# Mapping the next forest generation reveals multiple regeneration gaps across German forests

Leonie C. Gass[1*], ORCID: 0009-0002-6339-1363, leonie.gass@uni-bayreuth.de

Lisa Hülsmann[1,2], ORCID: 0000-0003-4252-2715, lisa.huelsmann@uni-bayreuth.de

[1]Ecosystem Analysis and Simulation (EASI) Lab, University of Bayreuth, Bayreuth, Germany

[2]Bayreuth Center of Ecology and Environmental Research (BayCEER), University of Bayreuth, Bayreuth, Germany

*Corresponding author

**Abstract**

1. In face of global change and increasing forest disturbances, forest regeneration is crucial for ensuring future generations of trees and resilient forest ecosystems. However, spatially explicit information on the current availability and climate suitability of seedlings and saplings remains scarce.
2. We assessed the potential to predict species-specific forest regeneration densities at high spatial resolution (1 ha) by calibrating generalized additive models (GAMs) using regeneration data from the German National Forest Inventory (NFI) and 44 environmental predictors. Regional regeneration gaps were then identified based on three indicators: low total density (<1,000 $ha^{-1}$), low species richness (≤2 species) and a high proportion (≥75%) of regeneration at high future cultivation risk.
3. For 22 tree species, we obtained regeneration density models that performed well in spatially blocked cross-validation. We were therefore able to generate regeneration density and indicator maps for a major part of the tree species.

4. The indicator maps revealed considerable regeneration gaps. 13.4% of Germany's forest area has low regeneration density, 47.1% has low species richness, and 25.2% of the Bavarian forest area lacks climate-adapted regeneration.
5. Our study demonstrates the potential of NFI regeneration data and its applicability for monitoring forest regeneration over large spatial scales. The regeneration indicator maps show that silvicultural interventions should prioritise increasing tree species richness and the proportion of species adapted to climate change. However, as regeneration gaps vary from region to region, management and policy must be adapted accordingly to ensure future forest resilience.
6. *Synthesis and applications:* Our study provides the first nationwide, high-resolution assessment of forest regeneration, offering a valuable baseline for monitoring forest development. The regeneration density and indicator maps enable forest managers and policymakers to identify regeneration deficits, prioritise adaptive management interventions, and contribute to the development of climate-resilient forests.

**Keywords**

forest regeneration, sapling density, tree species richness, climate-adapted species, cultivation risk, species distribution models SDMs, generalized additive models GAMs

## Introduction

Forest ecosystems are increasingly affected by ongoing climate change. In Europe, repeated droughts have caused increased spread of pests and diseases, defoliation of trees (Potočić et al., 2021), reduced tree growth (Martinez del Castillo et al., 2022) and higher tree mortality (George et al., 2022; Senf et al., 2020). The consequences are more open canopies and larger, more frequent disturbances (Senf & Seidl, 2021). This dynamic constitutes a partial loss of a forest generation,

46 making it necessary to consider the subsequent generation, the regenerating trees that are in the
47 seedling and sapling stage.

48 Forest regeneration can ensure future forest resilience, even under increased disturbances and
49 higher canopy mortality. A high density of regeneration can accelerate the regrowth of a closed
50 canopy, avoid arrested succession (Royo & Carson, 2006) and serve as an advanced start of post-
51 disturbance forest reorganization (Seidl et al., 2024; Seidl & Turner, 2022). Furthermore, regeneration
52 is key for the species composition and structure of future stands, and thus is targeted by
53 management to adapt forests to climate change (Fischer et al., 2016). While natural regeneration is
54 the dominant regeneration type in many European forest systems, seeding, planting and cutting are
55 selectively applied to ensure forest regeneration, increase the proportion of climate-adapted species
56 and create mixed stands (Erdozain et al., 2024). To assess how well forest regeneration is adapted to
57 future climates and where targeted forestry measures would be necessary, regional quantification of
58 regeneration is needed.

59 One of the most important data sources on forests at large spatial scales are national forest
60 inventories (NFIs). Besides statistically representative information on mature trees, most European
61 NFIs also include assessments of forest regeneration. Regeneration is often measured as a local
62 density by counting individuals below a threshold of diameter at breast height (dbh) per tree species
63 within small sampling areas, e.g. from 12 $m^2$ to 79 $m^2$ (Gschwantner et al., 2024; McRoberts et al.,
64 2011). The potential of such NFI regeneration data is largely untapped and underestimated. First,
65 despite the intense collection of such regeneration data, NFI reports either provide no information
66 on forest regeneration (Lackner et al., 2023) or only its dominant type, such as natural regeneration
67 or planting, at the national level (e.g. BMEL, 2024; Rigling & Schaffer, 2015). NFI reports thus lack
68 information on the quantity and quality of forest regeneration. Second, it is a widespread perception
69 that inference on forest regeneration and its patterns along large gradients using NFI data is
70 challenging or impossible due to high spatial heterogeneity, many interacting processes (Shoemaker

et al., 2020) and the relatively small size of regeneration plots. Nevertheless, inventory data on forest regeneration have been used to identify drivers of regeneration (Martini et al., 2024; Vayreda et al., 2013) and calibrate empirical models of regeneration distributions (Hasenauer et al., 2000; Kolo et al., 2017). This suggests that NFI regeneration data may have potential to map the next generation of forests at large spatial scales.

A common approach to creating maps from NFI sample plot data is to use species distribution models (SDMs; Xu et al., 2025), which make use of a species' ecological niche. However, these attempts (e.g. Bonannella et al., 2022; Dyderski et al., 2018) focus on large trees above the dbh threshold. Although the drivers of regeneration are becoming better understood, empirical models have not been applied to predict regeneration in space. The advantages of such regeneration maps would be their ability to provide information at unobserved locations, allowing for regional assessment of the regeneration and potential gaps of its quantity and quality. Species-specific regeneration maps could be used for early detection of post-disturbance reorganisation (Seidl et al., 2024), initialisation of dynamic forest simulation models (Díaz-Yáñez et al., 2024) and deriving regeneration indicators to inform forest management (Fischer et al., 2016).

Important indicators for the ability of forest regeneration to contribute to a more resilient next forest generation are its total density, species richness and proportion of climate-adapted species (Cerioni et al., 2024; König et al., 2022). High total regeneration density maintains the ability to establish the next forest generation (Hanbury-Brown et al., 2022). High species richness can reduce losses of productivity and biomass under more extreme climatic conditions (Jactel et al., 2017; Sebald et al., 2021). A high proportion of climate-adapted species indicates better resilience of the future stand and higher economic value (Erdozain et al., 2024; Hanewinkel et al., 2013). Evaluation of these indicators at high spatial resolution is essential to assess whether regeneration can secure future forests and maintain their multifunctionality in a changing climate.

Here, we assess the potential of regeneration density models calibrated with NFI data to infer and evaluate the current quantity and quality of forest regeneration at high spatial resolution (Figure 1). We built flexible species-specific regeneration models using the untapped regeneration density data of the German NFI in combination with 44 environmental variables, describing the environmental preferences of tree species in early life stages. Subsequently, we used the regeneration models to predict the regeneration density per tree species for the German forest area at a resolution of 1 ha. We then assessed potential regeneration gaps by calculating the currently available total regeneration density as a measure for regeneration quantity and two indicators for regeneration quality. For the latter, we derived species richness and the proportion of climate-adapted tree species in early life stages, indicated as a low proportion of regeneration at high cultivation risk.

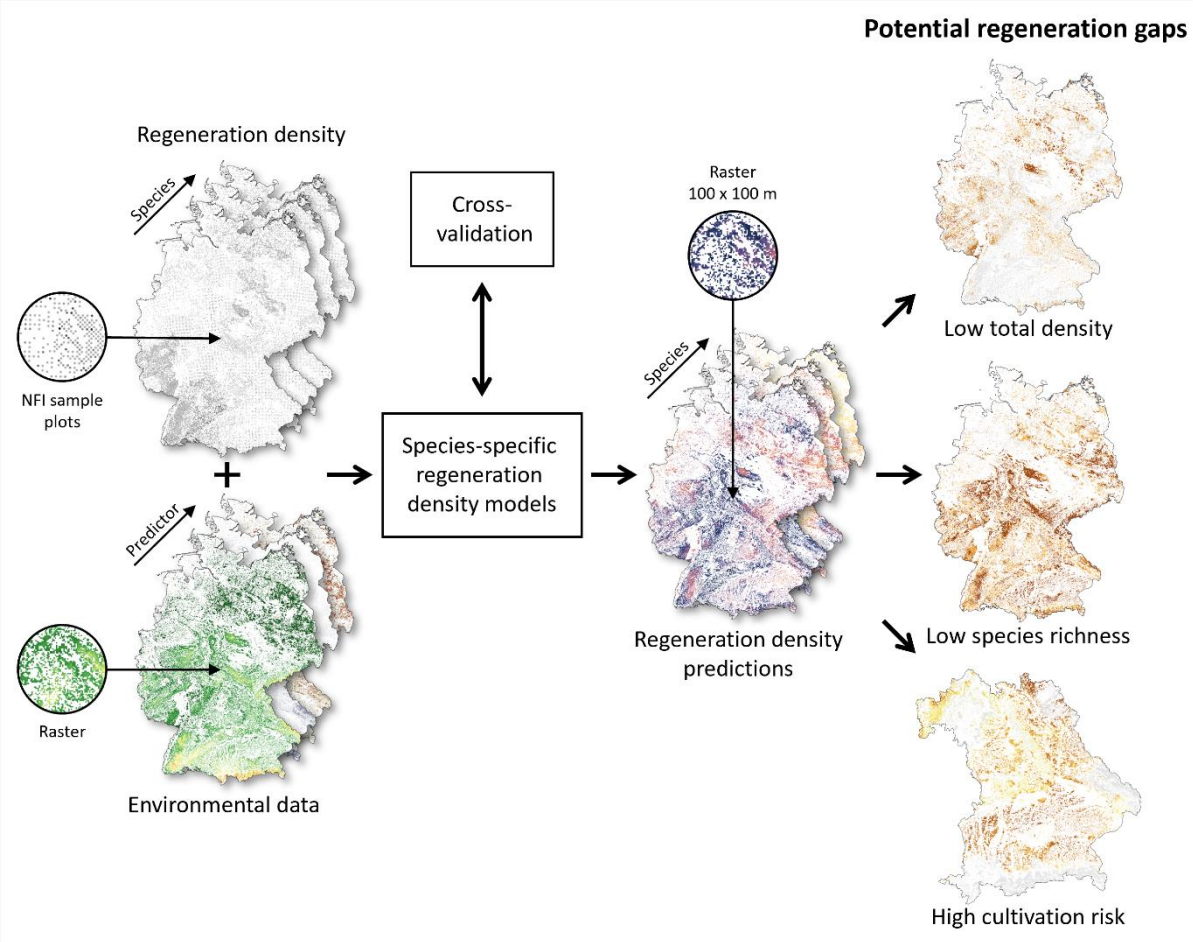


Figure 1: Workflow and indicators for the identification of potential regeneration gaps across German forests. To generate species-specific maps of current forest regeneration, we calibrated regeneration density models using data from the

German National Forest Inventory (NFI). These maps allowed us to identify regions where forest regeneration has low total density, low species richness, or high future cultivation risk.

## Materials and Methods

### Regeneration data

We used forest regeneration data from the most recent published German NFI, conducted in 2011 and 2012 (Thünen-Institut, 2015). The German NFI is conducted every ten years to assess tree and stand characteristics that are representative of the German forests. The sampling design is based on a regular grid with each cluster point consisting of four sample plots (survey design detailed in Riedel et al., 2017). We used regeneration counts of trees between 50 cm height and 7 cm dbh assessed per species within subplots of 2 m radius (12.57 $m^2$). All individuals were counted, whether they were naturally regenerated, sown, or planted. In total, our regeneration dataset covered information of 43 tree species at 59,848 NFI plot locations.

### Predictors of regeneration patterns

To calibrate predictive species distribution models, we used 44 environmental predictors related to topography, soil, macroclimate, microclimate, stand structure, space and time (Table S1). Besides previously used predictors for regeneration (e.g. Martini et al., 2024; Vayreda et al., 2013), we included the variables *month and year of NFI measurement* to account for seasonal differences in growing conditions and detection probability, *plot coordinates* to account for unobserved spatial predictors and *federal state* to account for potential management differences between states.

The environmental predictor values were preferably obtained from the NFI (meta)data and, if not available, from a corresponding raster layer (Table S1). Predictor information at each plot location was retrieved by the Thünen-Institute, as only anonymized plot locations on a 1 x 1 km grid are available (Hennig, 2022). The regeneration density and environmental datasets were then combined, and observations with missing predictor values were removed. The resulting dataset consisted of

52,305 NFI plot observations used for model calibration (available at Zenodo Data URL). For prediction we used raster layers of the same predictors (see Supporting information S1).

**Model calibration**

As predictive species-specific models of forest regeneration density, we calibrated generalized additive models (GAMs; Wood, 2017) with a negative binomial distribution and a log link function. We used GAMs with cubic regression splines (Wood et al., 2016) to allow for a broad spectrum of non-linear relationships between regeneration densities and our chosen environmental predictors (Table S1). *Month and year of NFI measurement* and *federal state* were included as random effects and *plot coordinates* as a tensor product smooth. GAM smoothness selection and estimation of the negative binomial functions theta value were performed using fast restricted maximum likelihood estimation. Basis dimensions of smoothing splines were kept at moderate complexity for environmental fixed effects (k = 10) and were set to 25 and 50 in x and y direction, respectively. We allowed fixed effects to be shrunk to zero, serving as a variable selection technique (Wood, 2017), and used a ridge penalty for random effects. To interpolate conspecific basal area for the German forest area as an additional predictor for regeneration, the same model structure was used (see Supporting information S1).

Models were fitted with the function bam() suited for large data sets (Wood et al., 2015) from the R package mgcv (v.1.9.1, Wood, 2023).

**Model evaluation**

Statistical assumptions of the regeneration models were assessed based on simulated residuals generated with the package DHARMa (v.0.4.6, Hartig, 2022). We visually evaluated distributional and residual assumptions as well as zero-inflation resulting in no critical violations (plots of simulated residuals can be found in Supporting information S3). To ensure that the observations are spatially independent, we tested for spatial autocorrelation within simulated residuals. We found a tendency

towards spatial autocorrelation for the regeneration models of 4 tree species (see Table S2). However, given the models' satisfactory performance in cross-validation (see subsequent paragraph), we assume that they generalize across space and likely capture meaningful spatial patterns.

Predictive model performance was assessed using 10-fold spatially blocked cross-validation with the blockCV package (v.3.1.4; Valavi et al., 2019). Blocks were set up with hexagonal block shapes and block sizes corresponding to the spatial autocorrelation range of the regeneration densities. Where block sizes were found to be too large, resulting in less than 10 blocks for some species, we set the range to 300 km resulting in 11 blocks across Germany (Table S2). The mean absolute error (MAE) as an indicator for model performance (Chai & Draxler, 2014) and pseudo-$R^2$ (Cameron & Windmeijer, 1997) as an indicator of explanatory power were computed for the test and training data of each fold. For MAE, we calculated the relative MAE from the test and training MAE $\left(\frac{MAE_{test}}{MAE_{train}}\right)$. The median was used to aggregate values of relative MAE and test pseudo-$R^2$ across all folds. We considered models where median relative MAE ≤2 and median pseudo-$R^2$ ≥0.1.

**Predictions**

After model evaluation, regeneration models for 22 tree species (Table 1) were available to be used for predicting regeneration densities across German forests. For creating regeneration maps, the variable *month and year of NFI measurement* was excluded, which results in predictions corresponding to average conditions. We converted the predicted regeneration counts per 2 m radius plot (approximately 12.6 $m^2$) to regeneration densities $ha^{-1}$.

Table 1: Evaluation and summary statistics of regeneration density models for 43 tree species. The availability of predicted regeneration density maps (Germany) or cultivation risk maps (only Bavaria; Falk & Mellert, 2011; Thurm et al., 2018) is indicated by a dot (available) or a circle (not available). Regeneration density maps were predicted when the model

performance criteria of median relative MAE ≤2 and median pseudo-$R^2$ ≥0.1 were met, as determined by 10-fold spatially blocked cross-validation.

| Species | Model performance | | Regeneration density map availability (Germany) | Regeneration density [#/ha] | | Cultivation risk map availability (Bavaria) |
|---|---|---|---|---|---|---|
| | Median relative MAE | Median pseudo-$R^2$ | | Mean | SD | |
| *Abies alba* | 1.02 | 0.48 | ● | 167 | 819 | ● |
| *Abies grandis* | 1.06 | 0.07 | ○ | | | ● |
| *Acer campestre* | 0.83 | 0.31 | ● | 18 | 345 | ● |
| *Acer platanoides* | 0.91 | 0.12 | ● | 8 | 154 | ● |
| *Acer pseudoplatanus* | 0.99 | -0.01 | ○ | | | ● |
| *Alnus glutinosa* | 1.12 | 0.16 | ● | 23 | 324 | ● |
| *Alnus incana* | 1.06 | 0.39 | ● | 84 | 9122 | ○ |
| *Betula pendula* | 1.00 | -0.12 | ○ | | | ● |
| *Betula pubescens* | 0.05 | 0.43 | ● | 25 | 533 | ○ |
| *Carpinus betulus* | 0.84 | 0.20 | ● | 208 | 1108 | ● |
| *Castanea sativa* | 1.01 | 0.32 | ● | 1 | 12 | ● |
| *Fagus sylvatica* | 1.05 | 0.26 | ● | 1192 | 1940 | ● |
| *Fraxinus excelsior* | 0.90 | 0.15 | ● | 329 | 1900 | ● |
| *Larix decidua* | 0.75 | 0.06 | ○ | | | ● |
| *Larix kaempferi* | 0.30 | 0.44 | ● | 7 | 88 | ● |
| *Malus sylvestris* | | | ○ | | | ○ |
| *Picea abies* | 0.75 | 0.16 | ● | 985 | 1572 | ● |
| *Picea sitchensis* | 0.20 | 0.09 | ○ | | | ○ |
| *Pinus mugo* | | | ○ | | | ○ |
| *Pinus nigra* | 0.50 | -0.28 | ○ | | | ● |
| *Pinus strobus* | 0.47 | -0.01 | ○ | | | ○ |
| *Pinus sylvestris* | 0.33 | 0.29 | ● | 257 | 805 | ● |
| *Populus alba* | 0.28 | 0.08 | ○ | | | ○ |
| *Populus nigra* | 0.13 | 0.20 | ● | 120 | 12213 | ○ |
| *Populus tremula* | 0.86 | 0.07 | ○ | | | ○ |
| *Populus trichocarpa x maximoviczii* | 0.35 | -0.98 | ○ | | | ○ |
| *Populus x canescens* | 0.06 | -0.09 | ○ | | | ○ |
| *Prunus avium* | 1.00 | 0.25 | ● | 11 | 43 | ● |
| *Prunus padus* | 0.54 | -0.57 | ○ | | | ○ |
| *Prunus serotina* | 0.33 | 0.11 | ● | 349 | 5338 | ○ |
| *Pseudotsuga menziesii* | 0.91 | 0.21 | ● | 26 | 101 | ● |
| *Pyrus communis* | | | ○ | | | ● |
| *Quercus petraea* | 0.74 | 0.02 | ○ | | | ● |
| *Quercus robur* | 1.06 | 0.20 | ● | 77 | 150 | ● |
| *Quercus rubra* | 0.84 | 0.15 | ● | 5 | 39 | ● |
| *Robinia pseudoacacia* | 1.09 | 0.45 | ● | 75 | 3850 | ● |
| *Salix spp.* | 1.04 | 0.03 | ○ | | | ○ |
| *Sorbus aria* | 0.89 | 0.12 | ● | 2 | 32 | ○ |
| *Sorbus aucuparia* | 0.99 | -0.10 | ○ | | | ● |
| *Sorbus torminalis* | | | ○ | | | ● |
| *Taxus baccata* | | | ○ | | | ○ |
| *Tilia spp.* | 0.92 | 0.29 | ● | 38 | 582 | ● |
| *Ulmus spp.* | 0.60 | -0.02 | ○ | | | ● |
| All species n = 22 | | | | 4006 | 17015.5 | |

## Regeneration indicators

Total regeneration density was calculated by summing up the densities for all 22 tree species per grid cell. Since reports of sufficient regeneration density thresholds vary, e.g. 1,591 $ha^{-1}$ (Kolo et al., 2017)

or 2,000 $ha^{-1}$ (StMELF, 2023), we chose an intermediate total regeneration density of 1,000-2,000 $ha^{-1}$ and defined <1,000 $ha^{-1}$ as insufficient and ≥2,000 $ha^{-1}$ as sufficient.

Tree species richness was calculated as the number of species with at least 5% of the total regeneration (BaySF, 2020). For Central European conditions, a species richness of three or four species has been proposed to be sufficient (BaySF, 2020; Lindner et al., 2025). Since our analyses included only 22 out of 43 species, we defined ≤2 species within the regeneration as insufficient, 3-4 species as intermediate and ≥5 species as sufficient.

To more precisely assess how the current regeneration fits future conditions, we used the federal state Bavaria as a case study. We combined our species-specific regeneration density maps with cultivation risk maps based on predicted occurrence probabilities of adult trees in the year 2100 (Falk & Mellert, 2011; Thurm et al., 2018). These were developed as a planning tool for forest practitioners throughout Bavaria and are actively used to select tree species considering climate projections and local site conditions. The maps categorize cultivation risk into five groups and are available for 32 tree species. Of these, 17 are also available as regeneration distribution maps (Table 1). For each grid cell, we calculated the percentage of regeneration density at high cultivation risk $R_{high\ risk}$ as:

$$R_{high\ risk}[\%] = \frac{N_{high\ risk}}{N_{total}} * 100$$

Here, $N_{high\ risk}$ is the regeneration density summed up over the species with the risk categories *very high risk* and *high risk* and $N_{total}$ the total regeneration density across all species of the grid cell. We defined $R_{high\ risk}$ ≥75% as problematic. The analysis of regeneration cultivation risk was possible for 76.8% of the Bavarian forest area.

The full workflow of modelling and data analysis can be found at GitHub URL and Zenodo Code URL. All analyses were conducted using R v.4.4.1 (R Core Team, 2024).

## Results

### Regeneration density models

From the 43 calibrated species-specific regeneration density models, 22 met the performance criteria of median pseudo-$R^2$ ≥0.1 and median relative MAE ≤2 from cross-validation (Table 1). We used these models to predict the regeneration density for 78.5% (8,615,918 ha) of the German forest area. The 22 species represented 74.9% of the regeneration measured within the NFI. In predictions across Germany, the most common tree species within the regeneration were *Fagus sylvatica* L., *Picea abies* (L.) H.Karst and *Prunus serotina* Ehrh. with mean densities of 1,192, 985 and 349 individuals $ha^{-1}$, respectively (Table 1). Species with lowest abundance in the regeneration throughout Germany were *Quercus rubra* L., *Sorbus aria* (L.) Crantz and *Pinus strobus* L. with average densities of ≤5 individuals $ha^{-1}$.

Of all 43 calibrated regeneration models, five did not converge and 16 did not meet the performance criteria (total 21; Table 1). Out of these, 15 were rare tree species with total regeneration density <1% within the German NFI (Table S3). The other six were common tree species *Acer pseudoplatanus* L., *Sorbus aucuparia* L., *Betula pendula* Roth, *Quercus petraea* (Matt.) Liebl., *Populus tremula* L. and *Prunus padus* L. (Table S3), that nevertheless could not be sufficiently modelled with our approach (Table 1). Median pseudo-$R^2$ was the primary factor to exclude models, as the median relative MAE criterion was consistently met.

### Species-specific regeneration maps for Germany

The predicted density maps showed distinct patterns in the availability of regeneration for each tree species (Figure 2, for all other tree species see Figure S1). For example, the regeneration of *Fagus sylvatica* was widely distributed with very high abundance in the centre of Germany and lower densities towards the east and the western lowlands (Figure 2). Similarly, the regeneration of *Picea abies* was widely abundant across Germany but showed lower densities towards the northeast. *Abies*

*alba* Mill., a less common tree species, showed a clear north-south trend with no occurrence in the northern half of Germany and a gradual increase in regeneration towards southern low mountain ranges. All maps can be explored online at Google Earth Engine URL.

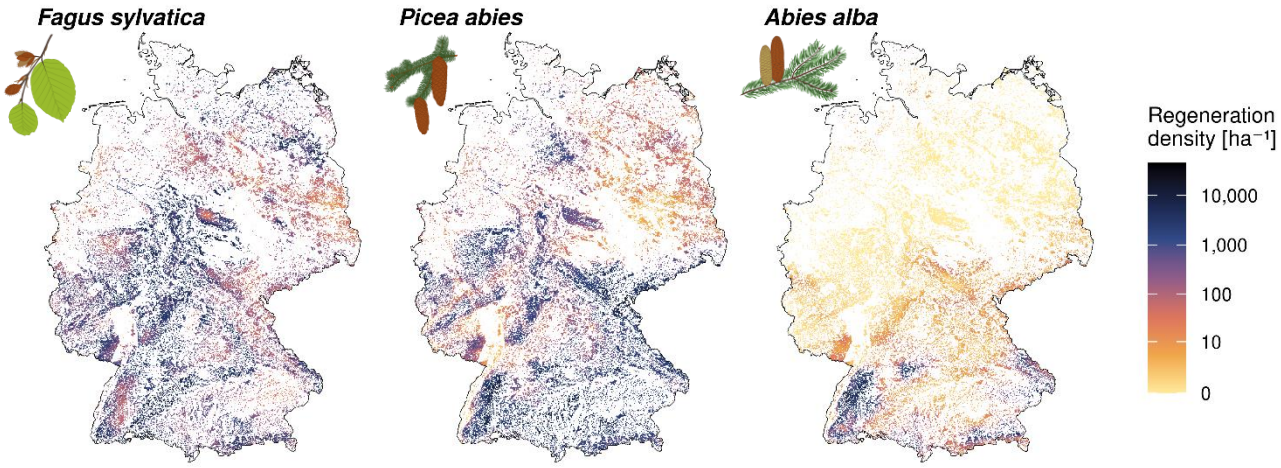


Figure 2: Regeneration densities shown for three important Central European tree species, i.e. *Fagus sylvatica, Picea abies* and *Abies alba*, in 1 ha grid cells for Germany (for remaining tree species maps see Figure S1). Maps are available for exploration at Google Earth Engine URL and for download at Zenodo Data URL.

**Indicators of regeneration quantity and quality**

The quantity of regeneration, evaluated as the total regeneration density based on 22 tree species, showed an average of 4,006 individuals $ha^{-1}$ (Table 1). We found a clear trend of insufficient (0-1,000 $ha^{-1}$) and intermediate (1,000-2,000 $ha^{-1}$) total regeneration densities in parts of Mid and North Germany (Figure 3, for continuous density scale see Figure S2), whereas the South mainly displayed sufficient regeneration (≥2,000 $ha^{-1}$). Overall, 60.1% of the predicted forest area had sufficient regeneration density, 26.4% had an intermediate density and 13.4% had an insufficient density.

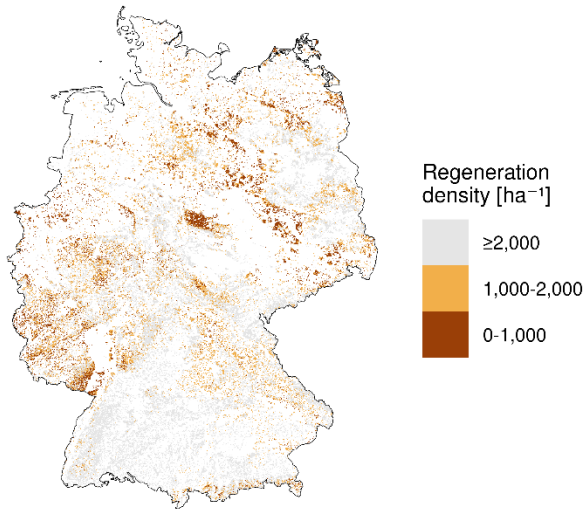


Figure 3: Spatial patterns of total regeneration density for the forest area of Germany based on 22 tree species. Colours indicate insufficient (0-1,000 $ha^{-1}$), intermediate (1,000-2,000 $ha^{-1}$) and sufficient (≥2,000 $ha^{-1}$) total regeneration densities (for continuous scale see Figure S2). The map is available for exploration at Google Earth Engine URL and for download at Zenodo Data URL.

As part of the quality assessment of the regeneration, we evaluated species richness (Figure 4, for continuous species richness scale see Figure S3), which was generally low with an average of 2.8 species $ha^{-1}$ across Germany. A total of 47.1% of the predicted forest area had too few (≤2) tree species in the regeneration (Figure 4B), while 43.5% and 9.4% of the area contained an intermediate (3-4) and sufficient number of species (≥5), respectively. Forests that were particularly species-rich in the regeneration were found towards the northeast (Figure 4A) but were otherwise restricted to local hotspots. Forests with a species richness of ≤2 were particularly common in low mountain ranges.

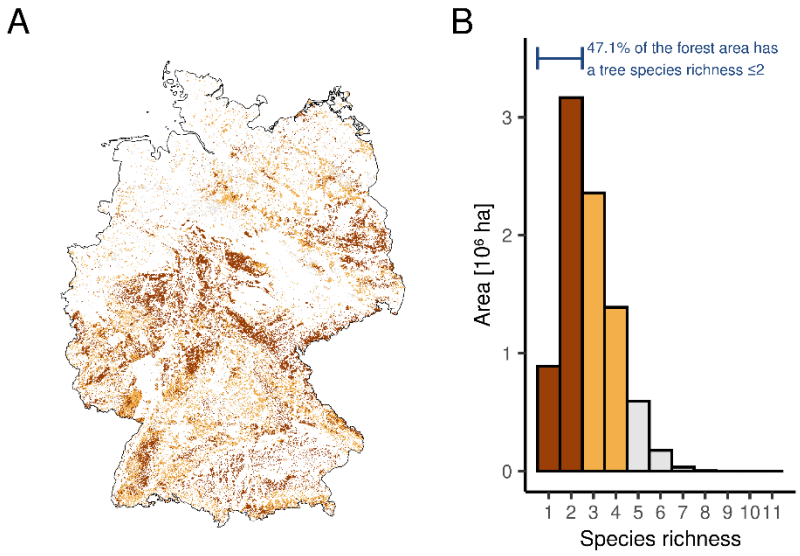


Figure 4: Tree species richness of regeneration for the forest area of Germany based on 22 tree species. The map (A) shows spatial patterns, the histogram (B) indicates the distribution of species richness values. Colours indicate insufficient (1-2), intermediate (3-4) and sufficient (≥5) regeneration species richness (for continuous scale see Figure S3). We considered a species present in a 1 ha-grid cell if its density was at least 5% of the total density. The map is available for exploration at Google Earth Engine URL and for download at Zenodo Data URL.

Regeneration quality was additionally assessed as the future suitability of tree species in the regeneration. We showcase this – and the identification of regeneration gaps and potential management strategies more generally – in Box 1.

Box 1: Bavaria (Germany) – A case study for identifying and managing regeneration gaps.

Using Bavaria as an example, we demonstrate the potential use of regeneration indicator maps to identify regeneration gaps (Figure 5) and derive regional recommendations for silvicultural interventions. Bavaria, a federal state in the southeast of Germany, has recently been affected by severe summer droughts and subsequent bark beetle outbreaks, which have led to a loss of tree canopies, especially in Norway spruce (*Picea abies*) forests (Thonfeld et al., 2022). We chose Bavaria because detailed cultivation risk maps are available for many tree species, which allowed us to derive not only the total regeneration density and species richness but also the proportion of regeneration at high future cultivation risk.

In Bavaria, only few regions, amounting to 3.5% of the forest area, showed a deficit of total regeneration density <1,000 $ha^{-1}$ (Figure 5A). Species richness of the regeneration was critically low (≤2 tree species; Figure 5B) in 50.0% of the Bavarian forest area, mainly found in the low mountain ranges. Regeneration at high cultivation risk (i.e. proportions ≥75%) dominated on 25.2% (489,385 ha; Figure 5D) of the forest area, e.g. in the northeast (Figure 5C), which is mainly the result of *Picea abies*, responsible for 94.5% of the regeneration densities at high risk (Table S4). Half of the analysed forest area had a proportion of less than 37.7% at high cultivation risk (Figure 5D), with a considerable area with no future risk in the regeneration. All indicators showed high spatial heterogeneity (Figure 5).

Such spatially resolved results on the quantity and quality of forest regeneration indicate regeneration gaps and allow for targeted silvicultural measures and incentives that can significantly contribute to the adaptation of forests to climate change. Regions like the Frankenwald and the Bavarian Alps (Figure 5A) are climate impact and adaptation hotspots, with the Frankenwald facing large-scale disturbances (Viana-Soto & Senf, 2024) and the Alps being increasingly prone to rockfall (e.g. Hillebrand et al., 2023). Combining this with forest regeneration indicators helps to prioritize forest management: In the Frankenwald, where species richness and climate-adapted tree species are lacking (Figure 5B and C), selective thinning and planting of additional climate-adapted tree species should be promoted. In the Bavarian Alps, smaller gaps in total regeneration density (Figure 5A) and species richness (Figure 5B) can be addressed by promoting natural regeneration and targeted planting. Overall, regions with severe regeneration gaps like the Frankenwald should be prioritized.

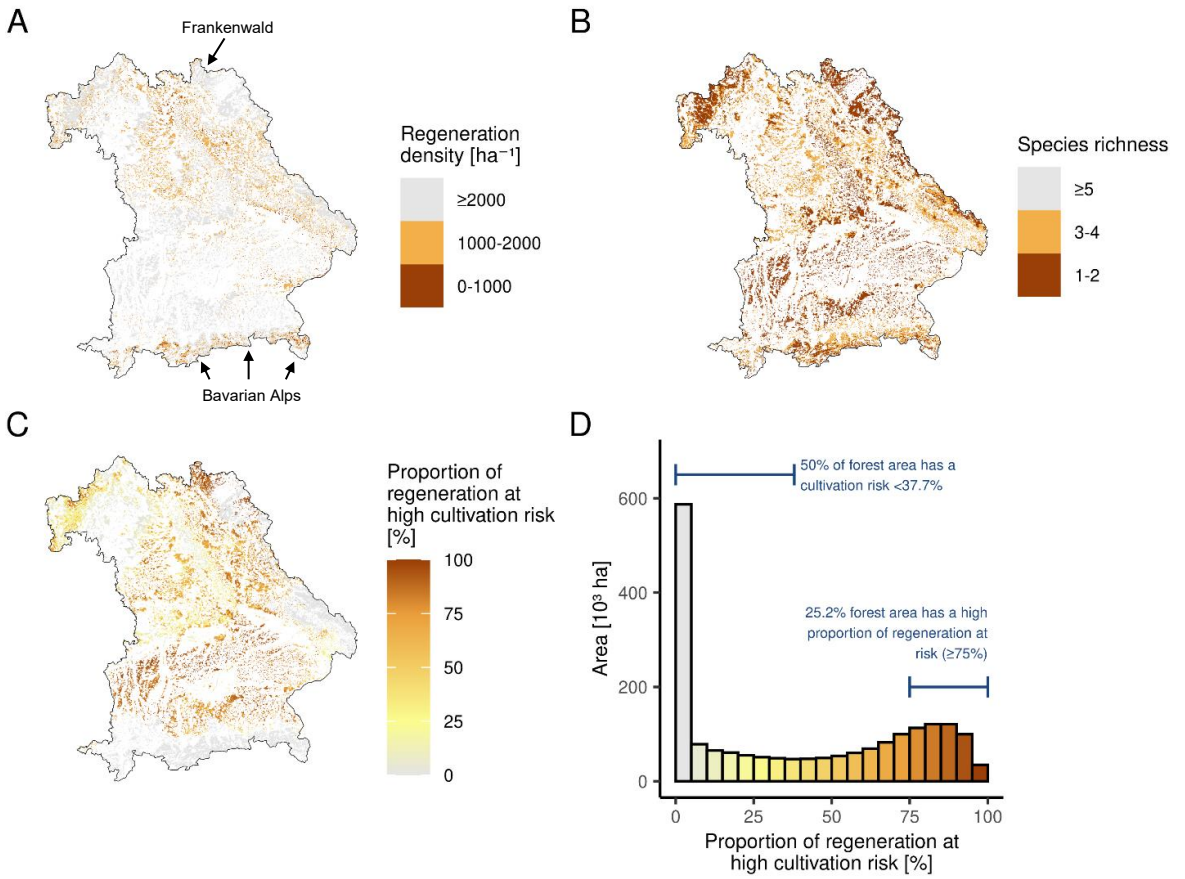


Figure 5: Maps of regeneration quantity and quality for Bavaria: (A) total density, (B) species richness, and (C) proportion of regeneration at high cultivation risk. (D) shows the distribution of values in (C). (A) and (B) were derived from regeneration density maps of 22 tree species, (C) and (D) are based on 17 tree species. Maps are available for exploration at Google Earth Engine URL and for download at Zenodo Data URL.

## Discussion

Our results demonstrate the potential to predict forest regeneration density at high spatial resolution from species-specific models calibrated with NFI regeneration data. Using the regeneration density maps predicted for Germany, we evaluated indicators of regeneration quantity and quality and identified regional gaps in forest regeneration.

**Predicting forest regeneration at large spatial scale**

We successfully predicted forest regeneration density for a large part of the modelled tree species in Central Europe. This contrasts with previous models of forest regeneration. These included only few species (Hasenauer et al., 2000; Kolo et al., 2017), covered only small environmental gradients (Hasenauer et al., 2000) and achieved low predictive accuracy at high spatial resolution (Zhu et al., 2014). Previous models were therefore not suited to reliably predict community composition and diversity across large environmental gradients.

Our modelling approach distinguishes itself by successfully cross-validating 22 of the 43 tree species models (Table 1). This is likely due to the large environmental gradient of the NFI data, the large number of environmental predictors (n = 44), partly at high spatial resolution, and the flexibility of our modelling approach (GAMs). We conclude that even though forest regeneration is subject to a variety of stochastic processes (Shoemaker et al., 2020) and is measured on small sample plots (12.57 $m^2$), there is enough signal in local regeneration densities to successfully predict the regional availability of forest regeneration.

**Tree species coverage of the regeneration models**

The predicted regeneration density maps (Figure 2 and Figure S1) cover a major part of the regeneration sampled within the German NFI. Therefore, our indicators derived from the regeneration maps provide reliable information about the dominant forest regeneration. Nevertheless, it would be desirable to expand the range of tree species modelled, especially since a large species pool and rare species will play a greater role as climate change progresses (Huth et al., 2025). Fifteen species (Table 1) that could not be modelled occurred at average densities <1% in the German NFI regeneration dataset (Table S3) and are therefore not well represented by the small NFI sample plots. To better cover the environmental preferences of such rare tree species, future predictive regeneration models, could be calibrated with regeneration data from previous German NFI surveys, other European NFIs or local inventories.

We could also not reliably predict the regeneration density for more generalist species such as *Acer pseudoplatanus* and *Betula pendula* found across large environmental gradients (Caudullo et al., 2016). This may have made it difficult to relate the regeneration densities of these species to the environmental predictors available to us. Future models could include even more predictors to better reflect environmental niches.

**Predictors of forest regeneration**

The regeneration models were calibrated using 44 predictive variables describing the environment with respect to topography, soil, microclimate, macroclimate, stand structure and spatial patterns (Table S1). However, it has been shown that forest regeneration density is also related to other predictors such as browsing intensity (Martini et al., 2024; Vayreda et al., 2013), understory light availability (Harris et al., 2024; Martini et al., 2024) or silvicultural management and ownership (Kolo et al., 2017).

We could not include these additional predictors in our forest regeneration maps because they are not (yet) available as spatial datasets for the German forest area, only available at low spatial resolution or not homogenized across federal states. We consider it promising to evaluate how much these additional predictors can contribute to the predictability of forest regeneration, and to invest accordingly in datasets for these predictors with better spatial coverage. Although our approach already allows for highly flexible effects (GAM), the complexity of environmental relationships could be further enhanced using machine learning (Pichler & Hartig, 2023).

**Application of regeneration density and indicator maps**

Creating species-specific regeneration density maps was motivated by the need to assess the potential contribution of forest regeneration to a more resilient next forest generation. To this end, we used three indicators that are widely used in forest management and planning: total regeneration density, species richness and proportion of climate-adapted tree species (Cerioni et al., 2024; König

et al., 2022). Typically, these indicators are assessed for individual stands by forest practitioners. Our results demonstrate the potential to monitor these indicators at national scales and to identify regional differences in forest regeneration.

For Germany, we found that regeneration gaps are small in terms of total density (Figure 3) but are of concern regarding species richness, with a deficit for almost half of the German forest area (Figure 4). In addition, one quarter of the forest area in Bavaria is affected by a lack of climate-adapted tree species (Figure 5D). While the forest regeneration indicator maps cannot replace a local, on-site assessment for stand level silvicultural decisions, they can provide an indication of potential regeneration gaps at the regional scale (cf. Box 1). Such knowledge can help forest policymakers identify potential priority areas to reduce future risks, increase species richness and regeneration density. These actions can be implemented through direct hands-on management or through incentives for silvicultural practices that promote regeneration of a diverse set of climate-adapted species (Huth et al., 2025).

Beyond practical applications, our species-specific regeneration maps can be used to increase the robustness of projections of future forest dynamics by incorporating comprehensive information on regeneration availability and species composition (e.g. Díaz-Yáñez et al., 2024). In turn, this also allows for the evaluation of different regeneration management strategies.

## Conclusions

Currently available forest regeneration appears insufficient to secure future forests and maintain their multifunctionality in a changing climate. Furthermore, the nature of gaps in regeneration quantity and quality varies spatially. Here, we demonstrated this using the German NFI regeneration data as an example to build predictive models of species-specific regeneration densities. We strongly encourage the evaluation of regeneration patterns and the regional assessment of total regeneration

density, species richness, and climate-adapted species across other countries and at continental scales.

## Acknowledgements

We thank Lukas Heiland for laying the groundwork for working with German NFI regeneration data, and Simon Mayer for supporting map visualization and database maintenance. Special thanks to Lukas Blickensdörfer (Thünen-Institute) for providing predictor data at true NFI plot locations, and Michael Heym and Tobias Mette (Bavarian State Institute of Forestry) for their help with NFI data and cultivation risk maps. We also appreciate Ottmar Ruppert, Ralph König, and Jonas Duscher for their forestry insights. This work was supported by the Bavarian Ministry of Science and the Arts within the Bavarian Climate Research Network (bayklif).

## Author contributions

**Leonie Gass:** Conceptualization (equal), data curation (lead), formal analysis (lead), methodology (equal), project administration (supporting), visualization (lead), writing – original draft preparation (lead), writing – review & editing (equal).

**Lisa Hülsmann:** Conceptualization (equal), formal analysis (supporting), funding acquisition (lead), methodology (equal), project administration (lead), resources (lead), supervision (lead), visualization (supporting), writing original draft preparation (supporting), writing – review & editing (equal).

Our study was based on secondary rather than primary data. Therefore, no local data was collected. However, all of the authors are based in the country where the study was conducted. We discussed our research with local forest practitioners whenever possible to seek feedback related to our regeneration indicators.

## Conflict of interest

The authors have no conflicts of interest to disclose.

## Data availability statement

All code supporting the findings of this study is openly available at Zenodo (https://doi.org/10.5281/zenodo.15552196) and GitHub (https://github.com/LeonieCG/GermanRegenerationMaps2012). The data used to calibrate the regeneration models was compiled from the German national forest inventory together with metadata sources, originally collected by various institutions. As far as we were permitted, we have republished the data at Zenodo (https://doi.org/10.5281/zenodo.15550864) and provided the code to work with the reduced set of environmental variables.

## References


BaySF. (2020). *Waldbauhandbuch Bayerische Staatsforsten, Richtlinie zur Baumartenwahl.* (WNJF-RL-007; p. 9). Bayerische Staatsforsten.

BMEL. (2024). *Der Wald in Deutschland—Ausgewählte Ergebnisse der vierten Bundeswaldinventur* (p. 60). Bundesministerium für Ernährung und Landwirtschaft.

Bonannella, C., Hengl, T., Heisig, J., Parente, L., Wright, M. N., Herold, M., & Bruin, S. de. (2022). Forest tree species distribution for Europe 2000–2020: Mapping potential and realized distributions using spatiotemporal machine learning. *PeerJ*, *10*, e13728. https://doi.org/10.7717/peerj.13728

Cameron, A. C., & Windmeijer, F. A. G. (1997). An R-squared measure of goodness of fit for some common nonlinear regression models. *Journal of Econometrics*, *77*(2), 329–342. https://doi.org/10.1016/S0304-4076(96)01818-0

Caudullo, G., De Rigo, D., Mauri, A., Houston Durrant, T., & San-Miguel-Ayanz, J. (2016). *European atlas of forest tree species*. Publications Office of the European Union. https://doi.org/doi/10.2760/776635

Cerioni, M., Brabec, M., Bače, R., Bāders, E., Bončina, A., Brůna, J., Chećko, E., Cordonnier, T., de Koning, J. H. C., Diaci, J., Dobrowolska, D., Dountchev, A., Engelhart, J., Fidej, G., Fuhr, M.,

Garbarino, M., Jansons, Ā., Keren, S., Kitenberga, M., … Nagel, T. A. (2024). Recovery and resilience of European temperate forests after large and severe disturbances. *Global Change Biology*, *30*(2), e17159. https://doi.org/10.1111/gcb.17159

Chai, T., & Draxler, R. R. (2014). Root mean square error (RMSE) or mean absolute error (MAE)? – Arguments against avoiding RMSE in the literature. *Geoscientific Model Development*, *7*(3), 1247–1250. https://doi.org/10.5194/gmd-7-1247-2014

Díaz-Yáñez, O., Käber, Y., Anders, T., Bohn, F., Braziunas, K. H., Brůna, J., Fischer, R., Fischer, S. M., Hetzer, J., Hickler, T., Hochauer, C., Lexer, M. J., Lischke, H., Mairota, P., Merganič, J., Merganičová, K., Mette, T., Mina, M., Morin, X., … Bugmann, H. (2024). Tree regeneration in models of forest dynamics: A key priority for further research. *Ecosphere*, *15*(3), e4807. https://doi.org/10.1002/ecs2.4807

Dyderski, M. K., Paź, S., Frelich, L. E., & Jagodziński, A. M. (2018). How much does climate change threaten European forest tree species distributions? *Global Change Biology*, *24*(3), 1150–1163. https://doi.org/10.1111/gcb.13925

Erdozain, M., Alberdi, I., Aszalós, R., Bollmann, K., Detsis, V., Diaci, J., Đodan, M., Efthimiou, G., Gálhidy, L., Haase, M., Hoffmann, J., Jaymond, D., Johann, E., Jørgensen, H., Krumm, F., Kuuluvainen, T., Lachat, T., Lapin, K., Lindner, M., … de-Miguel, S. (2024). The Evolution of Forest Restoration in Europe: A Synthesis for a Step Forward Based on National Expert Knowledge. *Current Forestry Reports*, *11*(1), 4. https://doi.org/10.1007/s40725-024-00235-3

Falk, W., & Mellert, K. H. (2011). Species distribution models as a tool for forest management planning under climate change: Risk evaluation of Abies alba in Bavaria. *Journal of Vegetation Science*, *22*(4), 621–634. https://doi.org/10.1111/j.1654-1103.2011.01294.x

Fischer, H., Huth, F., Hagemann, U., & Wagner, S. (2016). Developing restoration strategies for temperate forests using natural regeneration processes. In *Restoration of Boreal and Temperate Forests* (pp. 103–164). CRC Press.

George, J.-P., Bürkner, P.-C., Sanders, T. G. M., Neumann, M., Cammalleri, C., Vogt, J. V., & Lang, M. (2022). Long-term forest monitoring reveals constant mortality rise in European forests. *Plant Biology*, *24*(7), 1108–1119. https://doi.org/10.1111/plb.13469

Gschwantner, T., Schodterer, H., Kainz, C., & Freudenschuß, A. (2024). Regeneration of the Austrian forests and browsing impact – Insights from the latest National Forest Inventory. *Central European Forestry Journal*, *70*(4), 235–247. https://doi.org/10.2478/forj-2024-0010

Hanbury-Brown, A. R., Ward, R. E., & Kueppers, L. M. (2022). Forest regeneration within Earth system models: Current process representations and ways forward. *The New Phytologist*, *235*(1), 20–40. https://doi.org/10.1111/nph.18131

Hanewinkel, M., Cullmann, D. A., Schelhaas, M.-J., Nabuurs, G.-J., & Zimmermann, N. E. (2013). Climate change may cause severe loss in the economic value of European forest land. *Nature Climate Change*, *3*(3), 203–207. https://doi.org/10.1038/nclimate1687

Harris, L. B., Woodall, C. W., & D'Amato, A. W. (2024). Relationships between juvenile tree survival and tree density, shrub cover and temperature vary by size class based on ratios of abundance. *Canadian Journal of Forest Research*, *54*(2), 122–133. https://doi.org/10.1139/cjfr-2023-0097

Hartig, F. (2022). *DHARMa: Residual Diagnostics for Hierarchical (Multi-Level / Mixed) Regression Models* (Version 0.4.6) [Computer software]. https://CRAN.R-project.org/package=DHARMa

Hasenauer, H., Kindermann, G., & Merkl, D. (2000). Zur Schätzung der Verjüngungssituation in Mischbeständen mit Hilfe Neuraler Netze. *Forstwissenschaftliches Centralblatt vereinigt mit Tharandter forstliches Jahrbuch*, *119*(1), 350–366. https://doi.org/10.1007/BF02769149

Hennig, P. (2022). *Informationen zur Nutzung / Weitergabe anonymisierter Trakt-Koordinaten der Bundeswaldinventur*. Thünen-Institut. https://bwi.info/Download/de/BWI-Basisdaten/_Hinweise_BWI-Koordinaten.pdf

Hillebrand, L., Marzini, S., Crespi, A., Hiltner, U., & Mina, M. (2023). Contrasting impacts of climate change on protection forests of the Italian Alps. *Frontiers in Forests and Global Change*, *6*. https://doi.org/10.3389/ffgc.2023.1240235

Huth, F., Tischer, A., Nikolova, P., Feldhaar, H., Wehnert, A., Hülsmann, L., Bauhus, J., Heer, K., Vogt, J., Ammer, C., Berger, U., Bernhardt-Römermann, M., Böhme, M., Bugmann, H., Buse, J., Demant, L., Dörfler, I., Ewald, J., Feldmann, E., … Schuldt, B. (2025). Ecological assessment of forest management approaches to develop resilient forests in the face of global change in Central Europe. *Basic and Applied Ecology*. https://doi.org/10.1016/j.baae.2025.05.001

Jactel, H., Bauhus, J., Boberg, J., Bonal, D., Castagneyrol, B., Gardiner, B., Gonzalez-Olabarria, J. R., Koricheva, J., Meurisse, N., & Brockerhoff, E. G. (2017). Tree Diversity Drives Forest Stand Resistance to Natural Disturbances. *Current Forestry Reports*, *3*(3), 223–243. https://doi.org/10.1007/s40725-017-0064-1

Kolo, H., Ankerst, D., & Knoke, T. (2017). Predicting natural forest regeneration: A statistical model based on inventory data. *European Journal of Forest Research*, *136*(5–6), 923–938. https://doi.org/10.1007/s10342-017-1080-1

König, L. A., Mohren, F., Schelhaas, M.-J., Bugmann, H., & Nabuurs, G.-J. (2022). Tree regeneration in models of forest dynamics – Suitability to assess climate change impacts on European forests. *Forest Ecology and Management*, *520*, 120390. https://doi.org/10.1016/j.foreco.2022.120390

Lackner, C., Schreck, M., & Walli. (2023). *Österreichischer Waldbericht 2023*. Bundesministerium für Land- und Forstwitschaft, Regionen und Wasserwirtschaft.

Lindner, M., Seidl, R., Grünig, M., Bauhus, J., Willig, J., Hlásny, T., Nabuurs, G.-J., Patacca, M., Peltoniemi, M., Espelta, J.-M., Picos, J., Hoeben, A., Cantarello, E., & Schifferdecker, G. (2025). *Managing Forest Disturbances in a Changing Climate*. European Forest Institute. https://doi.org/10.36333/rs9

Martinez del Castillo, E., Zang, C. S., Buras, A., Hacket-Pain, A., Esper, J., Serrano-Notivoli, R., Hartl, C., Weigel, R., Klesse, S., Resco de Dios, V., Scharnweber, T., Dorado-Liñán, I., van der Maaten-Theunissen, M., van der Maaten, E., Jump, A., Mikac, S., Banzragch, B.-E., Beck, W., Cavin, L., … de Luis, M. (2022). Climate-change-driven growth decline of European beech forests. *Communications Biology*, *5*(1), 1–9. https://doi.org/10.1038/s42003-022-03107-3

Martini, F., Buechling, A., Bače, R., Hofmeister, J., Janda, P., Matula, R., & Svoboda, M. (2024). Biotic and abiotic effects on tree regeneration vary by life stage in European primary forests. *Oikos*. https://doi.org/10.1111/oik.10755

McRoberts, R. E., Chirici, G., Winter, S., Barbati, A., Corona, P., Marchetti, M., Hauk, E., Brändli, U.-B., Beranova, J., Rondeux, J., Sanchez, C., Bertini, R., Barsoum, N., Asensio, I. A., Condés, S., Saura, S., Neagu, S., Cluzeau, C., & Hamza, N. (2011). Prospects for Harmonized Biodiversity Assessments Using National Forest Inventory Data. In G. Chirici, S. Winter, & R. E. McRoberts (Eds.), *National Forest Inventories: Contributions to Forest Biodiversity Assessments* (pp. 41–97). Springer Netherlands. https://doi.org/10.1007/978-94-007-0482-4_3

Pichler, M., & Hartig, F. (2023). Machine learning and deep learning—A review for ecologists. *Methods in Ecology and Evolution*, *14*(4), 994–1016. https://doi.org/10.1111/2041-210X.14061

Potočić, N., Timmermann, V., Ognjenović, M., Kirchner, T., Prescher, A.-K., & Ferretti, M. (2021). *Tree health is deteriorating in the European forests*. Johann Heinrich von Thünen-Institut. https://doi.org/10.3220/ICP1638780772000

R Core Team. (2024). *R: A Language and Environment for Statistical Computing* (Version 4.4.1) [Computer software]. R Foundation for Statistical Computing. https://www.R-project.org/

Riedel, T., Hennig, P., Kroiher, F., Polley, H., Schmitz, F., & Schwitzgebel, F. (2017). *Die dritte Bundeswaldinventur (BWI 2012): Inventur- und Auswertungsmethoden*. Johann Heinrich von Thünen-Institut.

Rigling, A., & Schaffer, H. P. (2015). *Waldbericht 2015. Zustand und Nutzung des Schweizer Waldes.* Bundesamt für Umwelt.

Royo, A., & Carson, W. P. (2006). On the formation of dense understory layers in forests worldwide: Consequences and implications for forest dynamics, biodiversity, and succession. *Canadian Journal of Forest Research*, *36*, 1345–1362. https://doi.org/10.1139/X06-025

Sebald, J., Thrippleton, T., Rammer, W., Bugmann, H., & Seidl, R. (2021). Mixing tree species at different spatial scales: The effect of alpha, beta and gamma diversity on disturbance impacts under climate change. *Journal of Applied Ecology*, *58*(8), 1749–1763. https://doi.org/10.1111/1365-2664.13912

Seidl, R., Potterf, M., Müller, J., Turner, M. G., & Rammer, W. (2024). Patterns of early post-disturbance reorganization in Central European forests. *Proceedings of the Royal Society B: Biological Sciences*, *291*(2031), 20240625. https://doi.org/10.1098/rspb.2024.0625

Seidl, R., & Turner, M. G. (2022). Post-disturbance reorganization of forest ecosystems in a changing world. *Proceedings of the National Academy of Sciences of the United States of America*, *119*(28), e2202190119. https://doi.org/10.1073/pnas.2202190119

Senf, C., Buras, A., Zang, C. S., Rammig, A., & Seidl, R. (2020). Excess forest mortality is consistently linked to drought across Europe. *Nature Communications*, *11*(1), 6200. https://doi.org/10.1038/s41467-020-19924-1

Senf, C., & Seidl, R. (2021). Persistent impacts of the 2018 drought on forest disturbance regimes in Europe. *Biogeosciences*, *18*(18), 5223–5230. https://doi.org/10.5194/bg-18-5223-2021

Shoemaker, L. G., Sullivan, L. L., Donohue, I., Cabral, J. S., Williams, R. J., Mayfield, M. M., Chase, J. M., Chu, C., Harpole, W. S., Huth, A., HilleRisLambers, J., James, A. R. M., Kraft, N. J. B., May, F., Muthukrishnan, R., Satterlee, S., Taubert, F., Wang, X., Wiegand, T., … Abbott, K. C. (2020). Integrating the underlying structure of stochasticity into community ecology. *Ecology*, *101*(2), e02922. https://doi.org/10.1002/ecy.2922

StMELF. (2023). *Richtlinie für Zuwendungen zu waldbaulichen Maßnahmen im Rahmen eines forstlichen Förderprogramms (WALDFÖPR 2020)* (Az. F2-7752.1-1/361; pp. 1–21). Bayerisches Staatsministerium für Ernährung, Landwirtschaft und Forsten.

Thonfeld, F., Gessner, U., Holzwarth, S., Kriese, J., Da Ponte, E., Huth, J., & Kuenzer, C. (2022). A First Assessment of Canopy Cover Loss in Germany's Forests after the 2018–2020 Drought Years. *Remote Sensing*, *14*(3), 562. https://doi.org/10.3390/rs14030562

Thünen-Institut. (2015). *Dritte Bundeswaldinventur—Basisdaten* (20.03.2015) [Dataset].

Thurm, E. A., Hernandez, L., Baltensweiler, A., Ayan, S., Rasztovits, E., Bielak, K., Zlatanov, T. M., Hladnik, D., Balic, B., Freudenschuss, A., Büchsenmeister, R., & Falk, W. (2018). Alternative tree species under climate warming in managed European forests. *Forest Ecology and Management*, *430*, 485–497. https://doi.org/10.1016/j.foreco.2018.08.028

Valavi, R., Elith, J., Lahoz-Monfort, J. J., & Guillera-Arroita, G. (2019). blockCV: An R package for generating spatially or environmentally separated folds for k-fold cross-validation of species distribution models. *Methods in Ecology and Evolution*, *10*(2), 225–232. https://doi.org/10.1111/2041-210X.13107

Vayreda, J., Gracia, M., Martinez-Vilalta, J., & Retana, J. (2013). Patterns and drivers of regeneration of tree species in forests of peninsular Spain. *Journal of Biogeography*, *40*(7), 1252–1265. https://doi.org/10.1111/jbi.12105

Viana-Soto, A., & Senf, C. (2024). The European Forest Disturbance Atlas: A forest disturbance monitoring system using the Landsat archive. *Earth System Science Data Discussions*, 1–42. https://doi.org/10.5194/essd-2024-361

Wood, S. N. (2017). *Generalized Additive Models: An Introduction with R, Second Edition* (2nd ed.). Chapman and Hall/CRC. https://doi.org/10.1201/9781315370279

Wood, S. N. (2023). *mgcv: Mixed GAM Computation Vehicle with Automatic Smoothness Estimation* (Version 1.9.1, p. 1.9-1) [Computer software]. https://CRAN.R-project.org/package=mgcv

Wood, S. N., Goude, Y., & Shaw, S. (2015). Generalized Additive Models for Large Data Sets. *Journal of the Royal Statistical Society Series C: Applied Statistics*, *64*(1), 139–155. https://doi.org/10.1111/rssc.12068

Wood, S. N., Pya, N., & Säfken, B. (2016). Smoothing Parameter and Model Selection for General Smooth Models. *Journal of the American Statistical Association*, *111*(516), 1548–1563. https://doi.org/10.1080/01621459.2016.1180986

Xu, W., Luo, D., Peterson, K., Zhao, Y., Yu, Y., Ye, Z., Sun, J., Yan, K., & Wang, T. (2025). Advancements in ecological niche models for forest adaptation to climate change: A comprehensive review. *Biological Reviews*. https://doi.org/10.1111/brv.70023

Zhu, K., Woodall, C. W., Ghosh, S., Gelfand, A. E., & Clark, J. S. (2014). Dual impacts of climate change: Forest migration and turnover through life history. *Global Change Biology*, *20*(1), 251–264. https://doi.org/10.1111/gcb.12382

## Supporting information S1 – Additional Methods

### Predictor rasters

For the prediction of forest regeneration, we prepared information on the environmental variables for the entire forest area of Germany. The base raster layer of the forest area was created by recalculating the forest area map by Langer et al. (2022) to a 1 ha resolution and to the coordinate system of the cultivation risk maps (see Methods). Then, each predictor raster dataset was transformed using the base raster layer, and all datasets were set to the same coordinate system, extent and resolution. The predictors *coordinate* and *conspecific basal area*, were only available at NFI plot location and not as raster layers. Raster layers for *x* and *y coordinates* were created using the cell centroid coordinates of the base layer. Whereas the raster layers for *conspecific basal area* were derived using the NFI basal area data and the same modelling and prediction approach used for regeneration.

### Basal area interpolation

To interpolate conspecific basal area for the German forest area to predict regeneration, the same model structure with basal area as the response, a Tweedie distribution and a log link function was used. We calibrated basal area models for each regeneration tree species which remained after model evaluation (see Methods) and used the same prediction approach as described for regeneration density, without cross-validation. The plausibility of the species-specific basal area distributions was assessed by visual comparison with distribution maps of the European atlas of forest tree species (Caudullo et al., 2016).

## References

Caudullo, G., De Rigo, D., Mauri, A., Houston Durrant, T., & San-Miguel-Ayanz, J. (2016). *European atlas of forest tree species*. Publications Office of the European Union. https://doi.org/doi/10.2760/776635

Langner, N., Oehmichen, K., Henning, L., Blickensdörfer, L., & Riedel, T. (2022). *Bestockte Holzbodenkarte 2018*. Johann Heinrich von Thünen-Institut. https://doi.org/10.3220/DATA20221205151218

## Supporting information S2 - Additional Figures and Tables

Table S1: Predictor variables used for the calibration of species-specific regeneration density models.

| Category | Variable | Unit | Spatial extent | Spatial resolution | Measurement time | Reference |
|---|---|---|---|---|---|---|
| **Topography** | Eastness exposition | - | Europe | 25 x 25 m | 2011 | Derived from Thünen-Institut (2015) or from EEA (2016) |
| | Northness exposition | - | | | | |
| | Elevation above sea level | meters | Europe | 25 x 25 m | 2011 | Thünen-Institut (2015) or EEA (2016) |
| **Soil** | Available water capacity | % | Europe | 500 x 500 m | 2009 | Ballabio et al. (2016) |
| | Bulk density | t $m^3$ | | | | |
| | Clay | % | | | | |
| | Coarse fragments | % | | | | |
| | Sand | % | | | | |
| | Silt | % | | | | |
| | $CaCO_3$ | g $kg^{-1}$ | Europe | 500 x 500 m | 2009-2012 | Ballabio et al. (2019) |
| | Cation exchange capacity | cmol $kg^{-1}$ | | | | |
| | C-N-ratio | - | | | | |
| | K | mg $kg^{-1}$ | | | | |
| | N | g $kg^{-1}$ | | | | |
| | P | mg $kg^{-1}$ | | | | |
| | pH in CaCl | - | | | | |
| | Available water capacity in effective rooting depth | mm | Germany | 250 x 250 m | NA | Duijnisveld (2015) |
| | Water and wetness probability index | % | Europe | 20 x 20 m | 2015 | EEA (2018b) |
| | organic carbon | % | Europe | 1000 x 1000 m | 1800-2000 | Jones et al. (2005) |
| | Total $NH_4$ immission | eq $ha^{-1}$ $a^{-1}$ | Germany | 1000 x 1000 m | 2013-2015 | Schaap et al. (2018) |
| | Total $NO_3$ immission | eq $ha^{-1}$ $a^{-1}$ | | | | |
| | Total N immission | eq $ha^{-1}$ $a^{-1}$ | | | | |
| **Macroclimate** | Climatic water balance over the GDD period | mm | Europe | 30 x 30 arcsec | 1979–2013 | Heiland et al. (2022) |
| | Climatic water balance | mm | | | | |
| | Growing degree days | °C d | | | | |
| | Mean annual precipitation | mm | Global | 30 x 30 arcsec | 1981-2010 | Karger et al. (2018) |
| | Precipitation seasonality | % | | | | |
| | Mean daily minimum air temperature of the coldest month | °C | | | | |
| | Mean annual air temperature | °C | | | | |
| | Annual range of air temperature | °C | | | | |
| | Mean diurnal air temperature range | °C | | | | |
| | Temperature seasonality | 0.01 °C | | | | |
| | Aridity index | - | Global | 30 x 30 arcsec | 1970-2000 | Trabucco and Zomer (2019) |
| | Potential evapotranspiration | 0.0001 mm | | | | |
| **Microclimate** | Minimum temperature of the coldest month | °C | Europe | 25 x 25 m | 2000-2020 | Haesen et al. (2023) |
| | Mean annual temperature | °C | | | | |
| | Annual temperature range | °C | | | | |
| | Mean diurnal temperature range | °C | | | | |
| | Temperature seasonality | 0.01 °C | | | | |
| **Stand structure** | Tree cover density | % | Europe | 20 x 20 m | 2011-2013 | EEA (2018a) |

| | | | | | | |
|---|---|---|---|---|---|---|
| | Conspecific basal area (from angle count unit 1 and 2) | $m^2$ $ha^{-1}$ | Germany | 100 x 100 m | 2011-2012 | Thünen-Institut (2015) and this study |
| **Space** | Federal state of Germany | - | Germany | none and 100 x 100 m | 2013 and 2022 | Thünen-Institut (2015) and derived from BKG (2022) |
| | NFI plot coordinate x and y value (anonymized) | - | Germany | 1000 x 1000 m | 2016 | Thünen-Institut (2015) and this study |
| **Time** | Month and year of NFI measurement | - | Germany | none | 2011-2012 | Thünen-Institut (2015) |

Table S2: Spatial autocorrelation of each calibrated model and set up for spatially blocked cross-validation. Spatial autocorrelation of the model was assessed by using the R-package DHARMa (Hartig, 2022) and spatial autocorrelation range of the response was calculated with the package blockCV (Valavi et al., 2019).

| **Species** | **Model spatial autocorrelation** | | | **Spatially blocked cross-validation** | | |
|---|---|---|---|---|---|---|
| | **Observed Morans I** | **p-value** | | **Spatial autocorrelation range [m]** | **Used spatial range [m]** | **Block number** |
| *Abies alba* | -0.00019 | 0.32 | n.s. | 2,502 | 2,502 | 16,616 |
| *Abies grandis* | -0.00030 | 0.08 | n.s. | 5,682 | 5,683 | 8,645 |
| *Acer campestre* | -0.00013 | 0.60 | n.s. | 39,754 | 39,754 | 303 |
| *Acer platanoides* | -0.00028 | 0.10 | n.s. | 71,751 | 71,752 | 108 |
| *Acer pseudoplatanus* | -0.00017 | 0.42 | n.s. | 24,913 | 24,914 | 732 |
| *Alnus glutinosa* | -0.00012 | 0.66 | n.s. | 41,710 | 41,710 | 279 |
| *Alnus incana* | -0.00021 | 0.25 | n.s. | 9,450 | 9,450 | 4,163 |
| *Betula pendula* | -0.00035 | 0.03 | * | 13,295,247 | 300,000 | 11 |
| *Betula pubescens* | -0.00035 | 0.03 | * | 3,078,096 | 300,000 | 11 |
| *Carpinus betulus* | 0.00003 | 0.54 | n.s. | 31,648 | 31,649 | 465 |
| *Castanea sativa* | -0.00014 | 0.53 | n.s. | 531 | 532 | 18,181 |
| *Fagus sylvatica* | -0.00003 | 0.87 | n.s. | 51,183 | 51,184 | 191 |
| *Fraxinus excelsior* | -0.00030 | 0.07 | n.s. | 50,850 | 50,851 | 193 |
| *Larix decidua* | -0.00032 | 0.05 | n.s. | 224,055 | 224,056 | 16 |
| *Larix kaempferi* | -0.00009 | 0.80 | n.s. | 20,003,371 | 300,000 | 11 |
| *Malus sylvestris* | | | | | | |
| *Picea abies* | -0.00004 | 0.92 | n.s. | 104,926 | 104,927 | 58 |
| *Picea sitchensis* | -0.00029 | 0.08 | n.s. | 466,836 | 300,000 | 11 |
| *Pinus mugo* | | | | | | |
| *Pinus nigra* | -0.00015 | 0.50 | n.s. | 15,141 | 15,142 | 1,822 |
| *Pinus strobus* | -0.00024 | 0.18 | n.s. | 6,477,058 | 300,000 | 11 |
| *Pinus sylvestris* | -0.00007 | 0.89 | n.s. | 110,621 | 110,621 | 52 |
| *Populus alba* | 0.00006 | 0.42 | n.s. | 10,705 | 10,706 | 3,368 |
| *Populus nigra* | -0.00017 | 0.41 | n.s. | 42,140 | 42,141 | 269 |
| *Populus tremula* | -0.00015 | 0.50 | n.s. | 74,889 | 74,890 | 99 |
| *Populus trichocarpa x maximoviczii* | -0.00011 | 0.66 | n.s. | 1,854,565 | 300,000 | 11 |
| *Populus x canescens* | -0.00008 | 0.88 | n.s. | 47,026 | 47,026 | 220 |
| *Prunus avium* | -0.00002 | 0.82 | n.s. | 29,395 | 29,395 | 535 |
| *Prunus padus* | -0.00020 | 0.29 | n.s. | 17,820 | 17,821 | 1,367 |
| *Prunus serotina* | -0.00011 | 0.67 | n.s. | 103,071 | 103,072 | 59 |
| *Pseudotsuga menziesii* | -0.00012 | 0.63 | n.s. | 104,926 | 104,927 | 58 |
| *Pyrus communis* | | | | | | |
| *Quercus petraea* | -0.00035 | 0.03 | * | 240,624 | 240,625 | 15 |
| *Quercus robur* | -0.00014 | 0.53 | n.s. | 77,579 | 77,580 | 94 |
| *Quercus rubra* | -0.00018 | 0.36 | n.s. | 10,775 | 10,776 | 3,348 |
| *Robinia pseudoacacia* | -0.00017 | 0.39 | n.s. | 105,582 | 105,583 | 56 |
| *Salix spp.* | -0.00024 | 0.18 | n.s. | 26,742 | 26,742 | 640 |
| *Sorbus aria* | -0.00012 | 0.64 | n.s. | 10,119 | 10,120 | 3,721 |
| *Sorbus aucuparia* | -0.00012 | 0.63 | n.s. | 15,991,026 | 300,000 | 11 |
| *Sorbus torminalis* | | | | | | |

| | | | | | | |
|---|---|---|---|---|---|---|
| *Taxus baccata* | | | | | | |
| *Tilia spp.* | -0.00038 | 0.02 | * | 30,387 | 30,388 | 500 |
| *Ulmus spp.* | -0.00007 | 0.94 | n.s. | 27,193 | 27,193 | 616 |

Table S3: Forest regeneration densities per tree species from the German national forest inventory of 2012. The availability of predicted regeneration density maps is indicated by a dot (available) or a circle (not available).

| **Species** | **Density proportion [%]** | **Mean [#/ha]** | **SD [#/ha]** | **Map availability** |
|---|---|---|---|---|
| *Fagus sylvatica* | 29.9 | 1052 | 5085 | ● |
| *Picea abies* | 16.9 | 594 | 3546 | ● |
| *Acer pseudoplatanus* | 8.7 | 305 | 2481 | ○ |
| *Fraxinus excelsior* | 7.0 | 245 | 2121 | ● |
| *Sorbus aucuparia* | 6.8 | 240 | 1617 | ○ |
| *Carpinus betulus* | 4.2 | 148 | 1686 | ● |
| *Betula pendula* | 4.0 | 140 | 1668 | ○ |
| *Pinus sylvestris* | 3.8 | 132 | 1380 | ● |
| *Prunus serotina* | 3.5 | 124 | 1467 | ● |
| *Abies alba* | 2.3 | 81 | 931 | ● |
| *Quercus robur* | 1.6 | 56 | 582 | ● |
| *Quercus petraea* | 1.4 | 48 | 1022 | ○ |
| *Populus tremula* | 1.2 | 41 | 804 | ○ |
| *Prunus padus* | 1.1 | 40 | 849 | ○ |
| *Tilia spp.* | 0.9 | 32 | 511 | ● |
| *Salix spp.* | 0.8 | 29 | 637 | ○ |
| *Acer campestre* | 0.6 | 22 | 407 | ● |
| *Acer platanoides* | 0.6 | 22 | 593 | ● |
| *Pseudotsuga menziesii* | 0.6 | 21 | 569 | ● |
| *Alnus glutinosa* | 0.6 | 20 | 477 | ● |
| *Alnus incana* | 0.6 | 19 | 651 | ● |
| *Ulmus spp.* | 0.5 | 19 | 366 | ○ |
| *Prunus avium* | 0.5 | 19 | 341 | ● |
| *Betula pubescens* | 0.4 | 15 | 437 | ● |
| *Quercus rubra* | 0.4 | 13 | 364 | ● |
| *Robinia pseudoacacia* | 0.3 | 9 | 243 | ● |
| *Larix decidua* | 0.1 | 5 | 126 | ○ |
| *Sorbus aria* | 0.1 | 4 | 143 | ● |
| *Pinus strobus* | <0.1 | 3 | 131 | ○ |
| *Larix kaempferi* | <0.1 | 3 | 108 | ● |
| *Picea sitchensis* | <0.1 | 2 | 126 | ○ |
| *Pinus mugo* | <0.1 | 2 | 147 | ○ |
| *Populus nigra* | <0.1 | 2 | 164 | ● |
| *Populus trichocarpa x maximoviczii* | <0.1 | 2 | 226 | ○ |
| *Castanea sativa* | <0.1 | 2 | 94 | ● |
| *Sorbus torminalis* | <0.1 | 2 | 76 | ○ |
| *Pinus nigra* | <0.1 | 1 | 77 | ○ |
| *Populus x canescens* | <0.1 | 1 | 70 | ○ |
| *Pyrus communis* | <0.1 | 1 | 38 | ○ |
| *Malus sylvestris* | <0.1 | 0 | 24 | ○ |
| *Abies grandis* | <0.1 | 0 | 30 | ○ |
| *Taxus baccata* | <0.1 | 0 | 19 | ○ |
| *Populus alba* | <0.1 | 0 | 37 | ○ |
| *Sorbus domestica* | 0.0 | 0 | 0 | ○ |

Table S4: Proportion of regeneration in Bavaria at high cultivation risk for 17 tree species.

| Species | Regeneration at high cultivation risk [%] |
|---|---|
| *Abies alba* | 0.49 |
| *Acer campestre* | <0.01 |
| *Acer platanoides* | <0.01 |
| *Alnus glutinosa* | 0.26 |
| *Carpinus betulus* | <0.01 |
| *Castanea sativa* | <0.01 |
| *Fagus sylvatica* | <0.01 |
| *Fraxinus excelsior* | <0.01 |
| *Larix kaempferi* | <0.01 |
| *Picea abies* | 94.48 |
| *Pinus sylvestris* | 4.52 |
| *Prunus avium* | 0.19 |
| *Pseudotsuga menziesii* | 0.01 |
| *Quercus robur* | <0.01 |
| *Quercus rubra* | 0.02 |
| *Robinia pseudoacacia* | <0.01 |
| *Tilia spp.* | <0.01 |

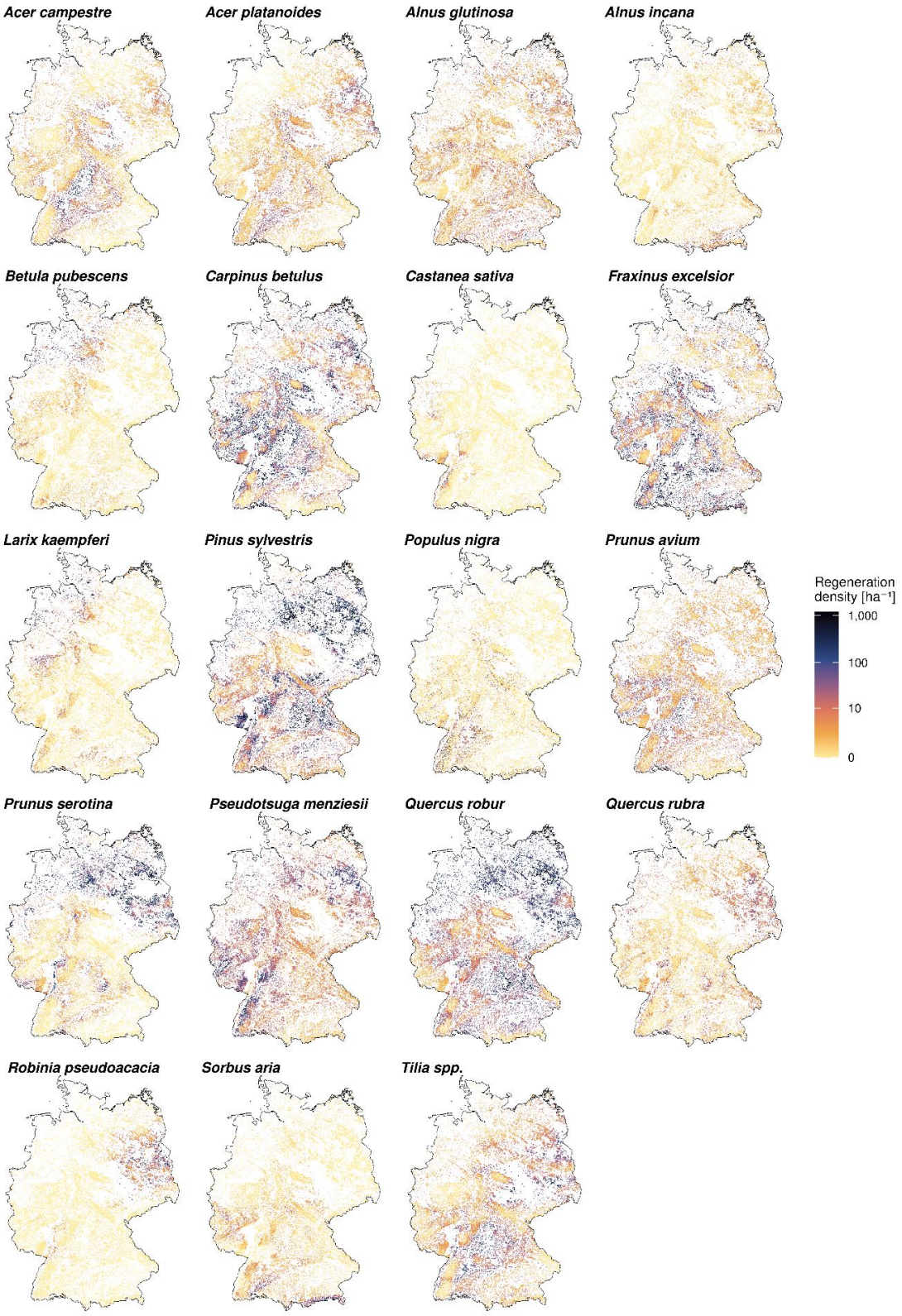


Figure S1: Total regeneration density maps of remaining tree species not displayed in Figure 2. Regeneration density scale was cut off at the 99% percentile across all species map values (1,186 $ha^{-1}$). All maps are available for exploration at Google Earth Engine URL and for download at Zenodo Data URL.

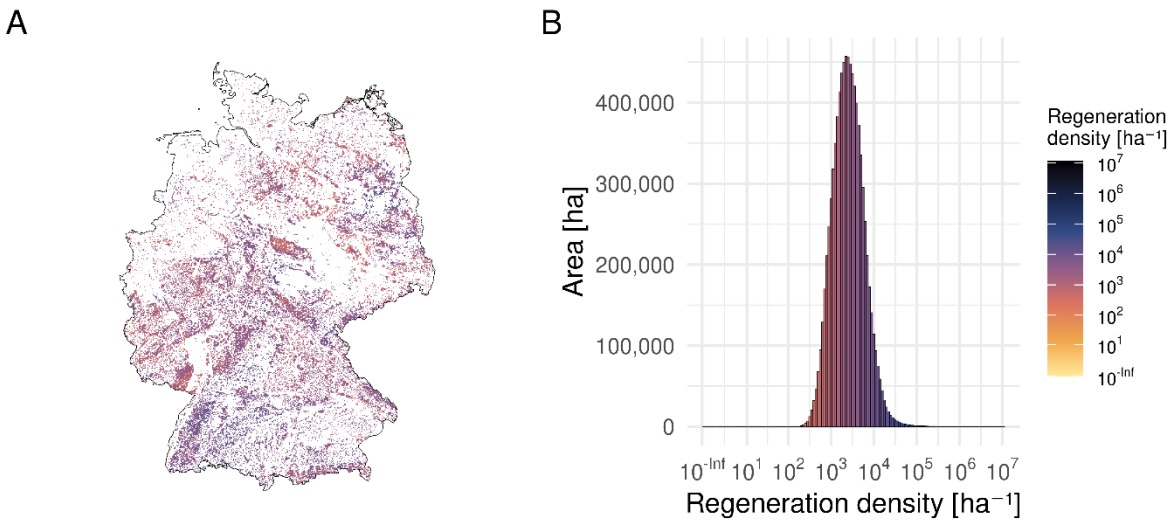


Figure S2: Spatial patterns of total regeneration density ($ha^{-1}$) for Germany based on 22 tree species.

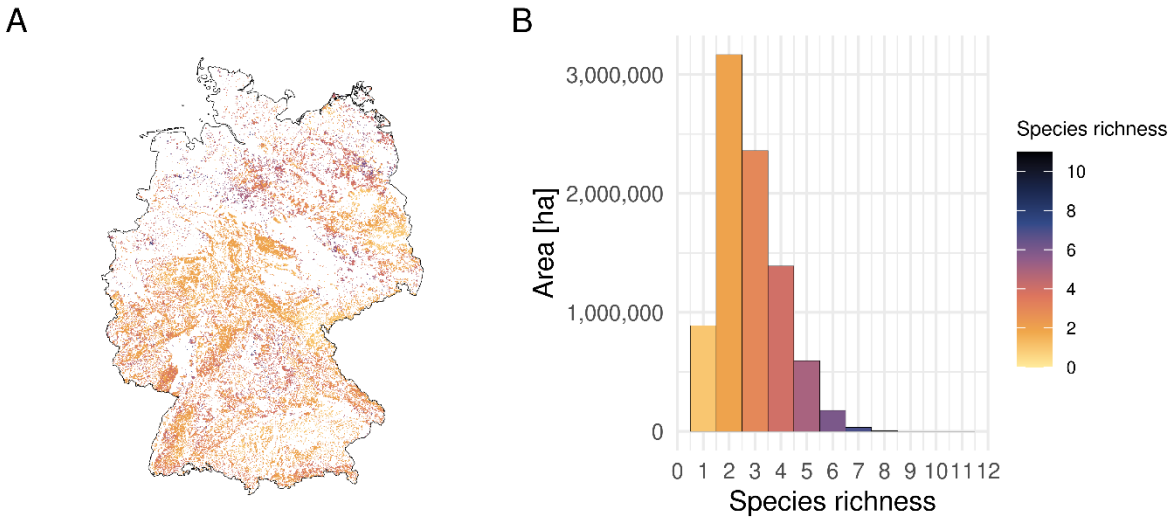


Figure S3: Regeneration tree species richness for the forest area of Germany based on 22 tree species. The map (A) shows spatial patterns, and the histogram (B) describes the distribution of species richness occurrence. We considered a species present in a 1 ha-grid cell if its density was at least 5% of the total regeneration density.

## References

Ballabio, C., Lugato, E., Fernández-Ugalde, O., Orgiazzi, A., Jones, A., Borrelli, P., Montanarella, L., & Panagos, P. (2019). Mapping LUCAS topsoil chemical properties at European scale using

Gaussian process regression. *Geoderma*, *355*, 113912. https://doi.org/10.1016/j.geoderma.2019.113912

Ballabio, C., Panagos, P., & Monatanarella, L. (2016). Mapping topsoil physical properties at European scale using the LUCAS database. *Geoderma*, *261*, 110–123. https://doi.org/10.1016/j.geoderma.2015.07.006

BKG. (2022). *Verwaltungsgebiete 1: 5 000 000.* (31.12.2022) [Dataset]. Bundesamt für Kartographie und Geodäsie. https://gdz.bkg.bund.de/index.php/default/digitale-geodaten/verwaltungsgebiete/verwaltungsgebiete-1-5-000-000-stand-31-12-vg5000-12-31.html

Duijnisveld, W. (2015). *Available water capacity in the rooting zone of German soils* (8e3f001c-9c6e-4eeb-8d0d-988456a20486; Version 1.0) [Dataset]. https://www.geoportal.de/Metadata/8e3f001c-9c6e-4eeb-8d0d-988456a20486

EEA. (2016). *European Digital Elevation Model (EU-DEM)* (copernicus_r_3035_25_m_eu-dem_p_2011_v01_r01; Version 1.1) [Dataset]. European Environment Agency.

EEA. (2018a). *Tree Cover Density 2012 (raster 20 m), Europe, 3-yearly, Mar. 2018* [Dataset]. European Environment Agency. https://doi.org/10.2909/91687EF2-F907-4F84-81F7-C9C81980C306

EEA. (2018b). *Water and Wetness 2015 (raster 20 m), Europe, 3-yearly, Nov. 2020* (Version 07.00) [Dataset]. European Environment Agency. https://doi.org/10.2909/25ED7A97-E3A6-42ED-A403-D636D6880E6D

Haesen, S., Lembrechts, J. J., De Frenne, P., Lenoir, J., Aalto, J., Ashcroft, M. B., Kopecký, M., Luoto, M., Maclean, I., Nijs, I., Niittynen, P., Van Den Hoogen, J., Arriga, N., Brůna, J., Buchmann, N., Čiliak, M., Collalti, A., De Lombaerde, E., Descombes, P., … Van Meerbeek, K. (2023). ForestClim—Bioclimatic variables for microclimate temperatures of European forests. *Global Change Biology*, *29*(11), 2886–2892. https://doi.org/10.1111/gcb.16678

Hartig, F. (2022). *DHARMa: Residual Diagnostics for Hierarchical (Multi-Level / Mixed) Regression Models* (Version 0.4.6) [Computer software]. https://CRAN.R-project.org/package=DHARMa

Heiland, L., Kunstler, G., Ruiz–Benito, P., Buras, A., Dahlgren, J., & Hülsmann, L. (2022). Divergent occurrences of juvenile and adult trees are explained by both environmental change and ontogenetic effects. *Ecography*, *2022*(3). https://doi.org/10.1111/ecog.06042

Jones, R. J. A., Hiederer, R., Rusco, E., & Montanarella, L. (2005). Estimating organic carbon in the soils of Europe for policy support. *European Journal of Soil Science*, *56*(5), 655–671. https://doi.org/10.1111/j.1365-2389.2005.00728.x

Karger, D. N., Conrad, O., Böhner, J., Kawohl, T., Kreft, H., Soria-Auza, R. W., Zimmermann, N. E., Linder, H. P., & Kessler, M. (2018). *Data from: Climatologies at high resolution for the earth's land surface areas* (Version 1) [Dataset]. Dryad. https://doi.org/10.5061/DRYAD.KD1D4

Schaap, M., Hendriks, C., Kranenburg, R., Kuenen, J., Segers, A., Schlutow, A., Nagel, H.-D., Ritter, A., & Banzhaf, S. (2018). *PINETI-3: Modellierung atmosphärischer Stoffeinträge von 2000 bis 2015 zur Bewertung der ökosystem-spezifischen Gefährdung von Biodiversität durch Luftschadstoffe in Deutschland*. Umweltbundesamt.

Thünen-Institut. (2015). *Dritte Bundeswaldinventur—Basisdaten* (20.03.2015) [Dataset].

Trabucco, A., & Zomer, R. (2019). *Global Aridity Index and Potential Evapotranspiration (ET0) Climate Database* (Version 2) [Dataset]. figshare. https://doi.org/10.6084/M9.FIGSHARE.7504448.V2

Valavi, R., Elith, J., Lahoz-Monfort, J. J., & Guillera-Arroita, G. (2019). blockCV: An R package for generating spatially or environmentally separated folds for k-fold cross-validation of species distribution models. *Methods in Ecology and Evolution*, *10*(2), 225–232. https://doi.org/10.1111/2041-210X.13107

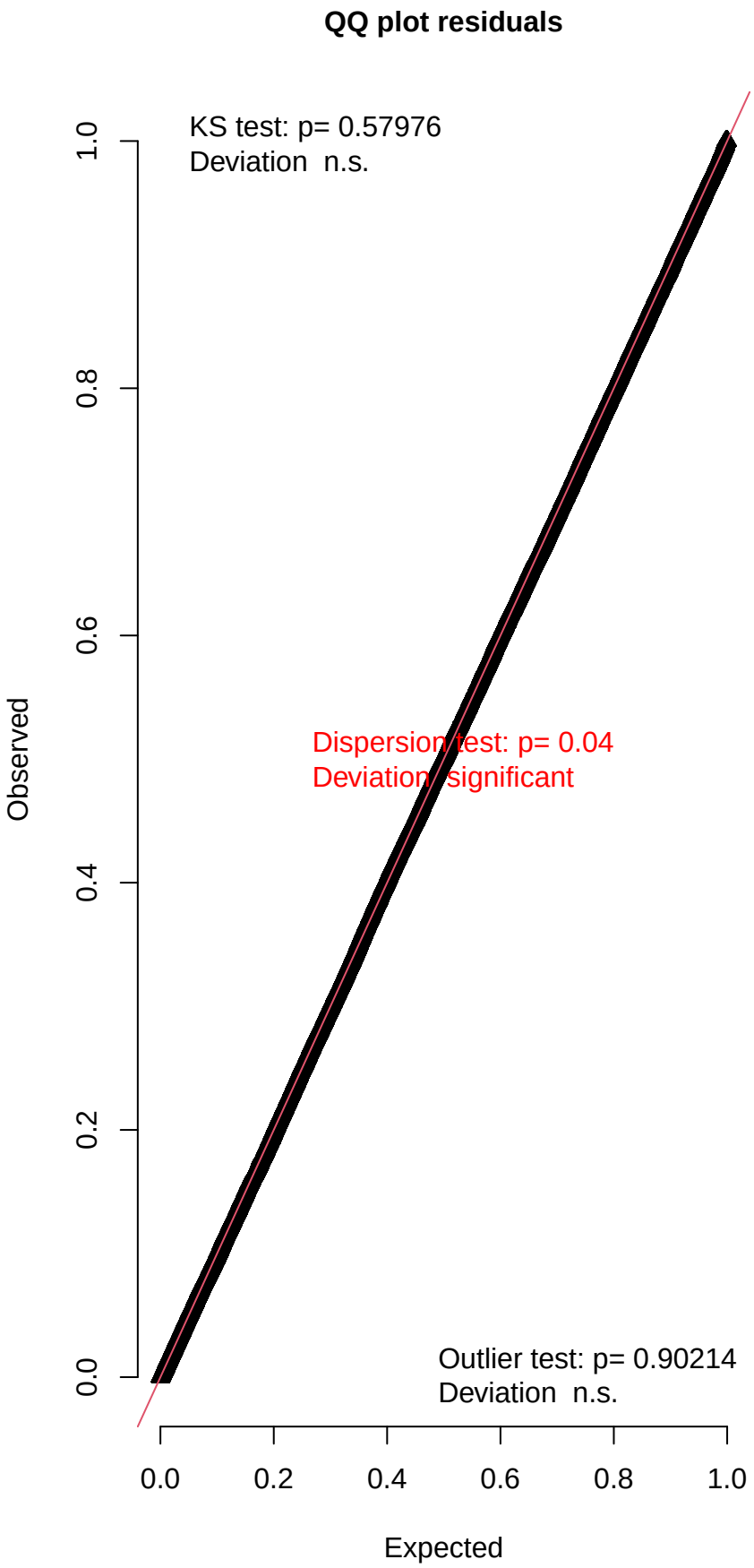
QQ plot residuals
KS test: p= 0.57976
Deviation n.s.
Dispersion test: p= 0.04
Deviation significant
Outlier test: p= 0.90214
Deviation n.s.
Observed
Expected
0.0
0.2
0.4
0.6
0.8
1.0

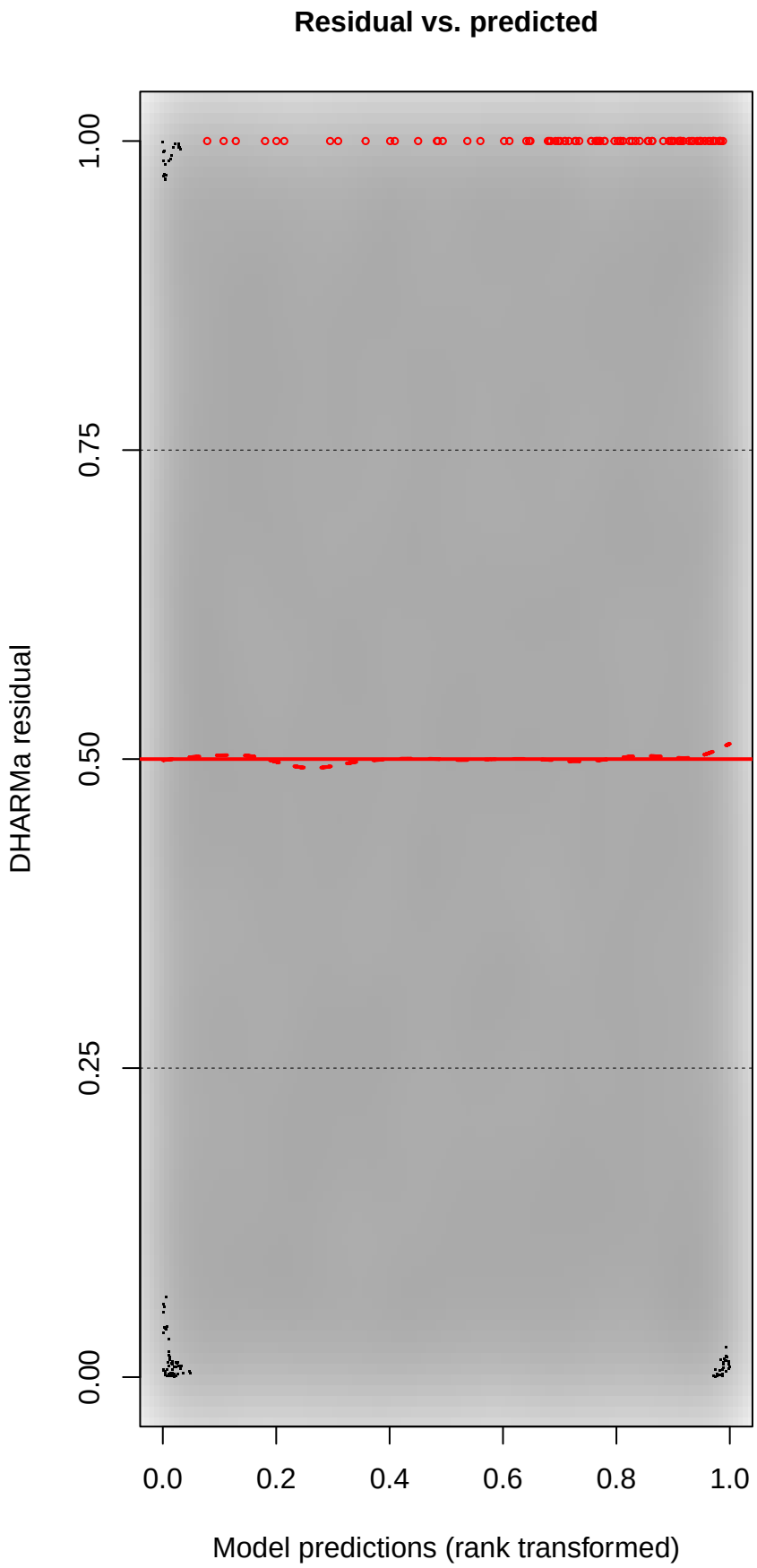
Residual vs. predicted
DHARMa residual
Model predictions (rank transformed)
0.00
0.25
0.50
0.75
1.00
0.0
0.2
0.4
0.6
0.8
1.0

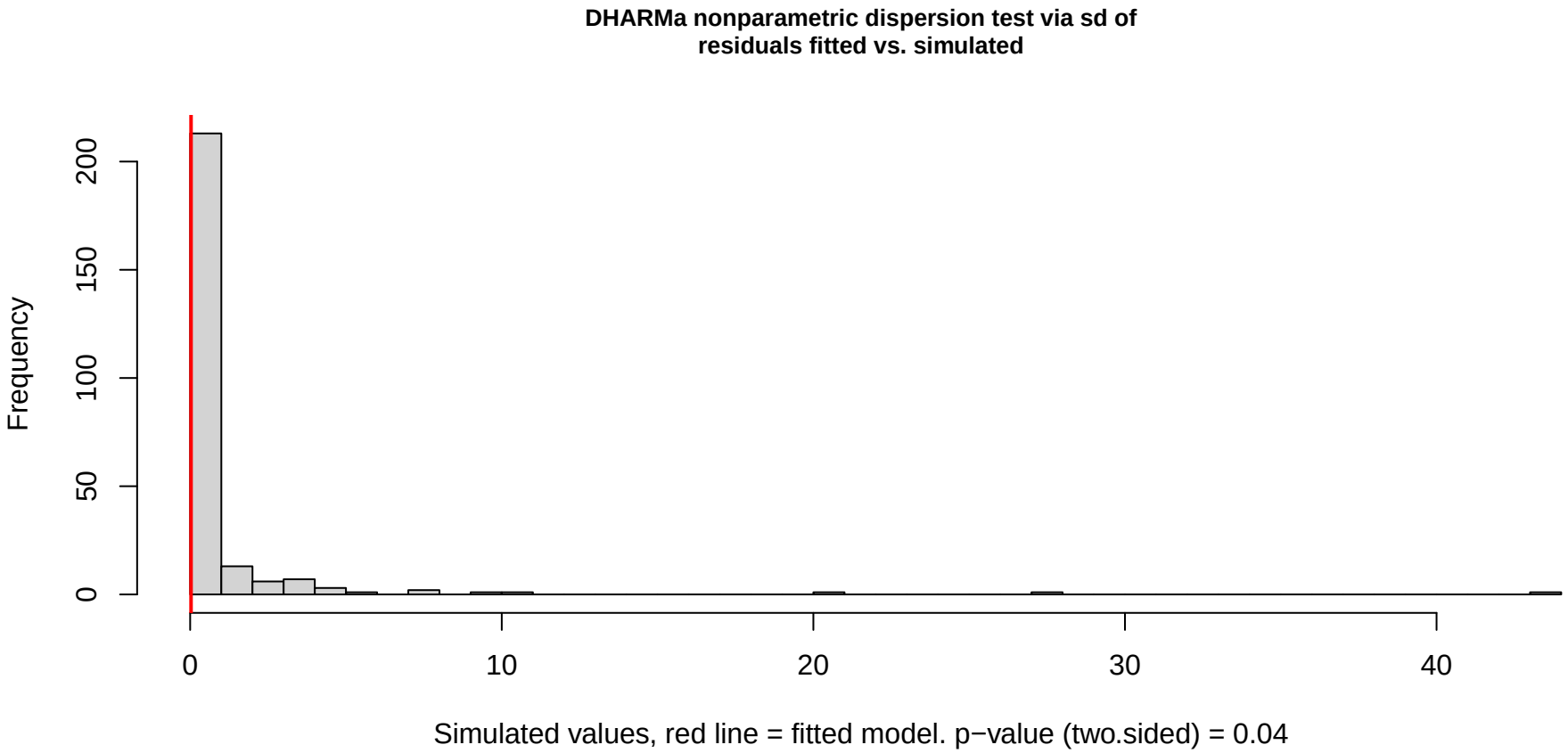
DHARMa nonparametric dispersion test via sd of residuals fitted vs. simulated
Frequency
0
50
100
150
200
0
10
20
30
40
Simulated values, red line = fitted model. p−value (two.sided) = 0.04

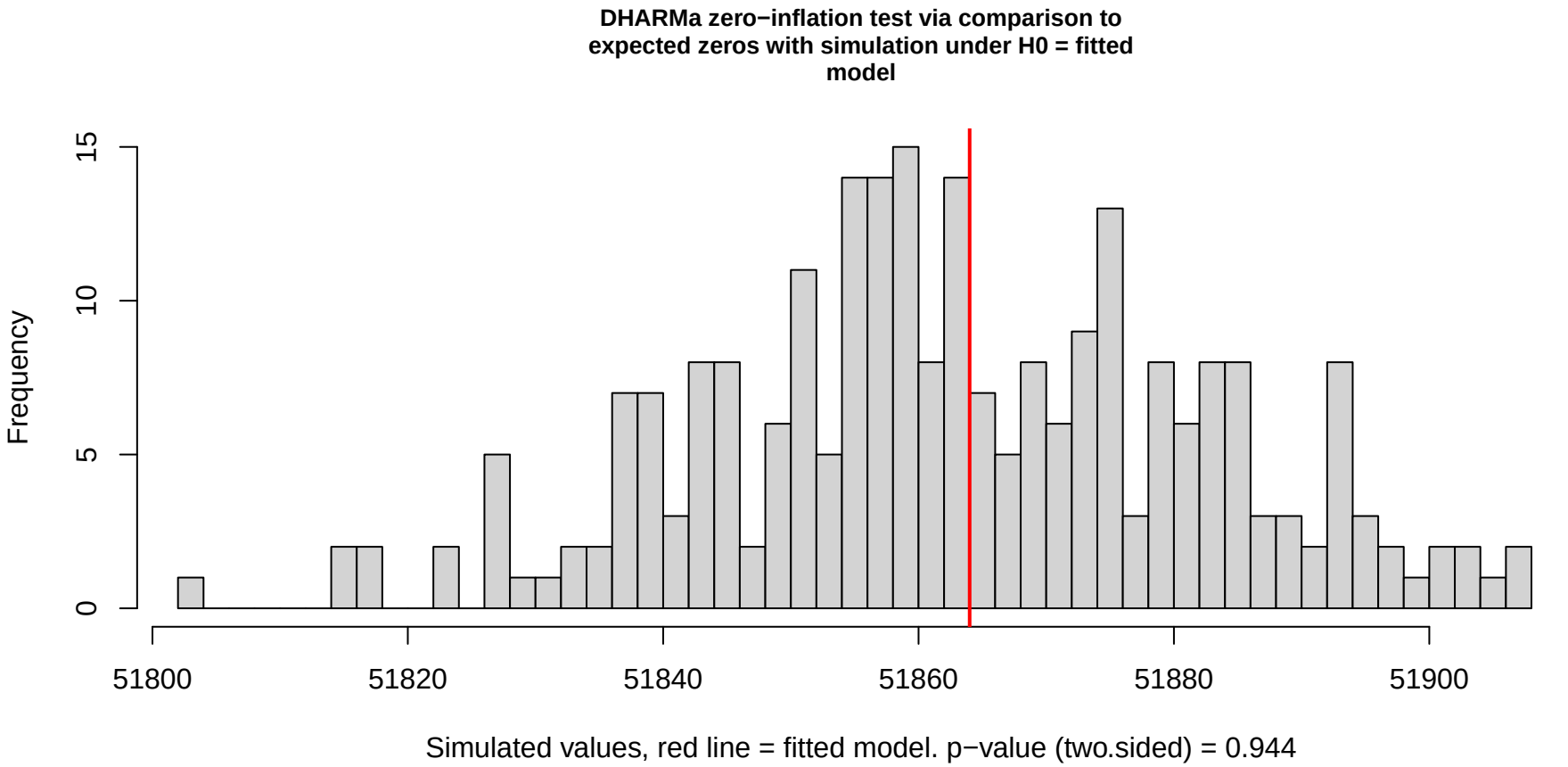
DHARMa zero−inflation test via comparison to expected zeros with simulation under H0 = fitted model
Frequency
0
5
10
15
51800
51820
51840
51860
51880
51900
Simulated values, red line = fitted model. p−value (two.sided) = 0.944

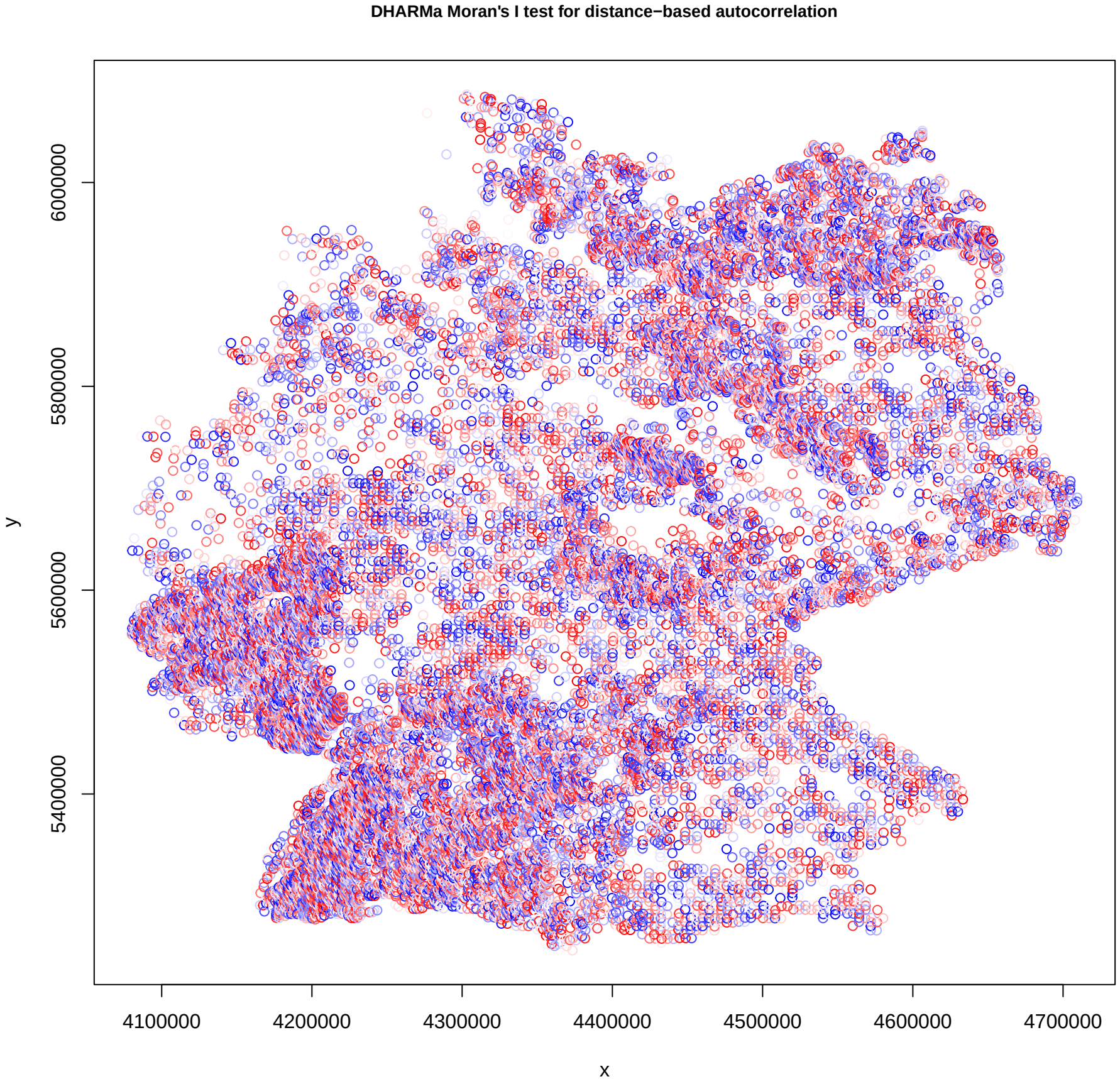
DHARMa Moran's I test for distance−based autocorrelation
y
6000000
5800000
5600000
5400000
4100000
4200000
4300000
4400000
4500000
4600000
4700000
x

DHARMa residual

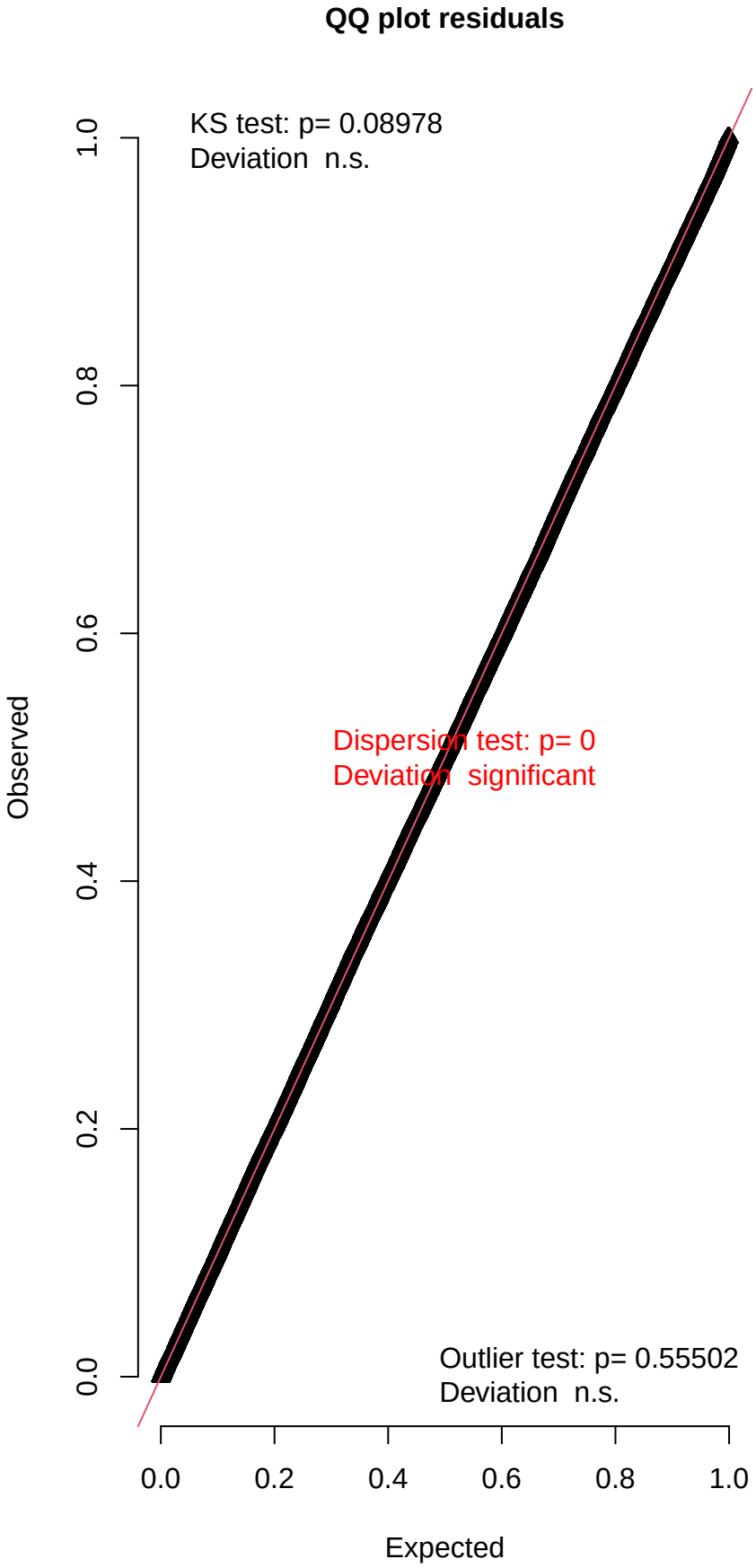


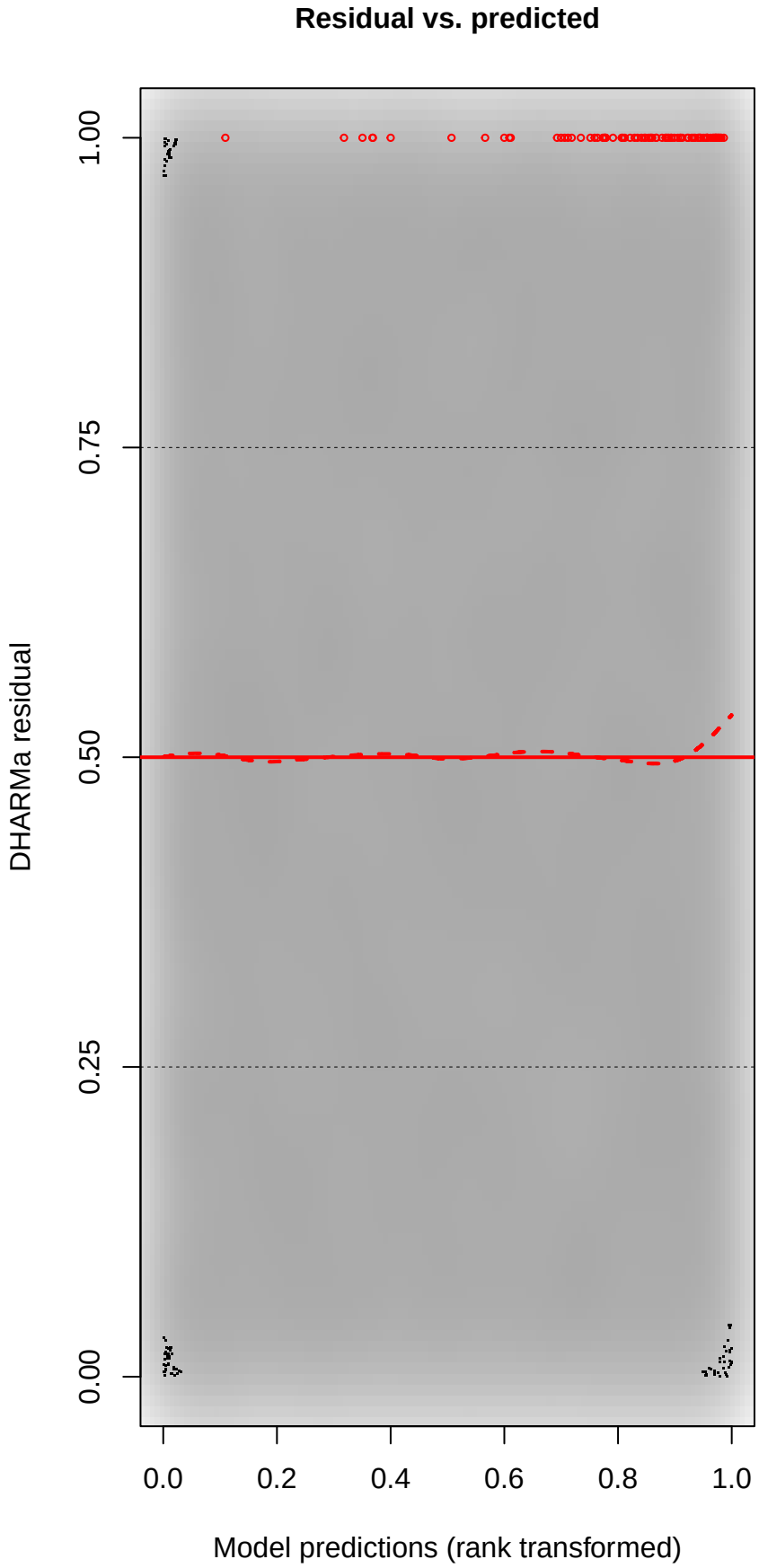

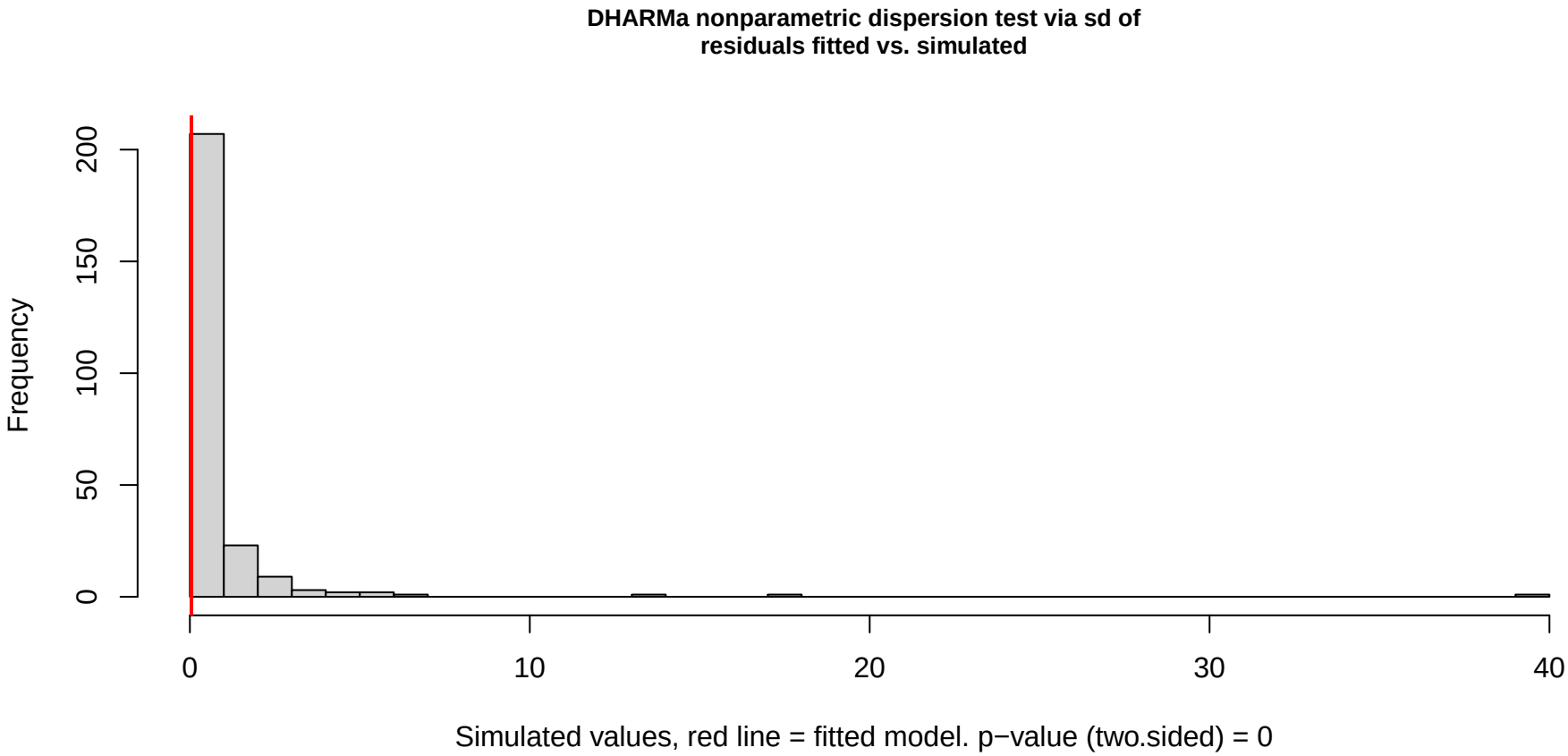
DHARMa nonparametric dispersion test via sd of residuals fitted vs. simulated
Frequency
0
50
100
150
200
0
10
20
30
40
Simulated values, red line = fitted model. p−value (two.sided) = 0

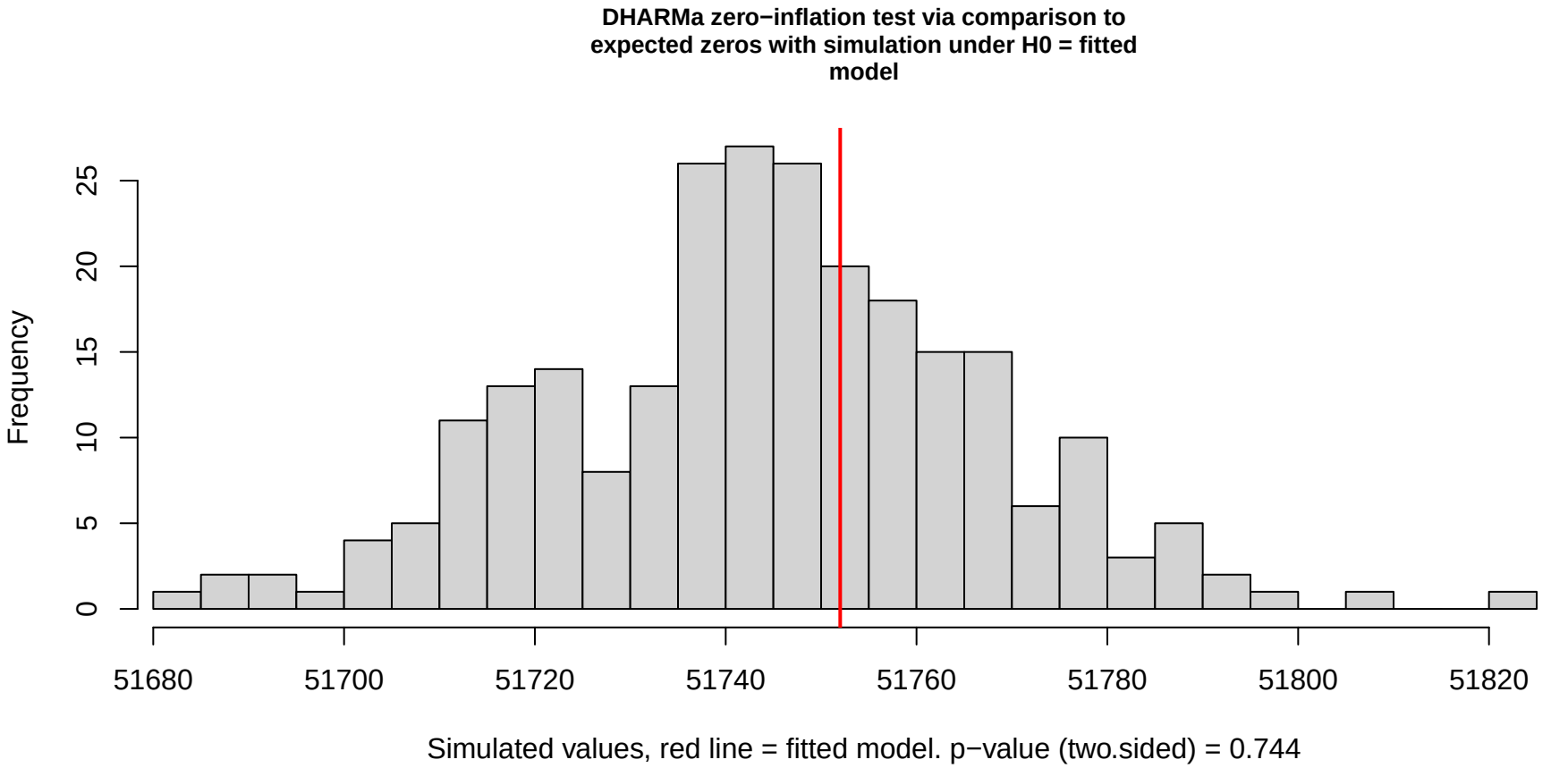
DHARMa zero−inflation test via comparison to expected zeros with simulation under H0 = fitted model
Frequency
0
5
10
15
20
25
51680
51700
51720
51740
51760
51780
51800
51820
Simulated values, red line = fitted model. p−value (two.sided) = 0.744

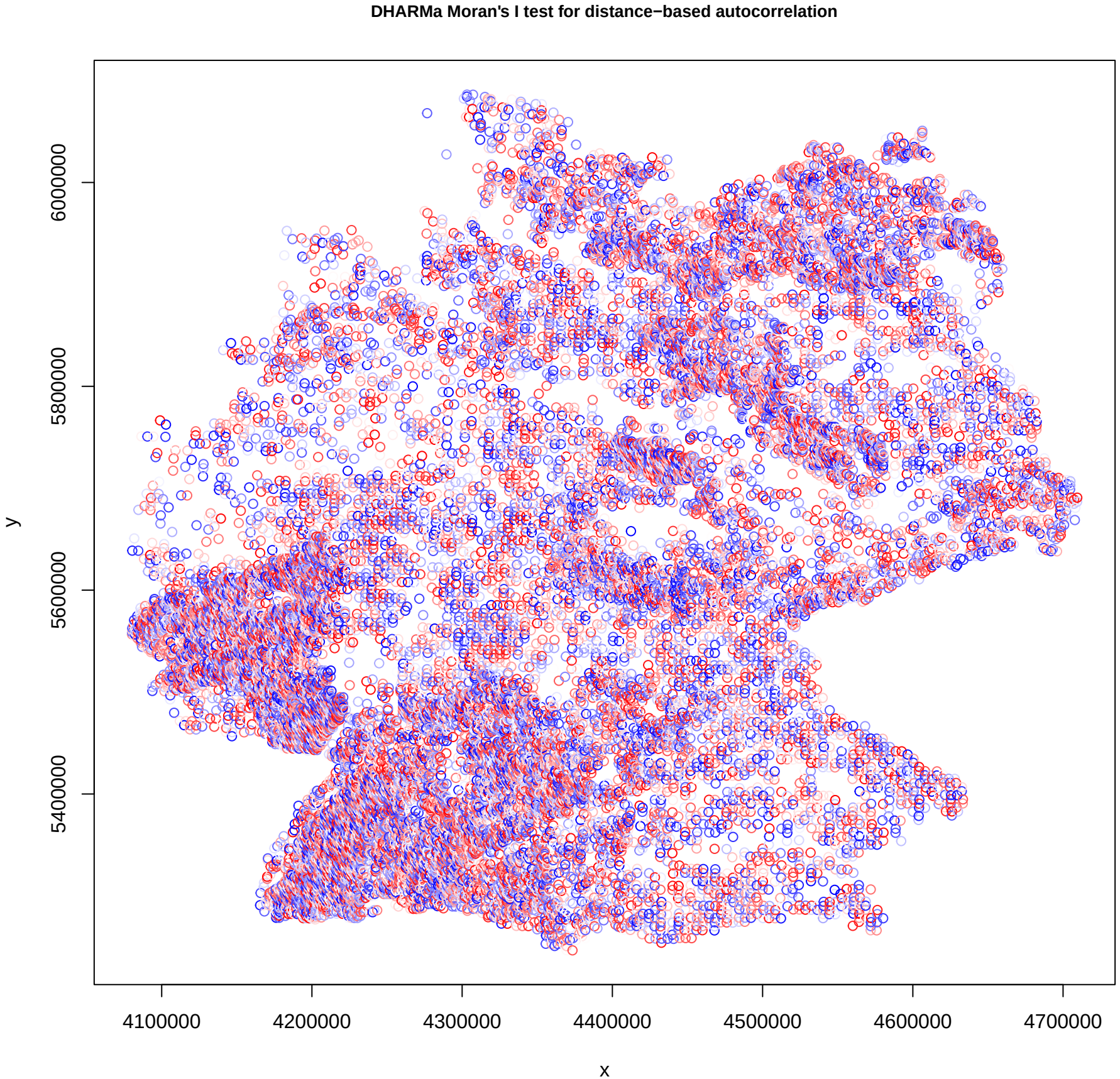
DHARMa Moran's I test for distance−based autocorrelation
y
6000000
5800000
5600000
5400000
4100000
4200000
4300000
4400000
4500000
4600000
4700000
x

DHARMa residual

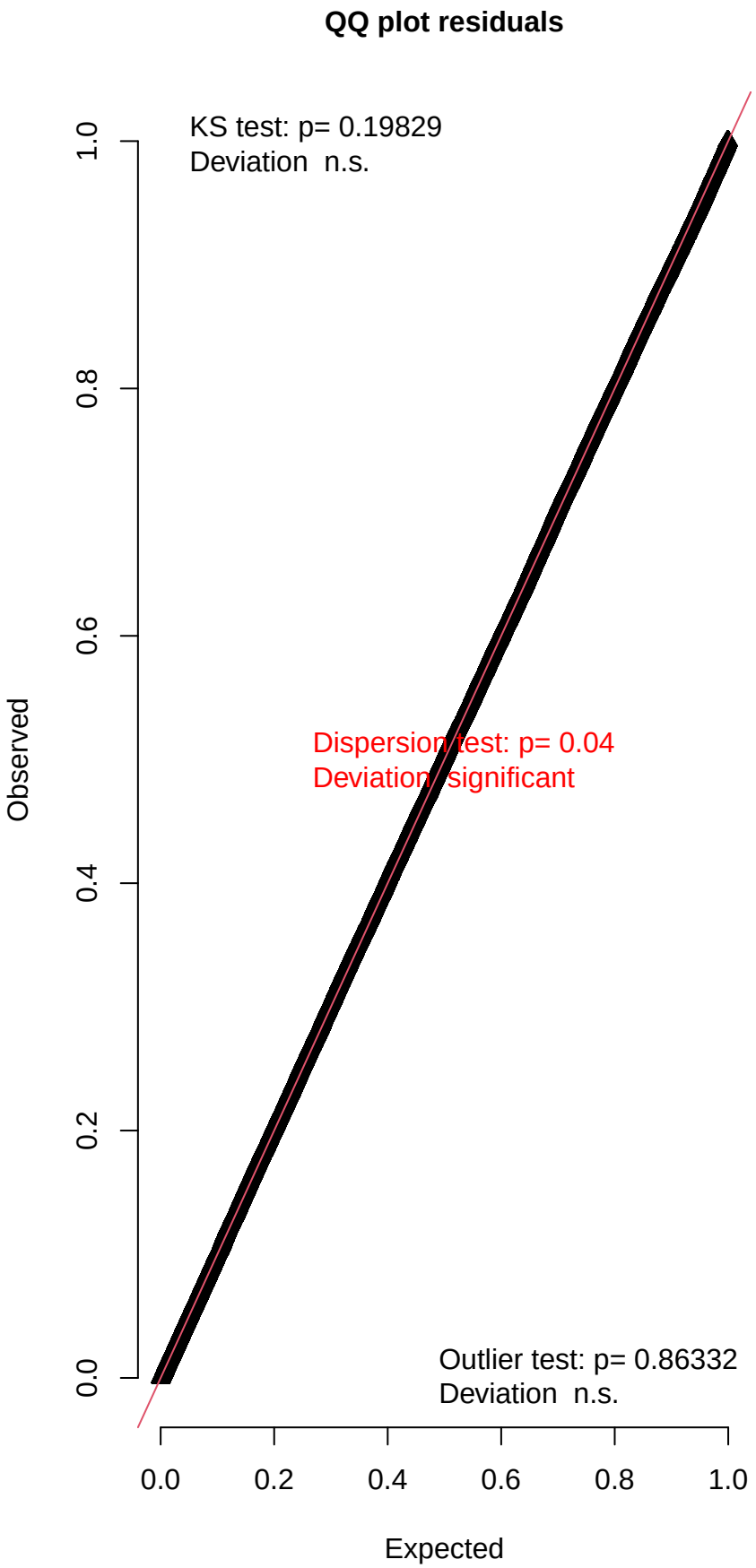


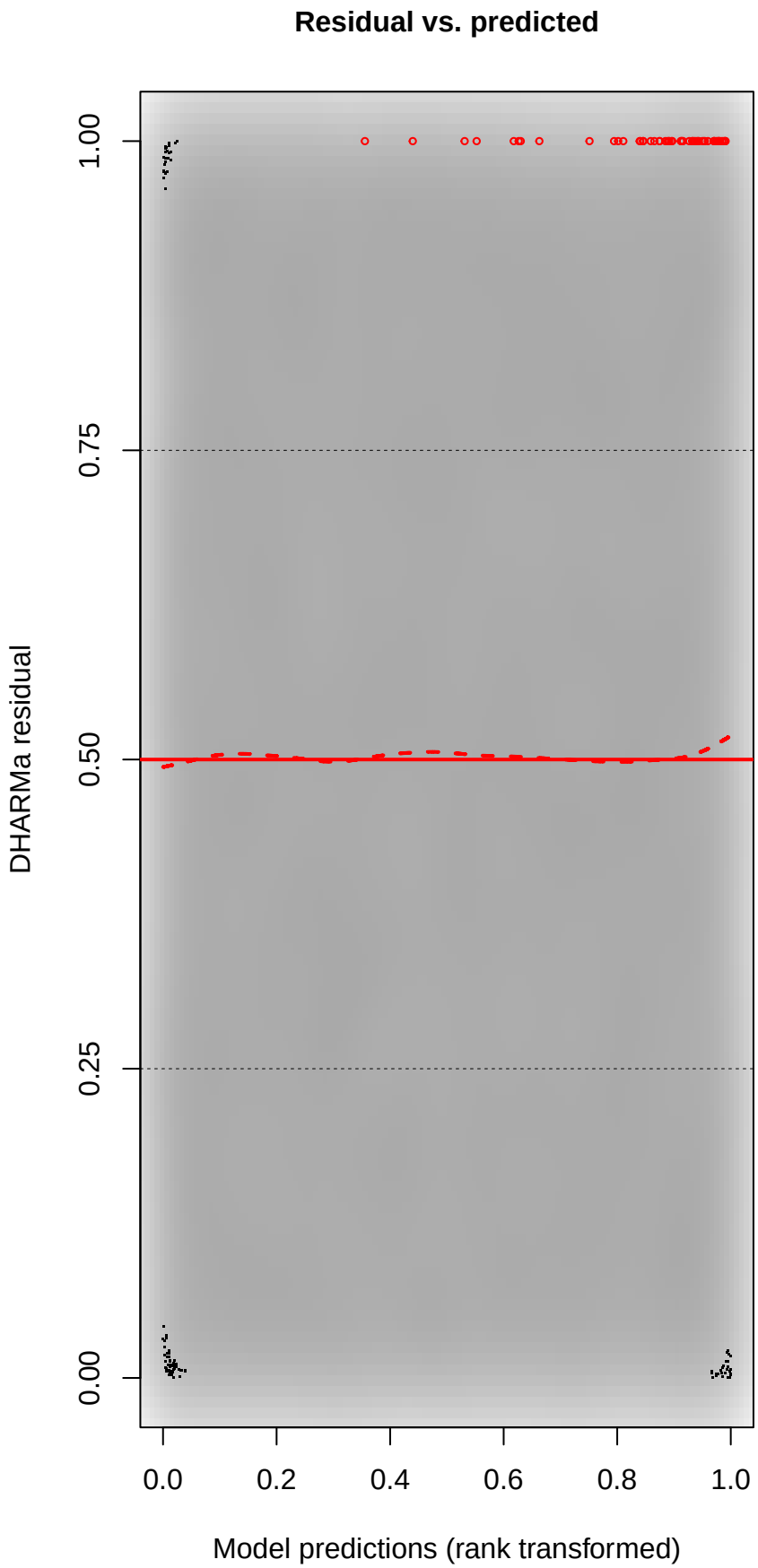

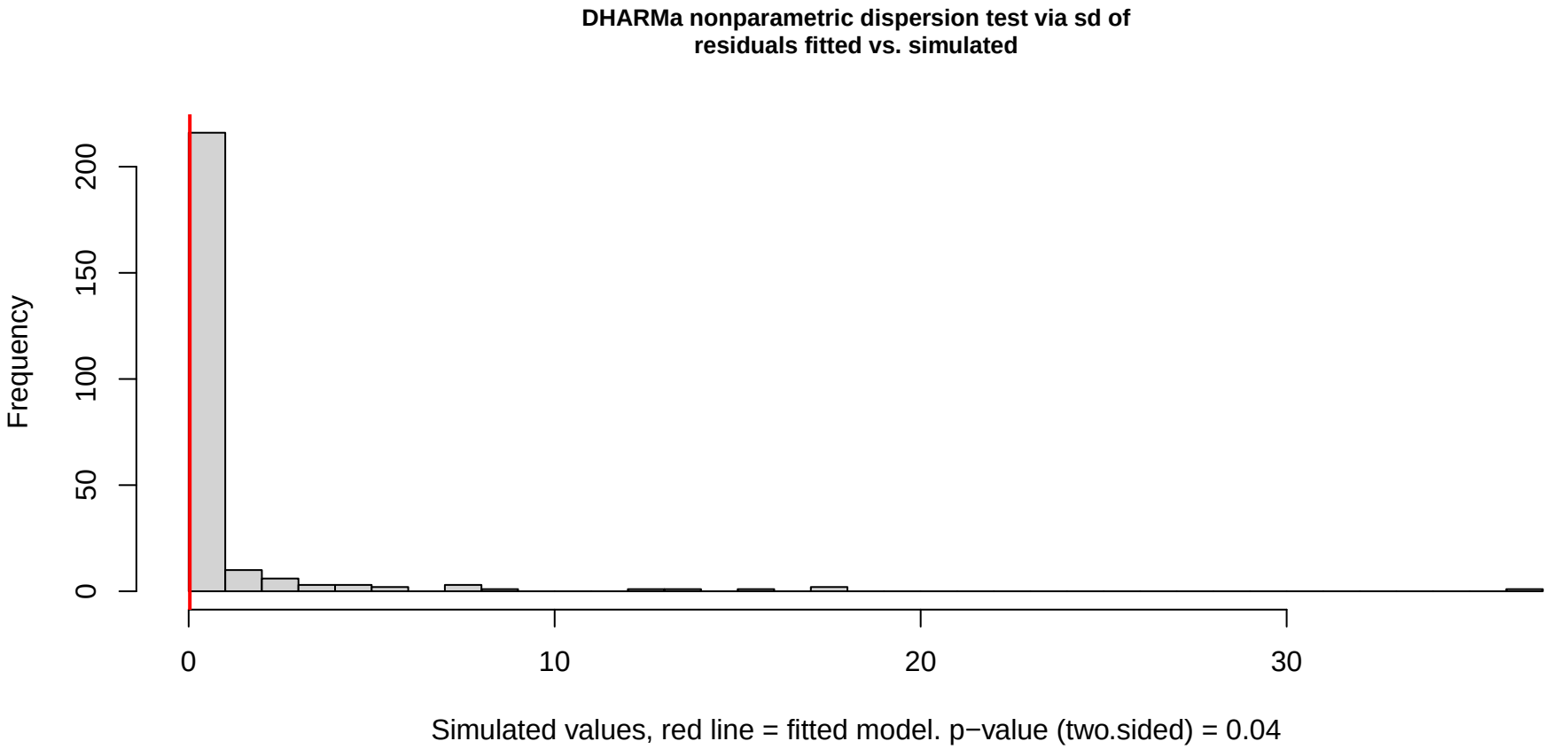
DHARMa nonparametric dispersion test via sd of residuals fitted vs. simulated
Frequency
0
50
100
150
200
0
10
20
30
Simulated values, red line = fitted model. p−value (two.sided) = 0.04

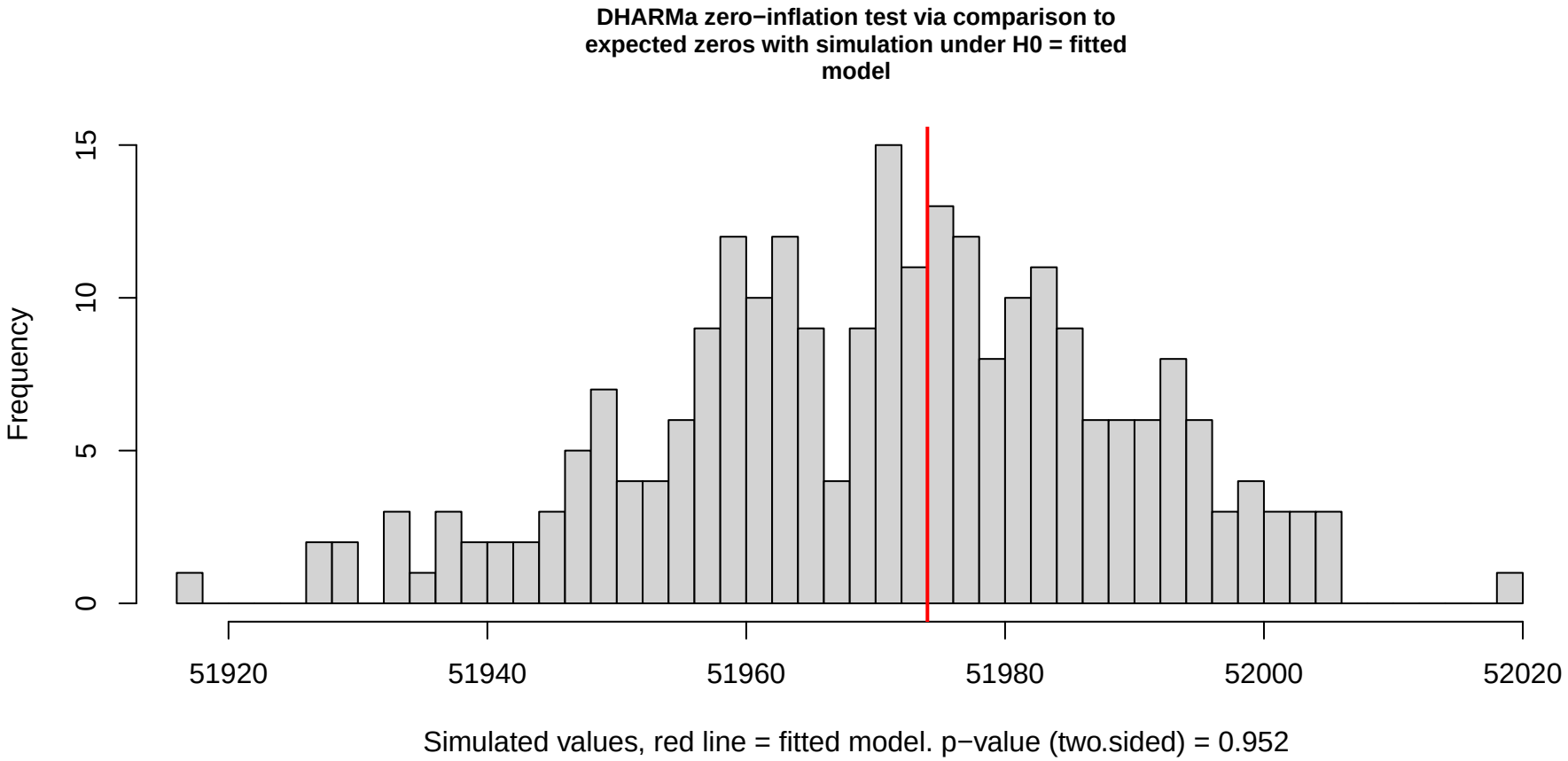
DHARMa zero−inflation test via comparison to expected zeros with simulation under H0 = fitted model
Frequency
0
5
10
15
51920
51940
51960
51980
52000
52020
Simulated values, red line = fitted model. p−value (two.sided) = 0.952

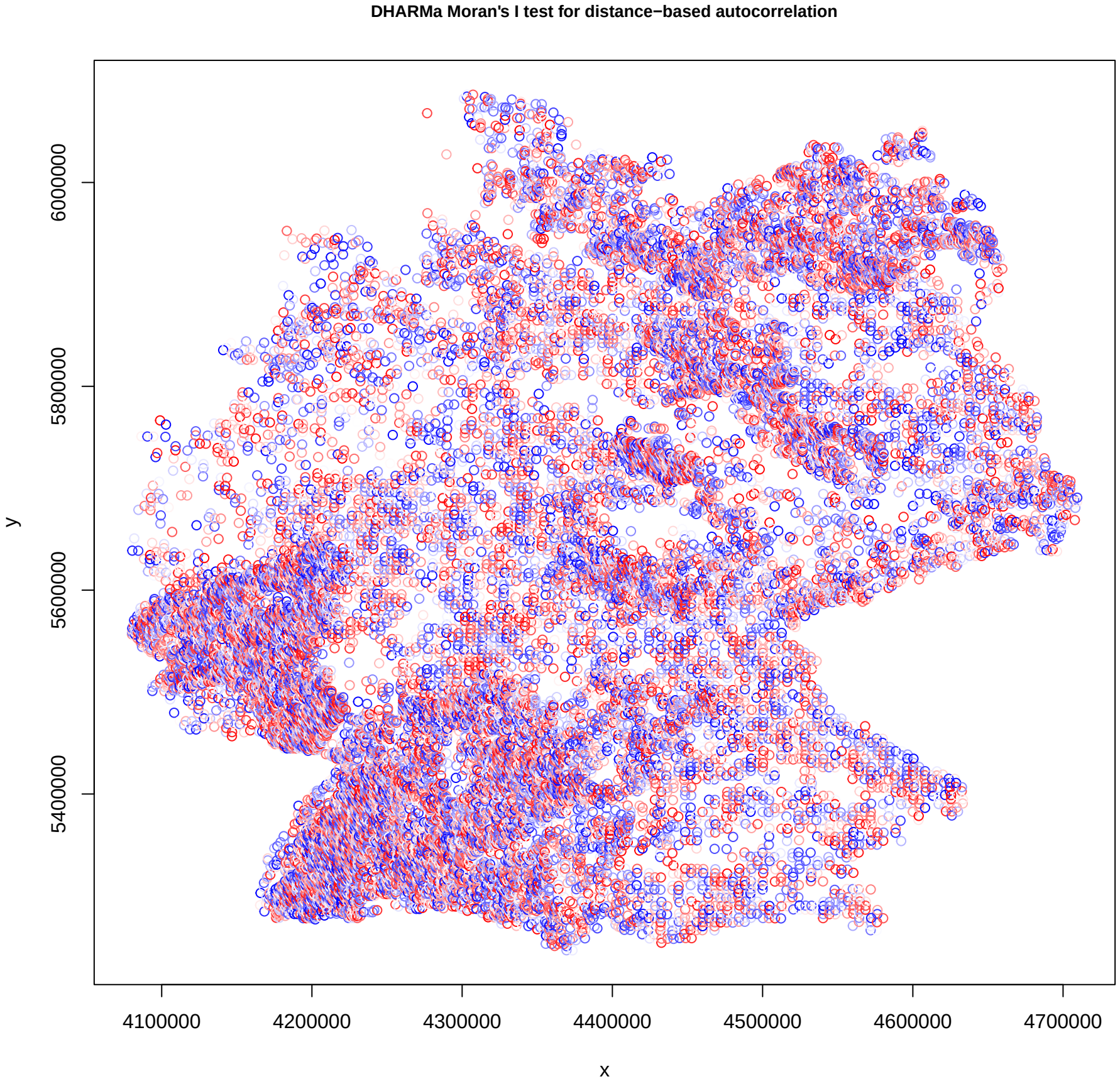
DHARMa Moran's I test for distance−based autocorrelation
y
6000000
5800000
5600000
5400000
4100000
4200000
4300000
4400000
4500000
4600000
4700000
x

*Robinia pseudoacacia*

DHARMa residual

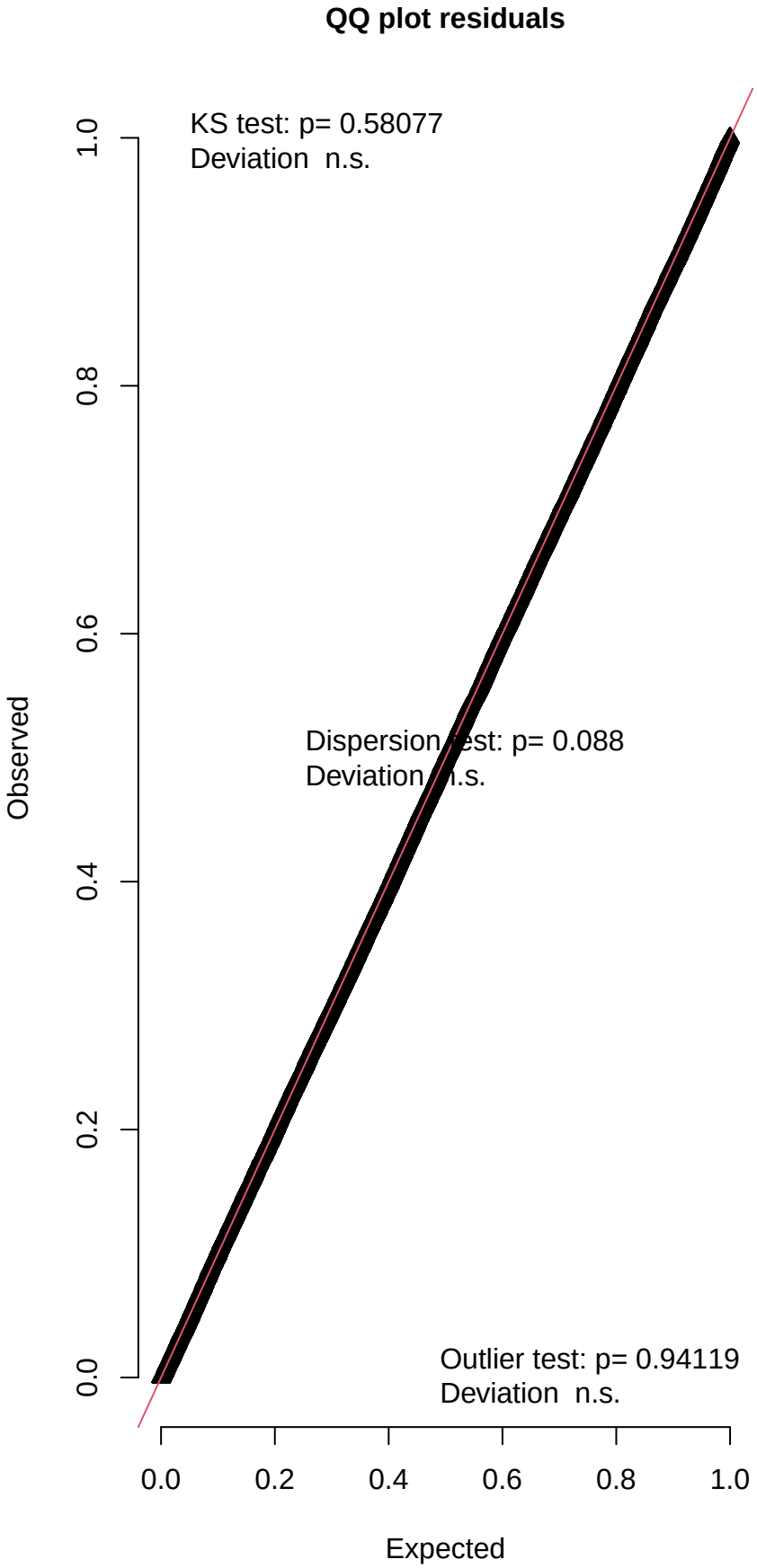


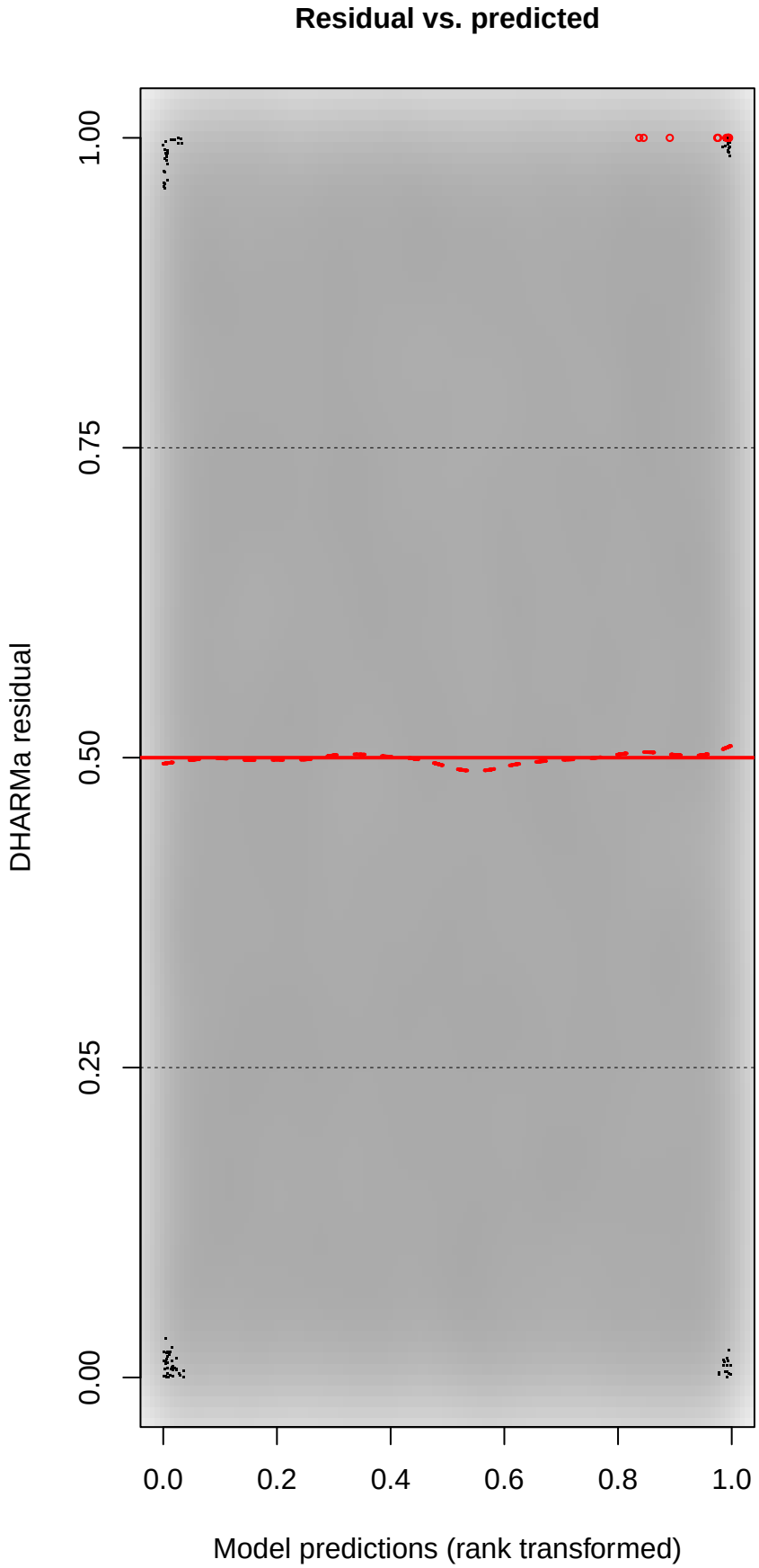

*Robinia pseudoacacia*

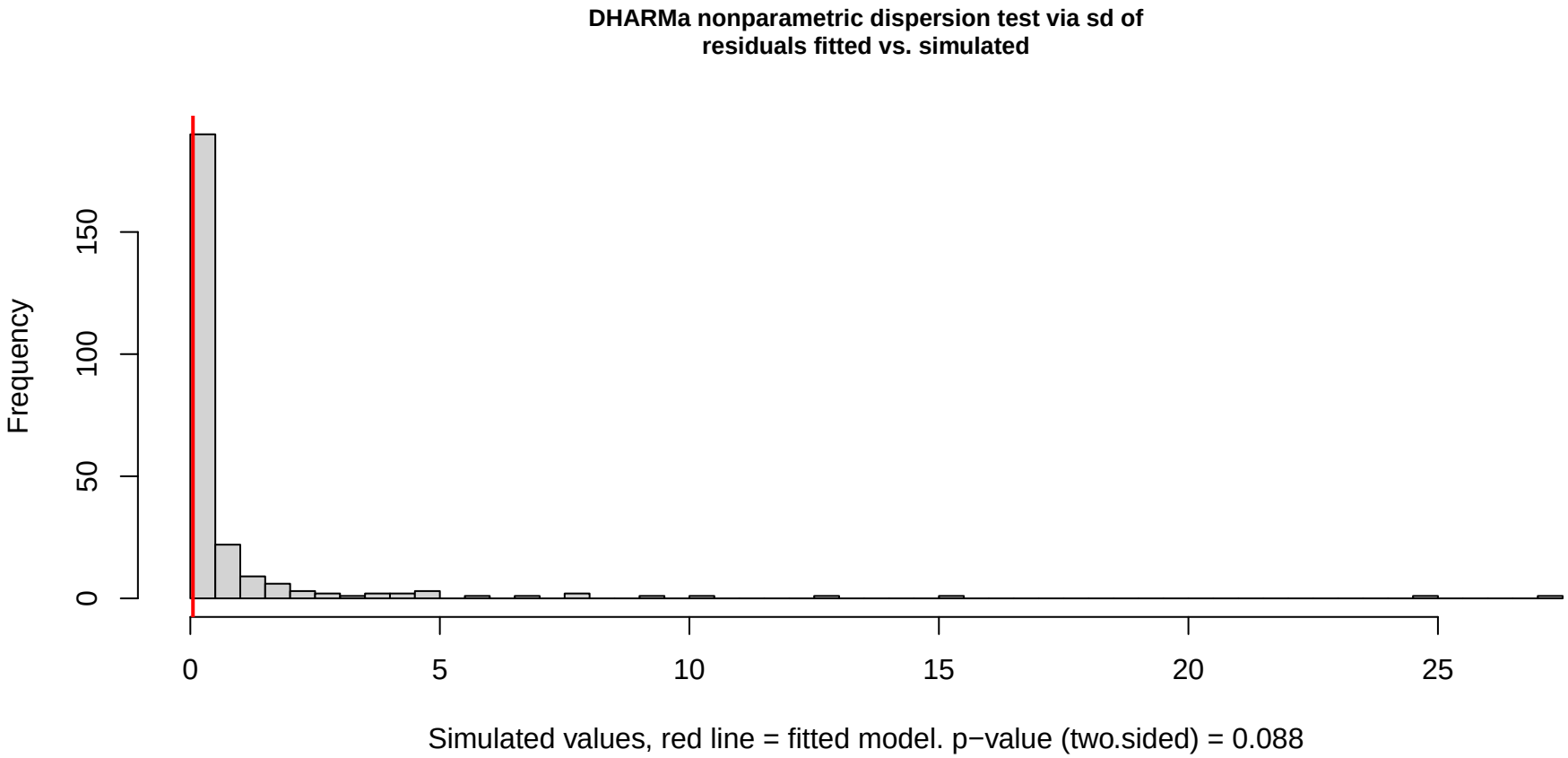


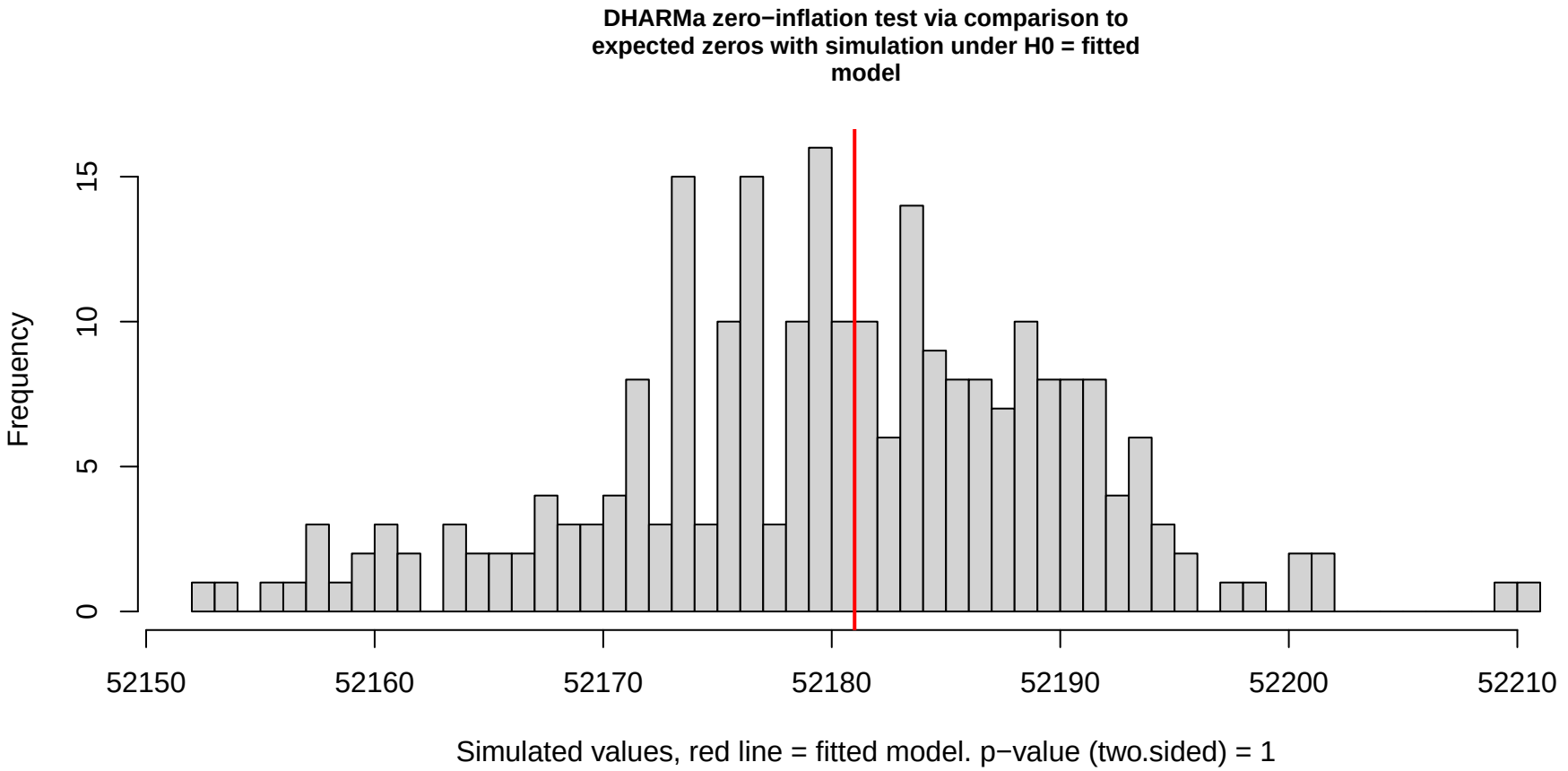

*Robinia pseudoacacia*

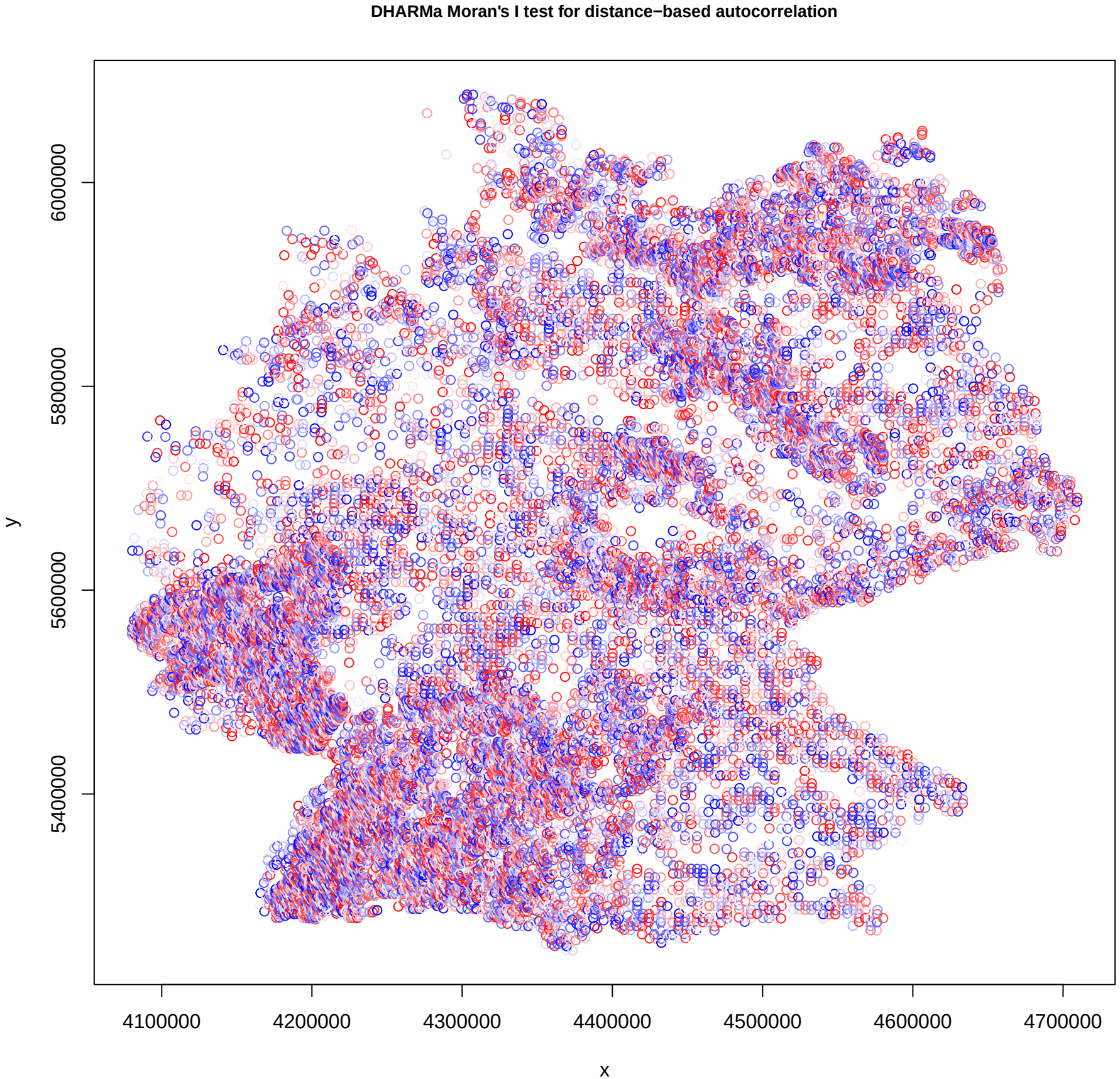

*Quercus petraea*

DHARMa residual

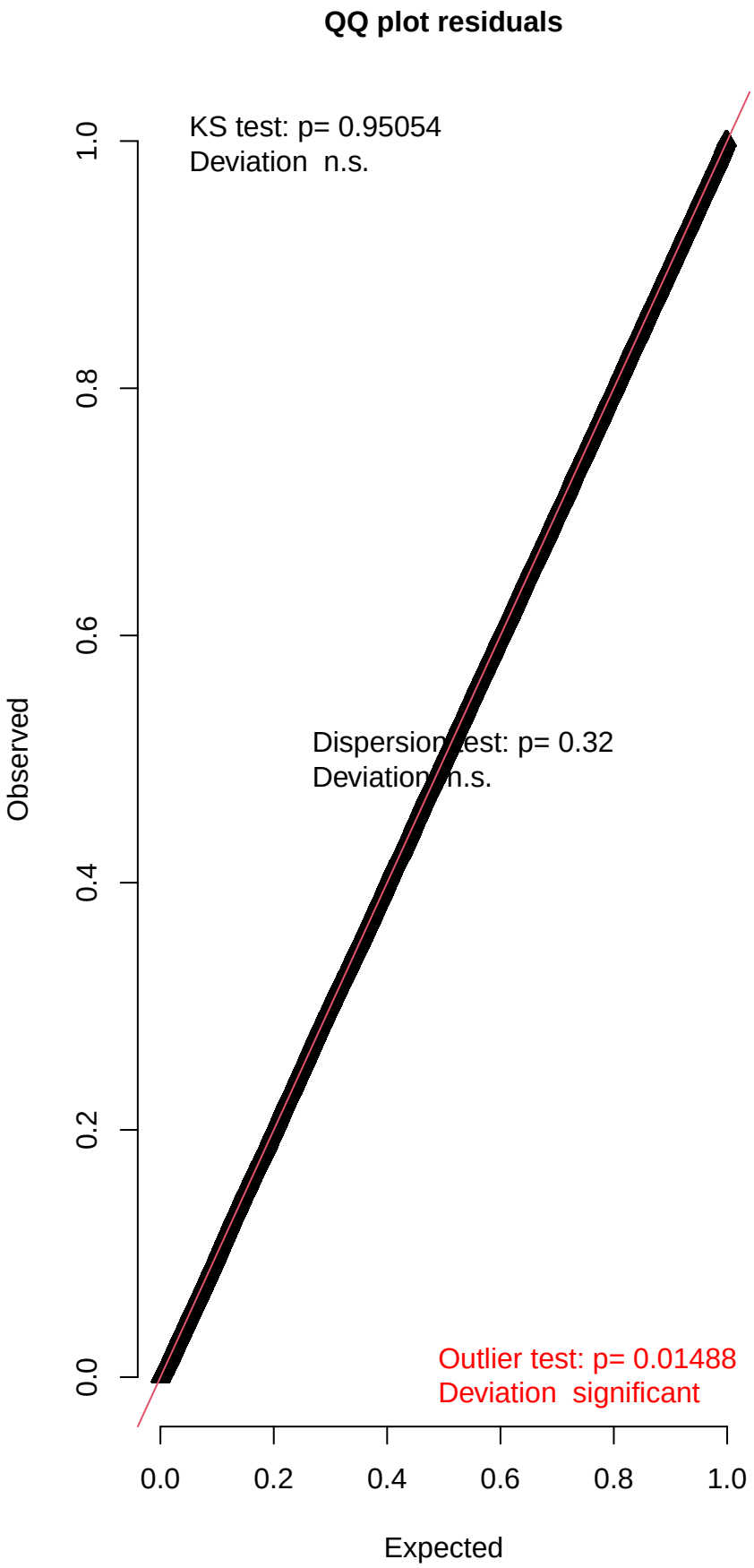


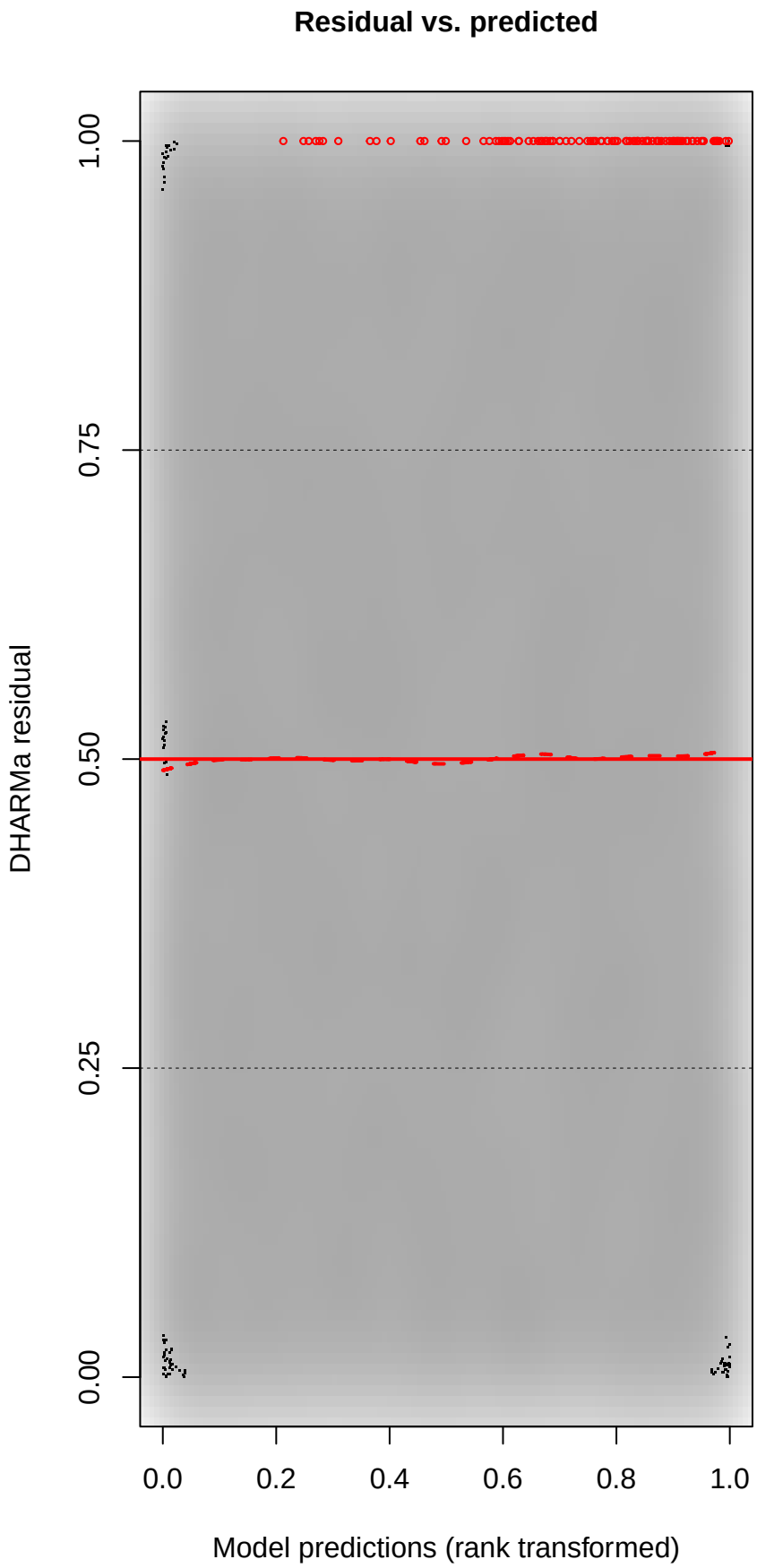

*Quercus petraea*

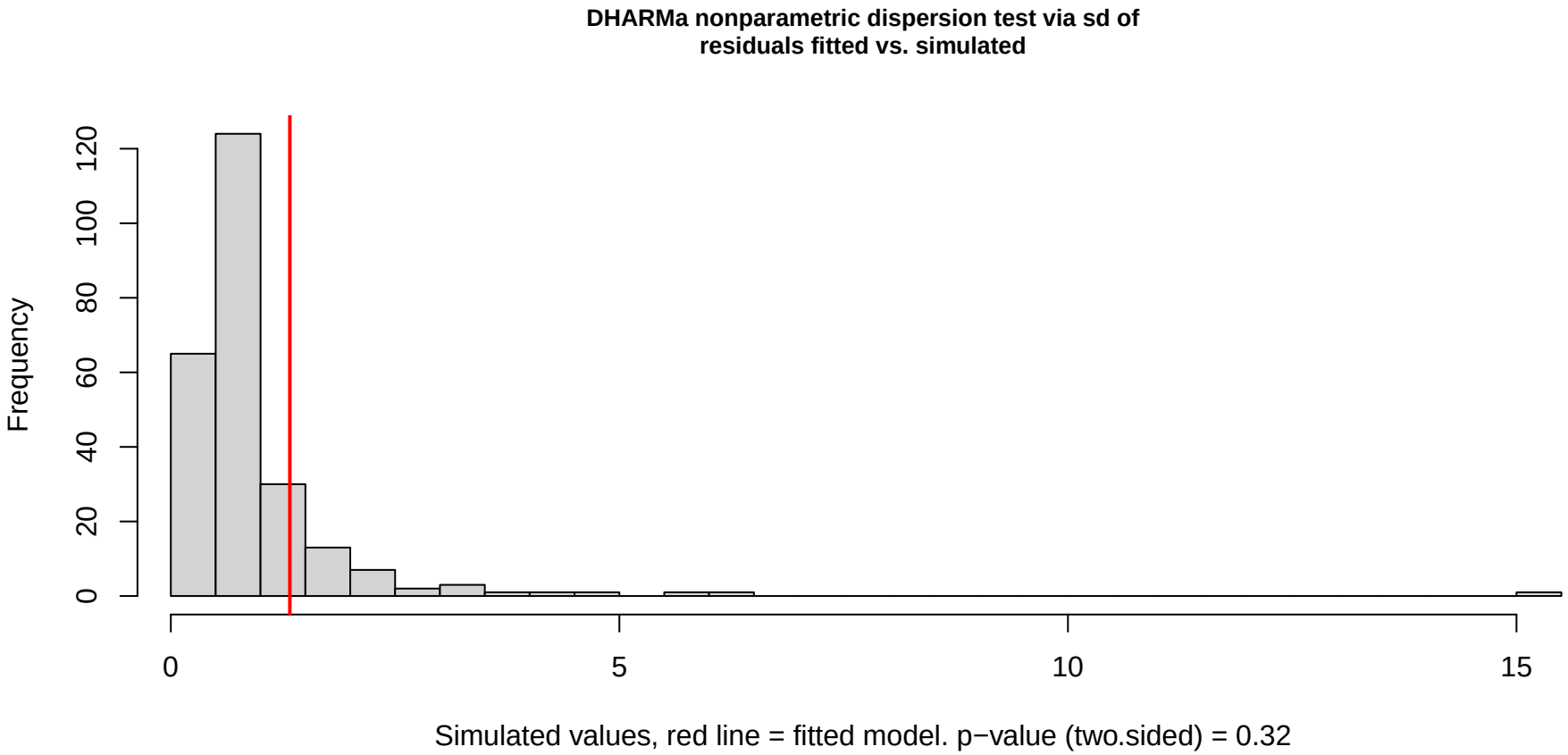


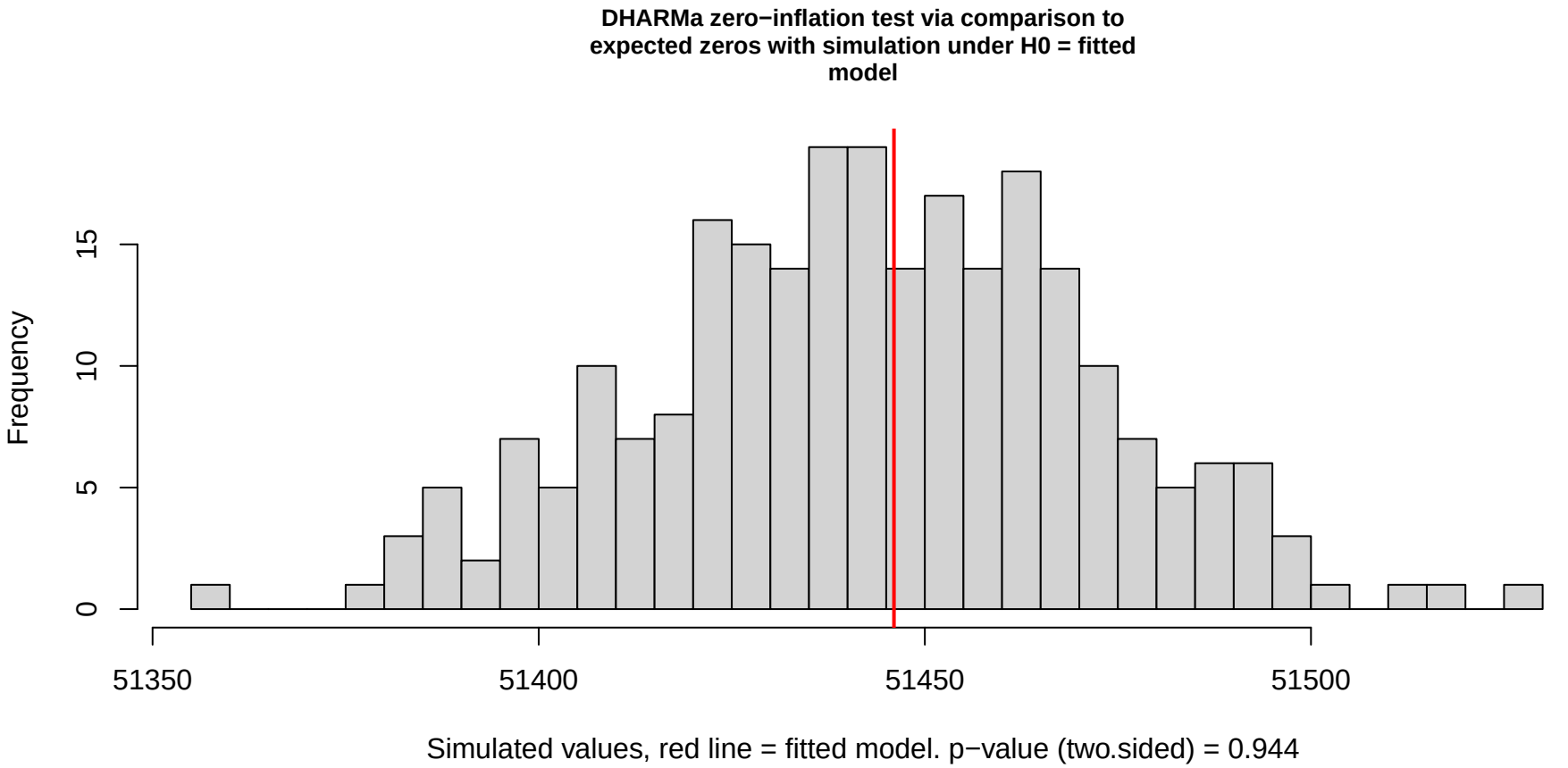

*Quercus petraea*

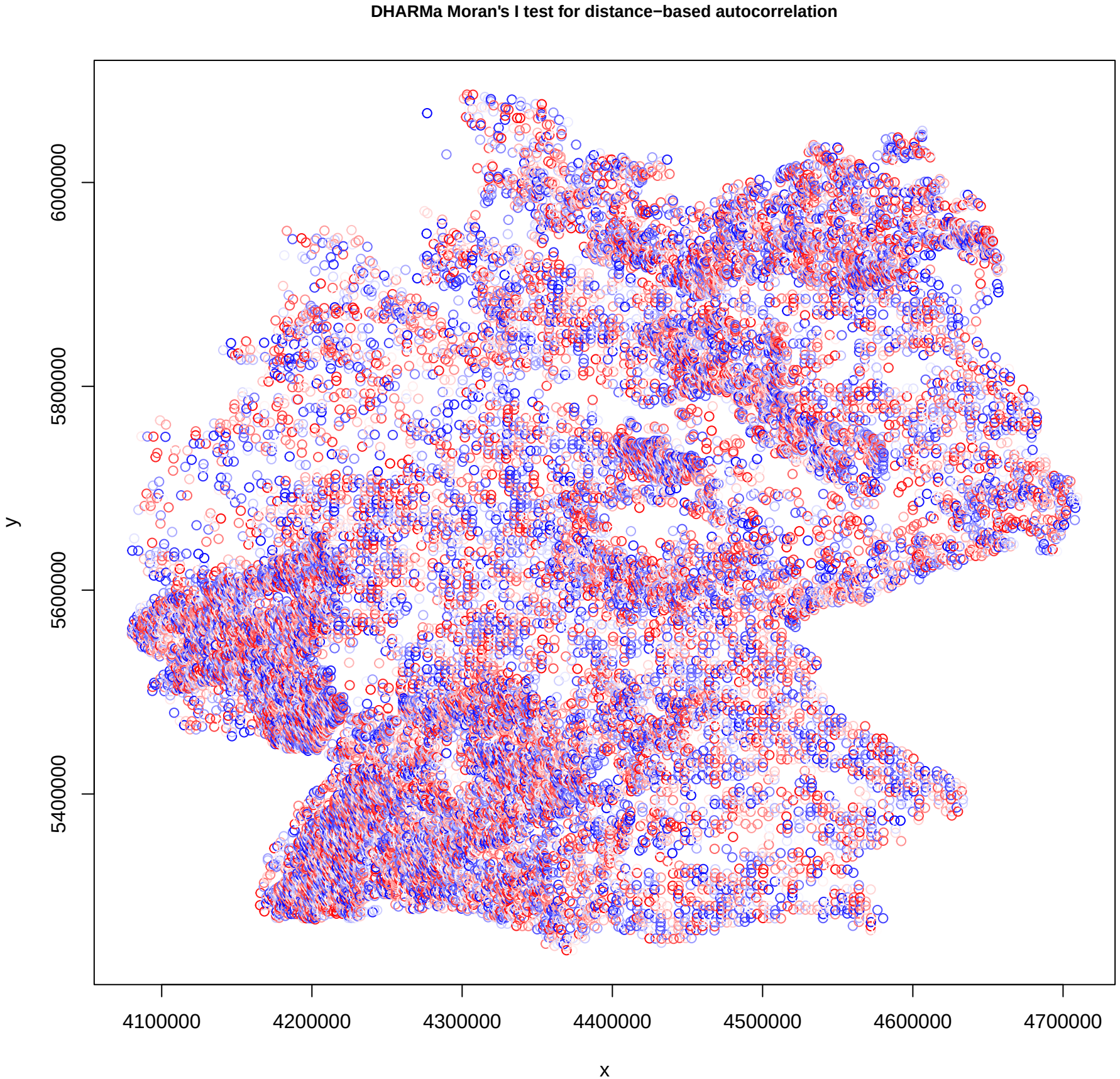

*Quercus robur*

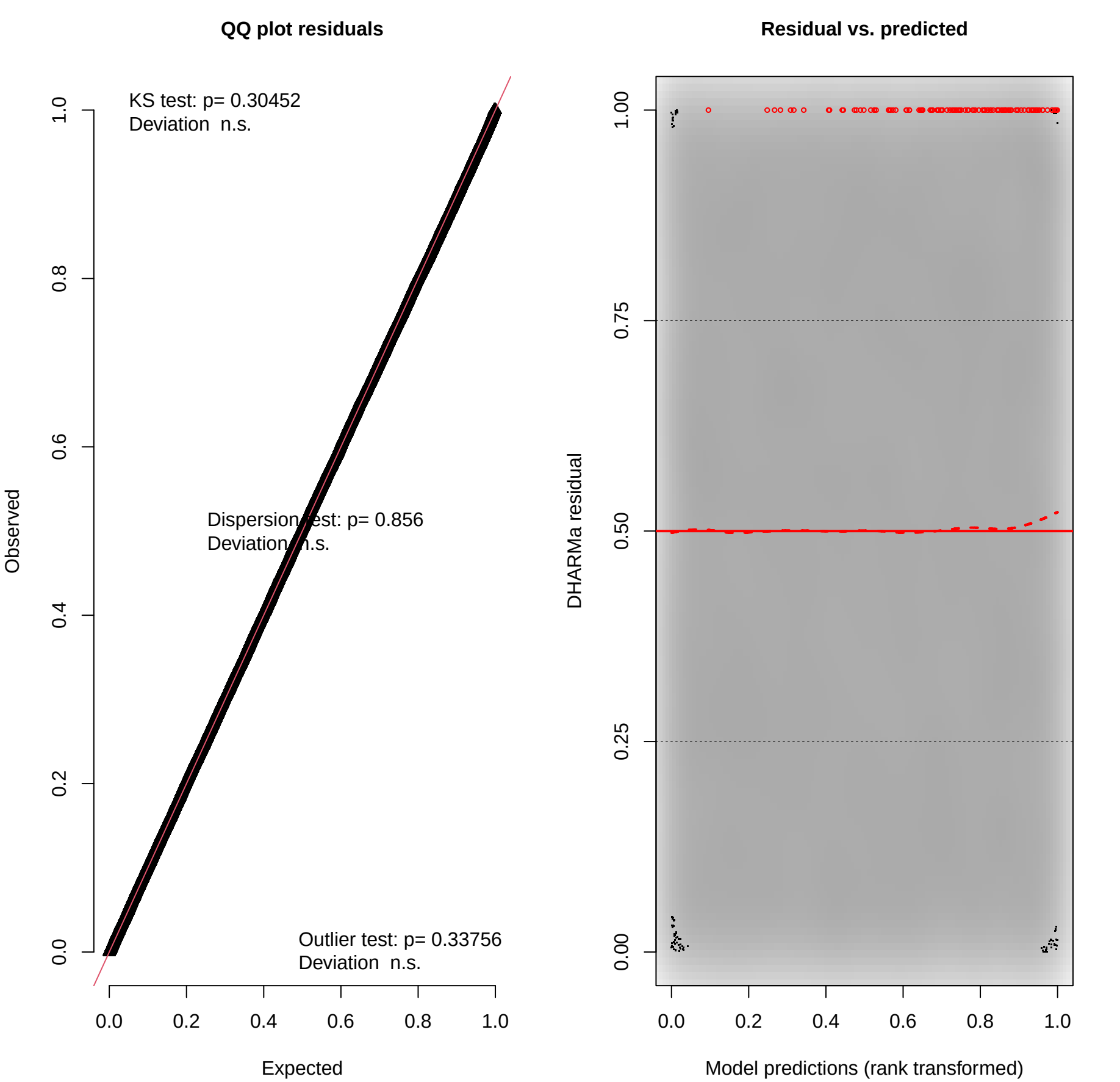

*Quercus robur*

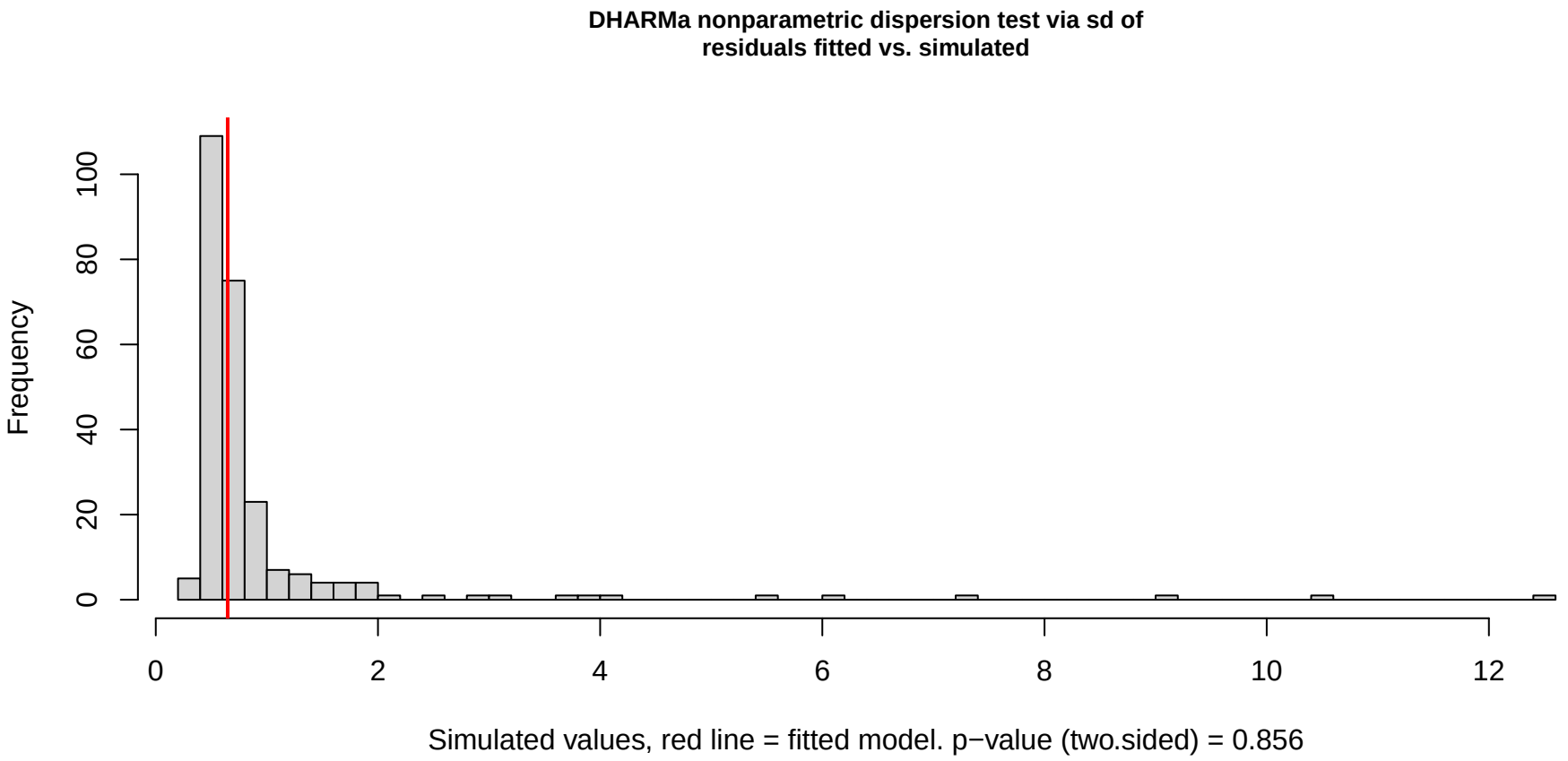


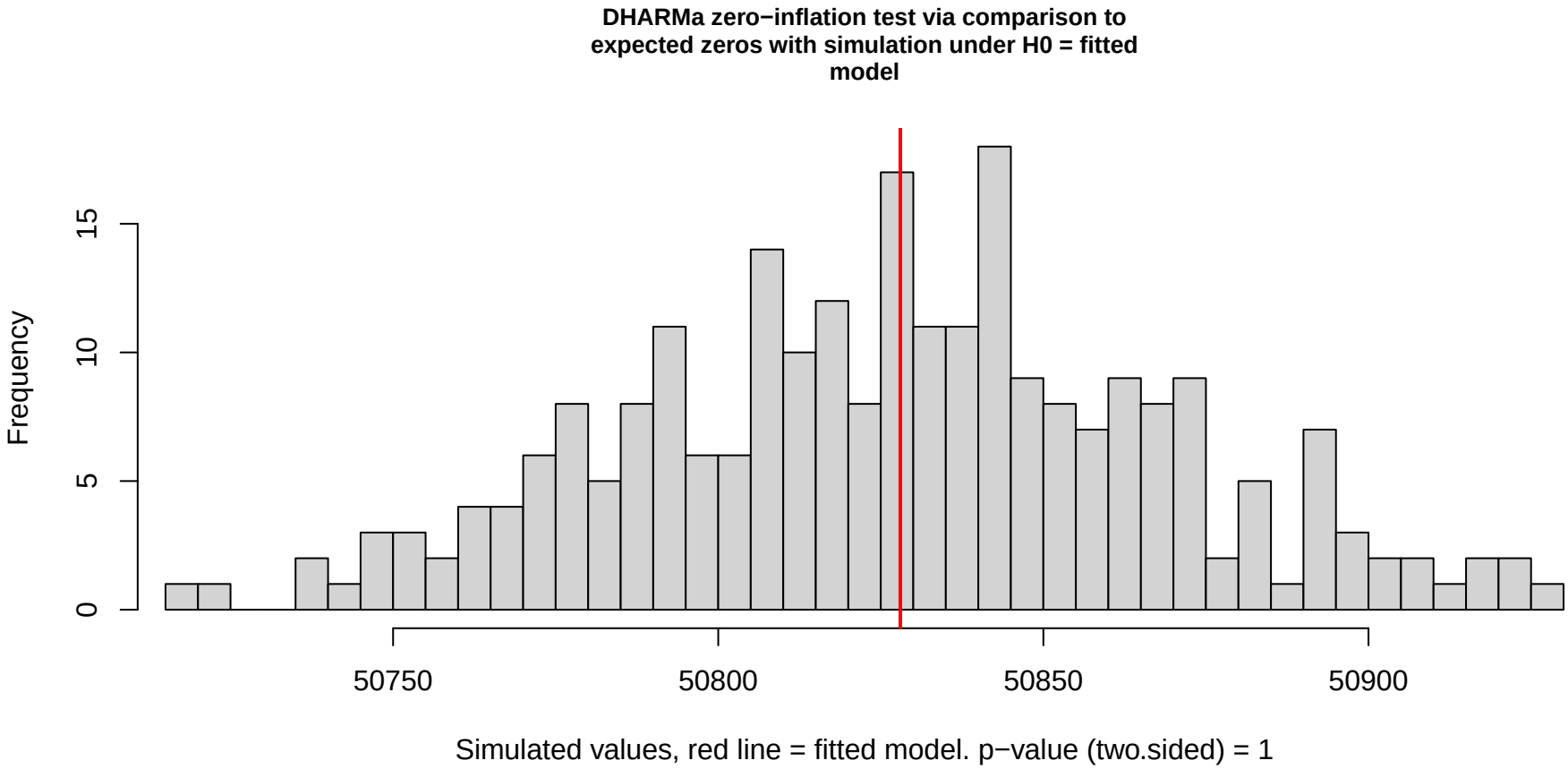

*Quercus robur*

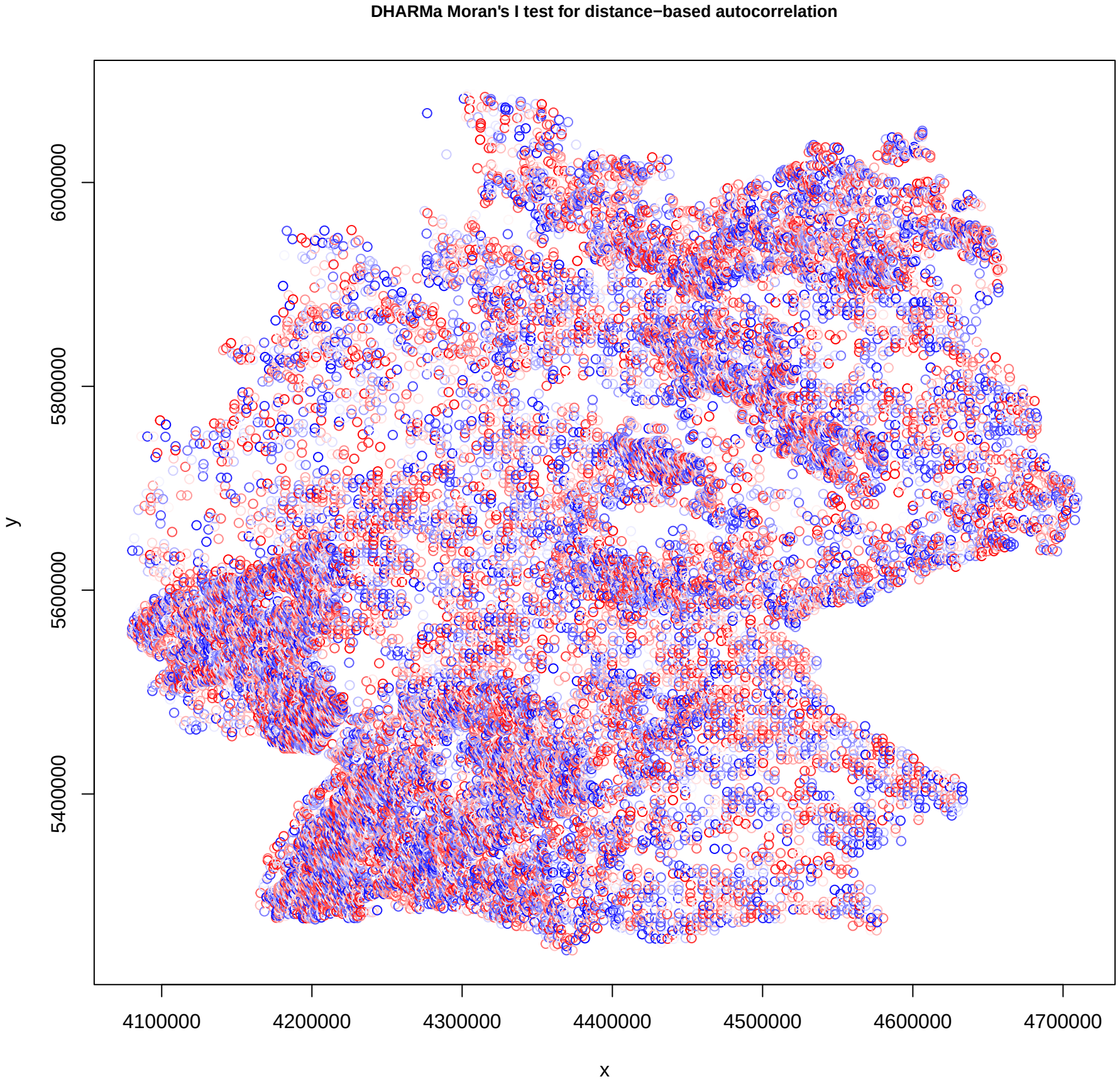

*Quercus rubra*

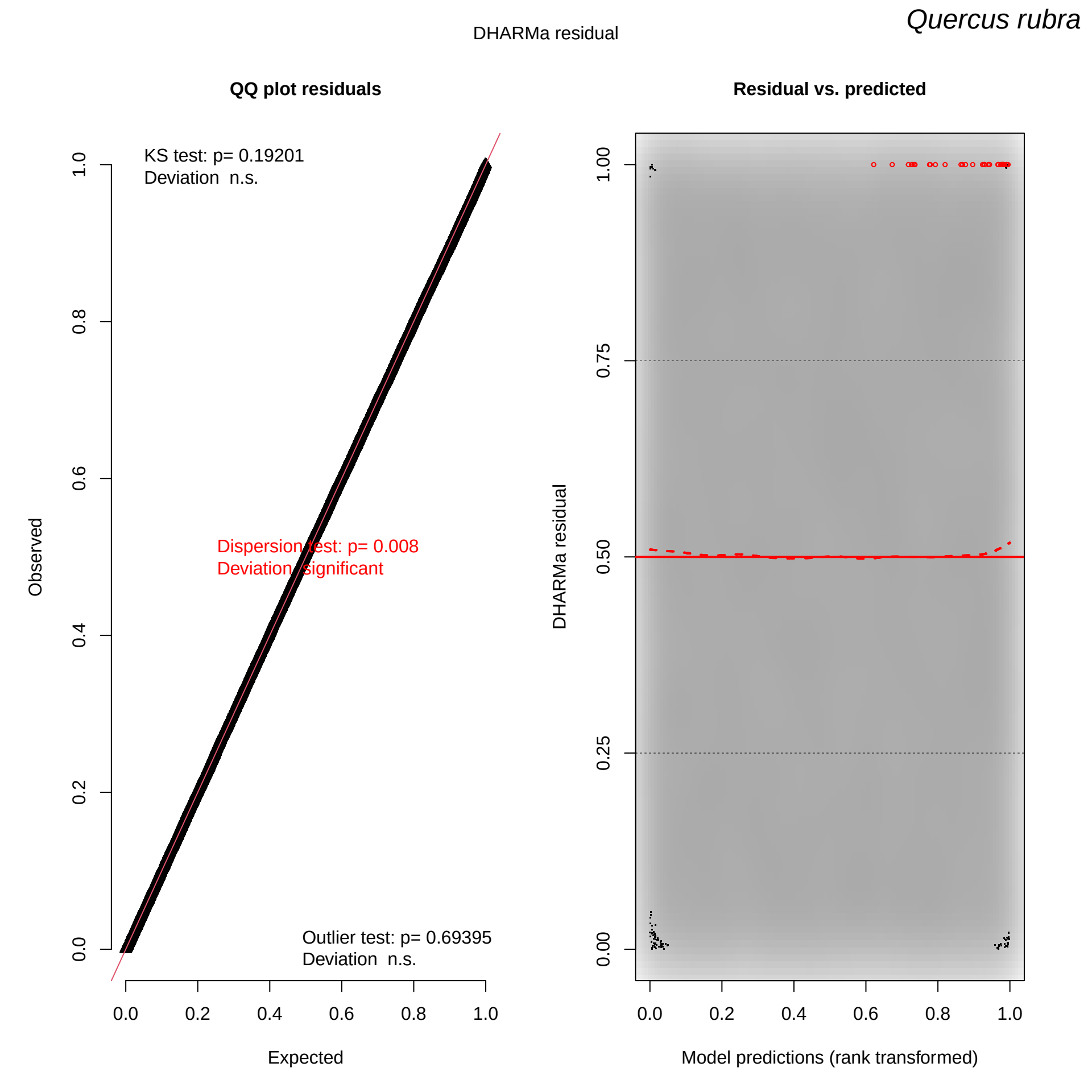

*Quercus rubra*

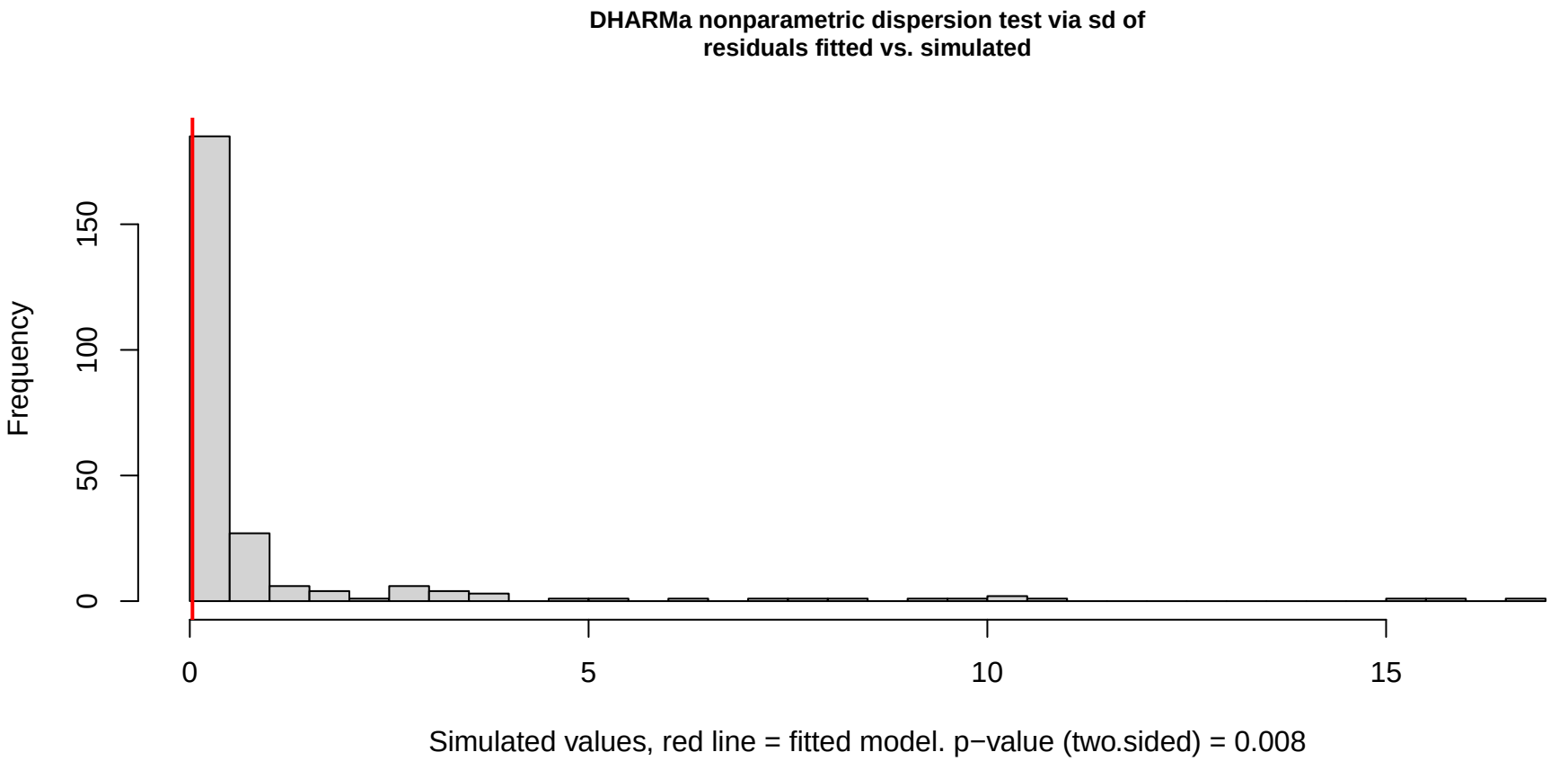


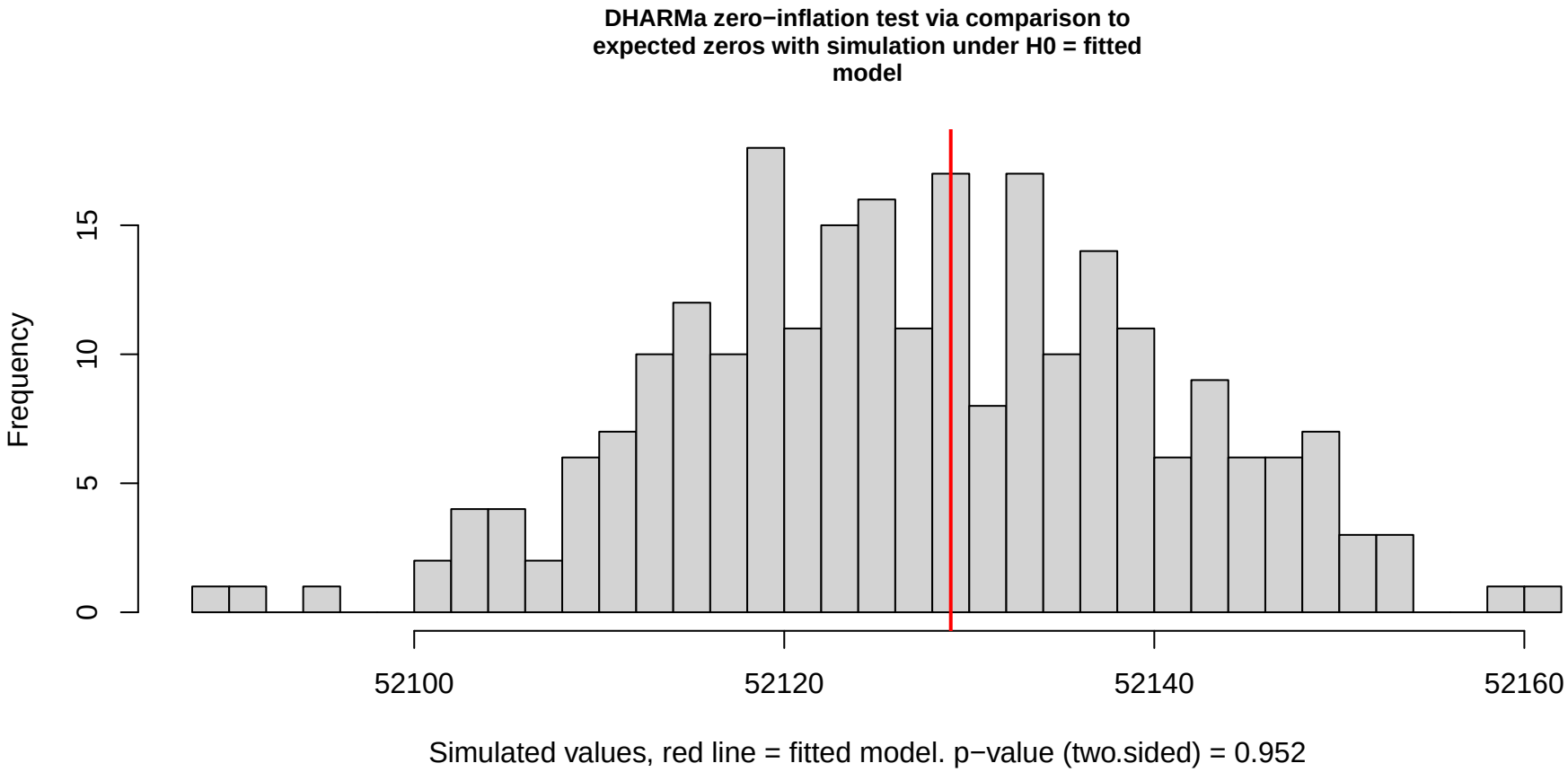

*Quercus rubra*

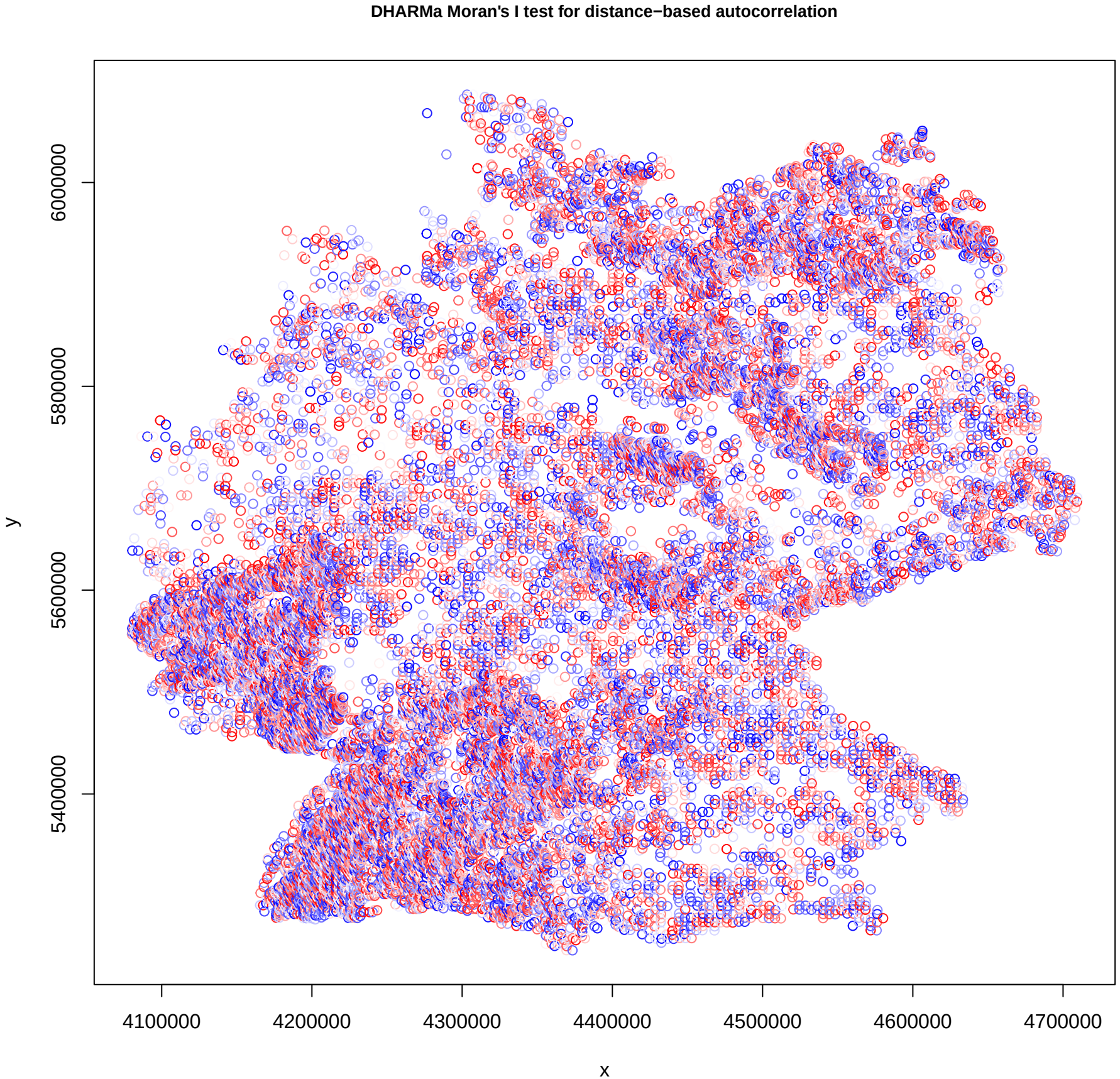

*Betula pendula*

DHARMa residual

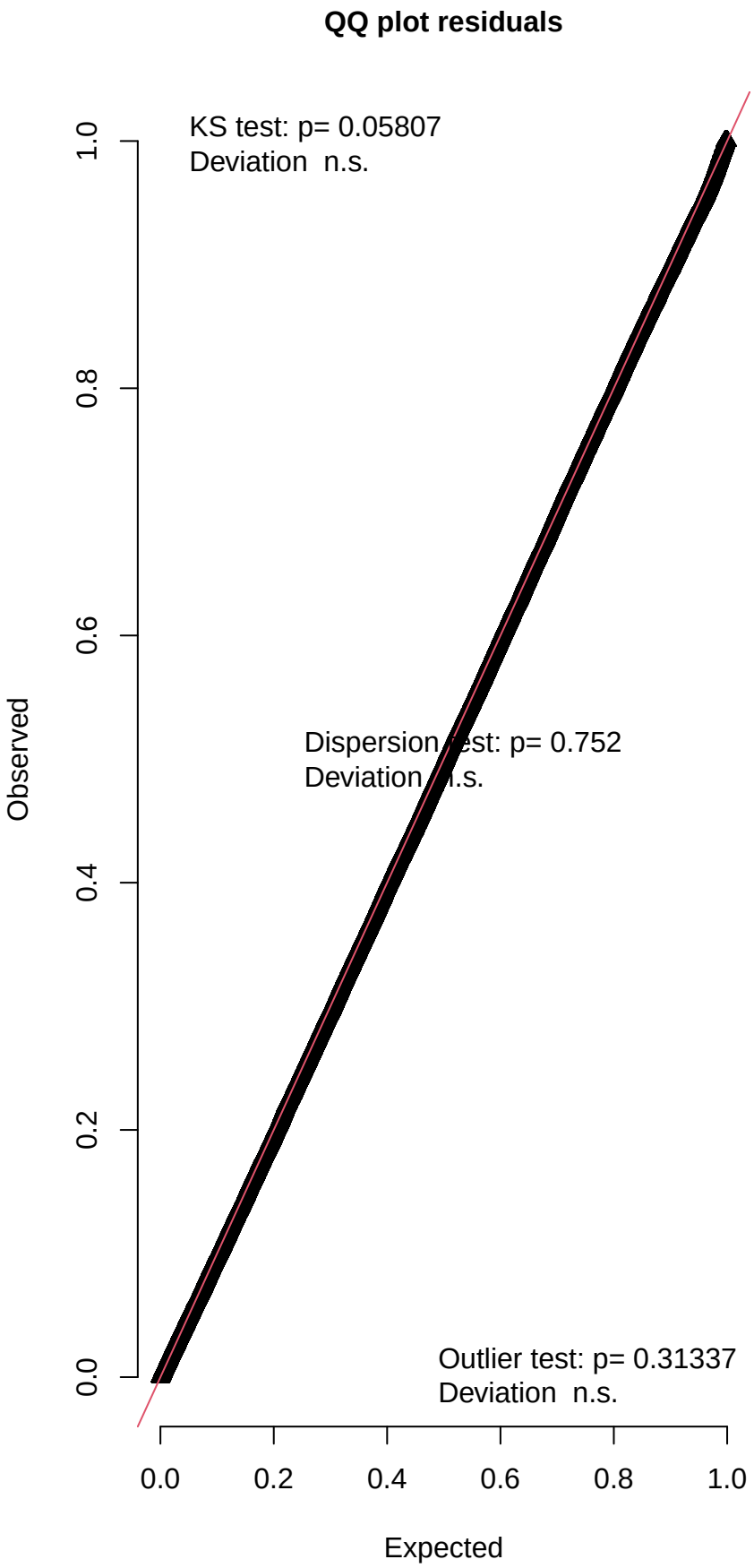


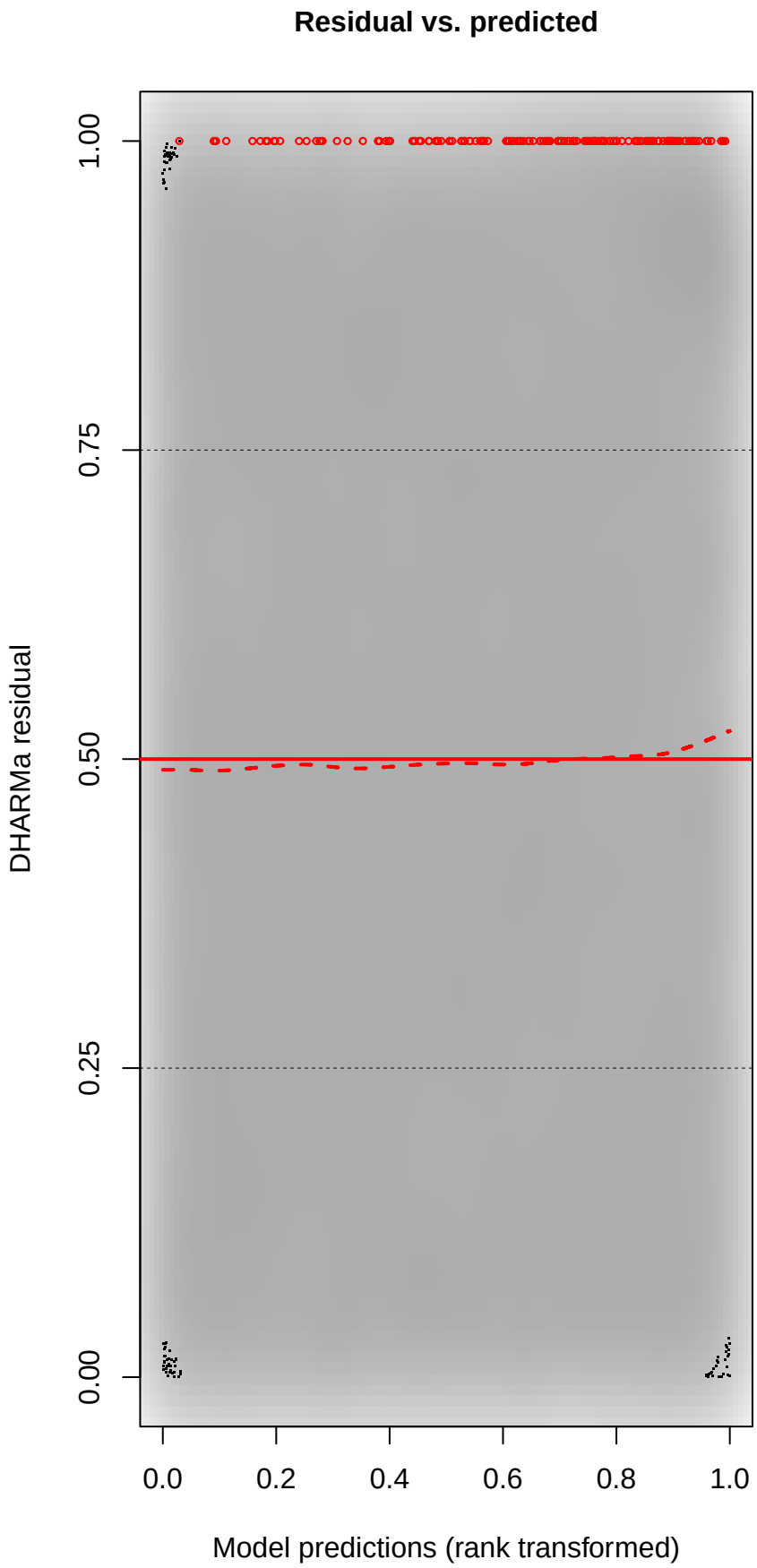

*Betula pendula*

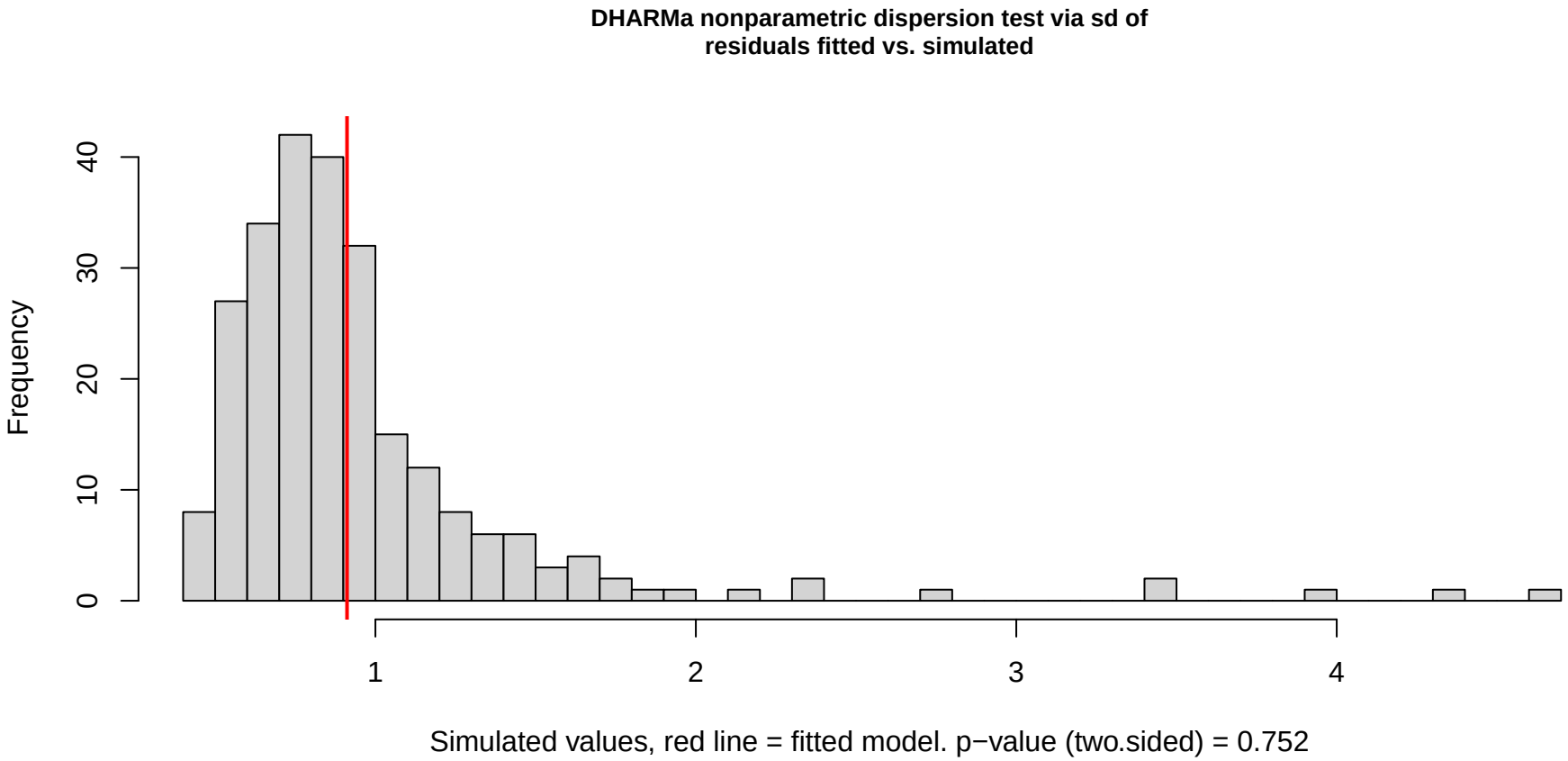


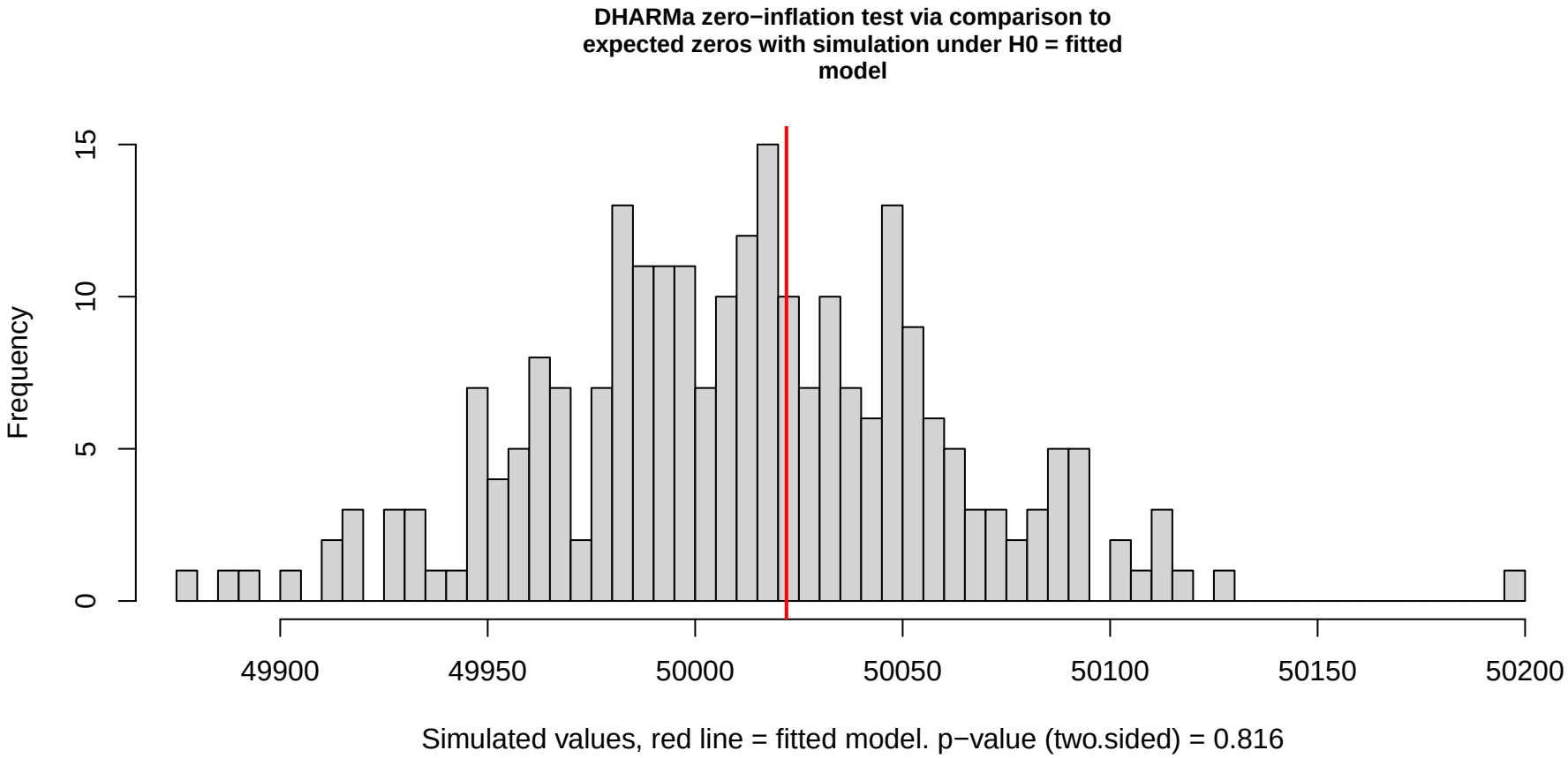

*Betula pendula*

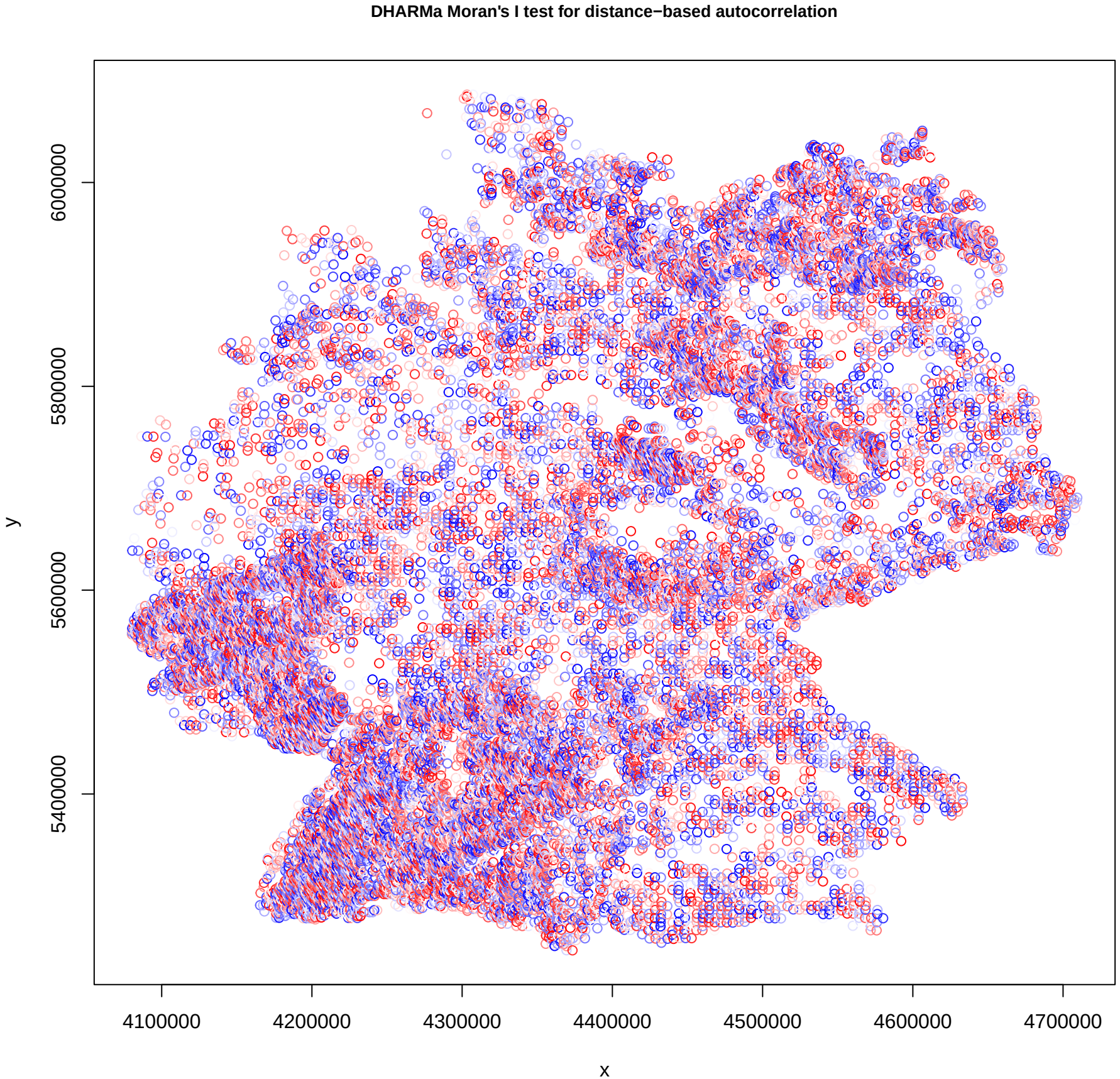

*Betula pubescens*

DHARMa residual

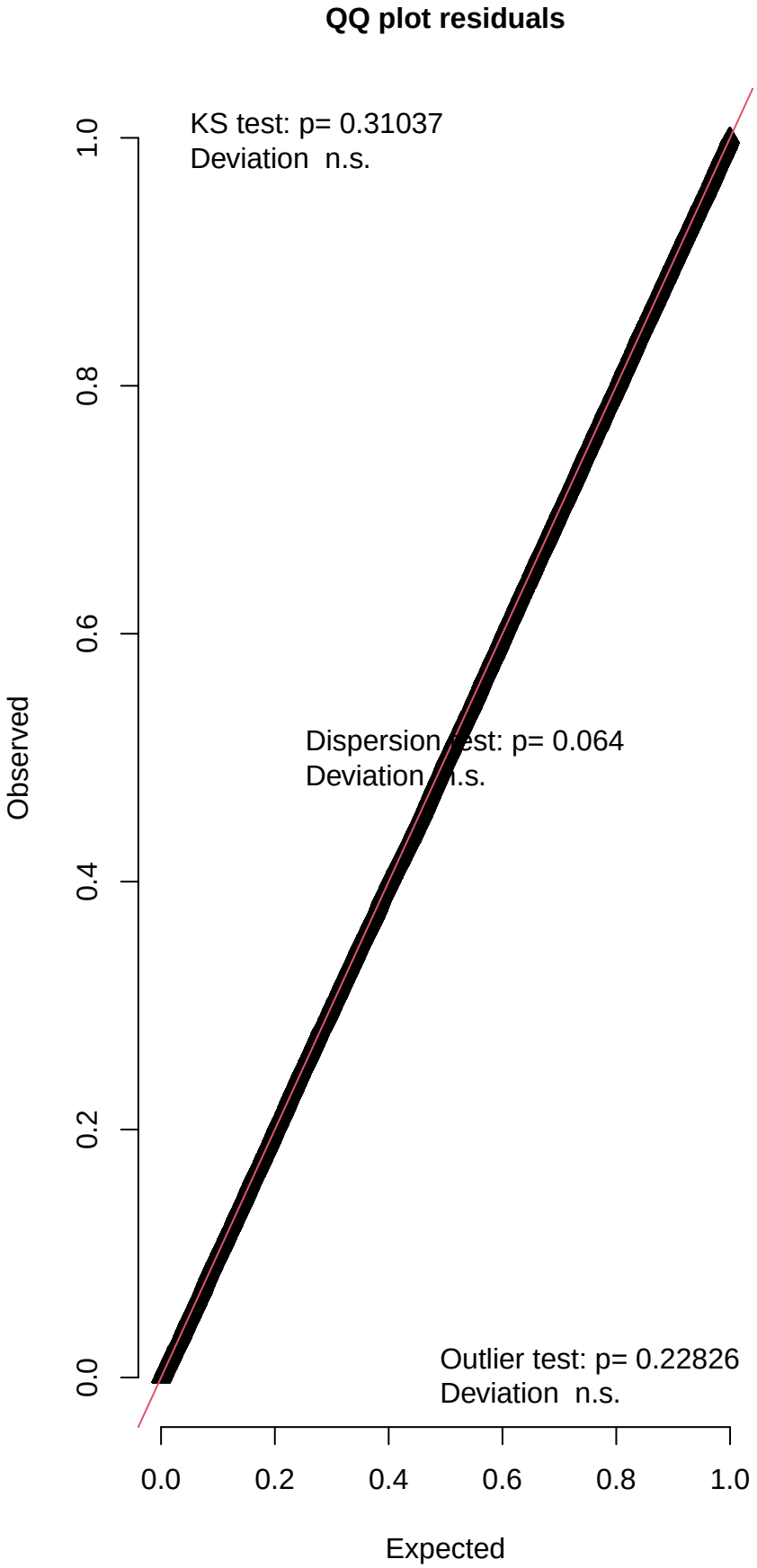


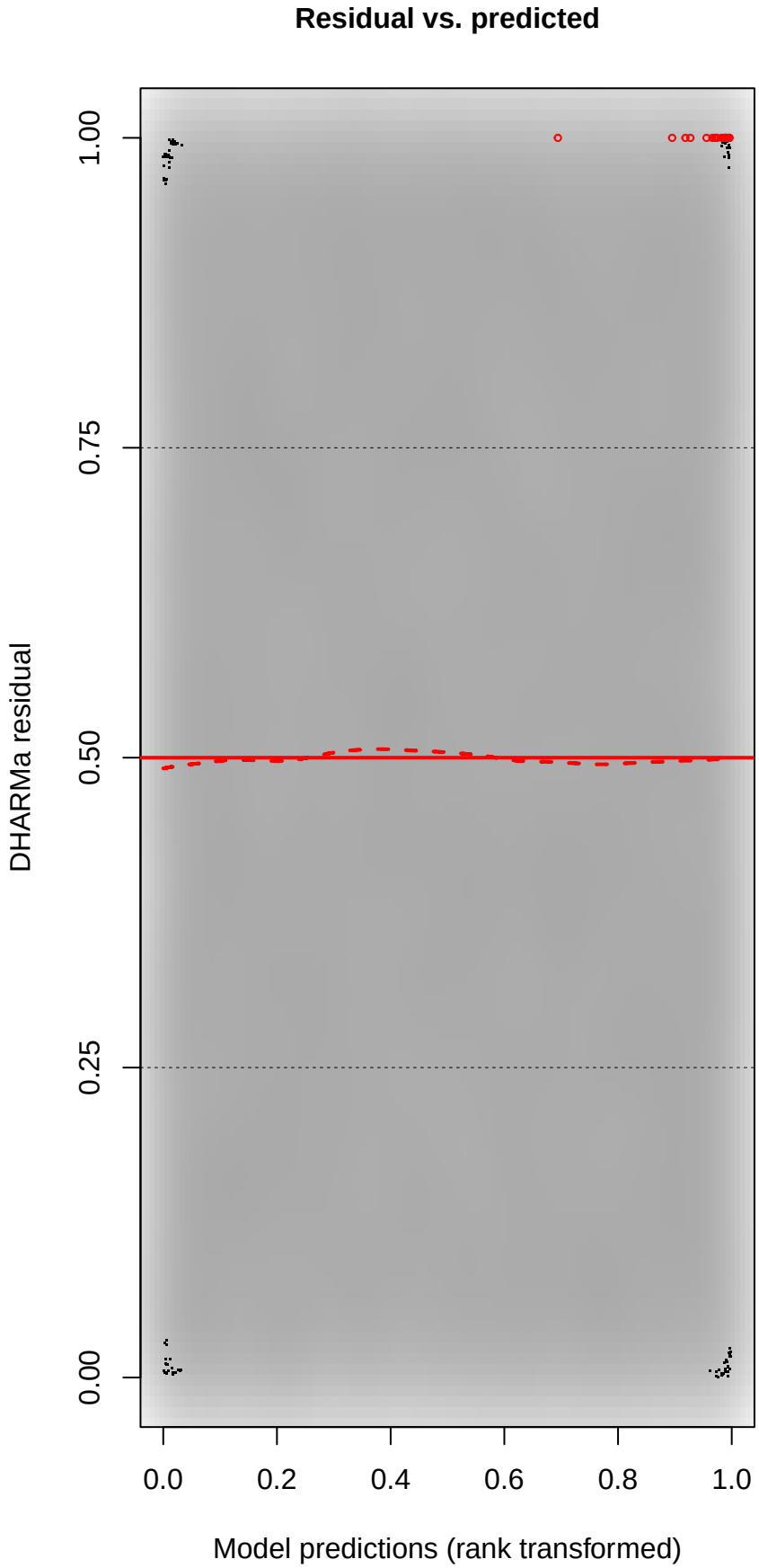

*Betula pubescens*

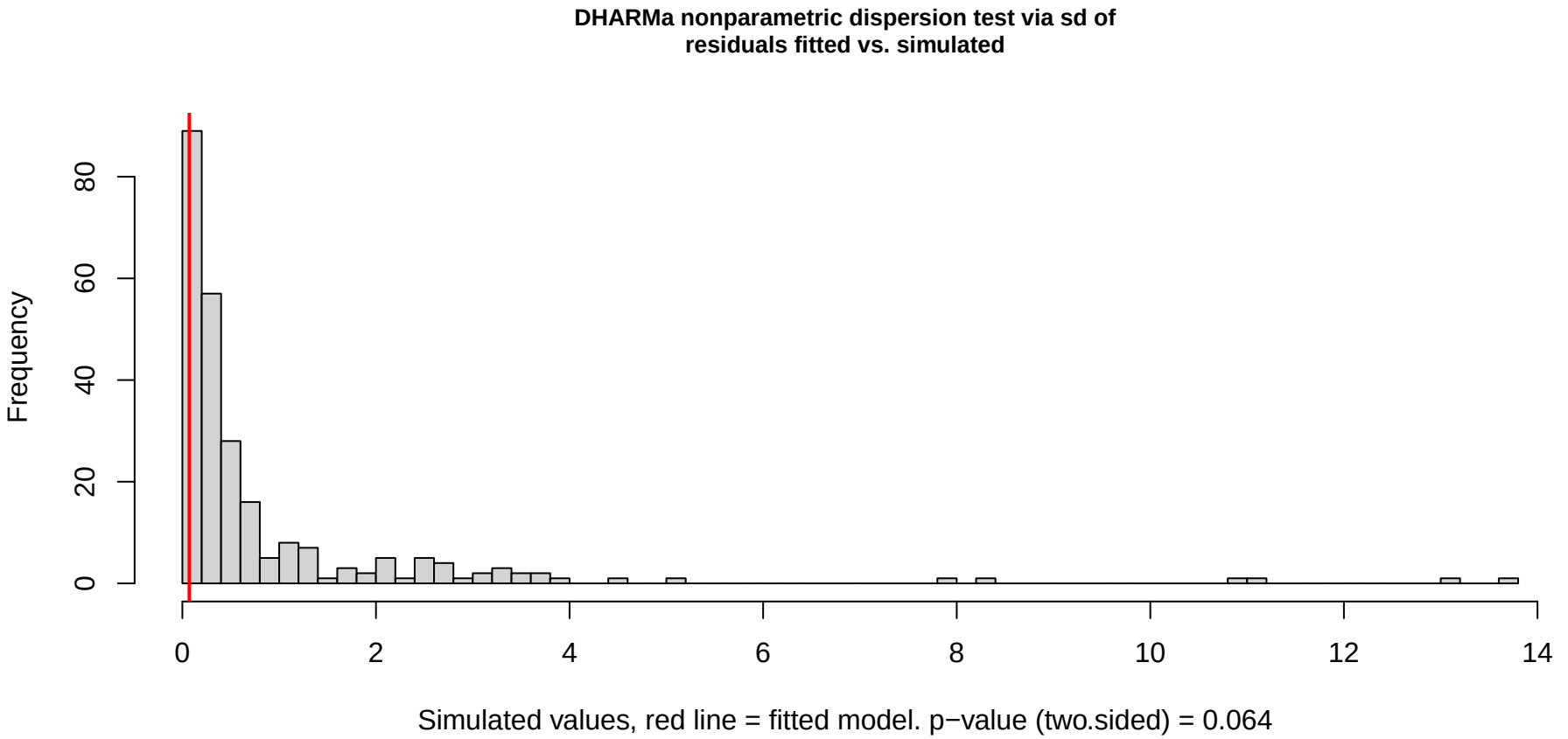


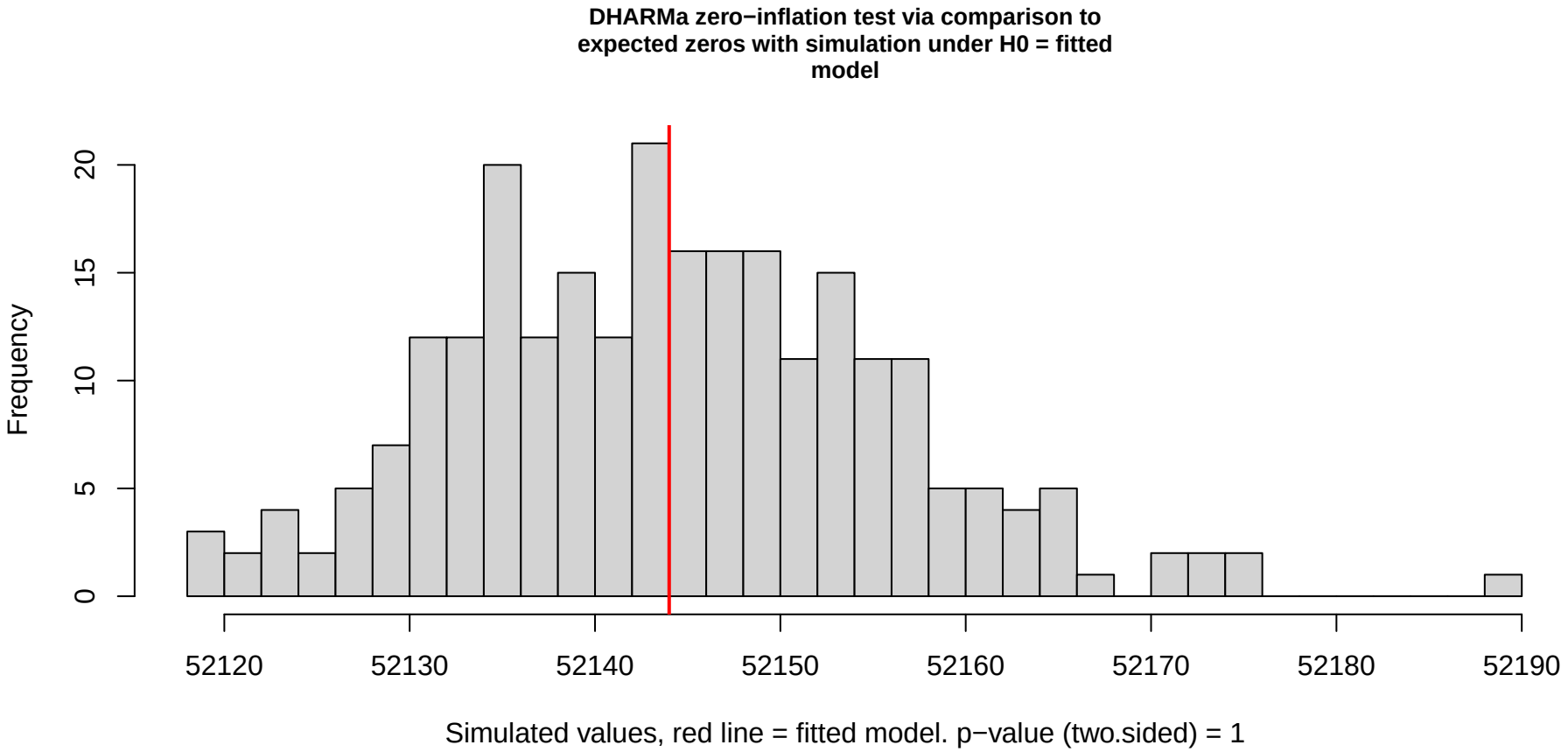

*Betula pubescens*

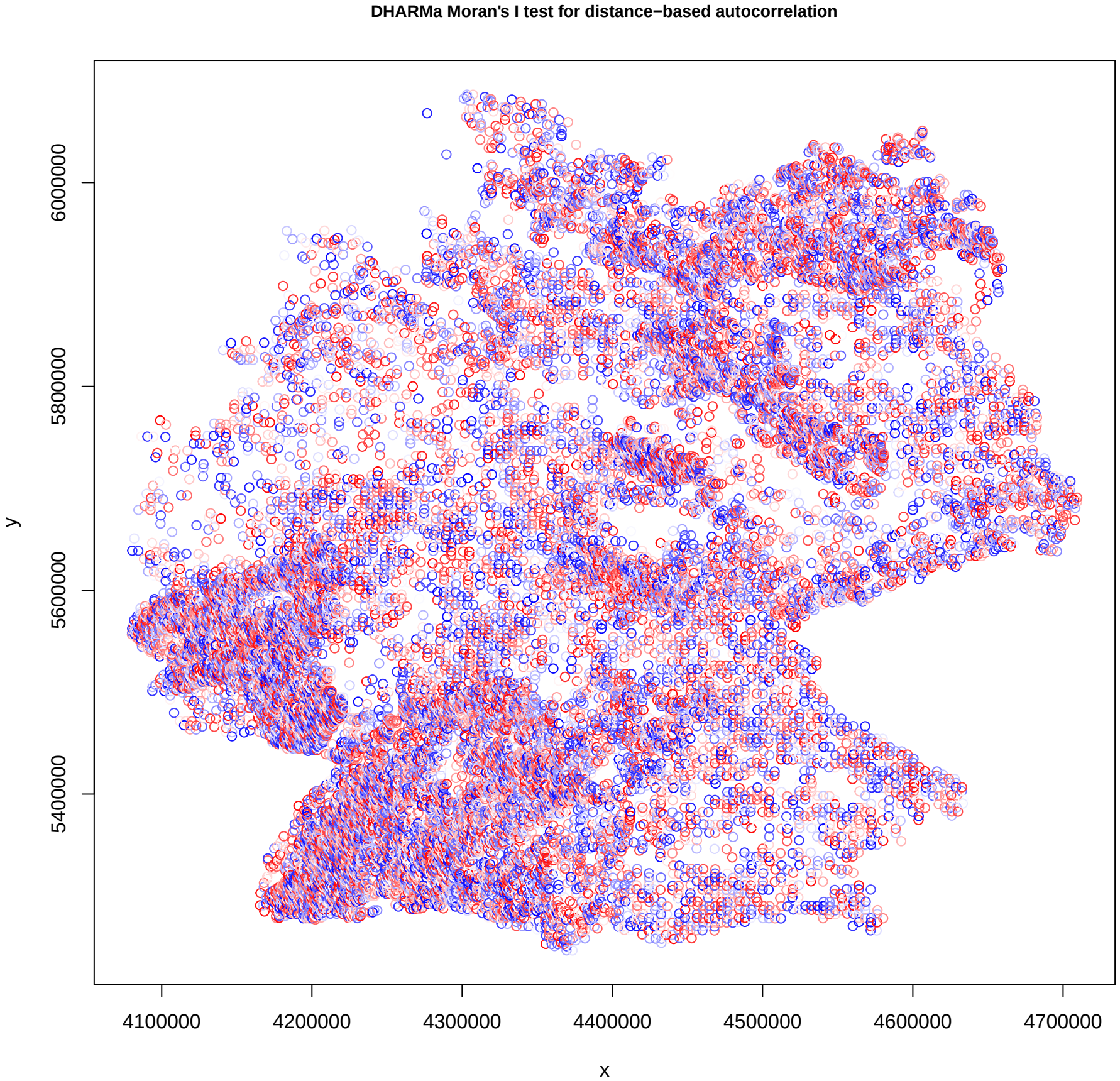

*Larix decidua*

DHARMa residual

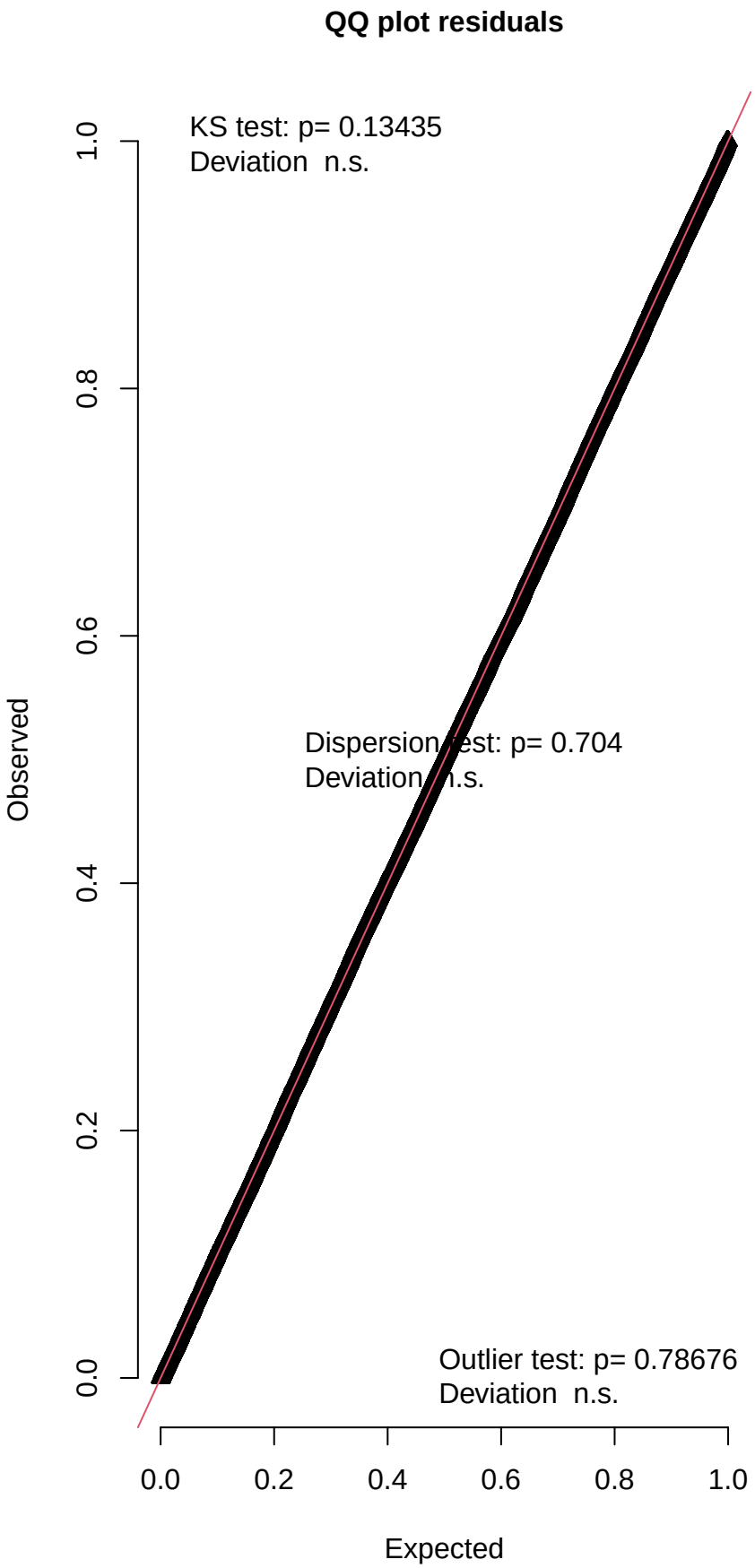


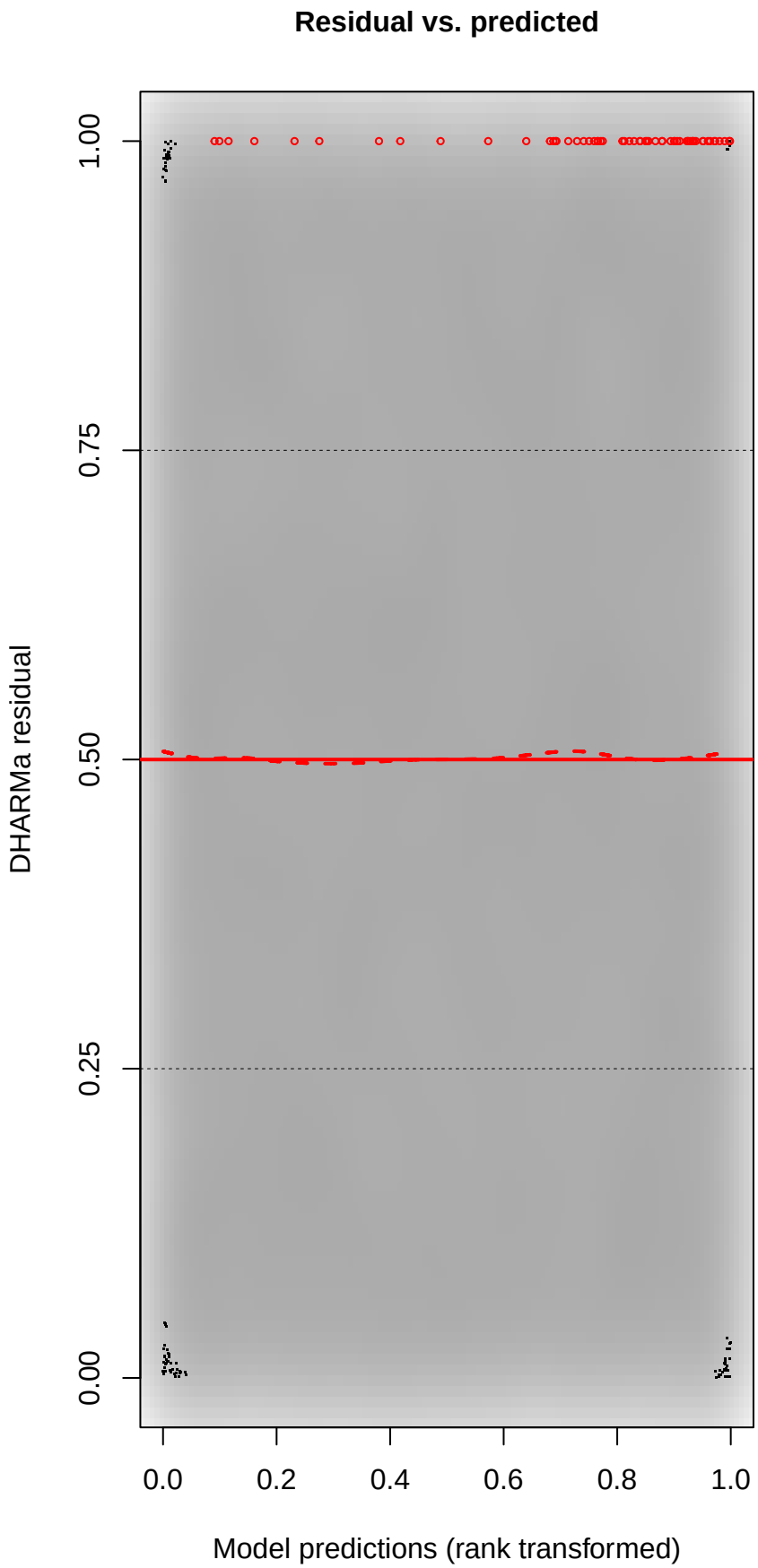

*Larix decidua*

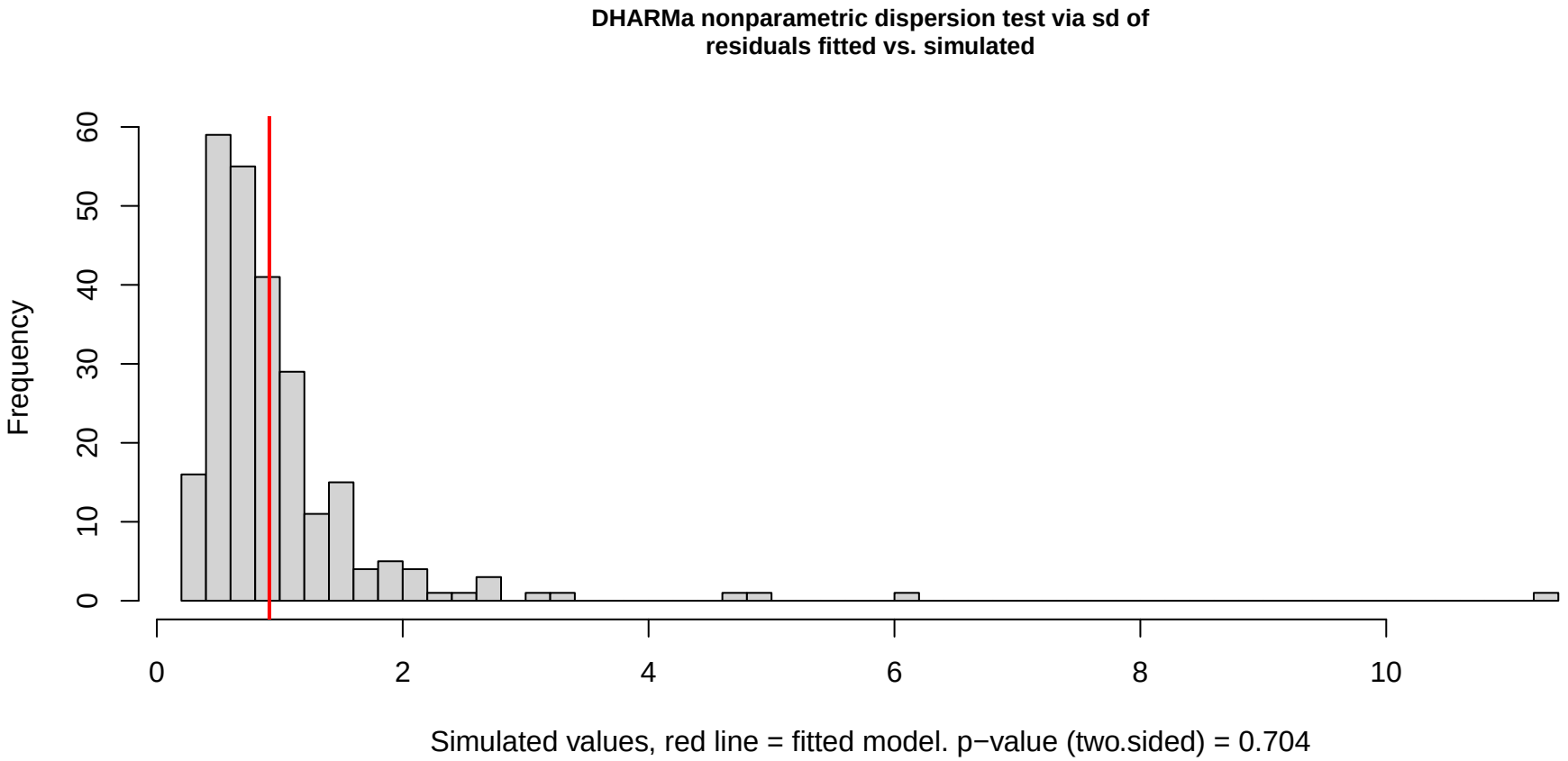


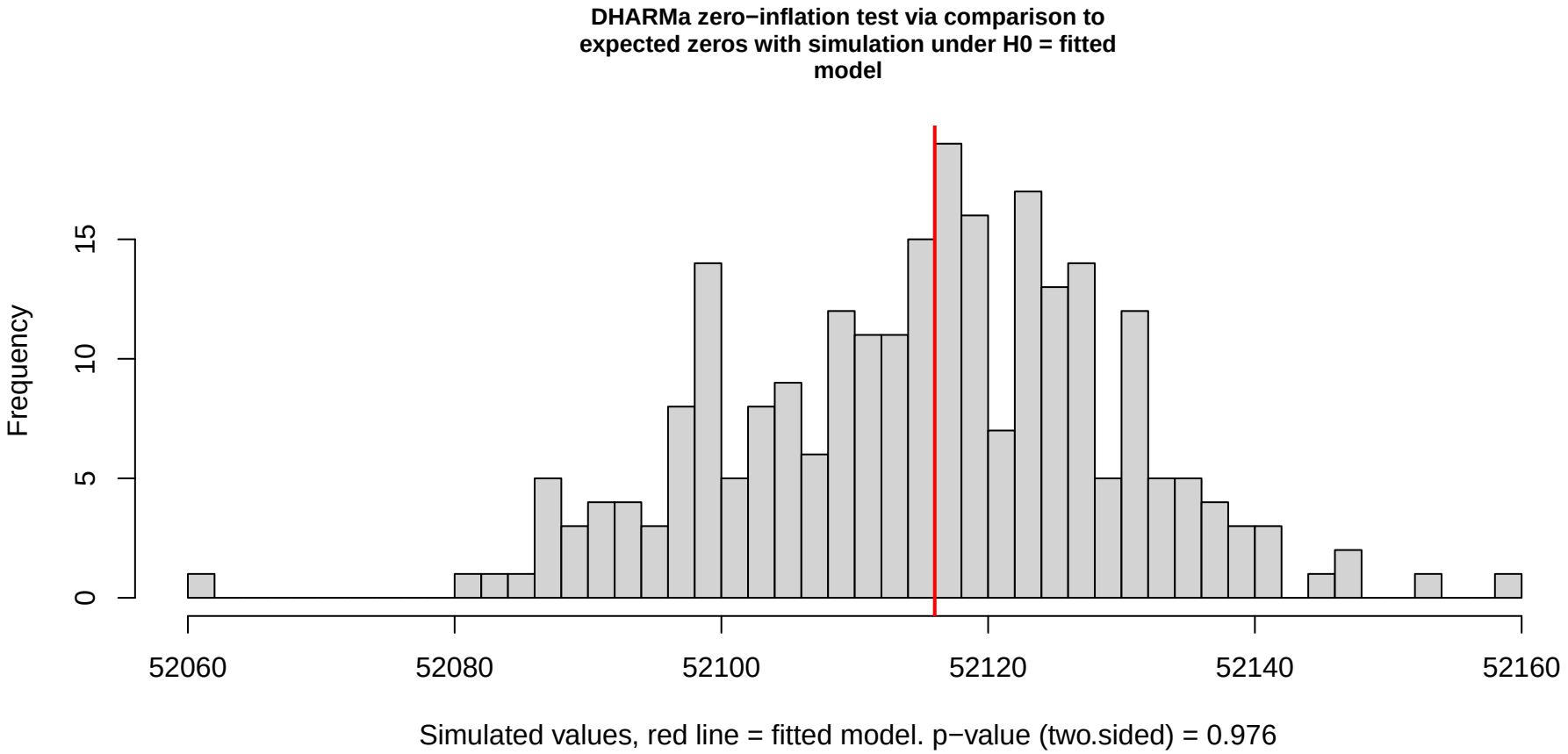

*Larix decidua*

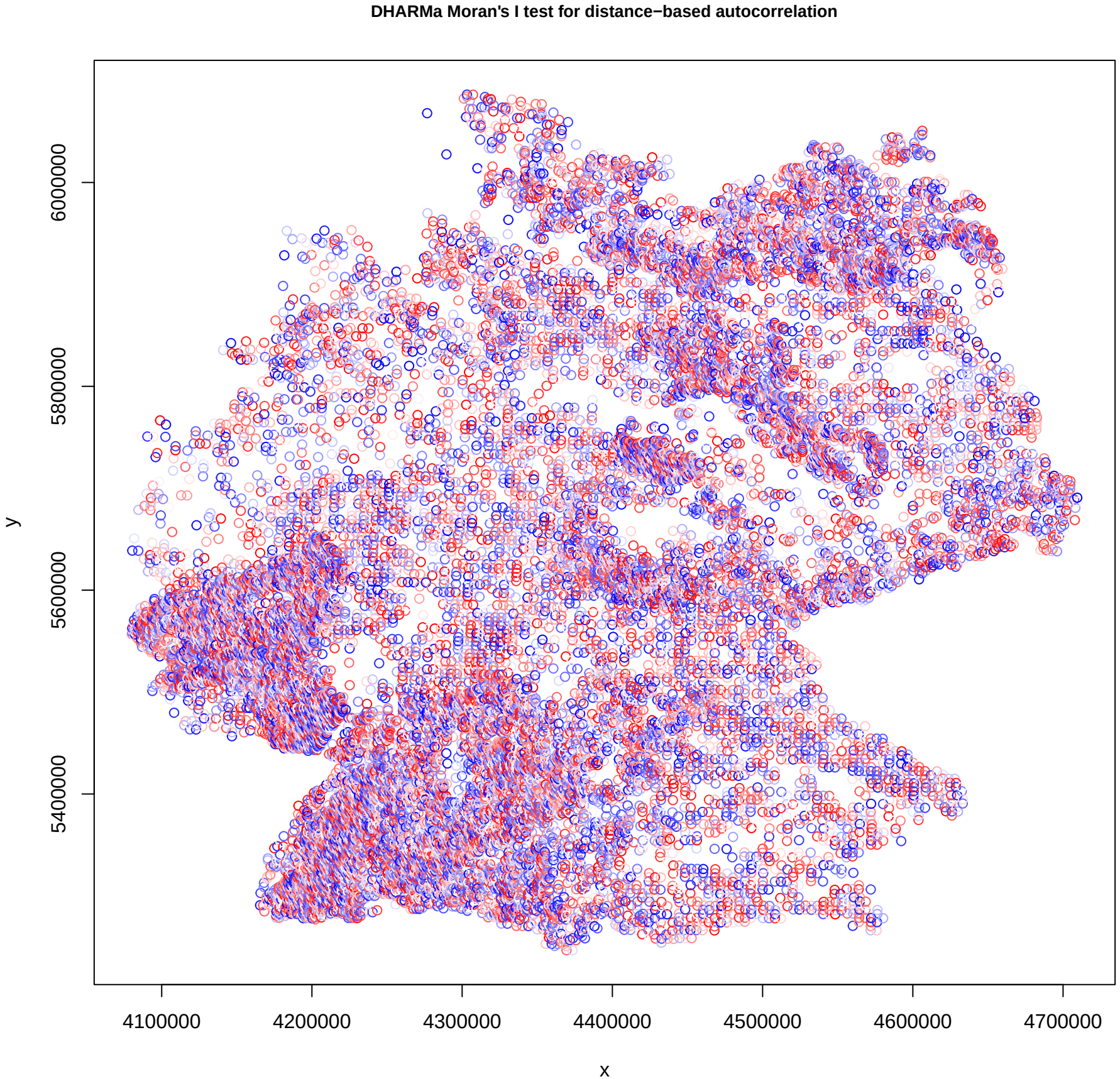

*Larix kaempferi*

DHARMa residual

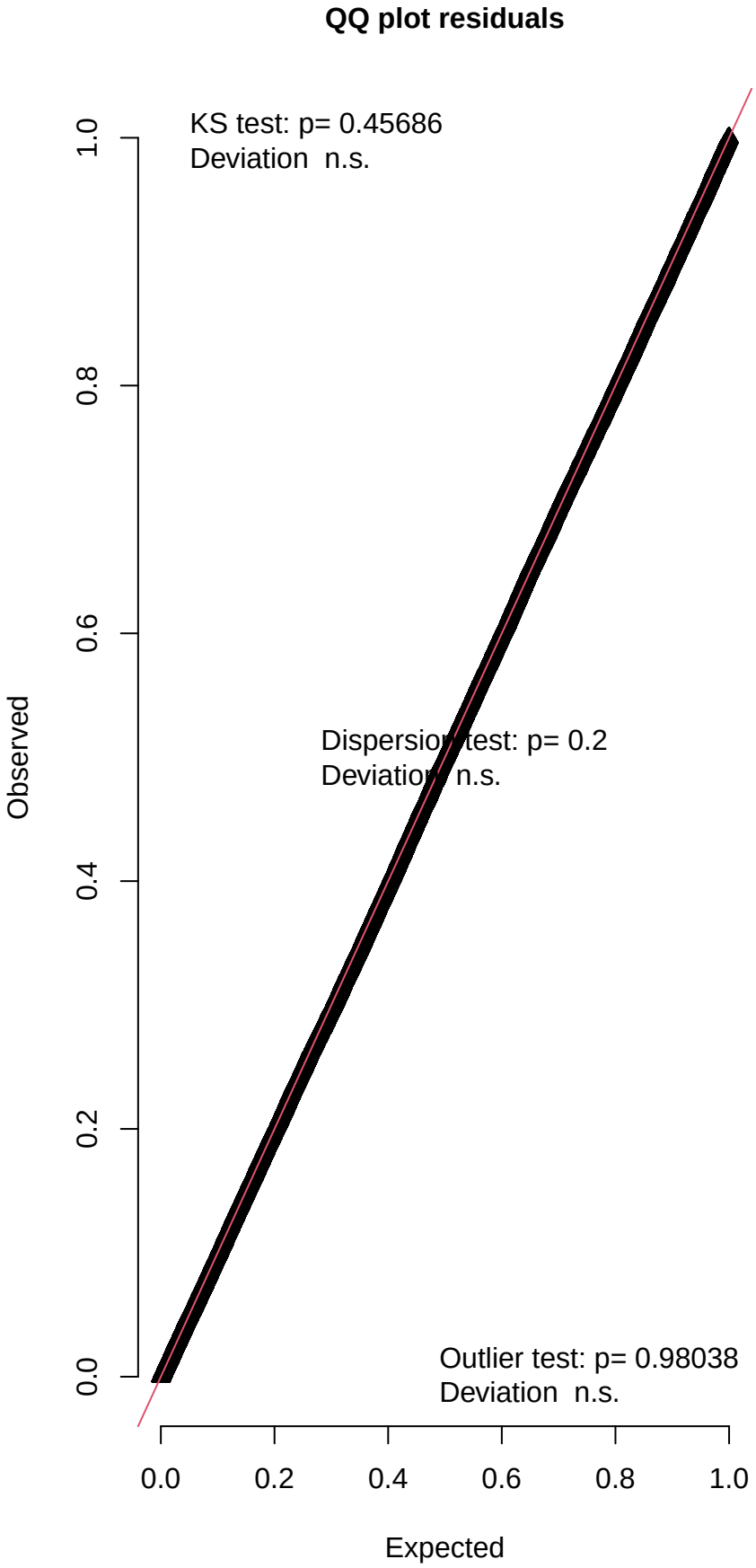


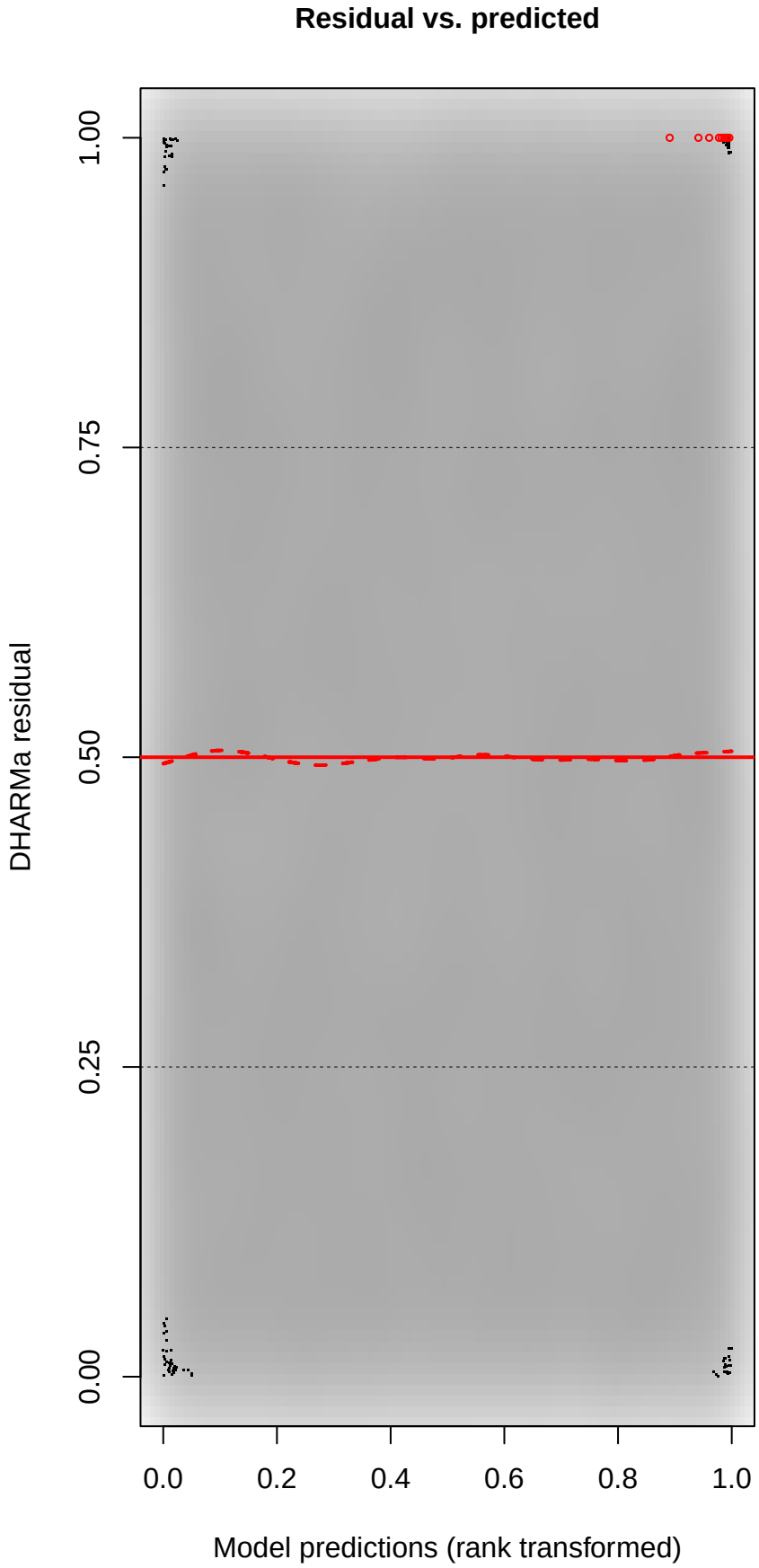

*Larix kaempferi*

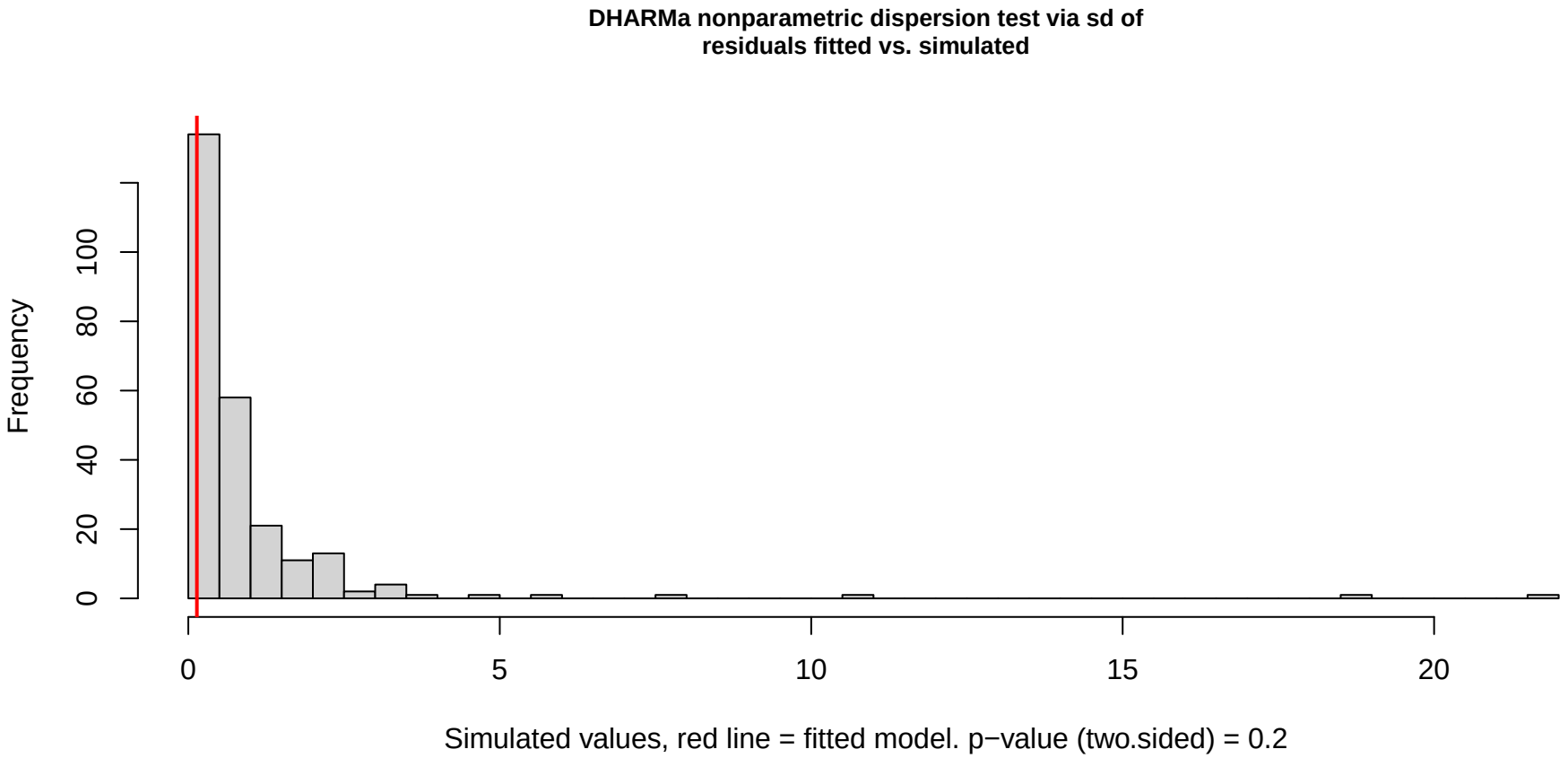


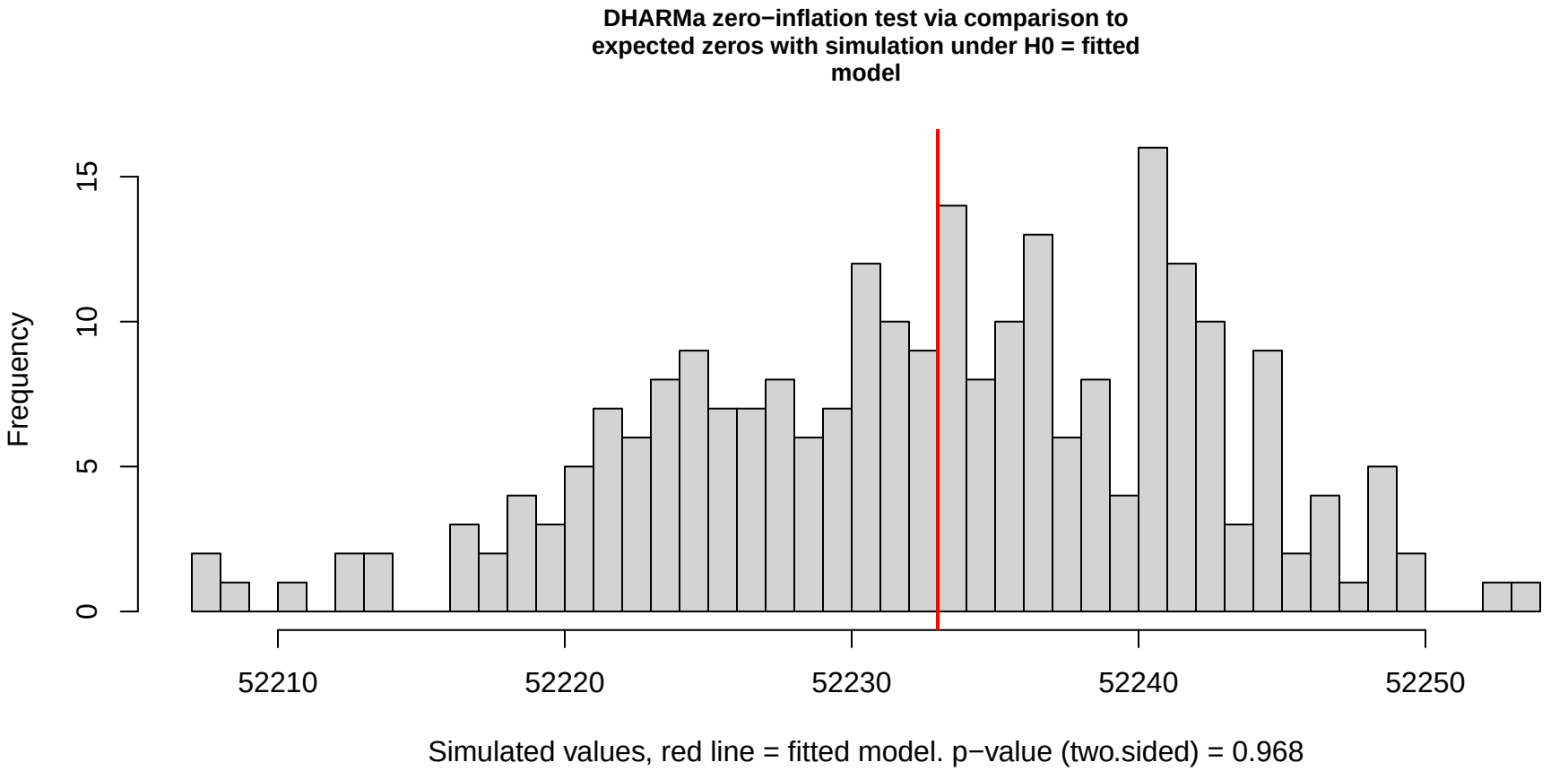

*Larix kaempferi*

DHARMa residual

*Pseudotsuga menziesii*

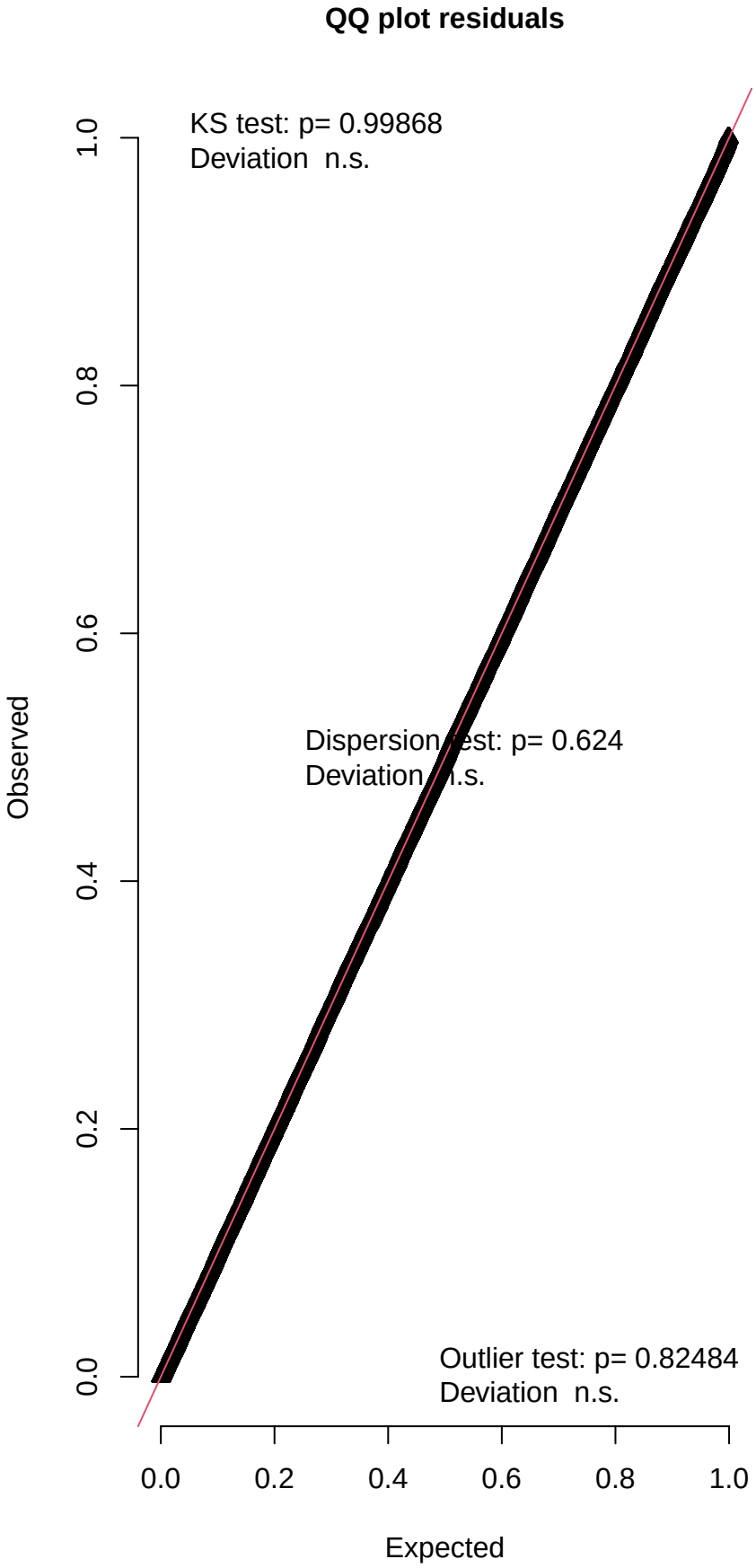


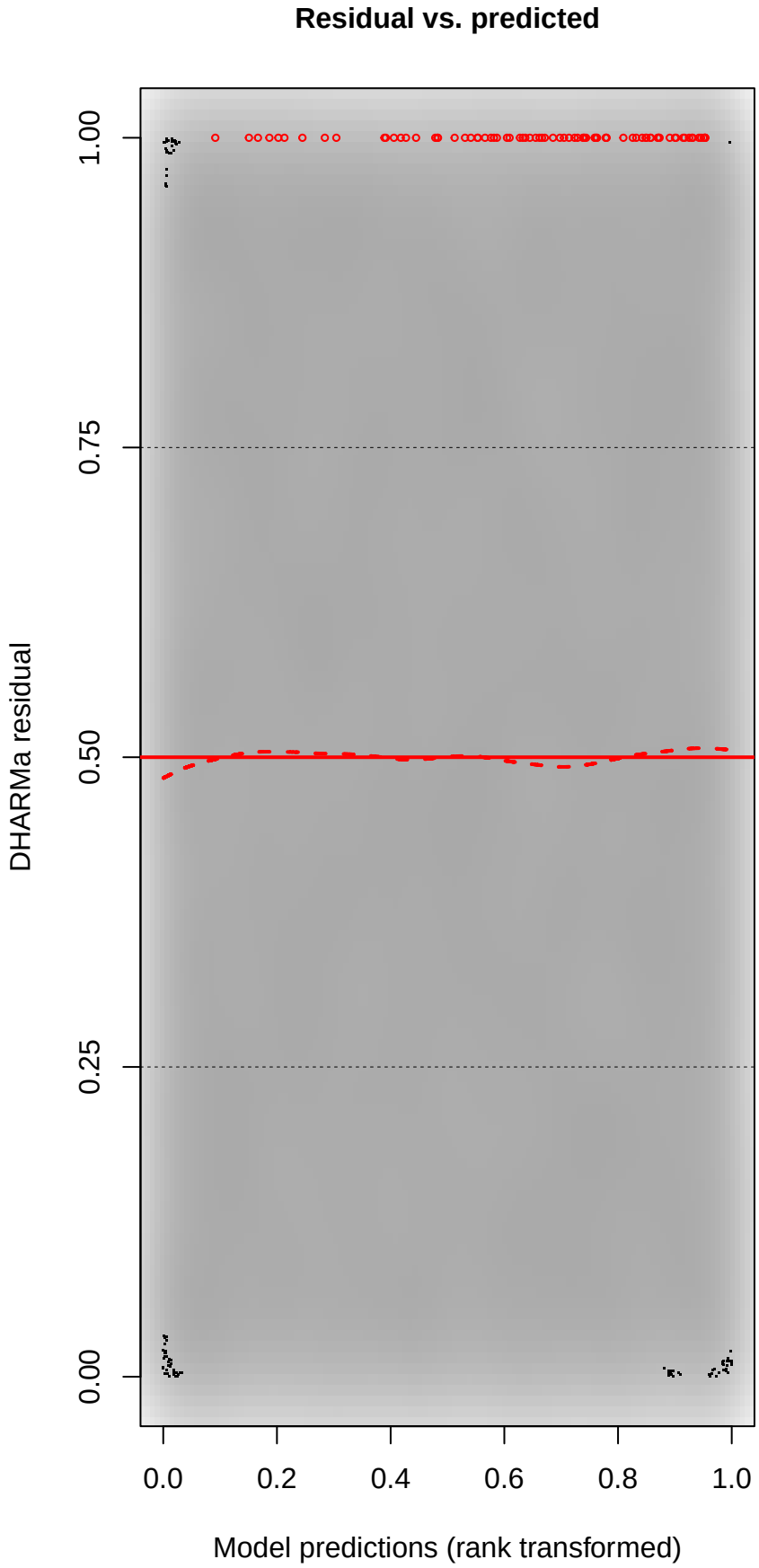

*Pseudotsuga menziesii*

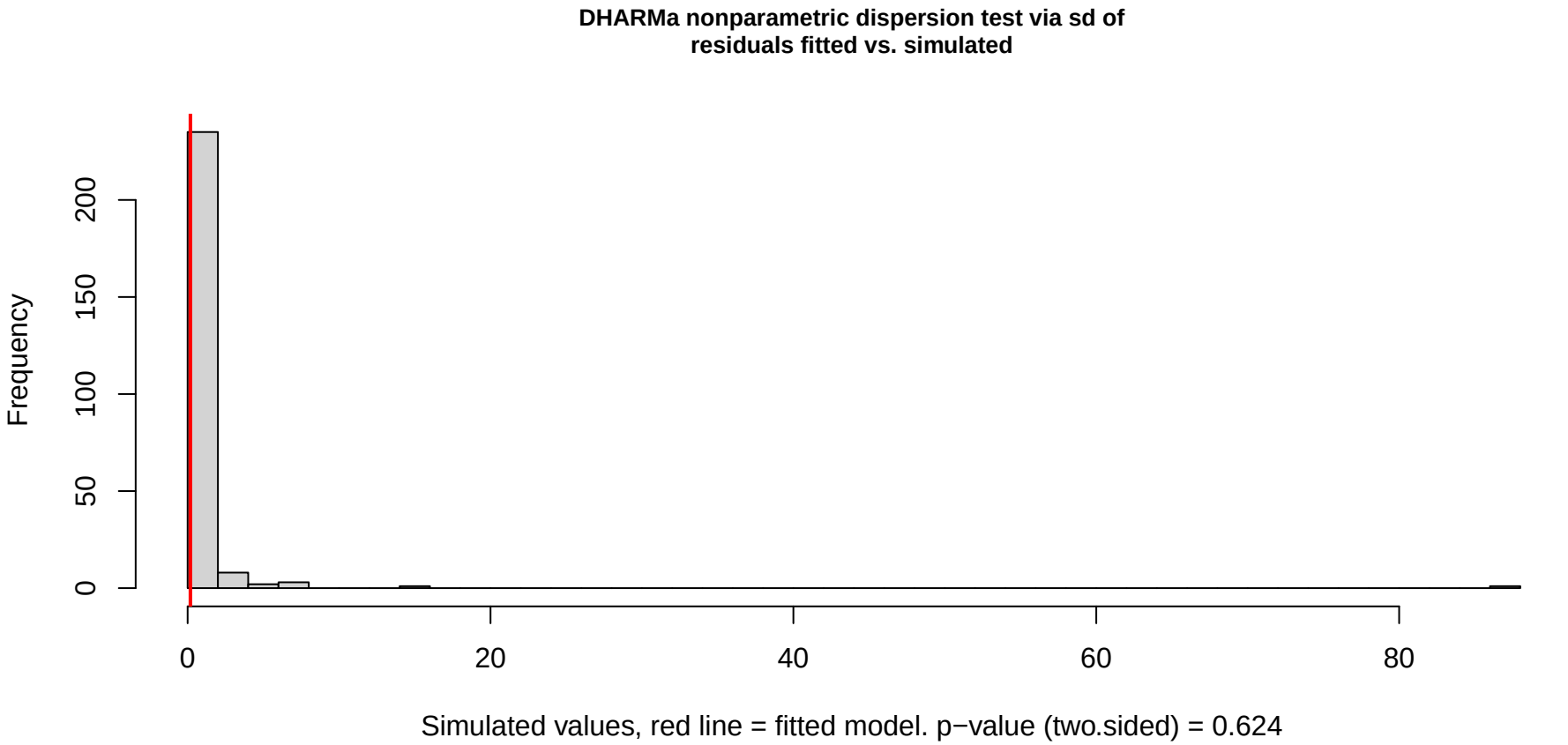


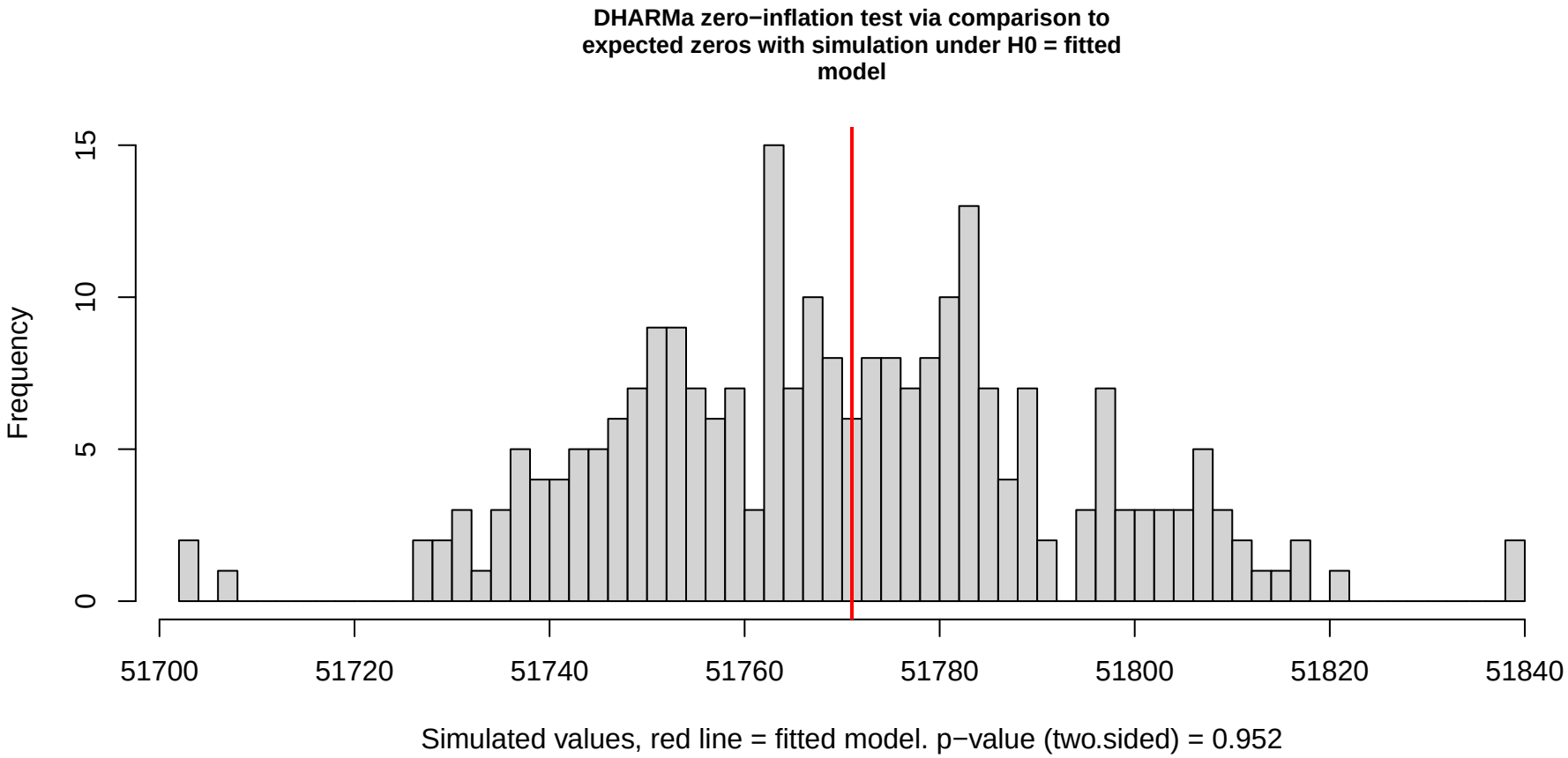

*Pseudotsuga menziesii*

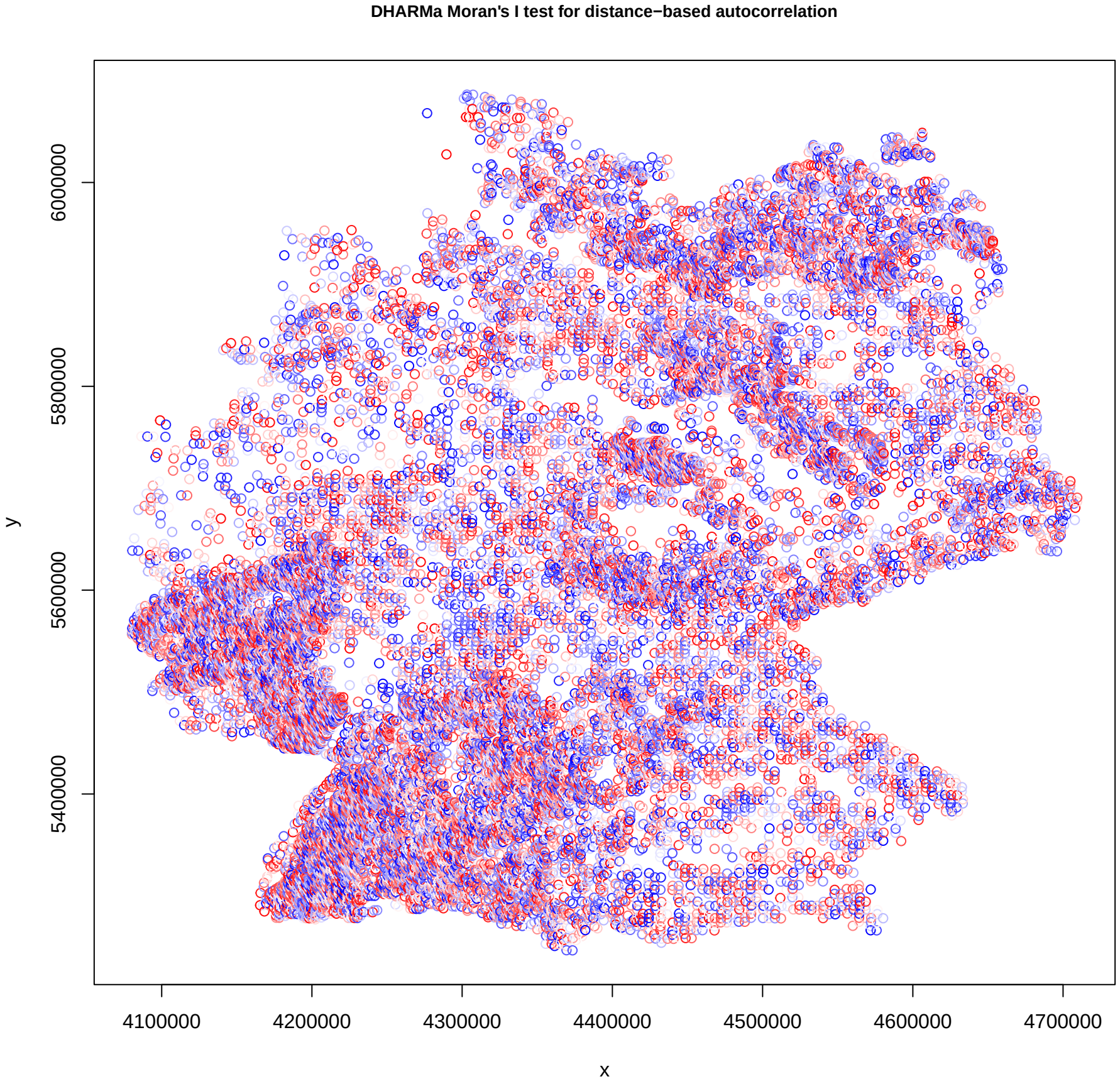

*Pinus strobus*

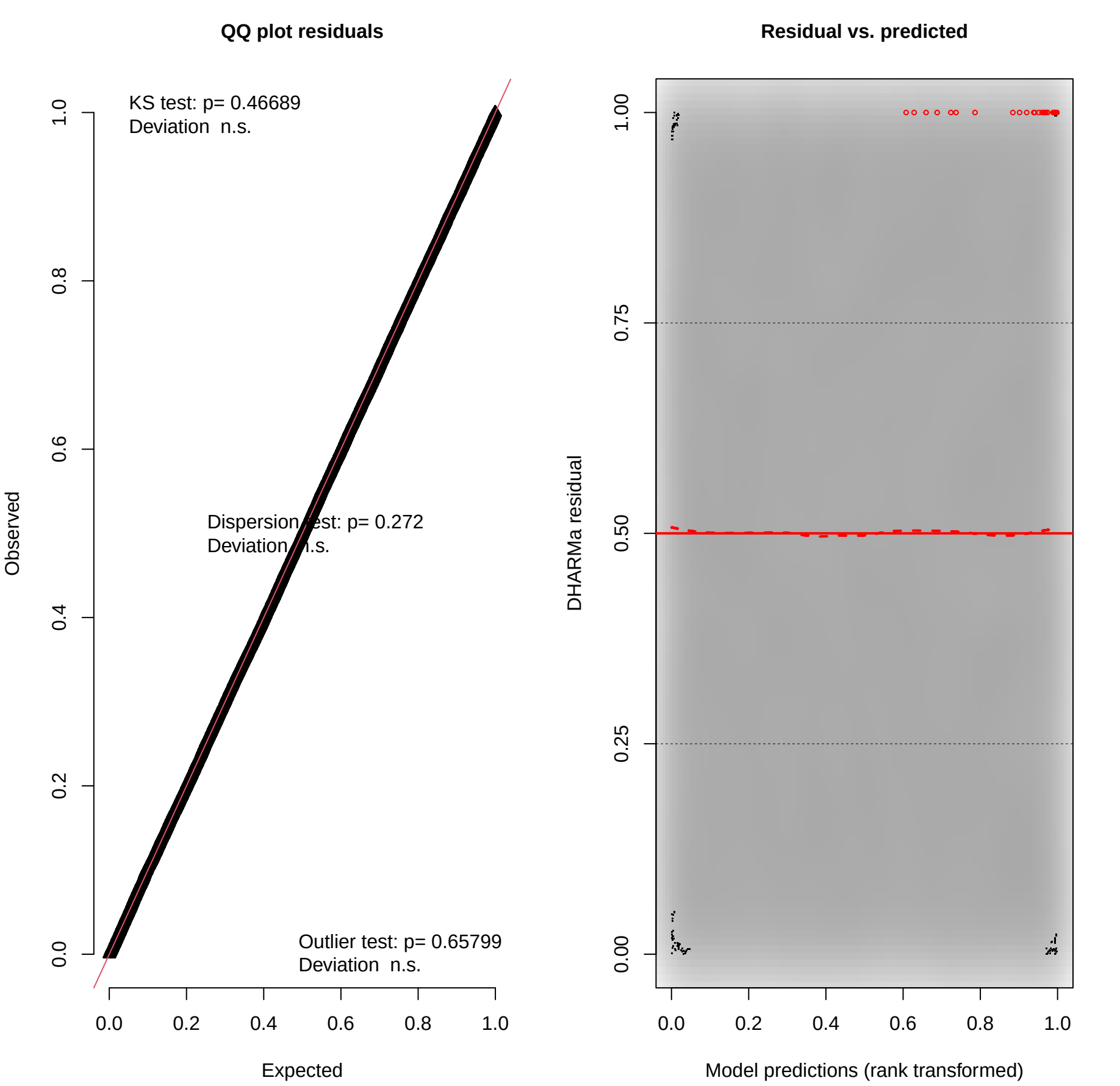

*Pinus strobus*

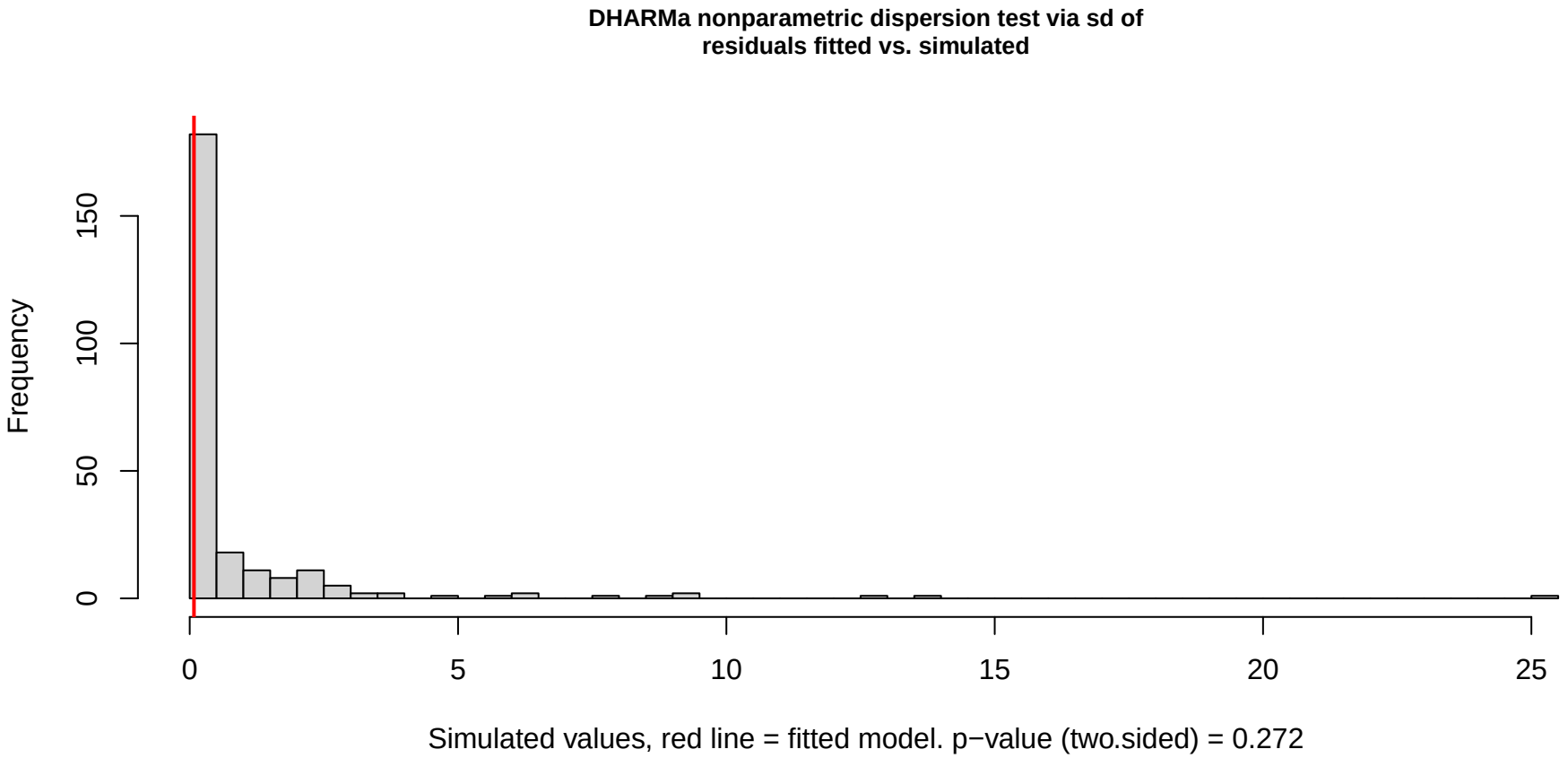


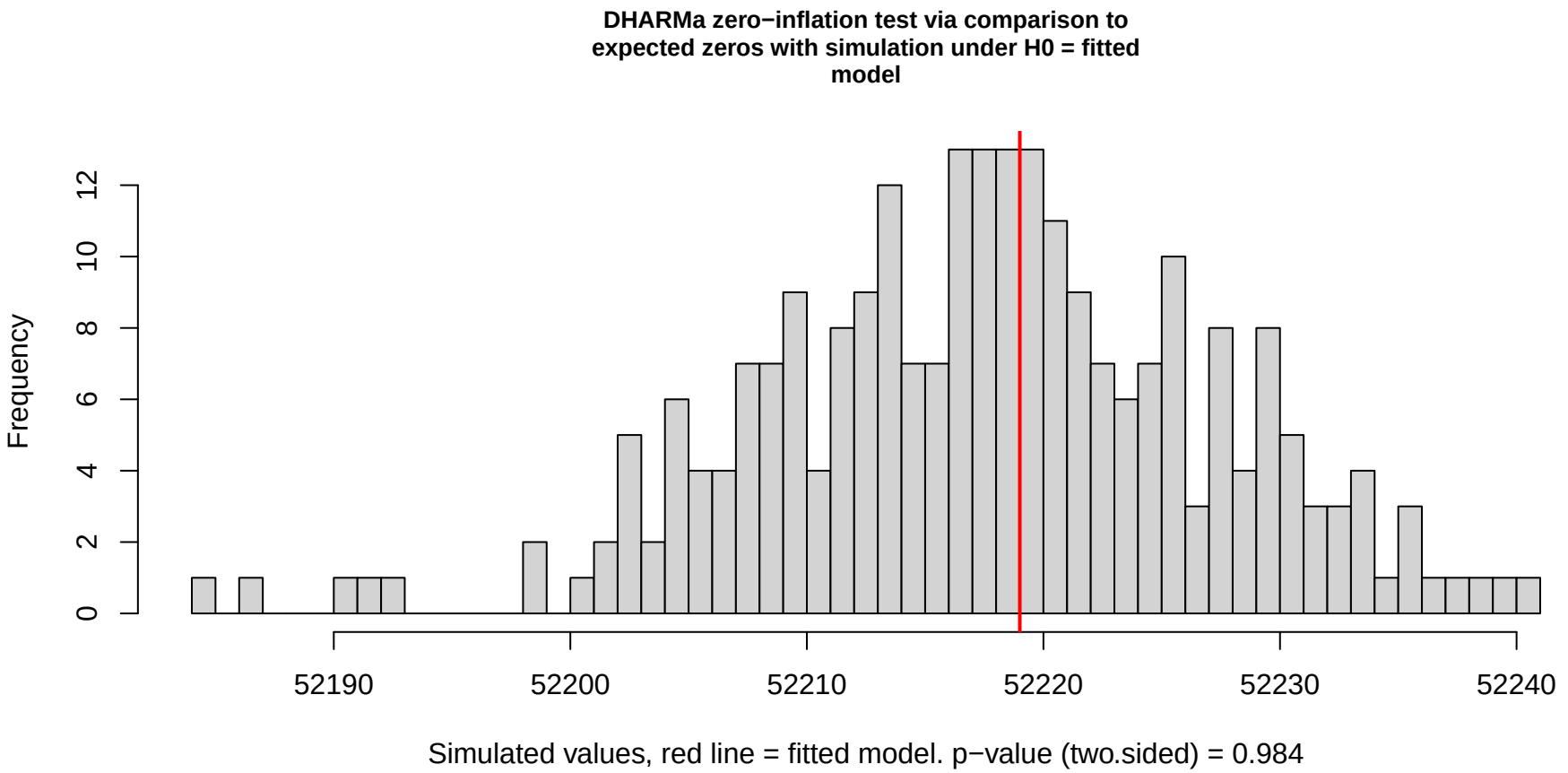

*Pinus strobus*

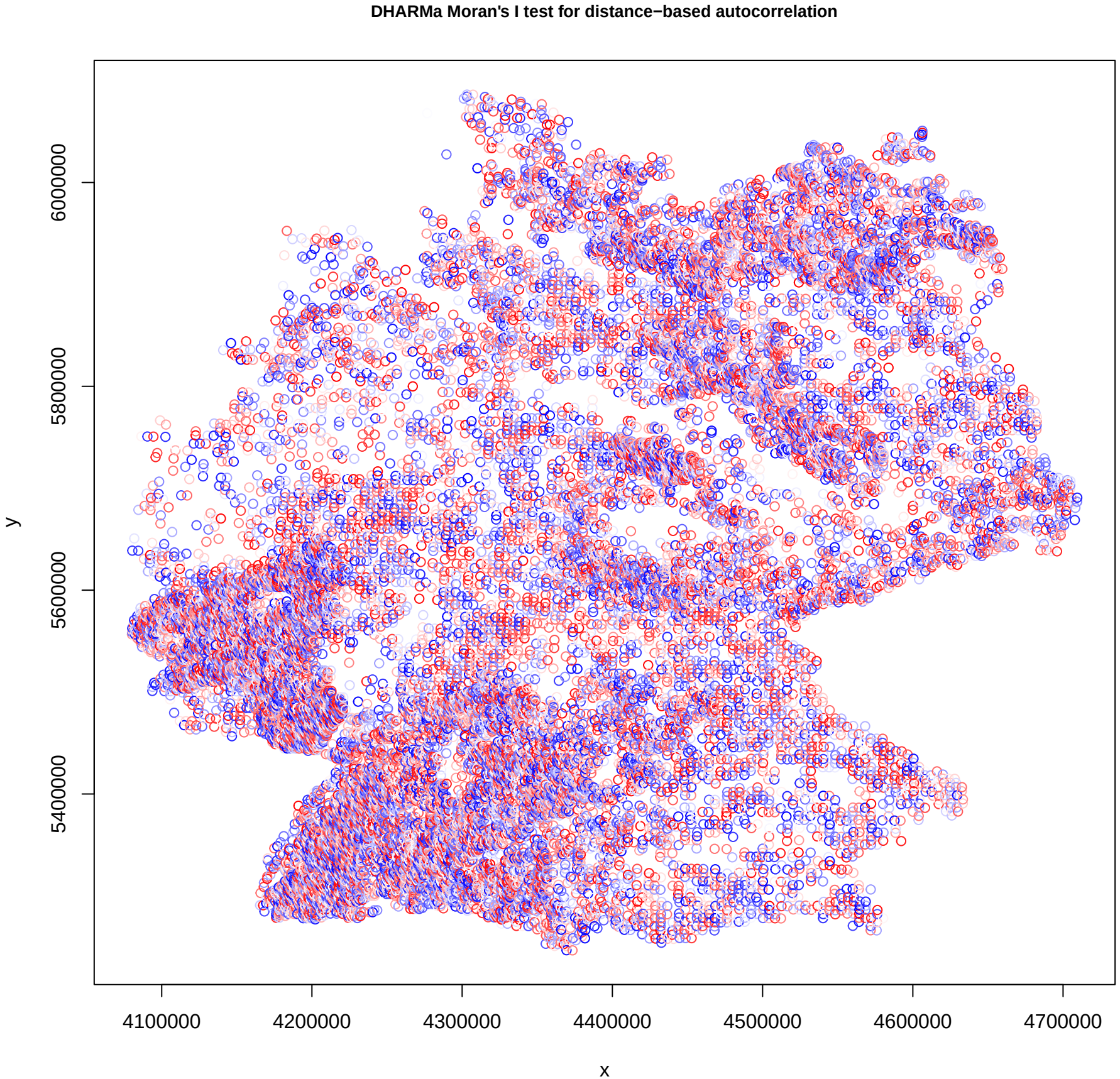

*Pinus sylvestris*

DHARMa residual

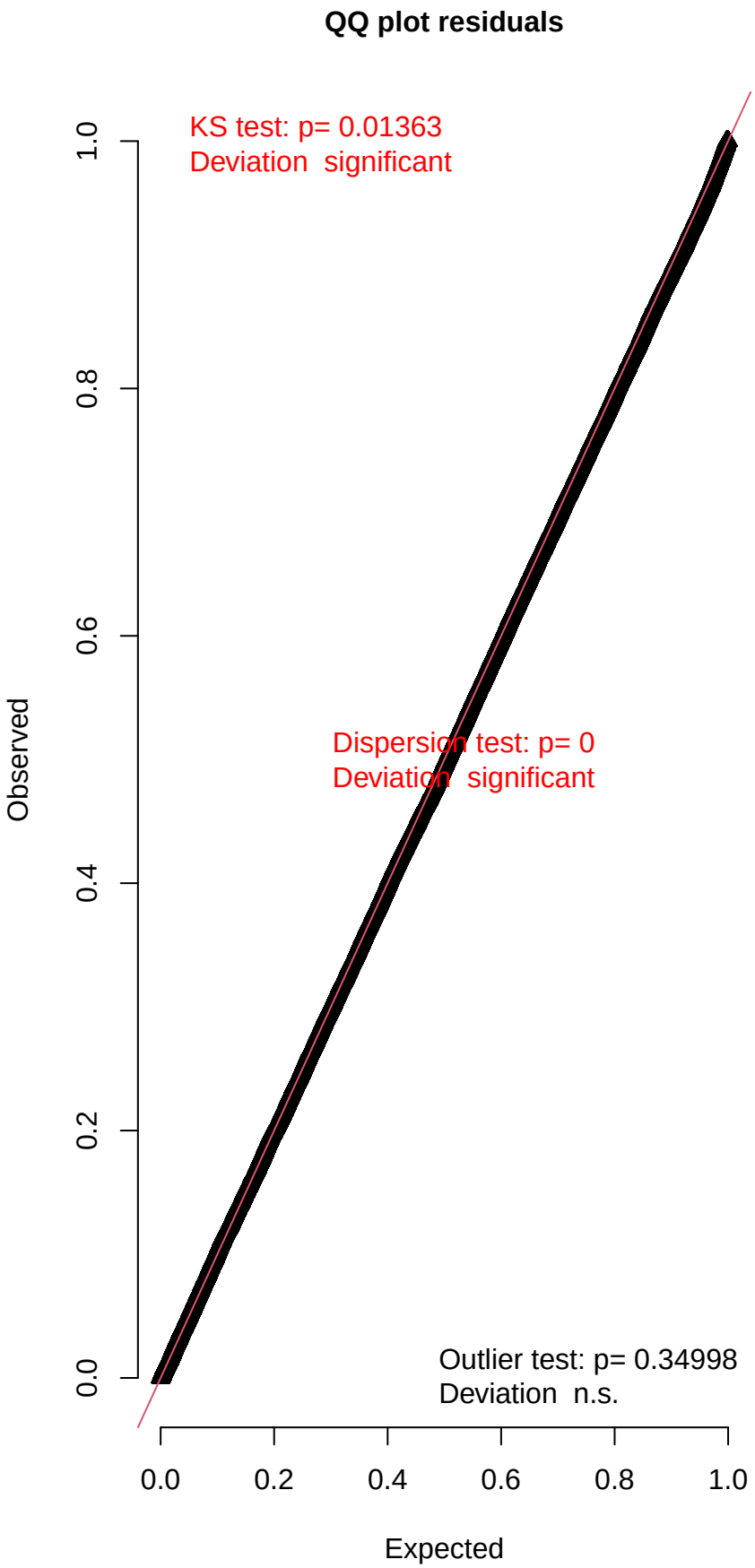


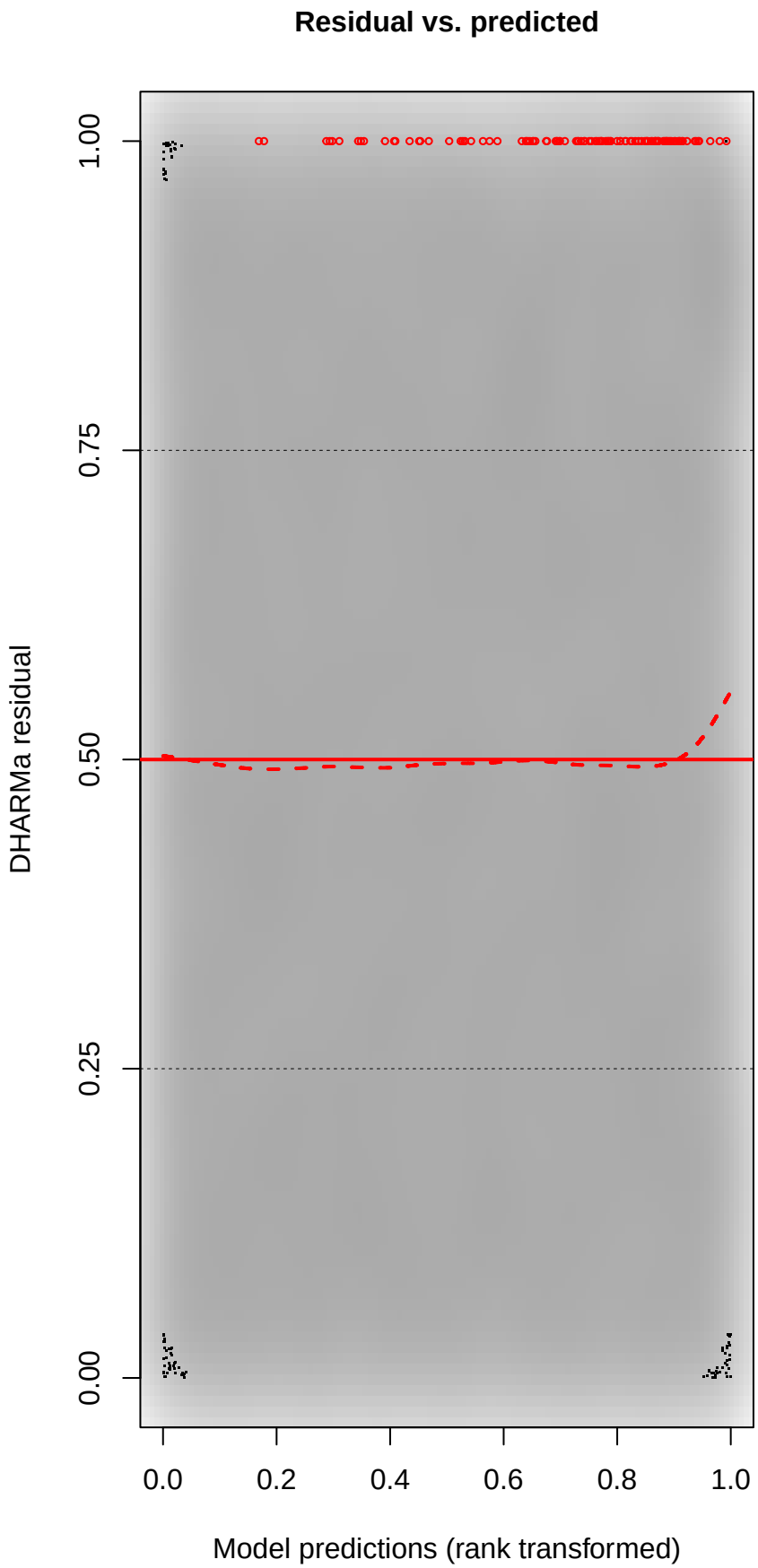

*Pinus sylvestris*

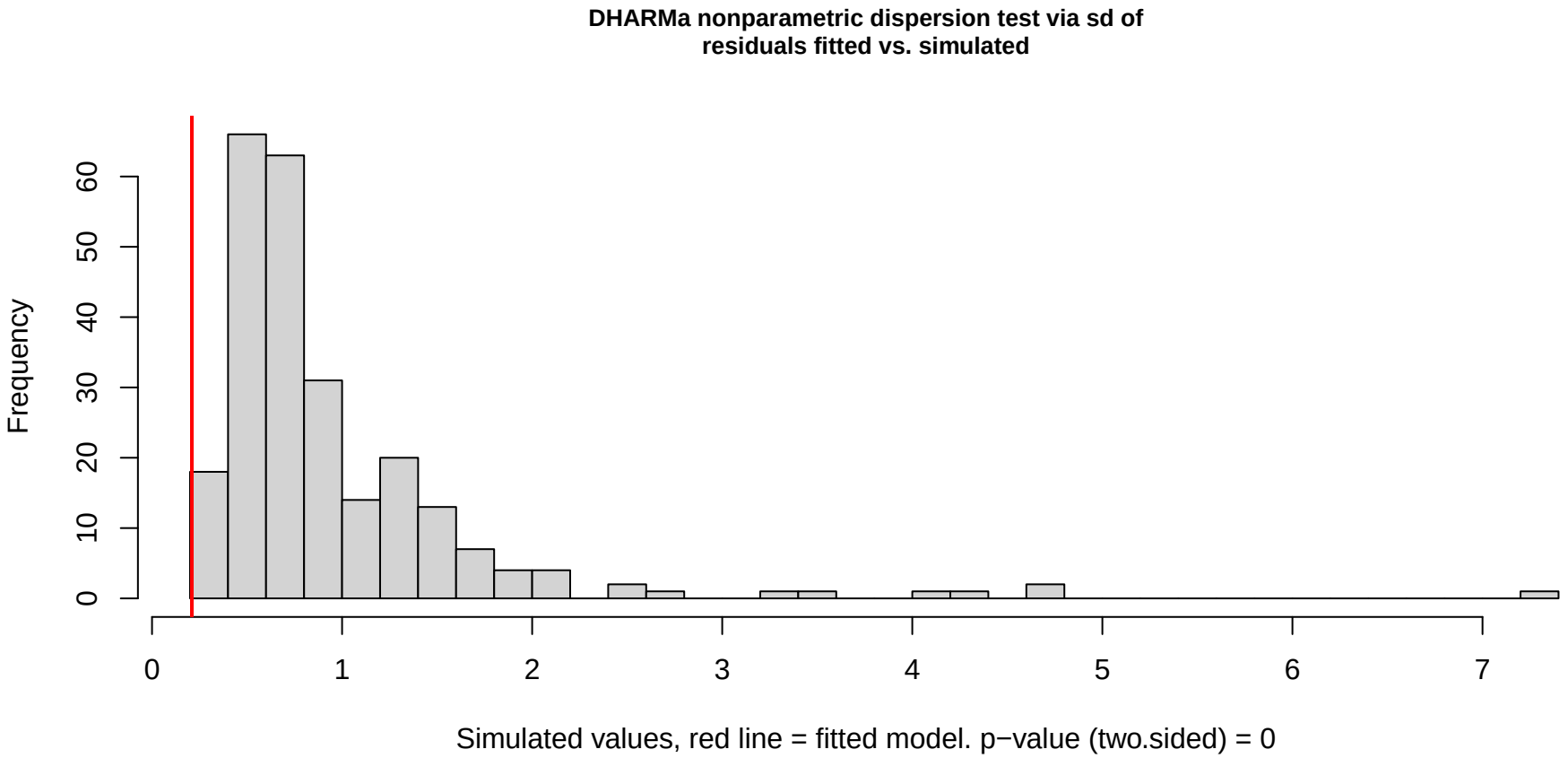


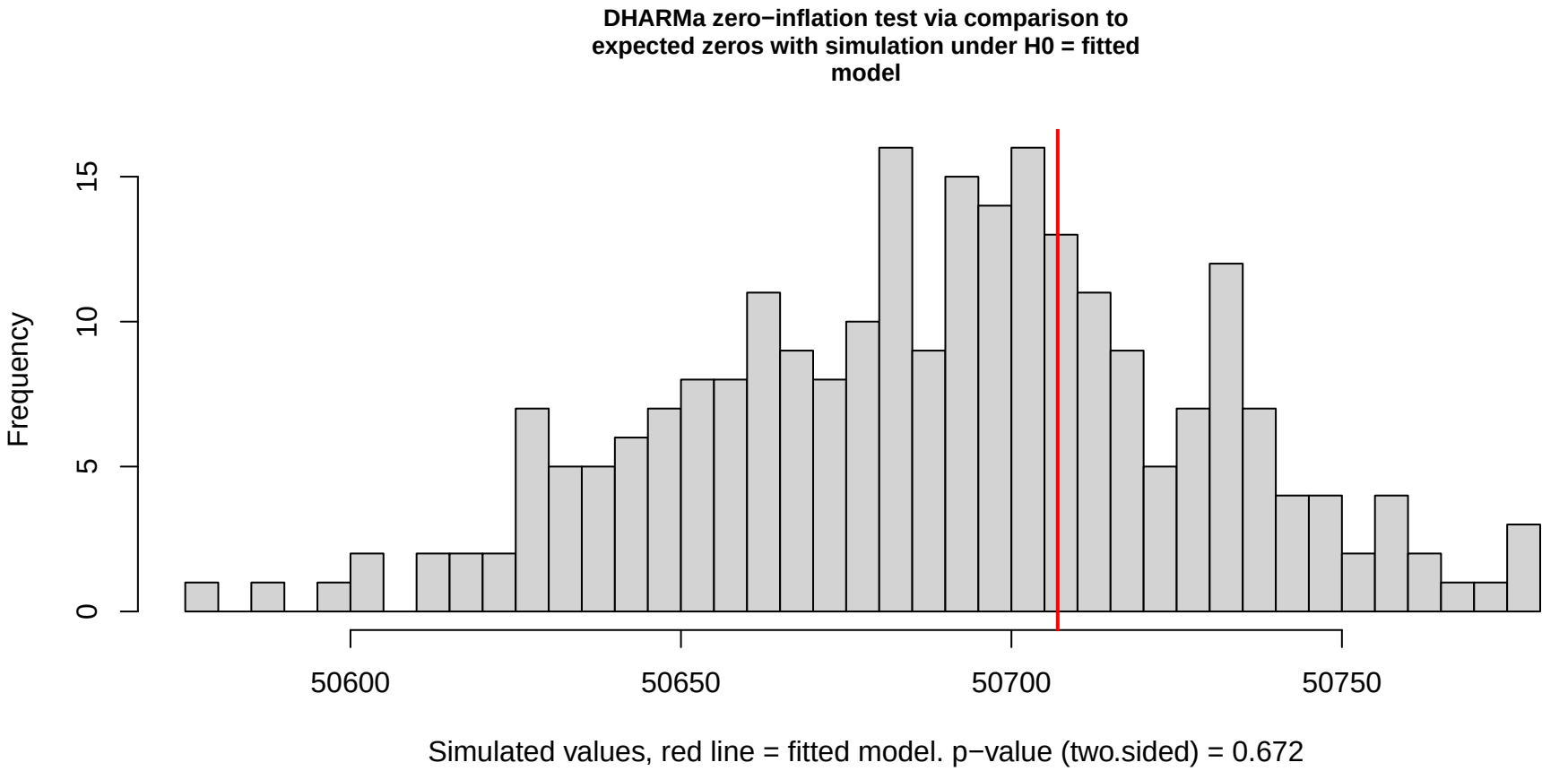

*Pinus sylvestris*

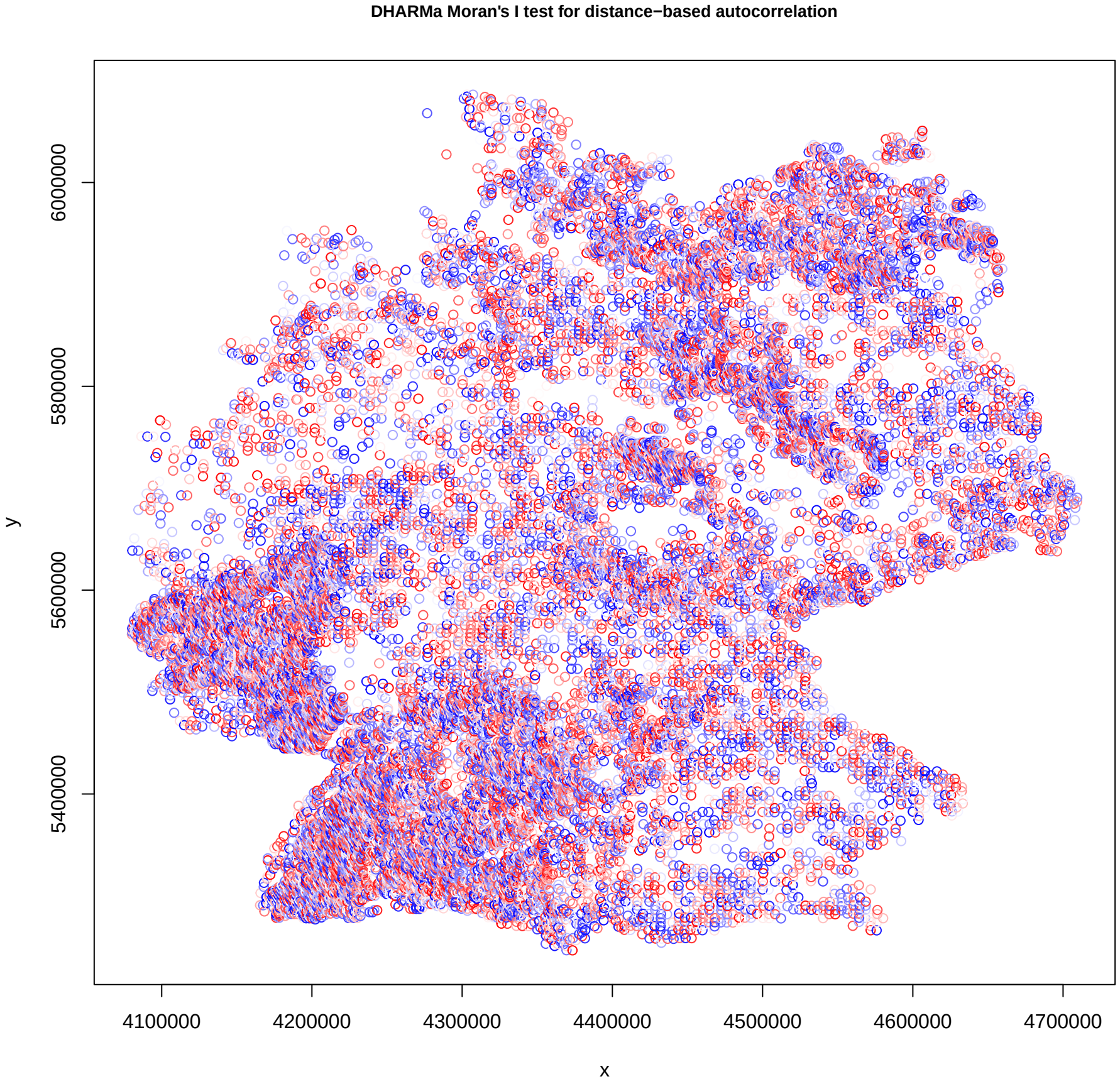

*Pinus nigra*

DHARMa residual

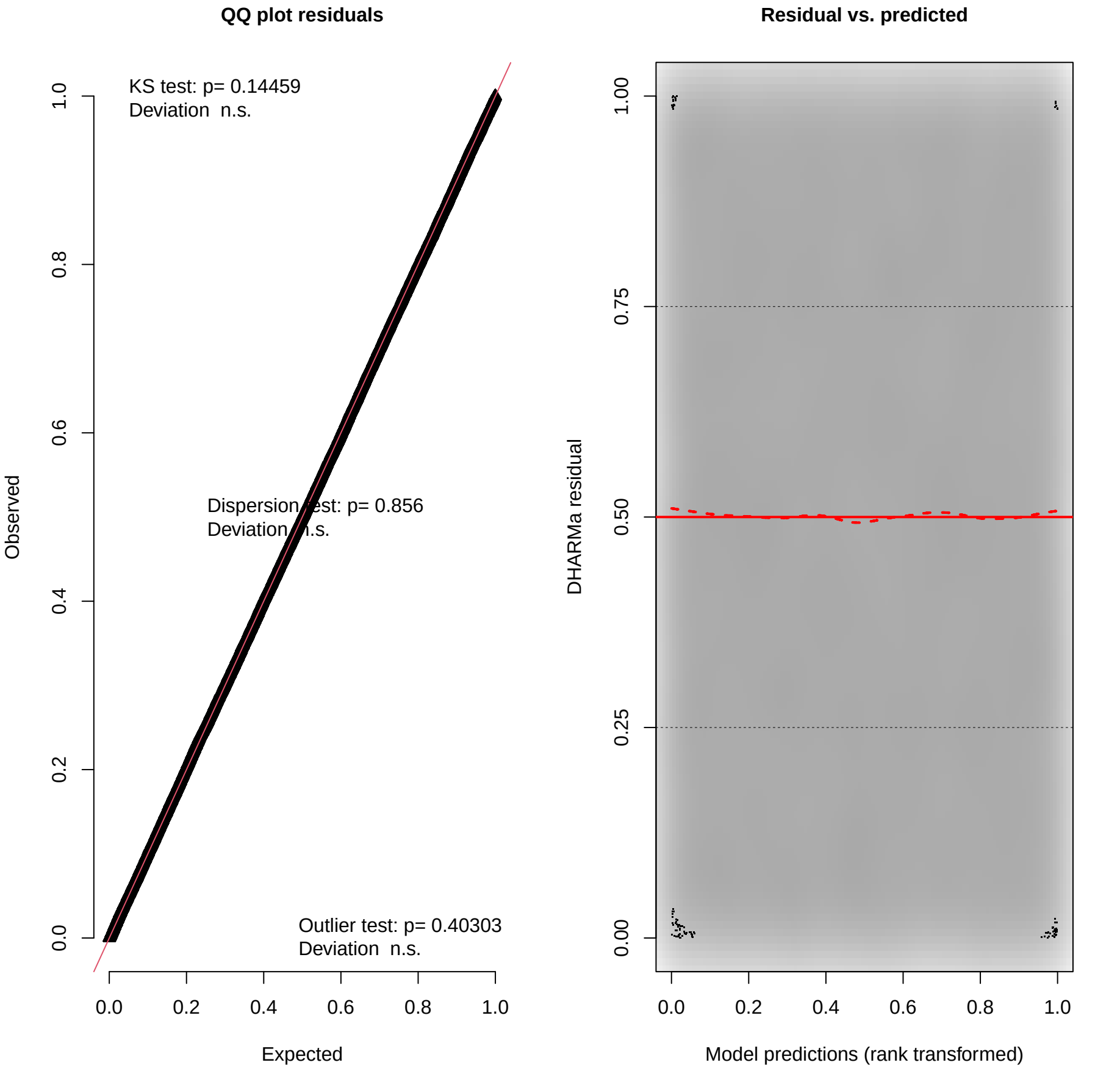

*Pinus nigra*

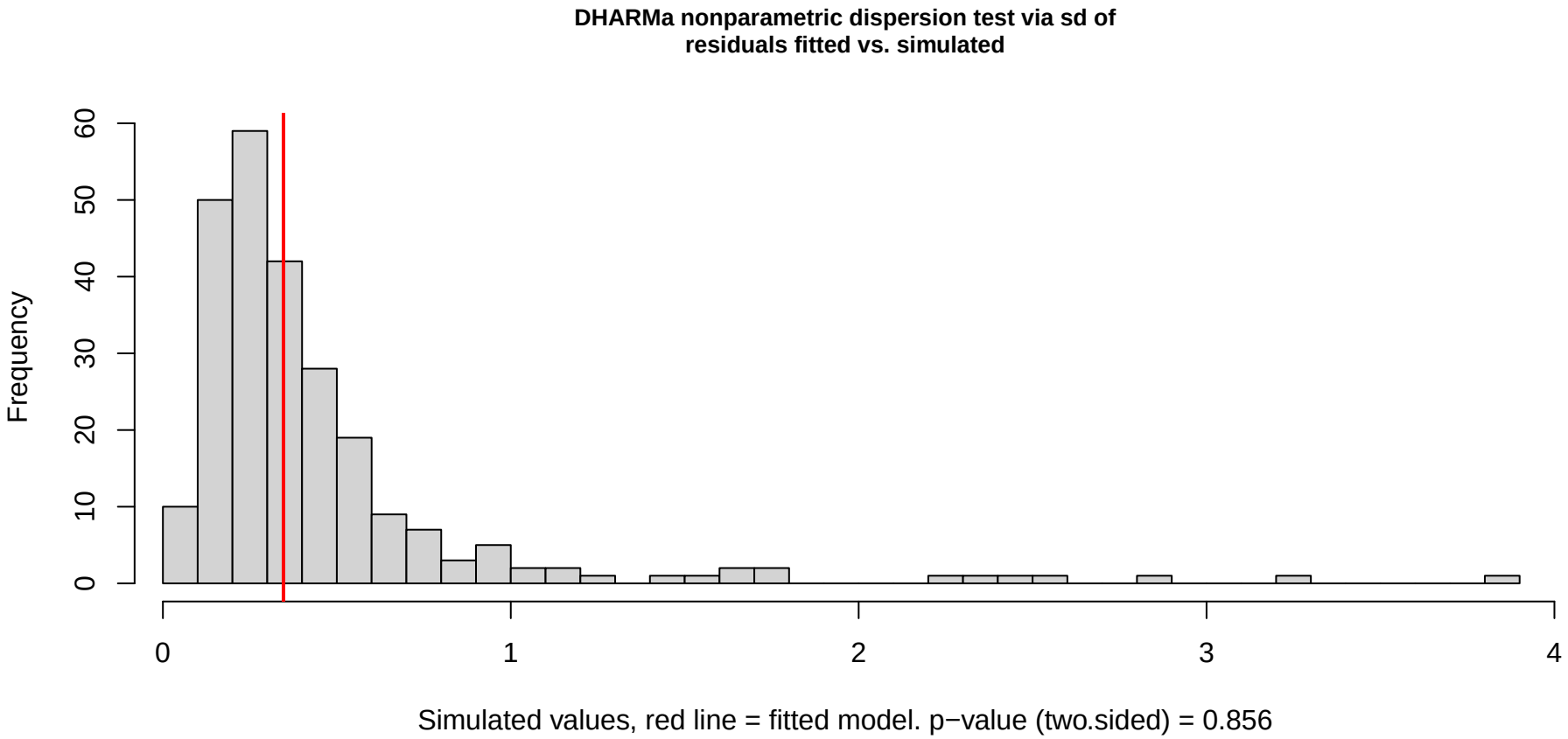
DHARMa nonparametric dispersion test via sd of residuals fitted vs. simulated
Frequency
0
10
20
30
40
50
60
0
1
2
3
4
Simulated values, red line = fitted model. p−value (two.sided) = 0.856

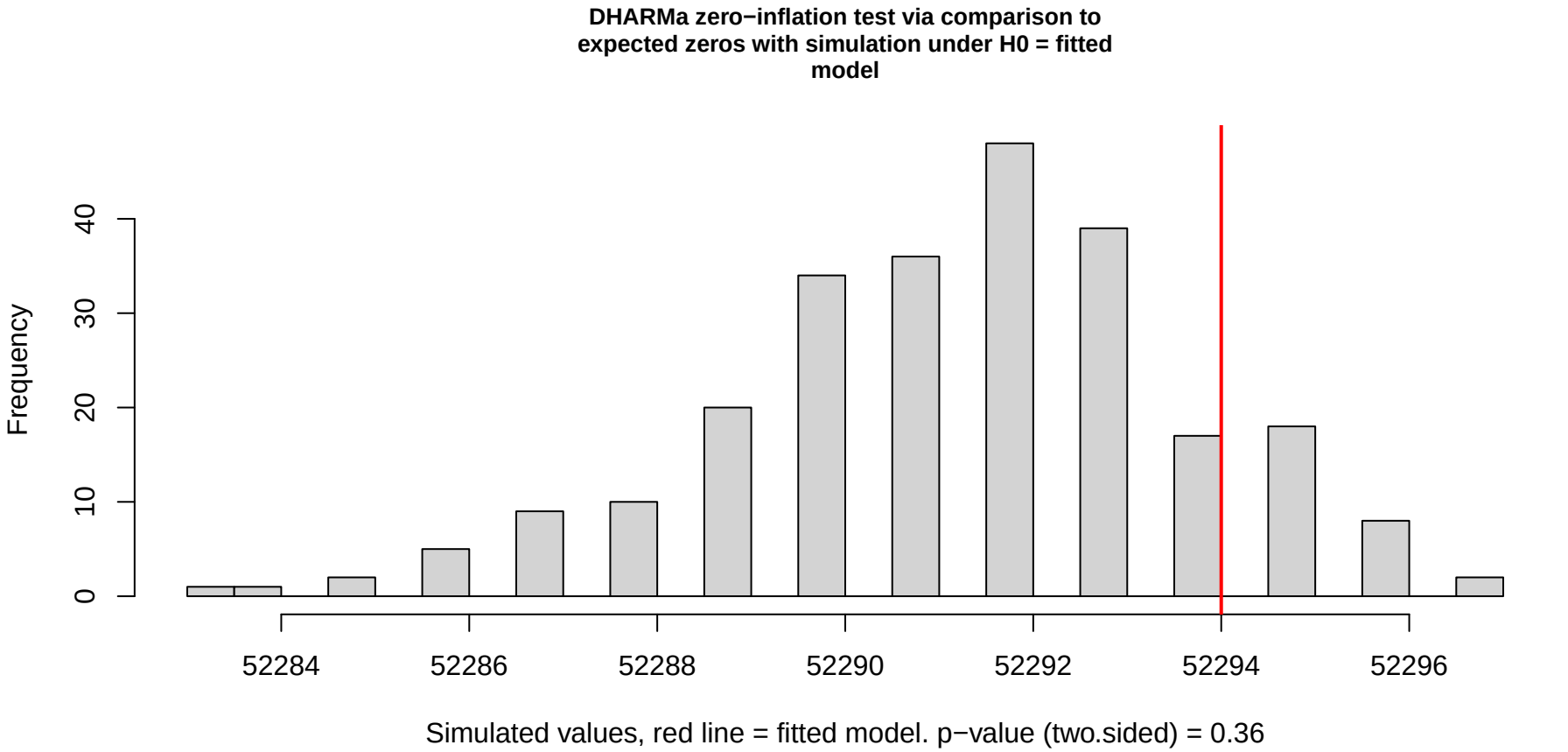
DHARMa zero−inflation test via comparison to expected zeros with simulation under H0 = fitted model
Frequency
0
10
20
30
40
52284
52286
52288
52290
52292
52294
52296
Simulated values, red line = fitted model. p−value (two.sided) = 0.36

*Pinus nigra*

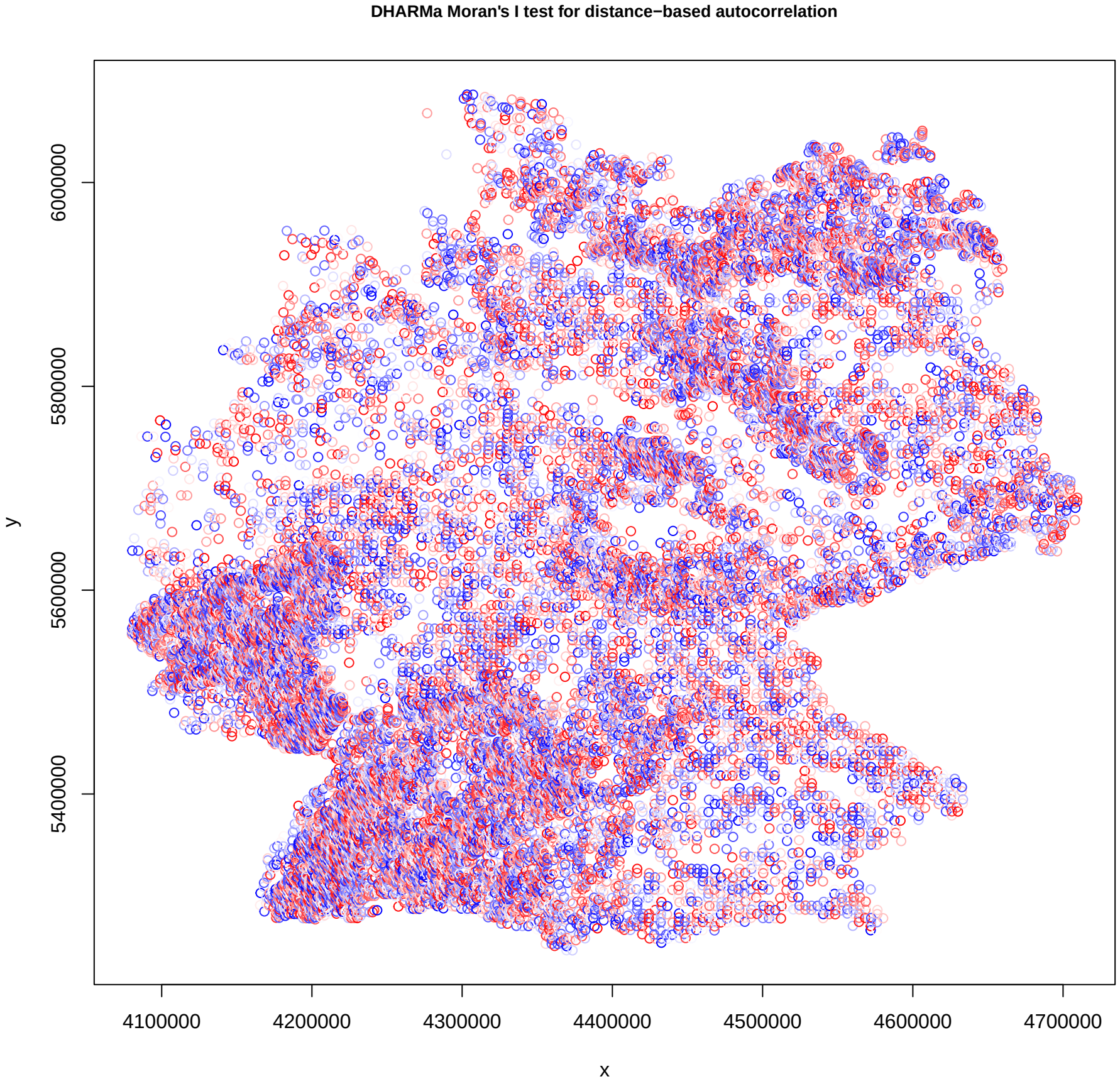
DHARMa Moran's I test for distance−based autocorrelation
y
6000000
5800000
5600000
5400000
4100000
4200000
4300000
4400000
4500000
4600000
4700000
x

*Picea abies*

DHARMa residual

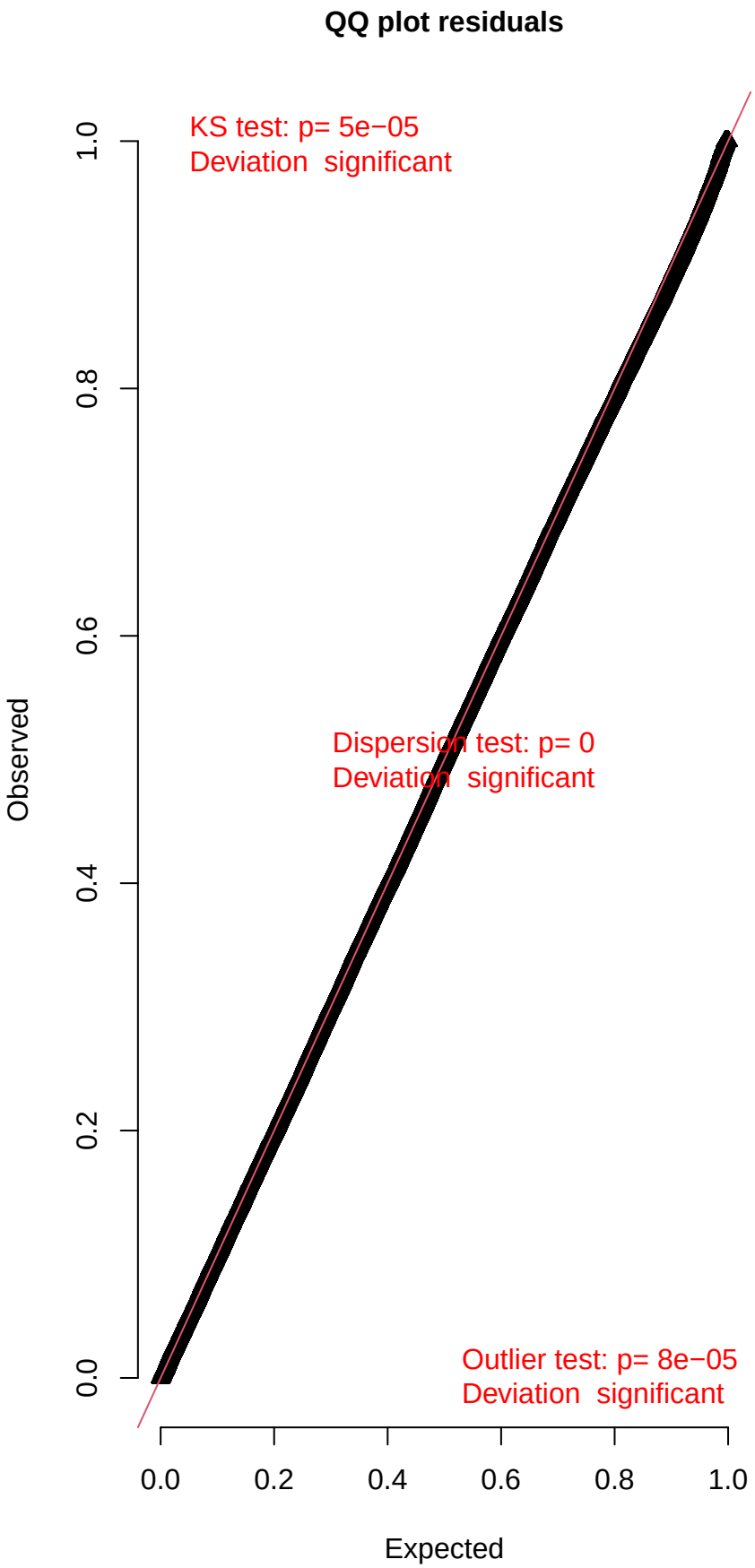


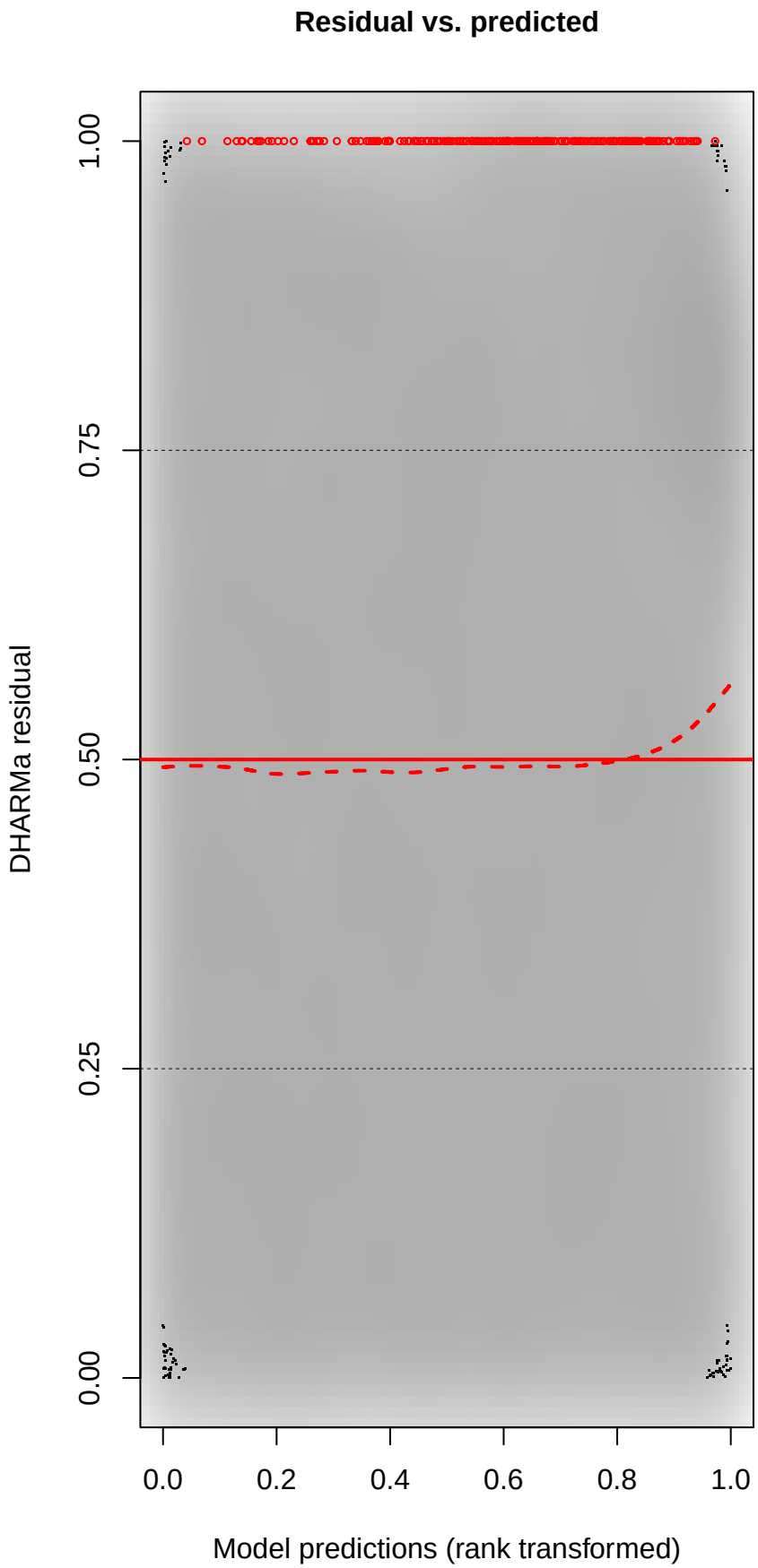

*Picea abies*

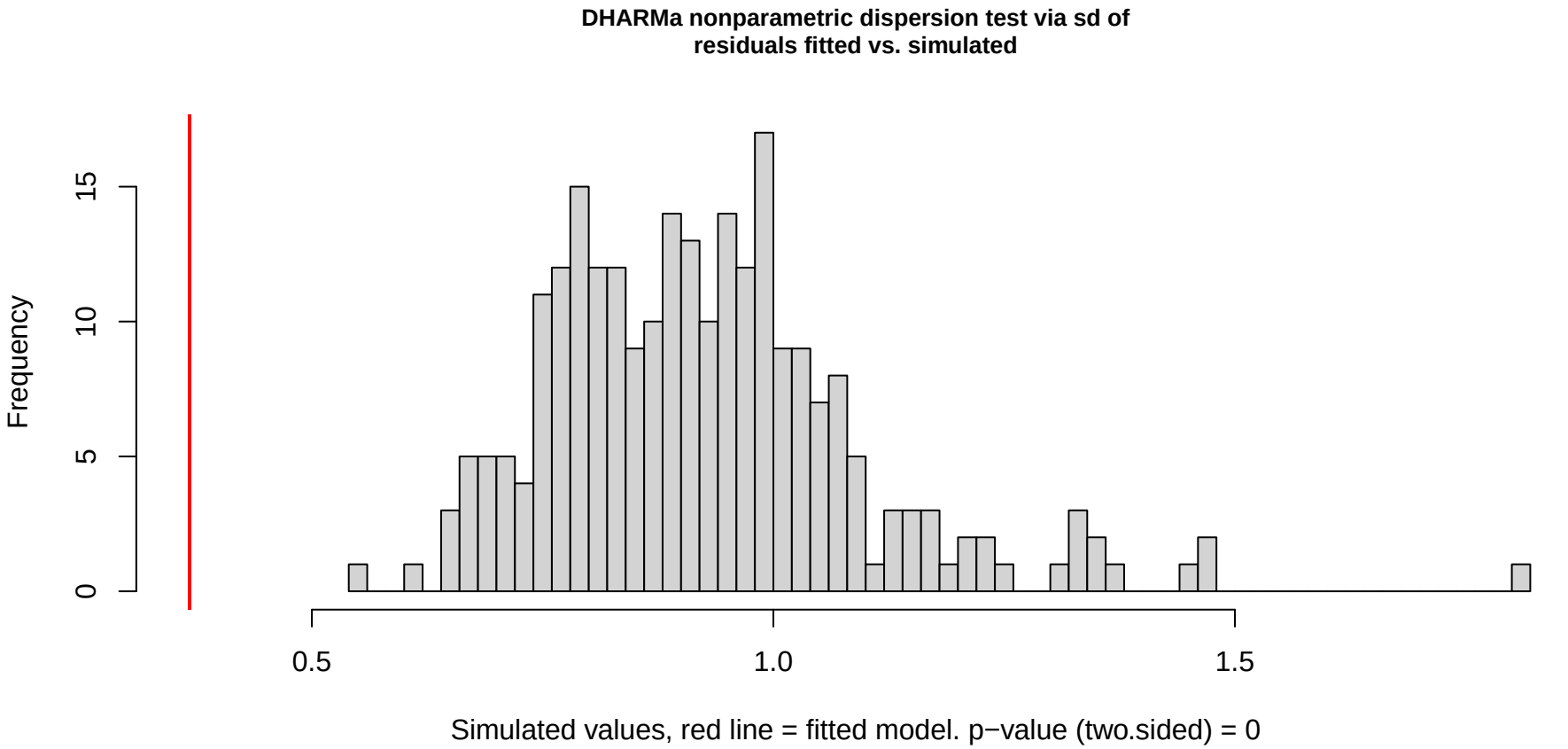
DHARMa nonparametric dispersion test via sd of residuals fitted vs. simulated
Frequency
0
5
10
15
0.5
1.0
1.5
Simulated values, red line = fitted model. p−value (two.sided) = 0

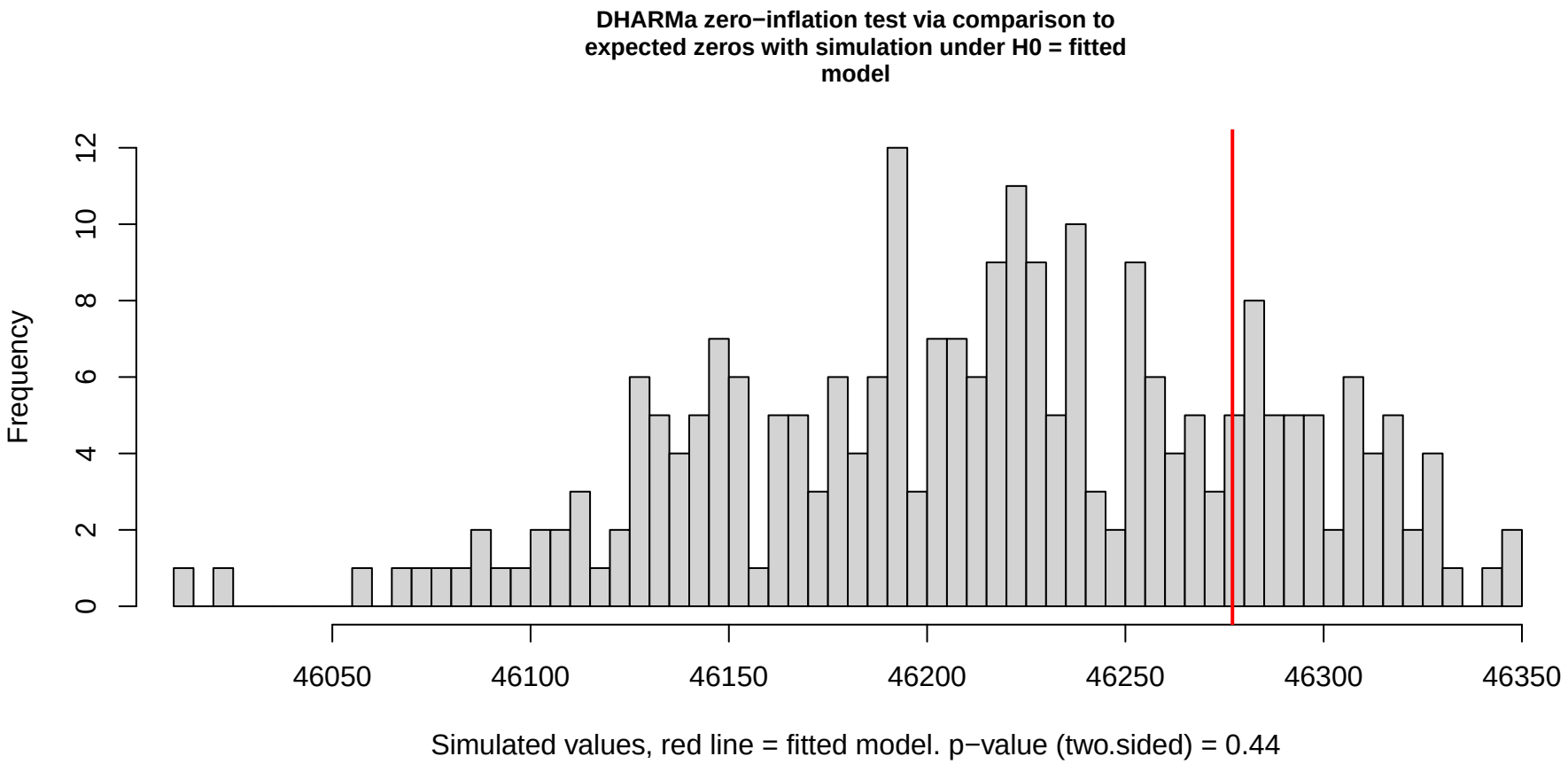
DHARMa zero−inflation test via comparison to expected zeros with simulation under H0 = fitted model
Frequency
0
2
4
6
8
10
12
46050
46100
46150
46200
46250
46300
46350
Simulated values, red line = fitted model. p−value (two.sided) = 0.44

*Picea abies*

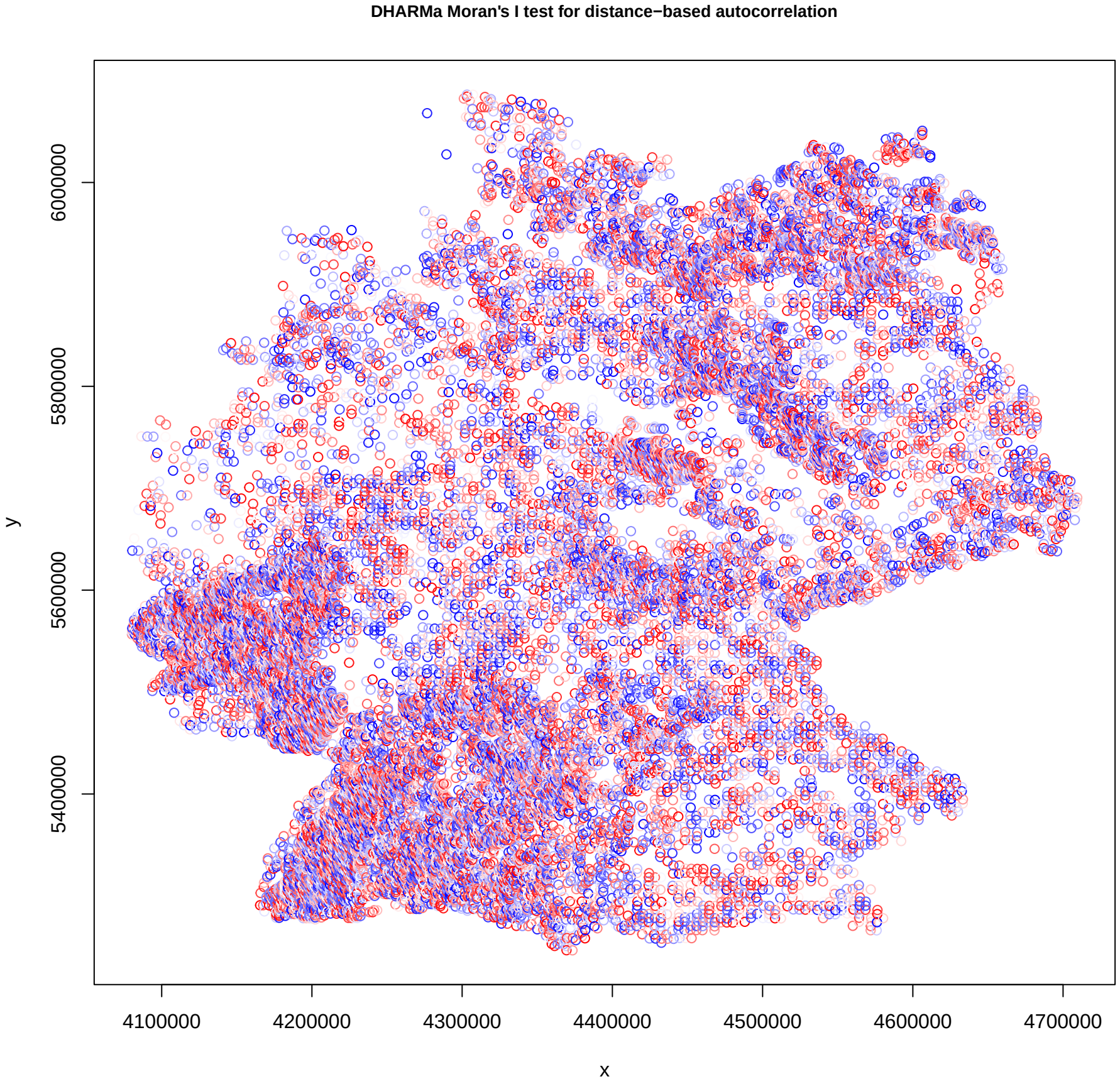
DHARMa Moran's I test for distance−based autocorrelation
y
6000000
5800000
5600000
5400000
4100000
4200000
4300000
4400000
4500000
4600000
4700000
x

*Picea sitchensis*

DHARMa residual

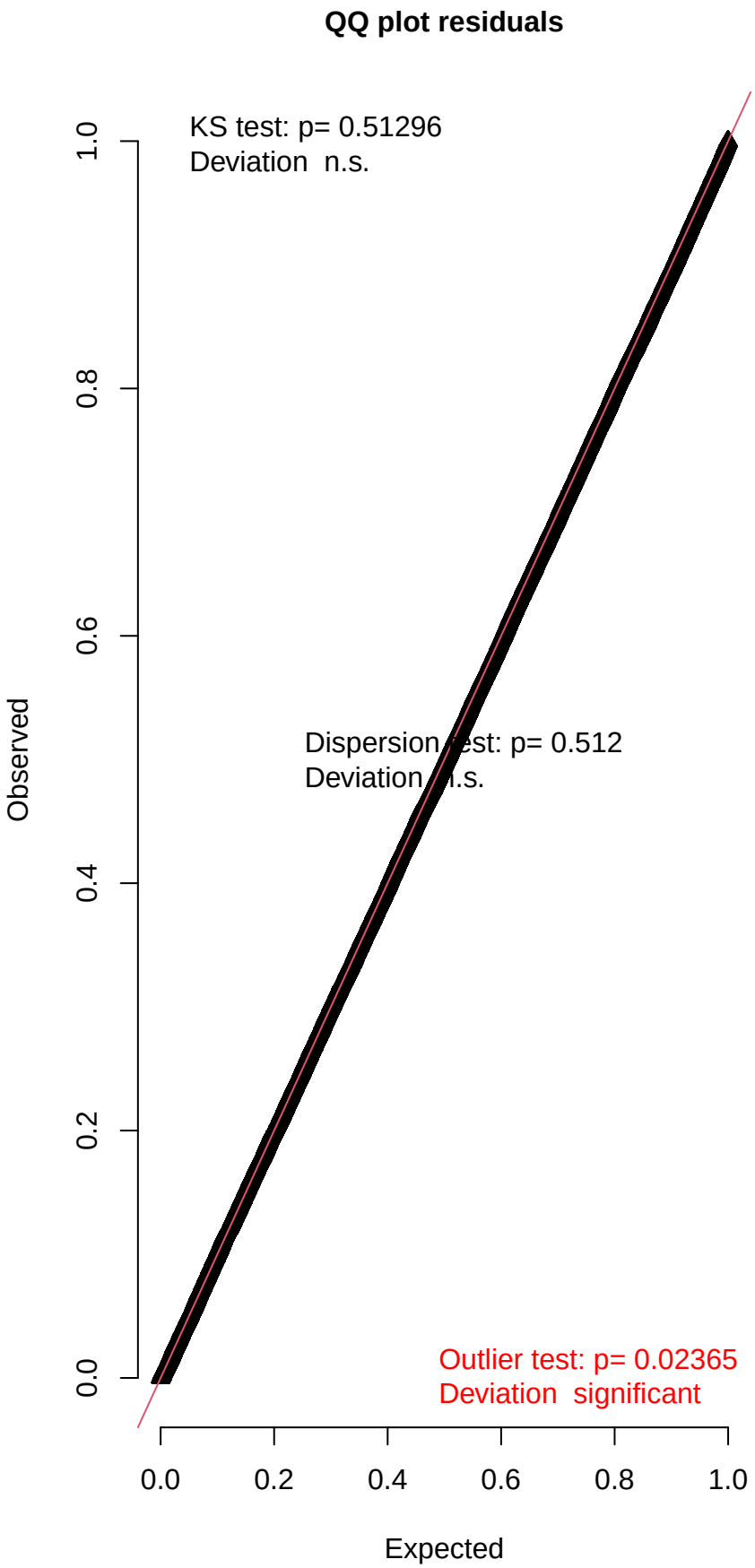


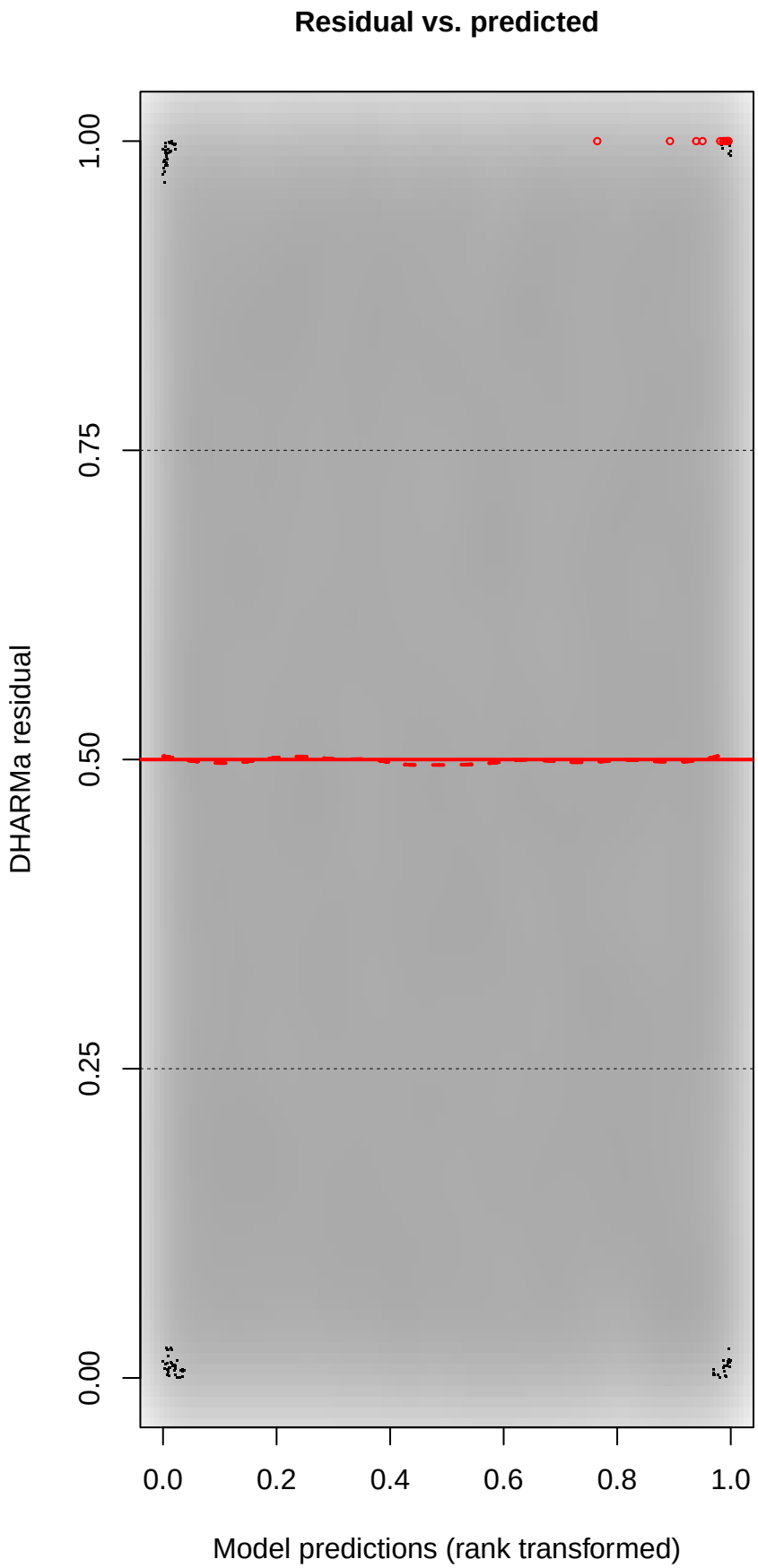

*Picea sitchensis*

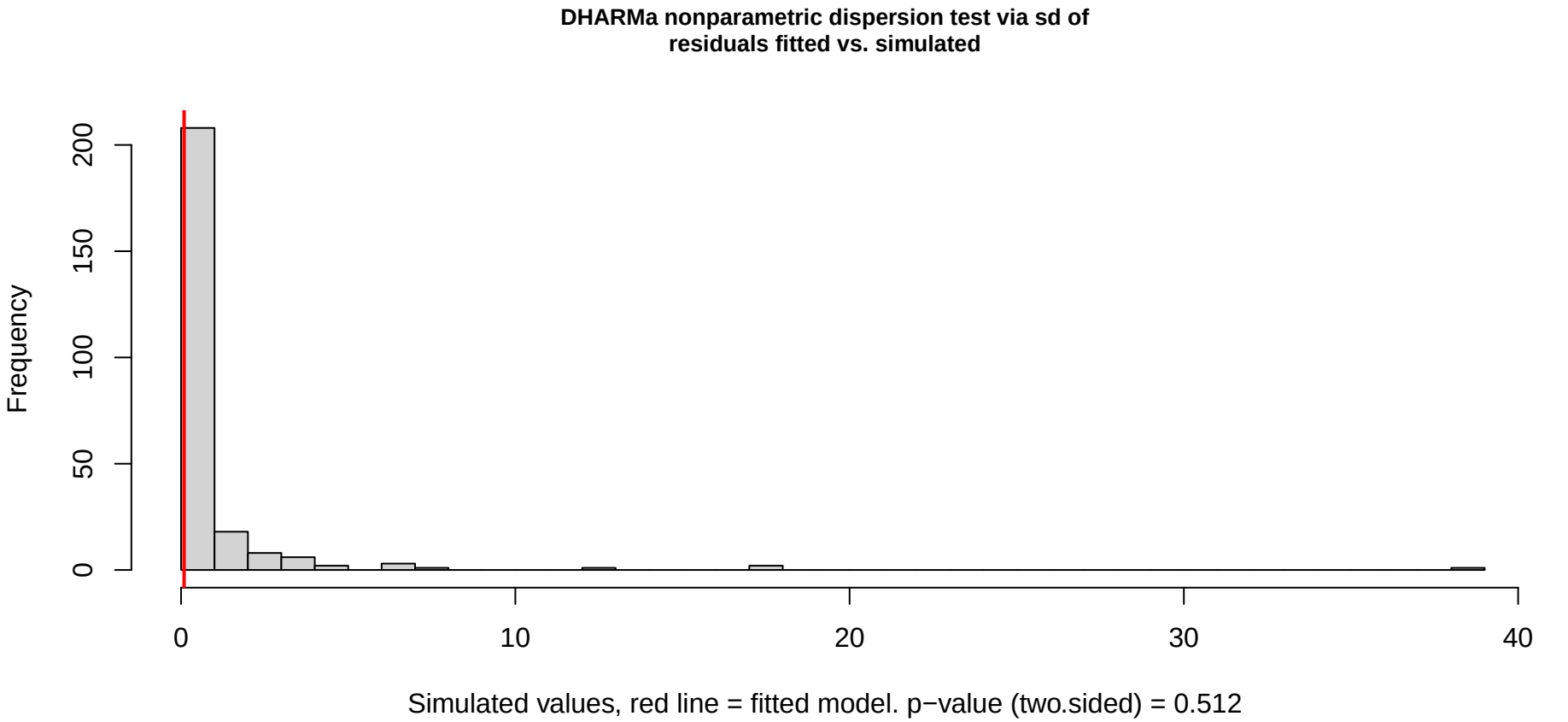


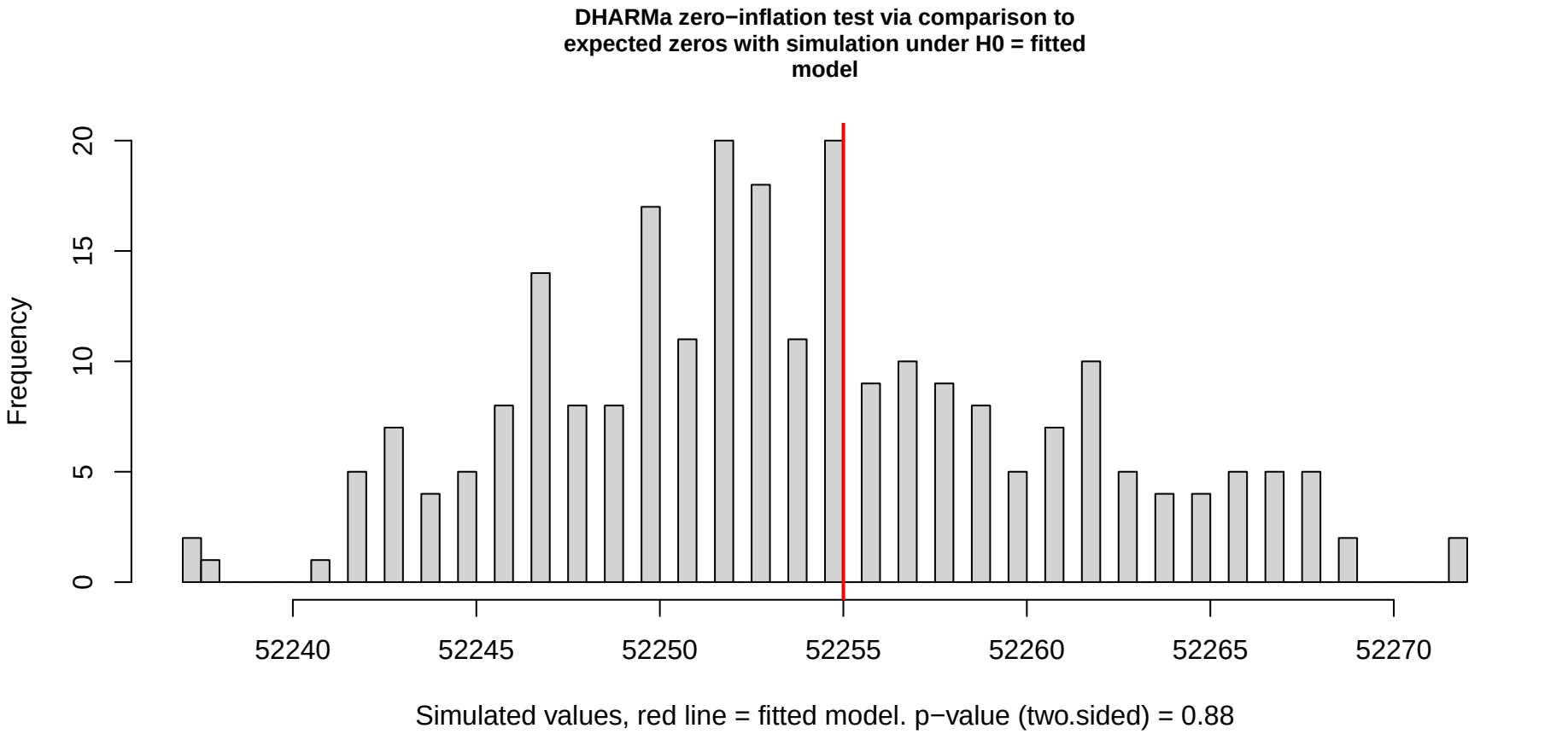

*Picea sitchensis*

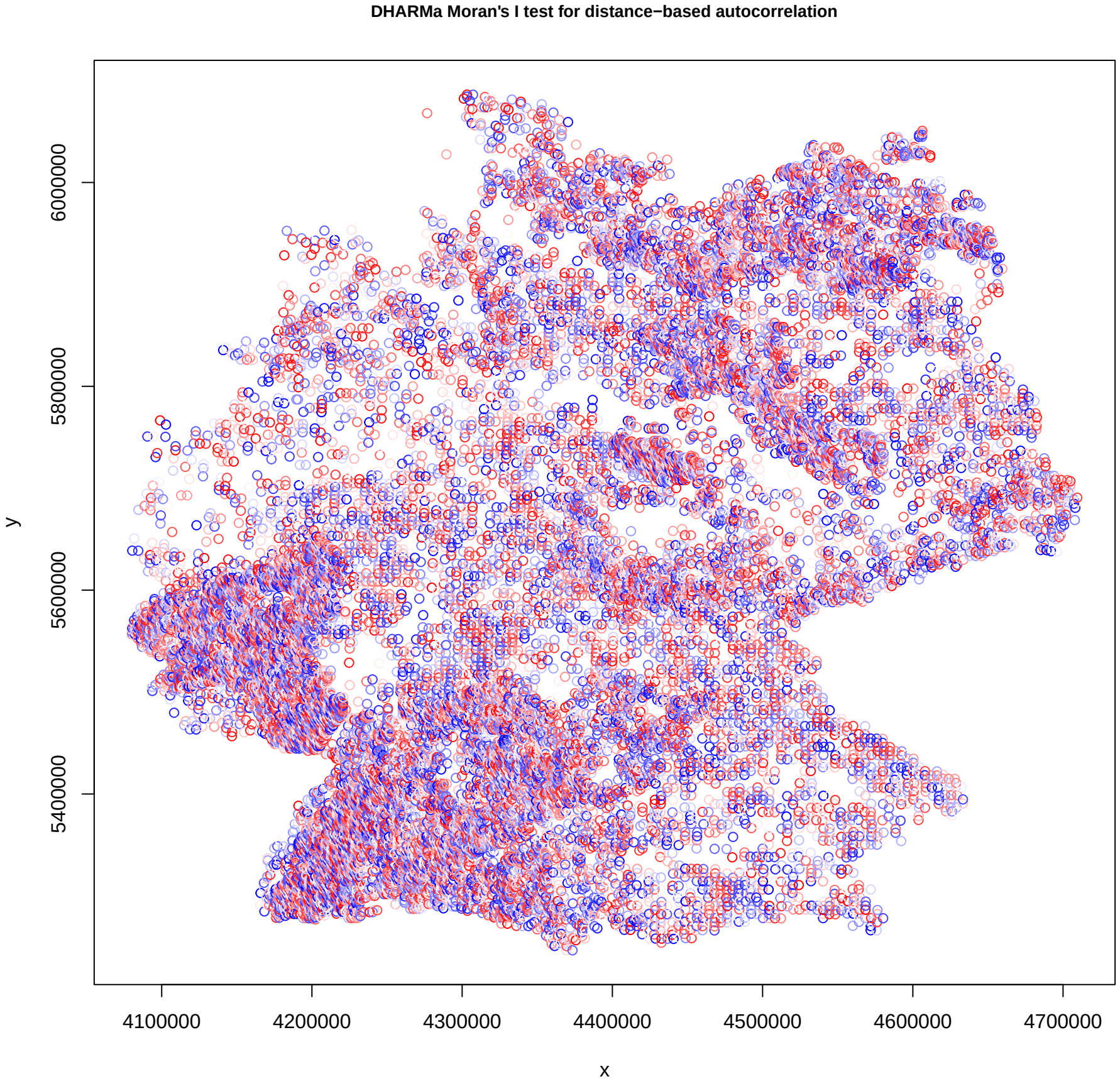

*Abies alba*

DHARMa residual

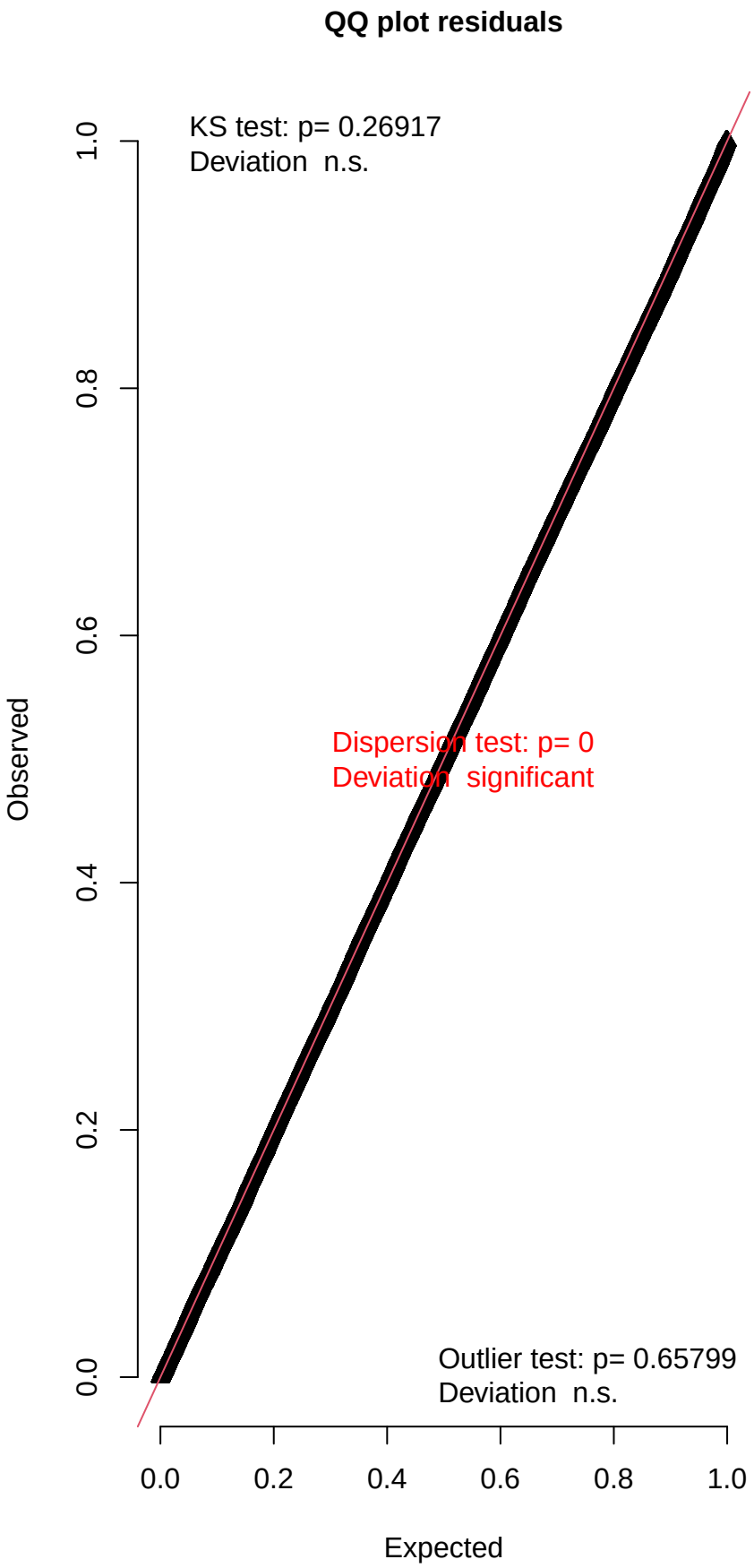


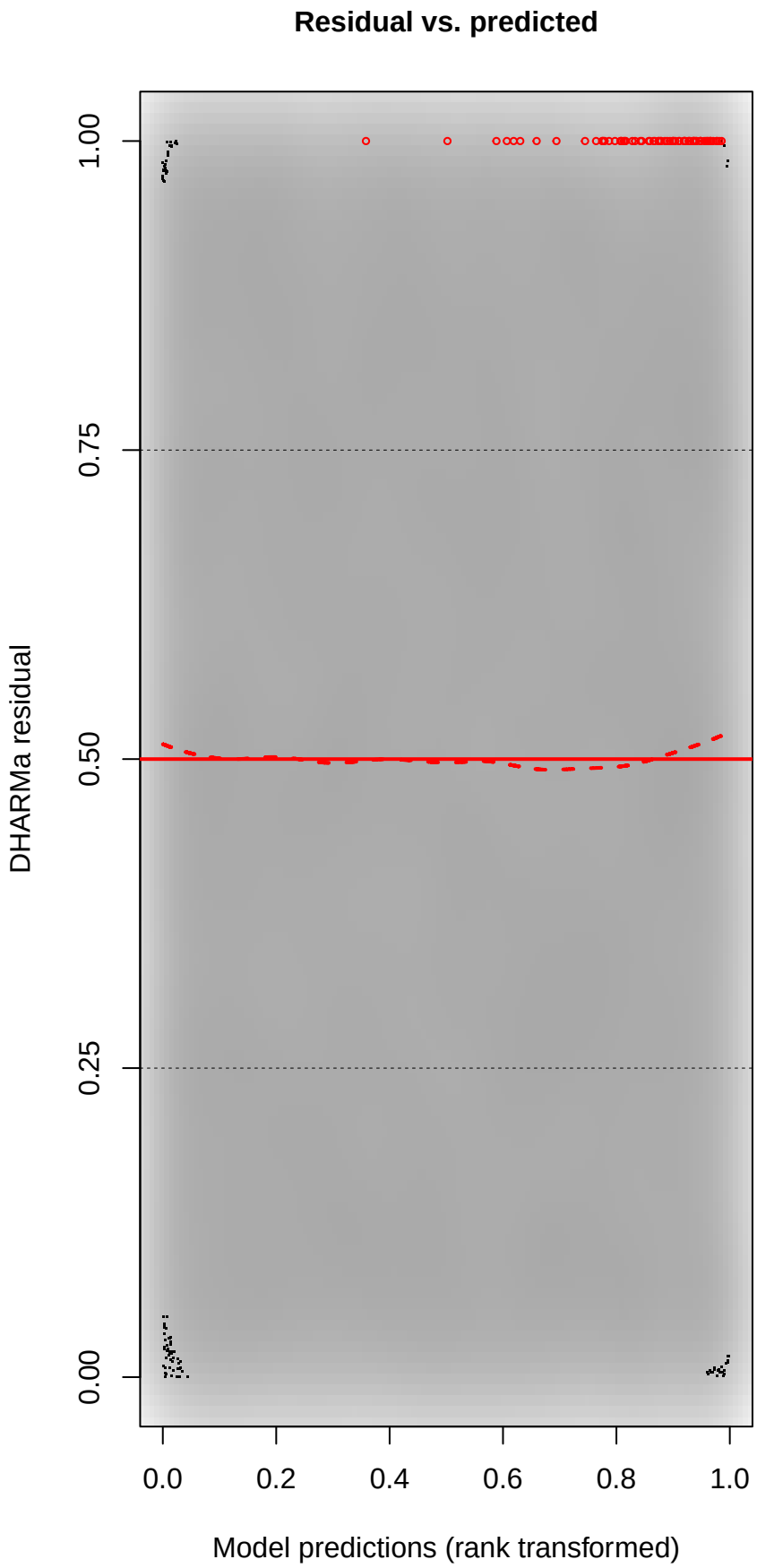

*Abies alba*

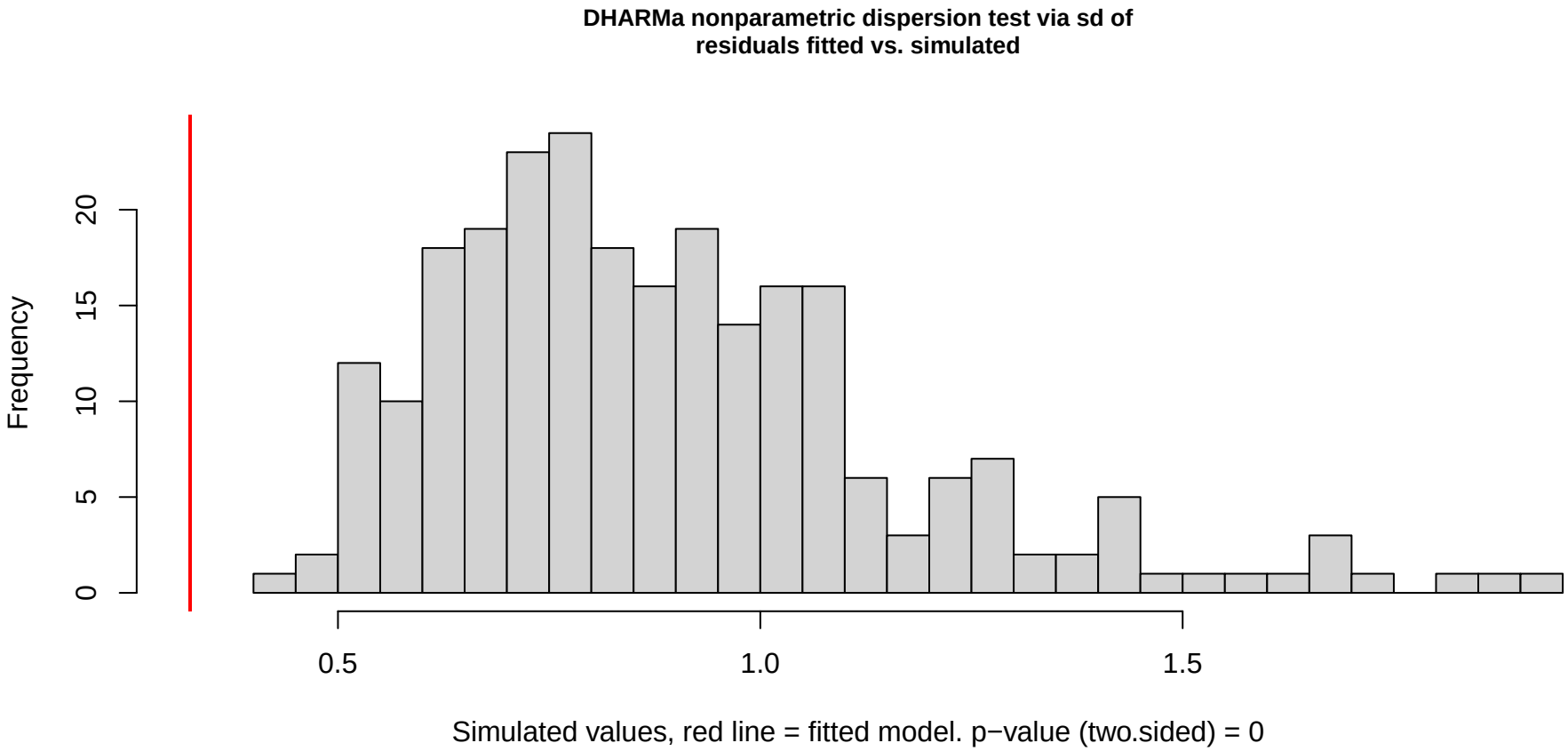
DHARMa nonparametric dispersion test via sd of residuals fitted vs. simulated
Frequency
0
5
10
15
20
0.5
1.0
1.5
Simulated values, red line = fitted model. p−value (two.sided) = 0

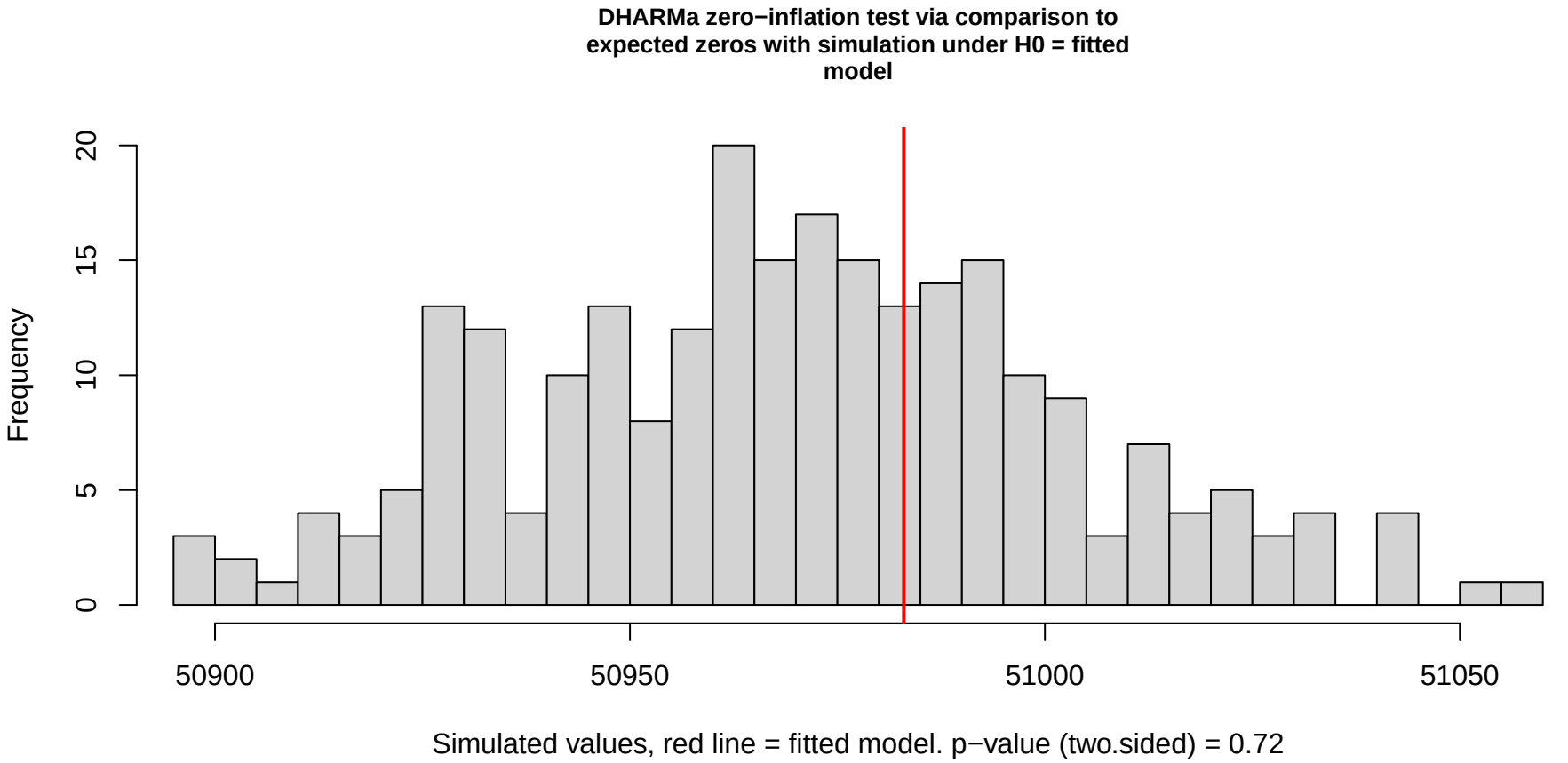
DHARMa zero−inflation test via comparison to expected zeros with simulation under H0 = fitted model
Frequency
0
5
10
15
20
50900
50950
51000
51050
Simulated values, red line = fitted model. p−value (two.sided) = 0.72

*Abies alba*

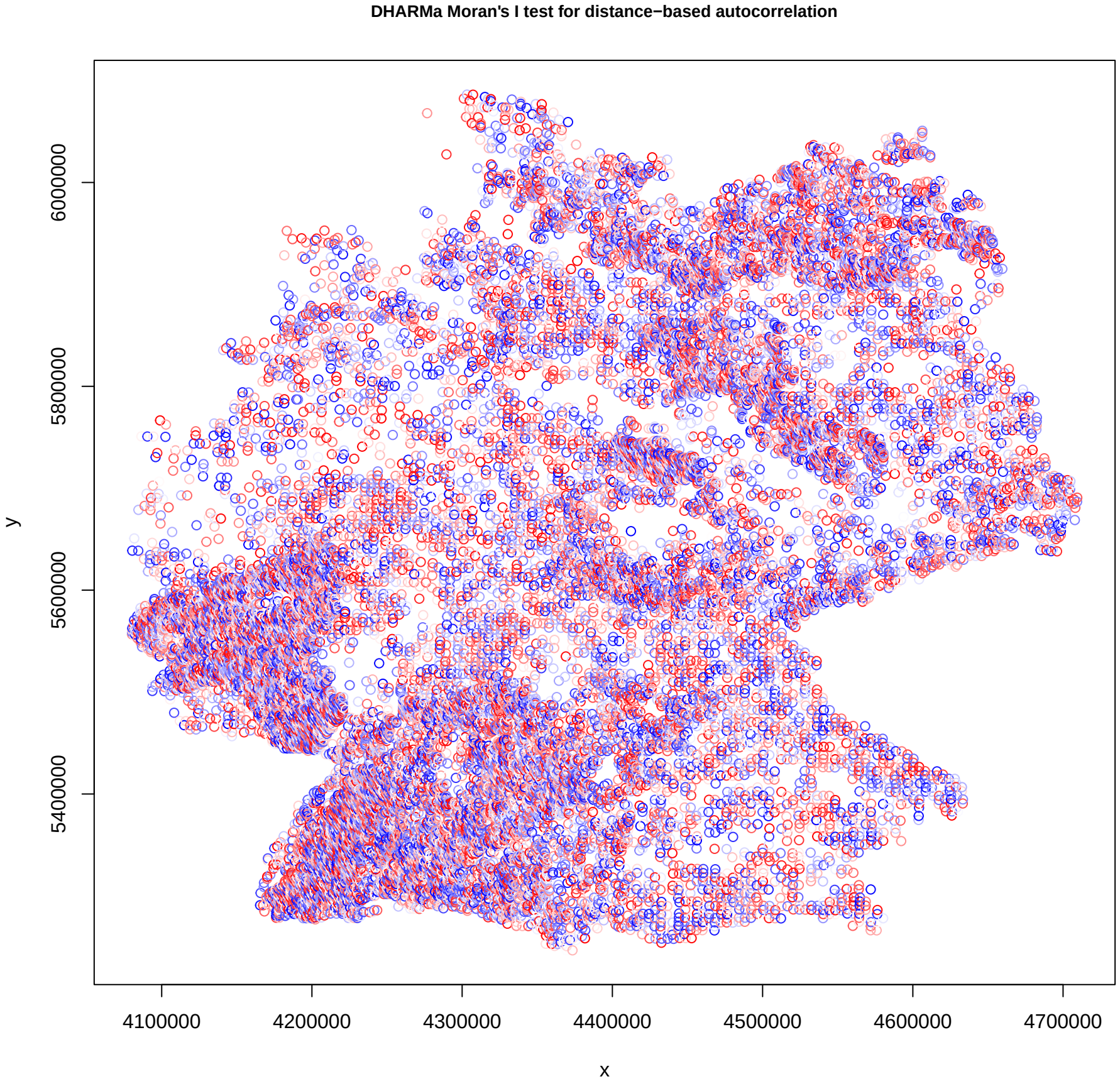
DHARMa Moran's I test for distance−based autocorrelation
y
6000000
5800000
5600000
5400000
4100000
4200000
4300000
4400000
4500000
4600000
4700000
x

*Abies grandis*

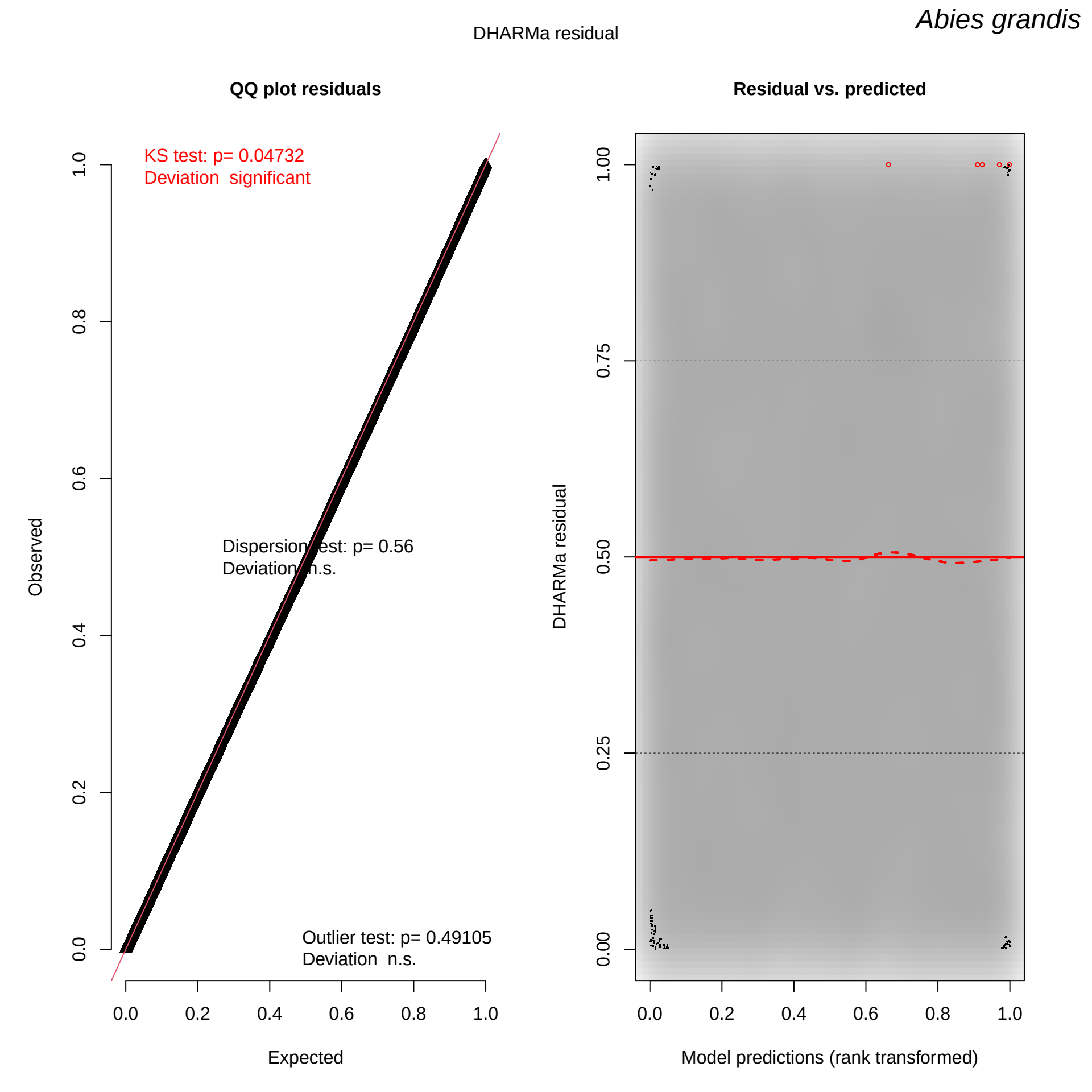

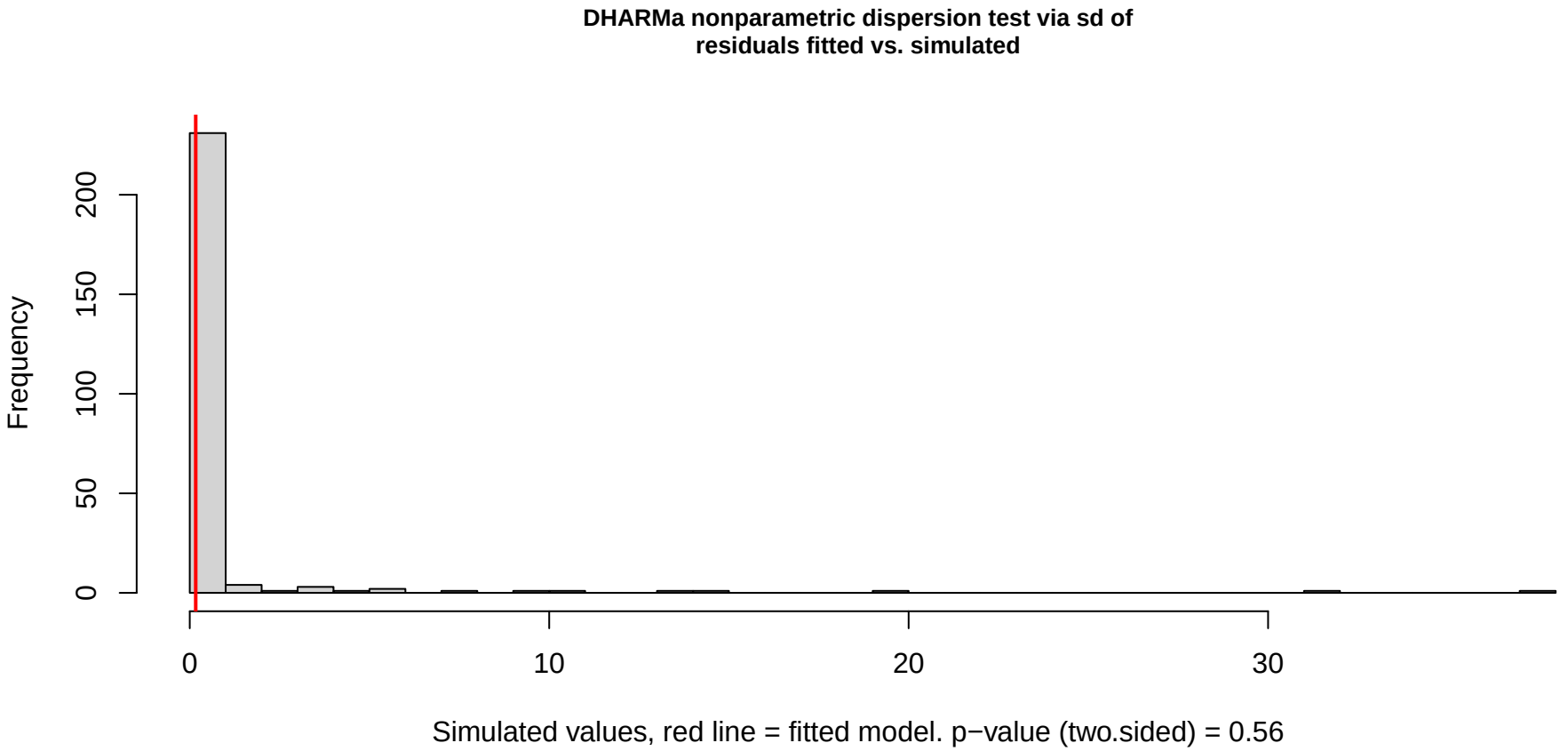
DHARMa nonparametric dispersion test via sd of residuals fitted vs. simulated
Frequency
0
50
100
150
200
0
10
20
30
Simulated values, red line = fitted model. p−value (two.sided) = 0.56

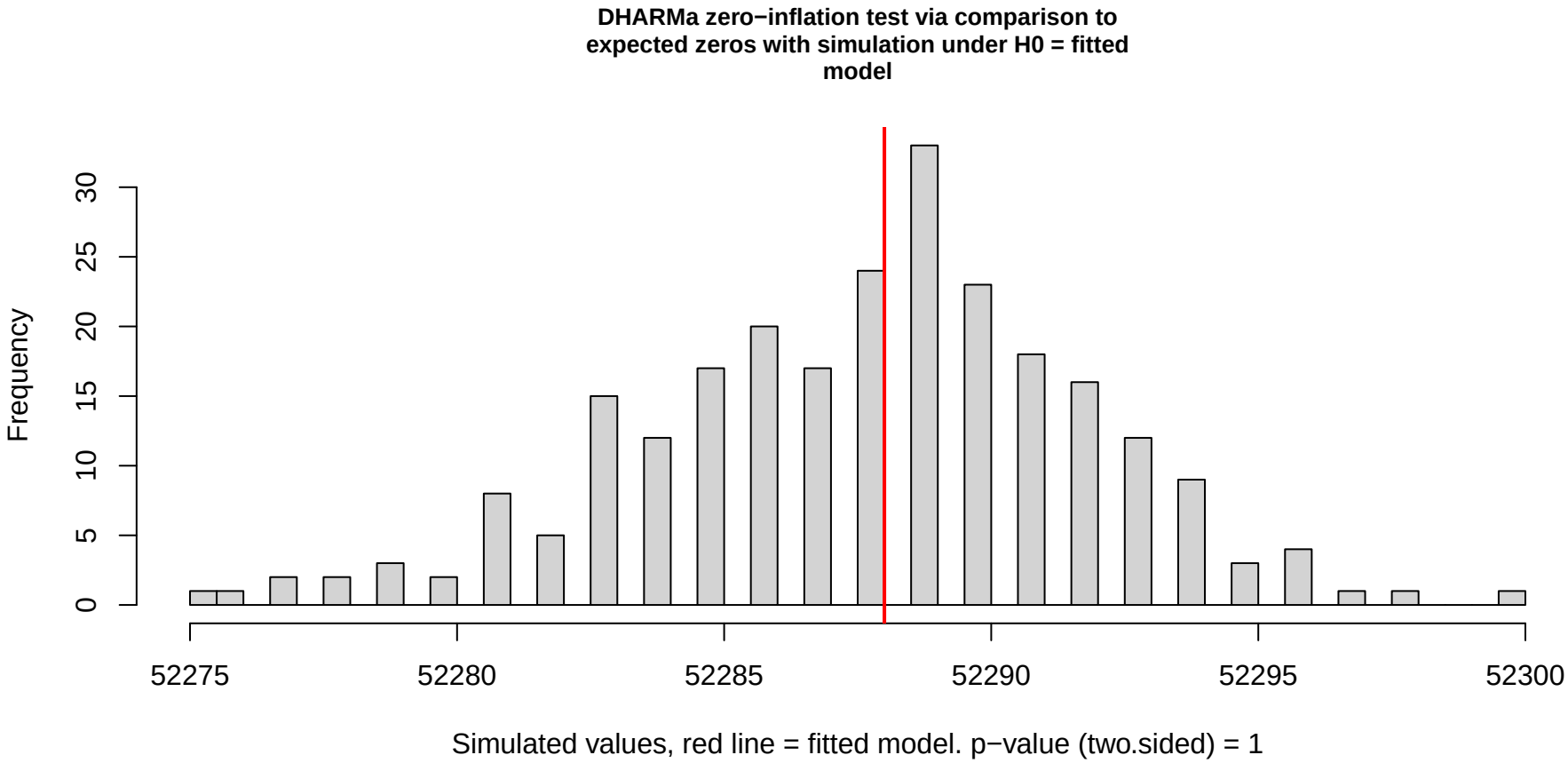
DHARMa zero−inflation test via comparison to expected zeros with simulation under H0 = fitted model
Frequency
0
5
10
15
20
25
30
52275
52280
52285
52290
52295
52300
Simulated values, red line = fitted model. p−value (two.sided) = 1

*Abies grandis*

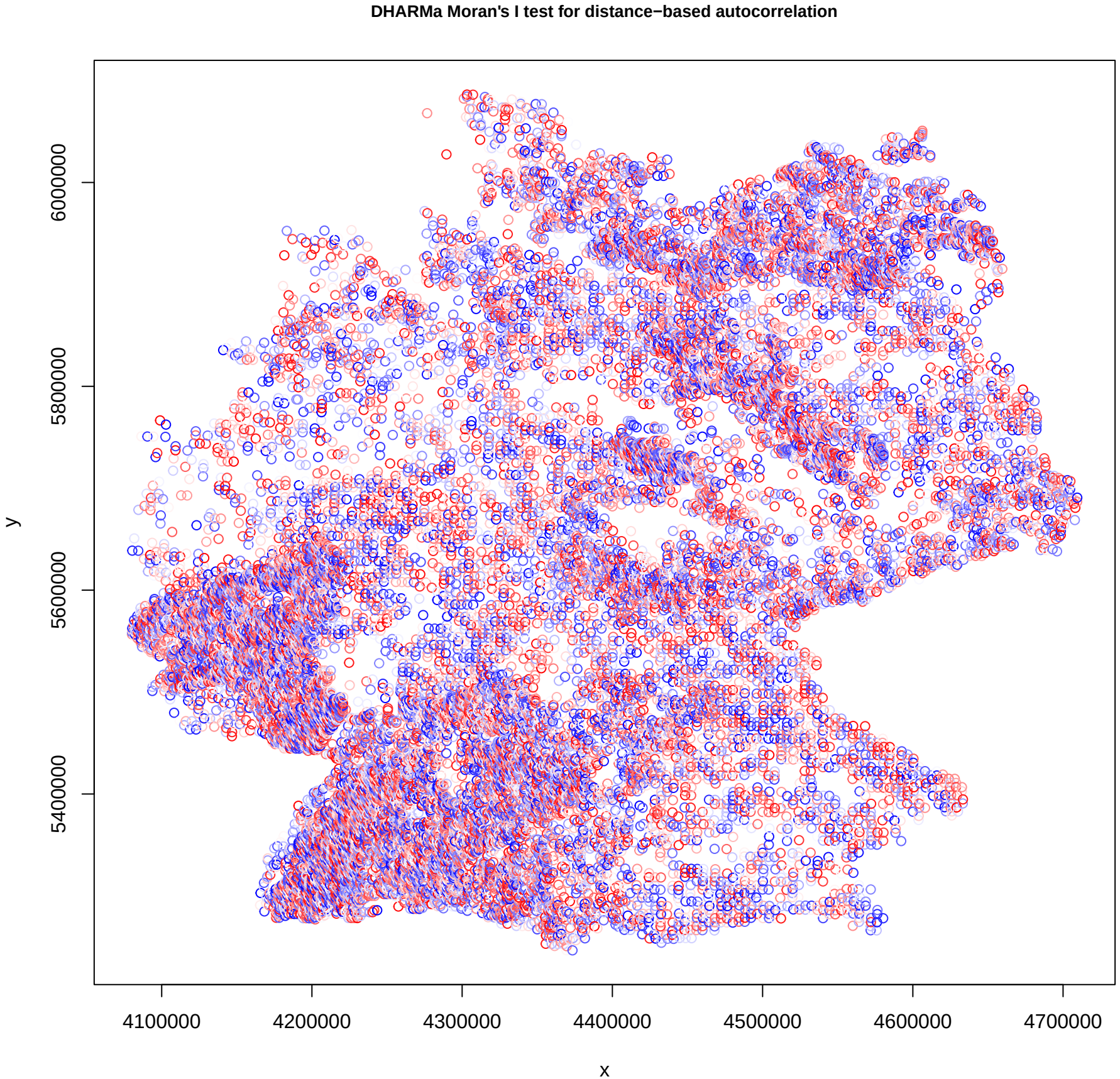

*Acer campestre*

DHARMa residual

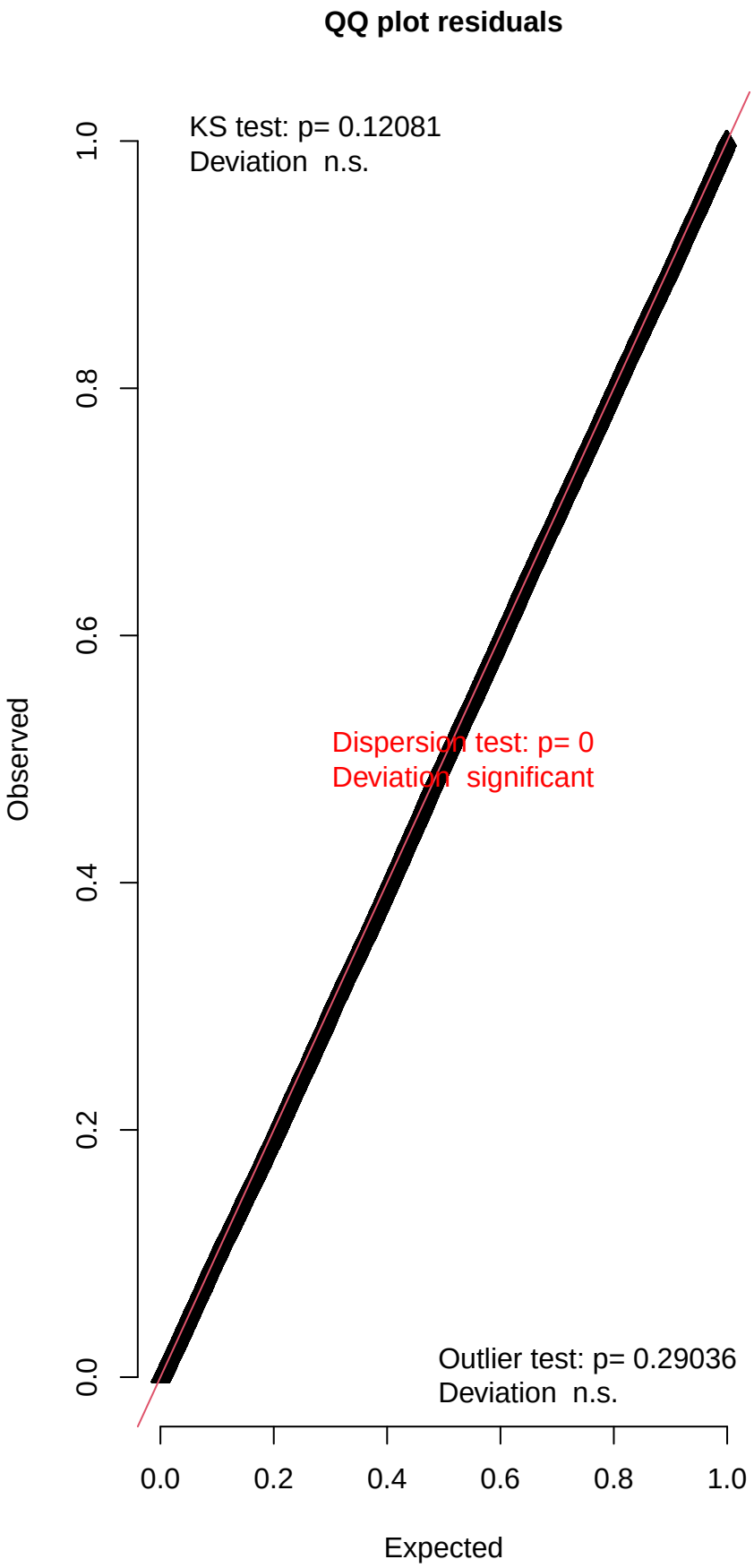


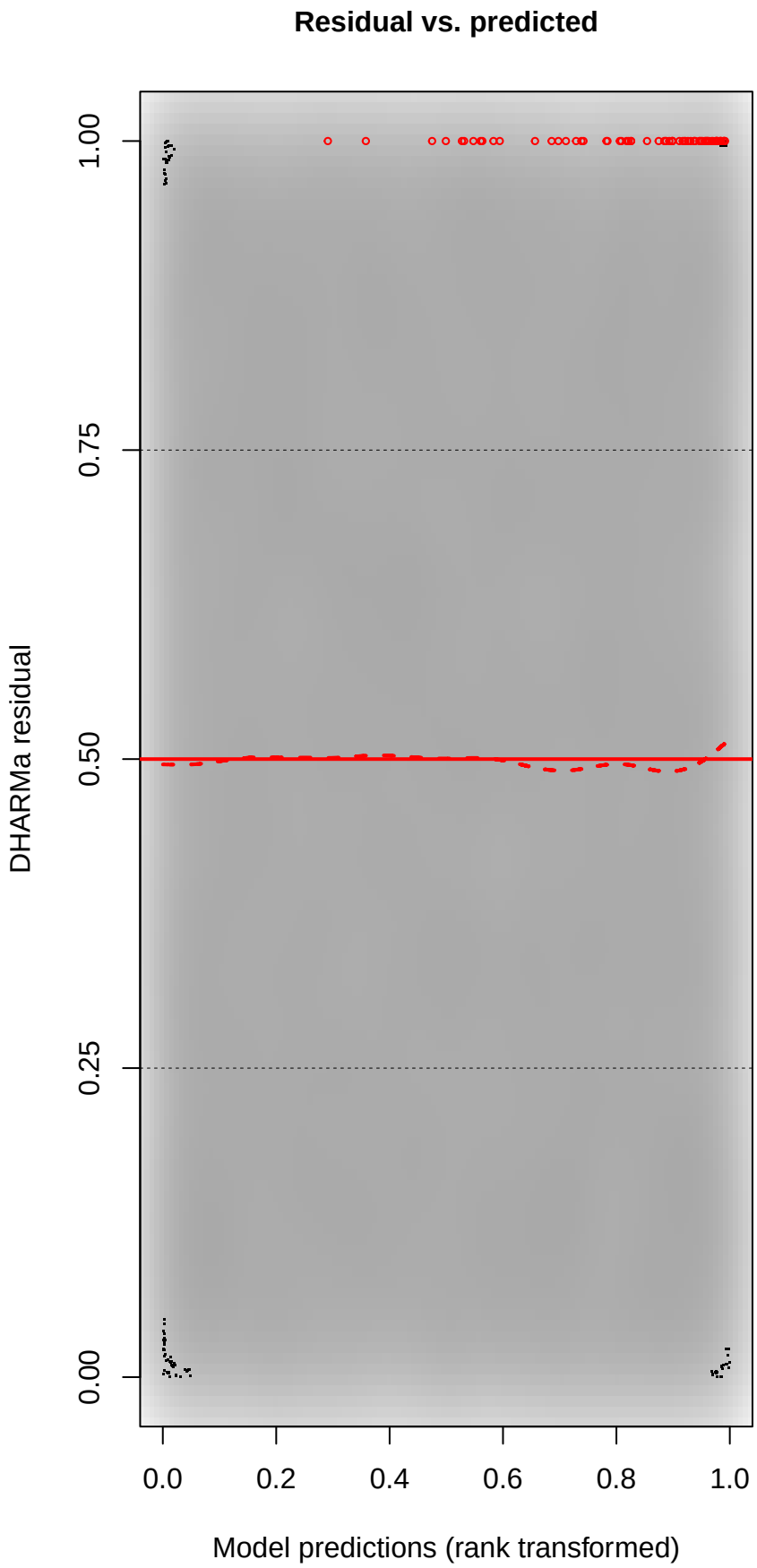

*Acer campestre*

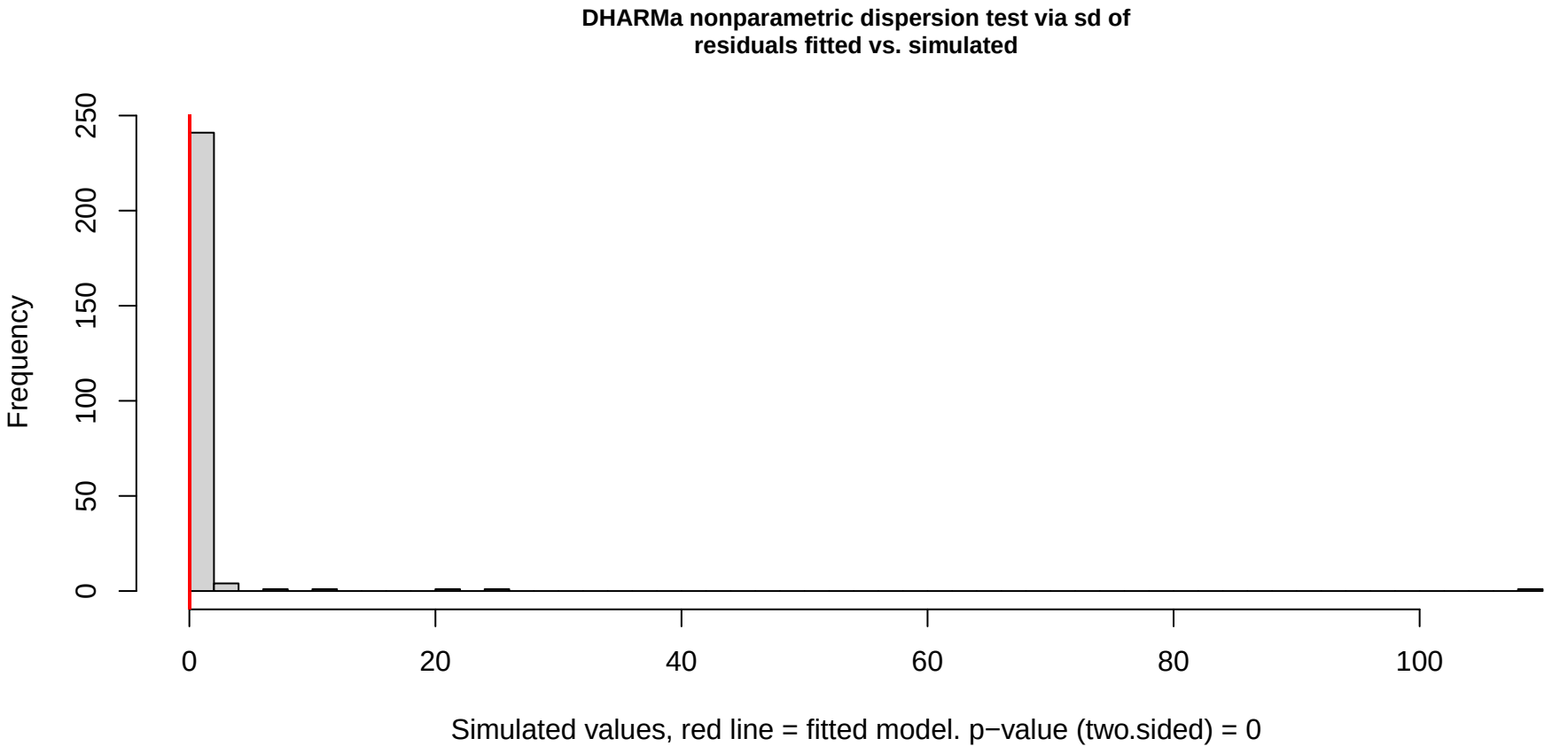


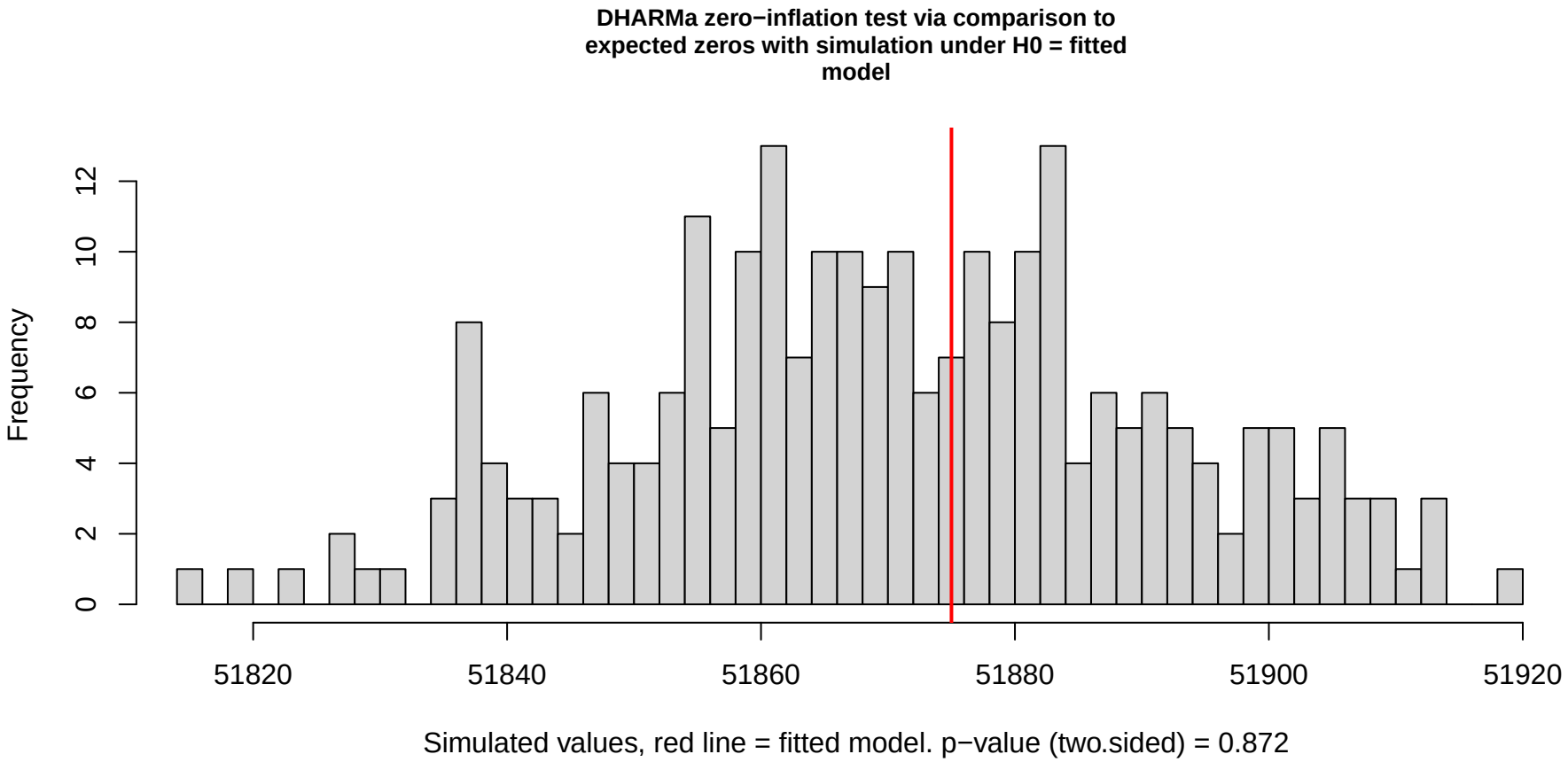

*Acer campestre*

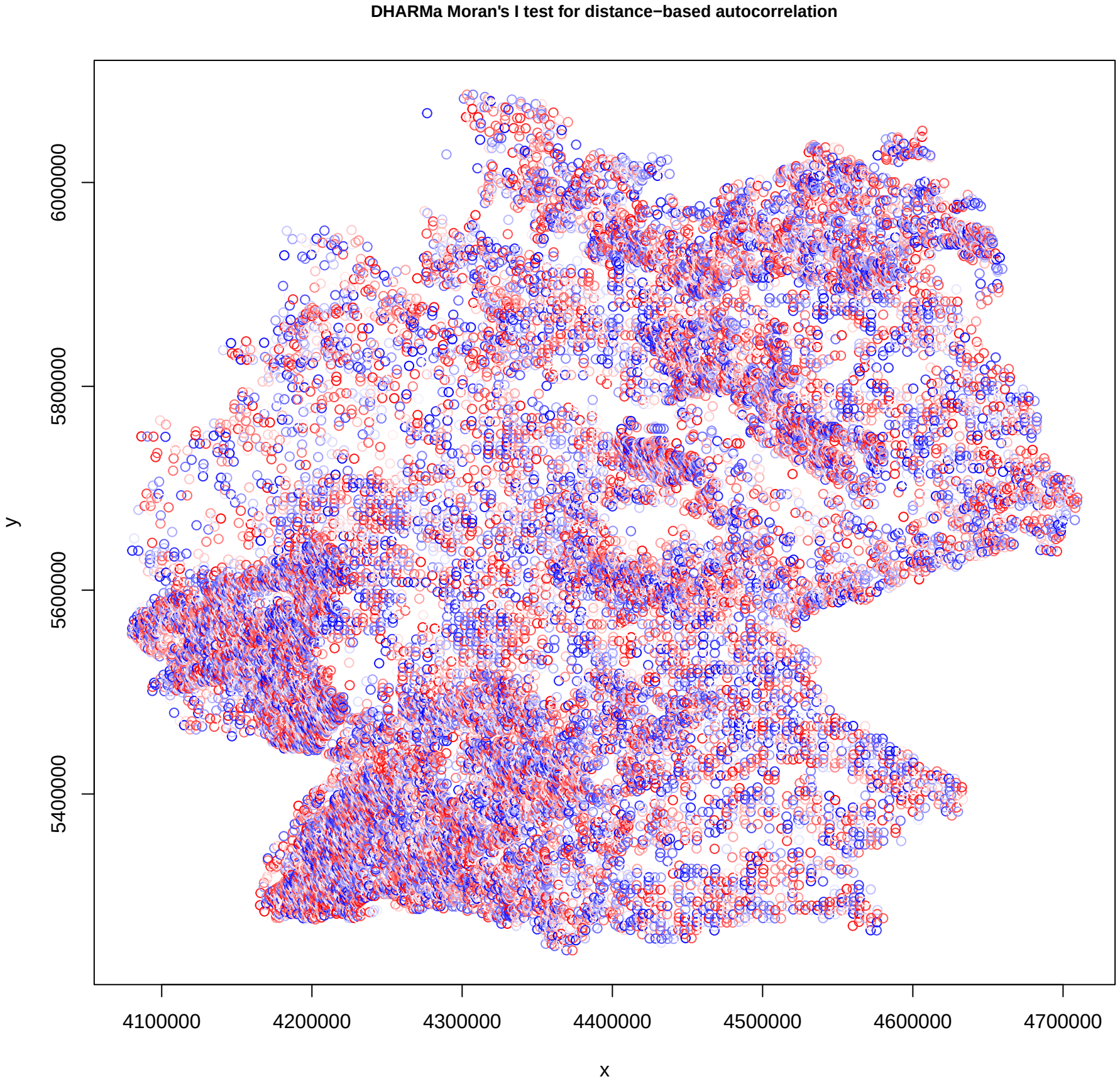

*Acer platanoides*

DHARMa residual

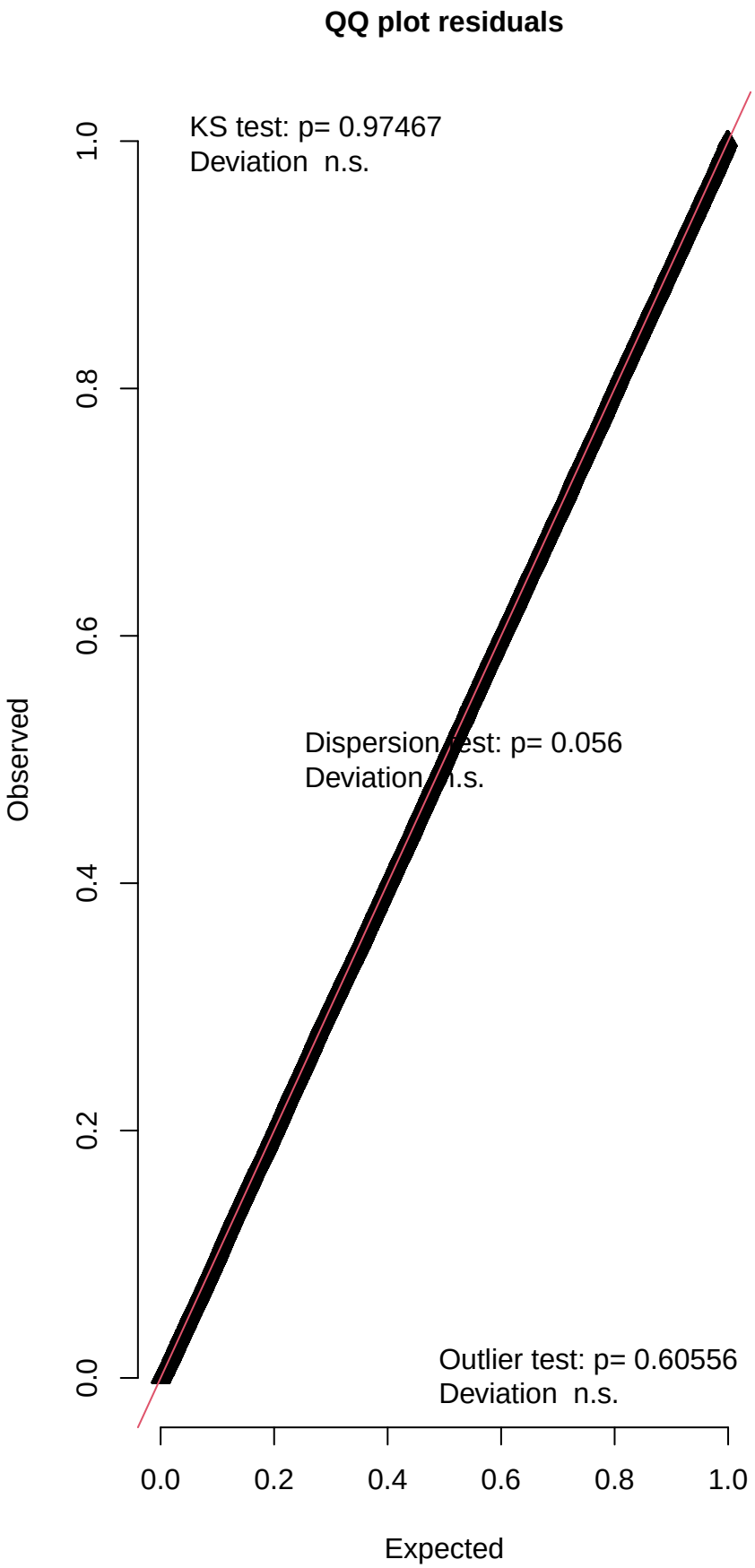


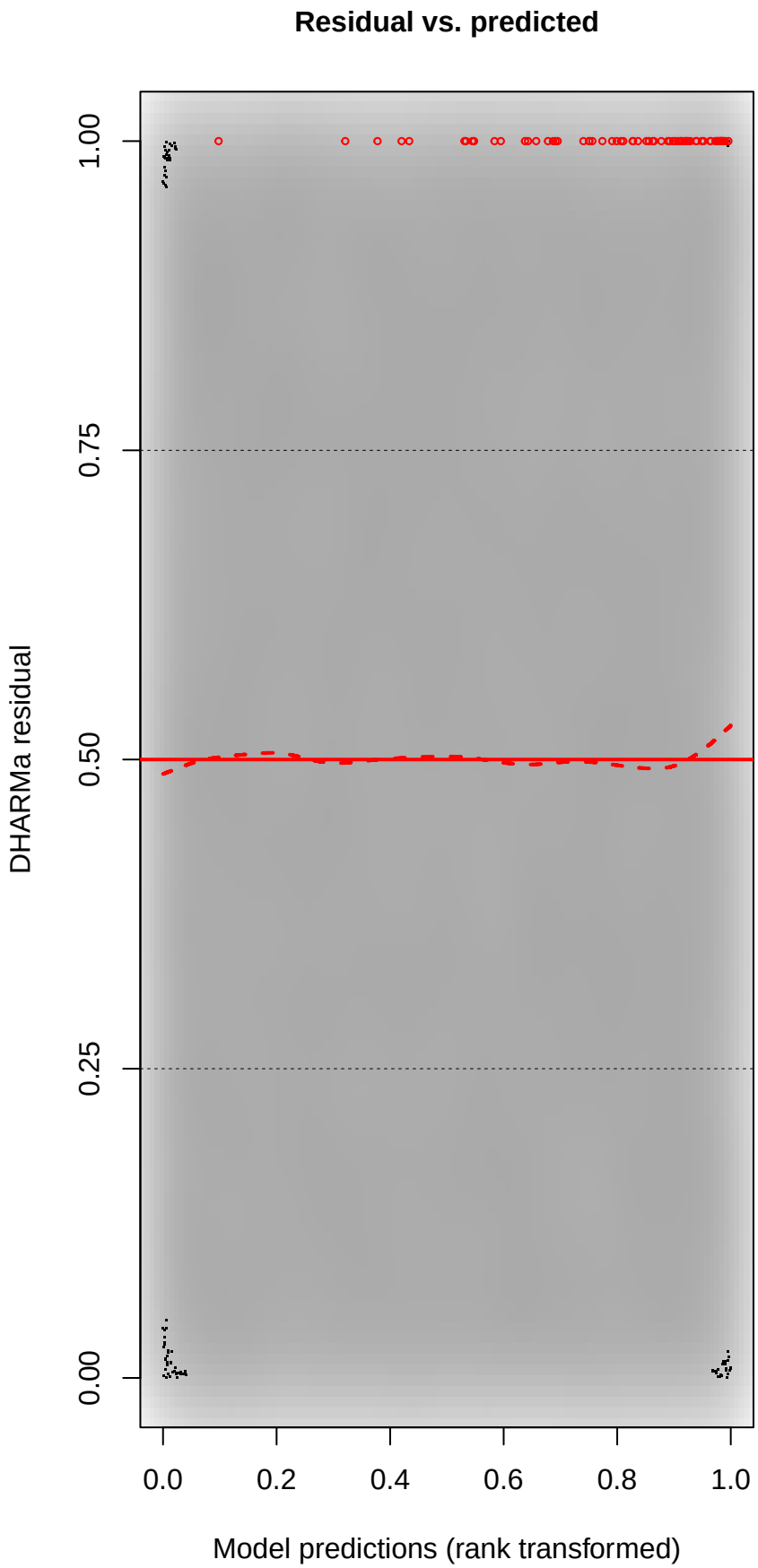

*Acer platanoides*

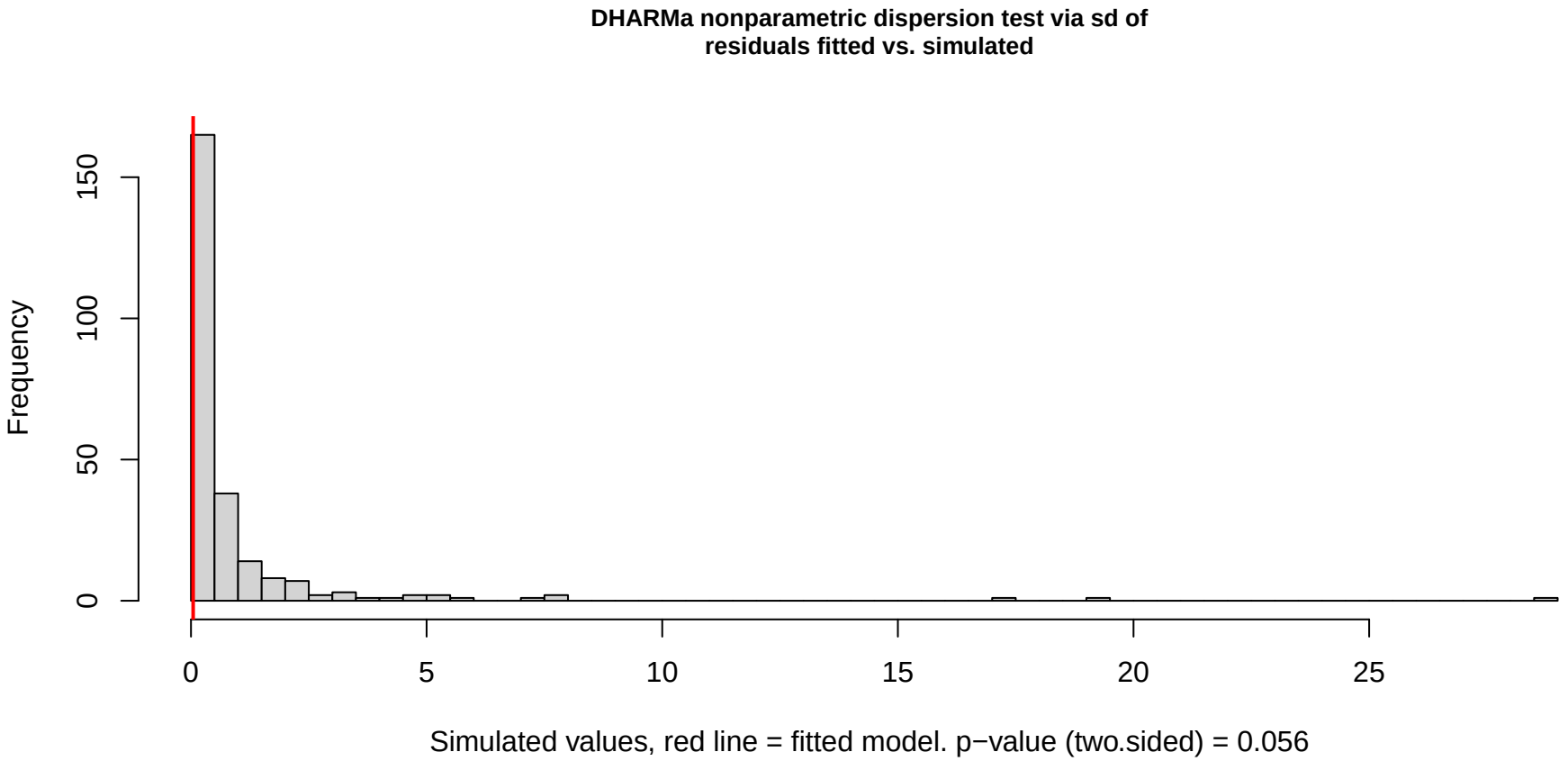


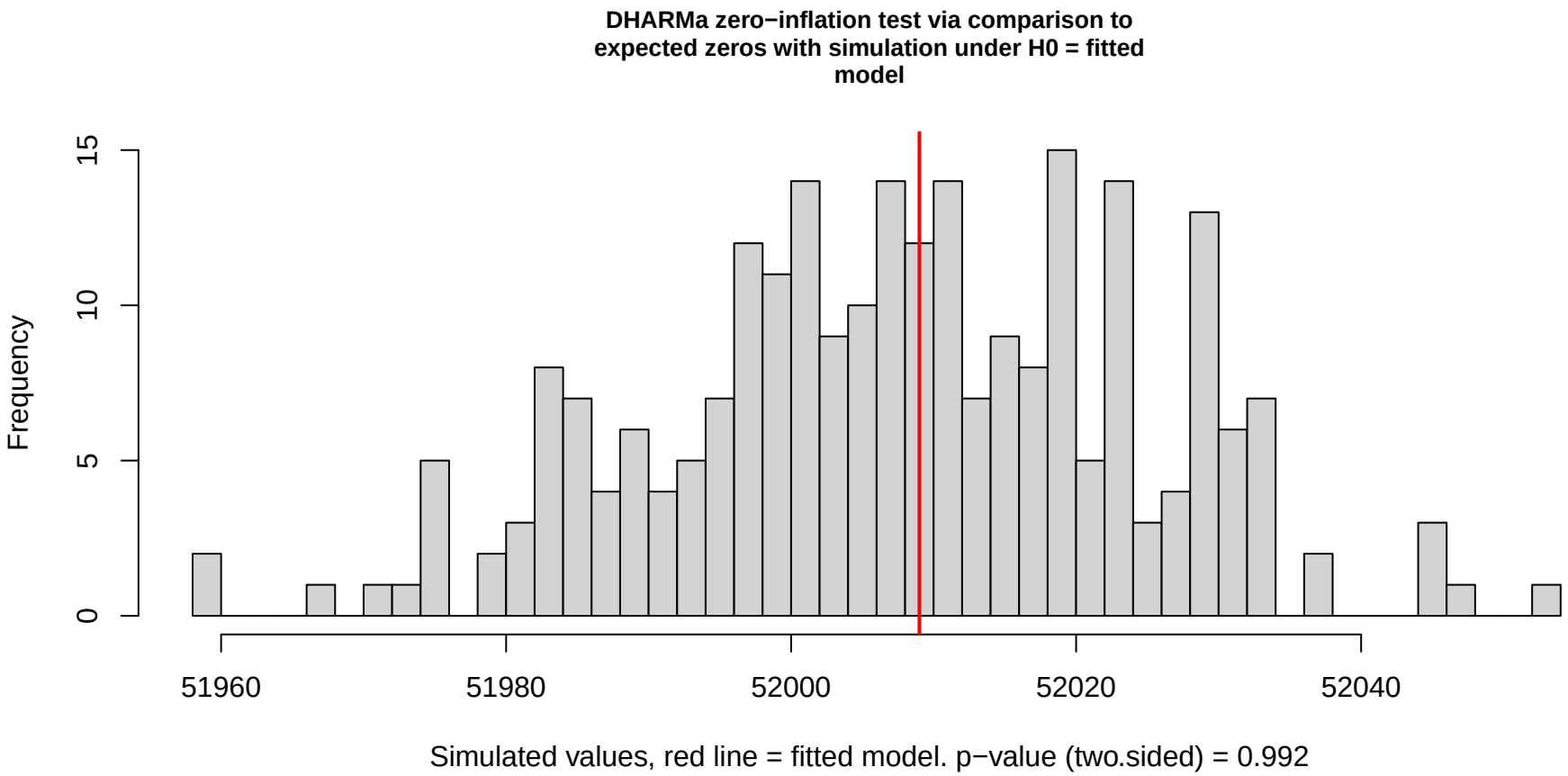

*Acer platanoides*

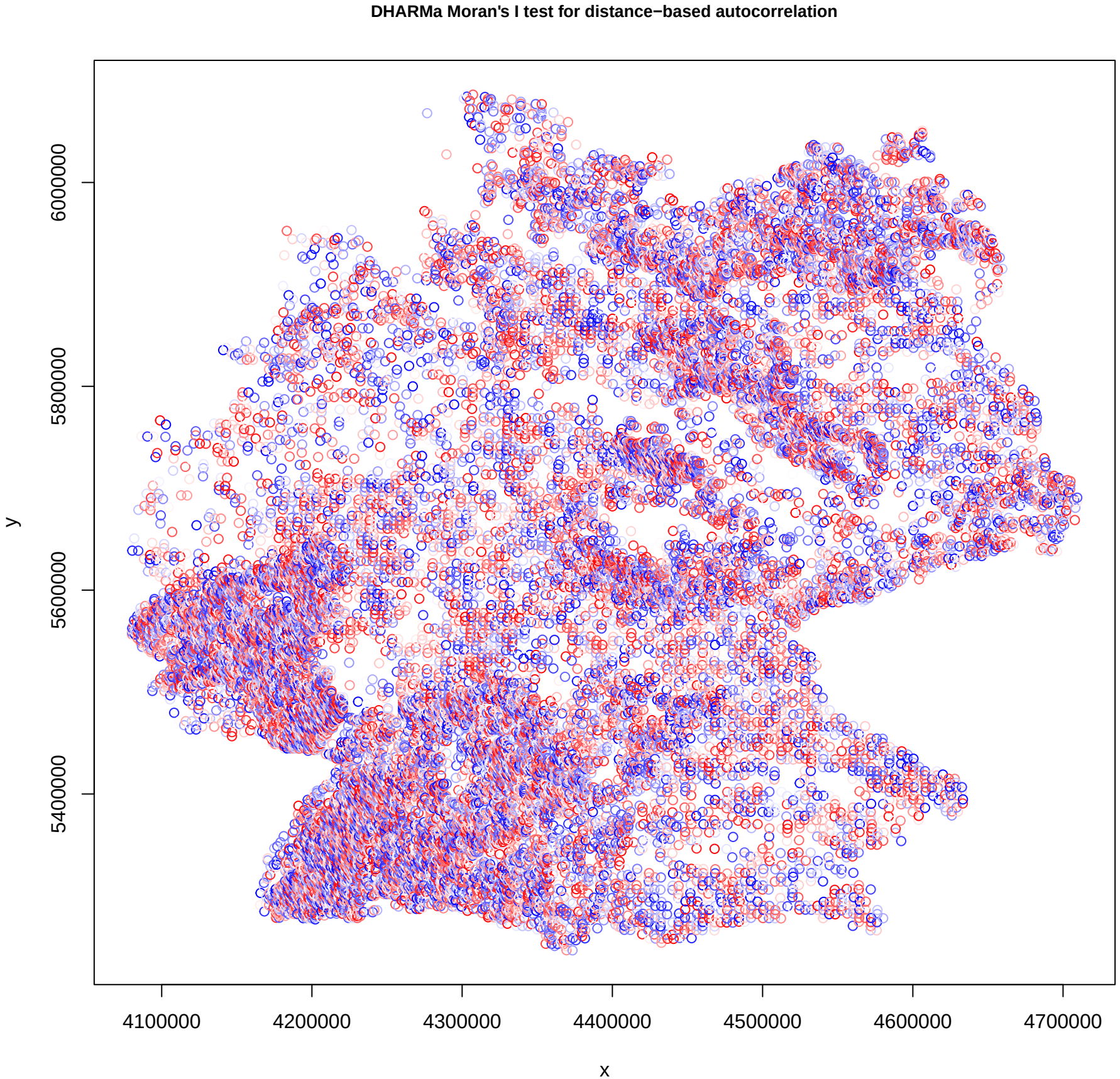

*Acer pseudoplatanus*

DHARMa residual

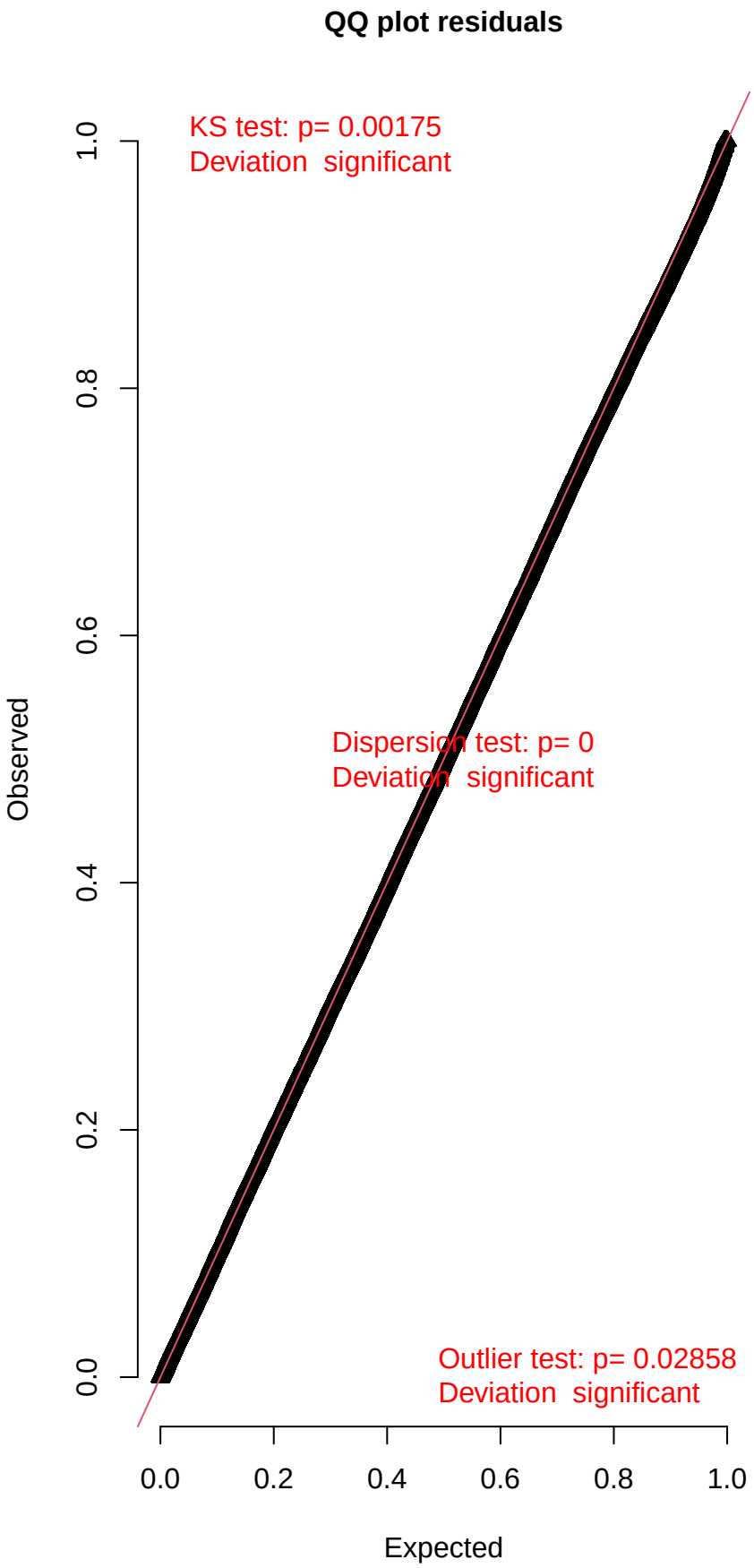


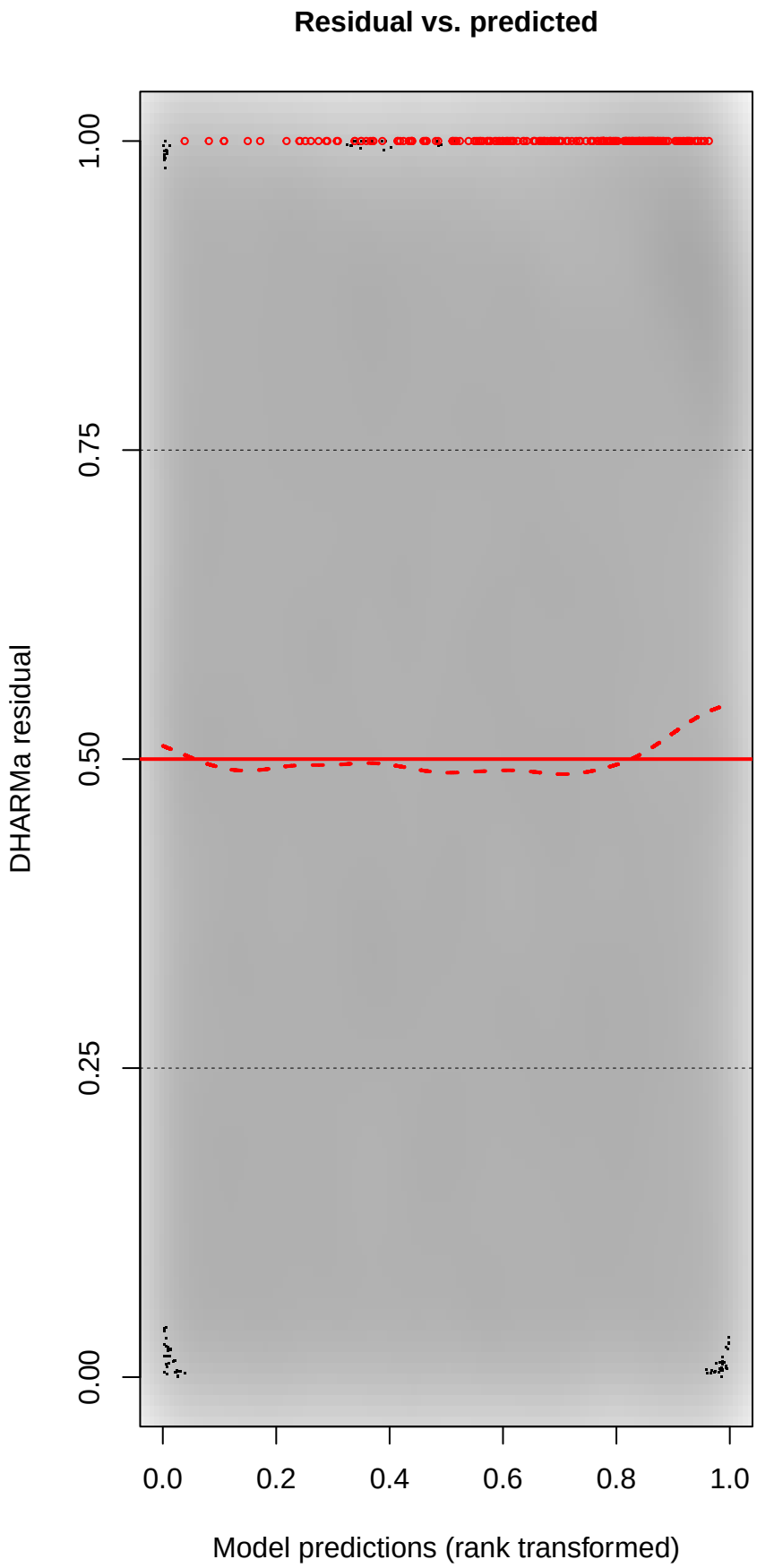

*Acer pseudoplatanus*

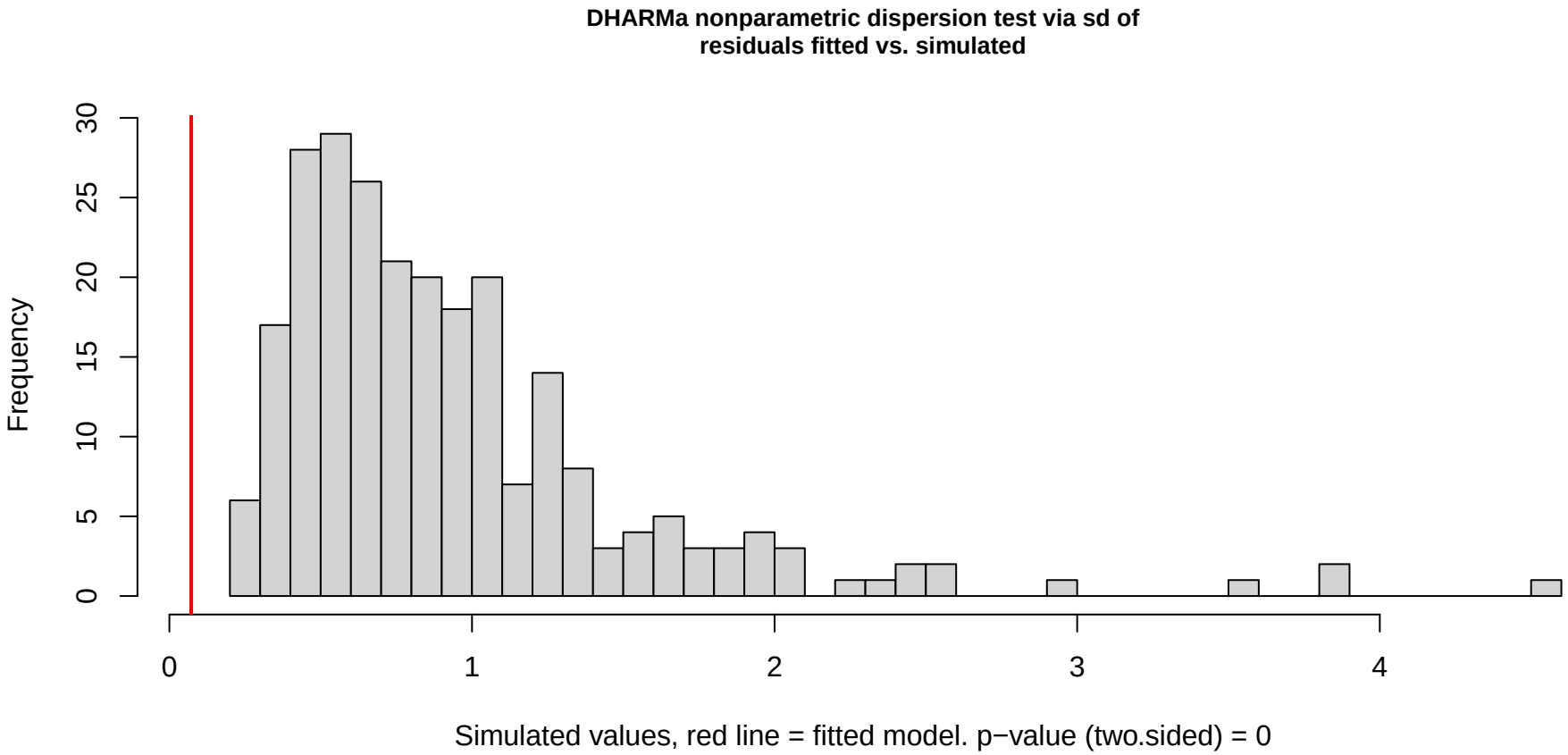


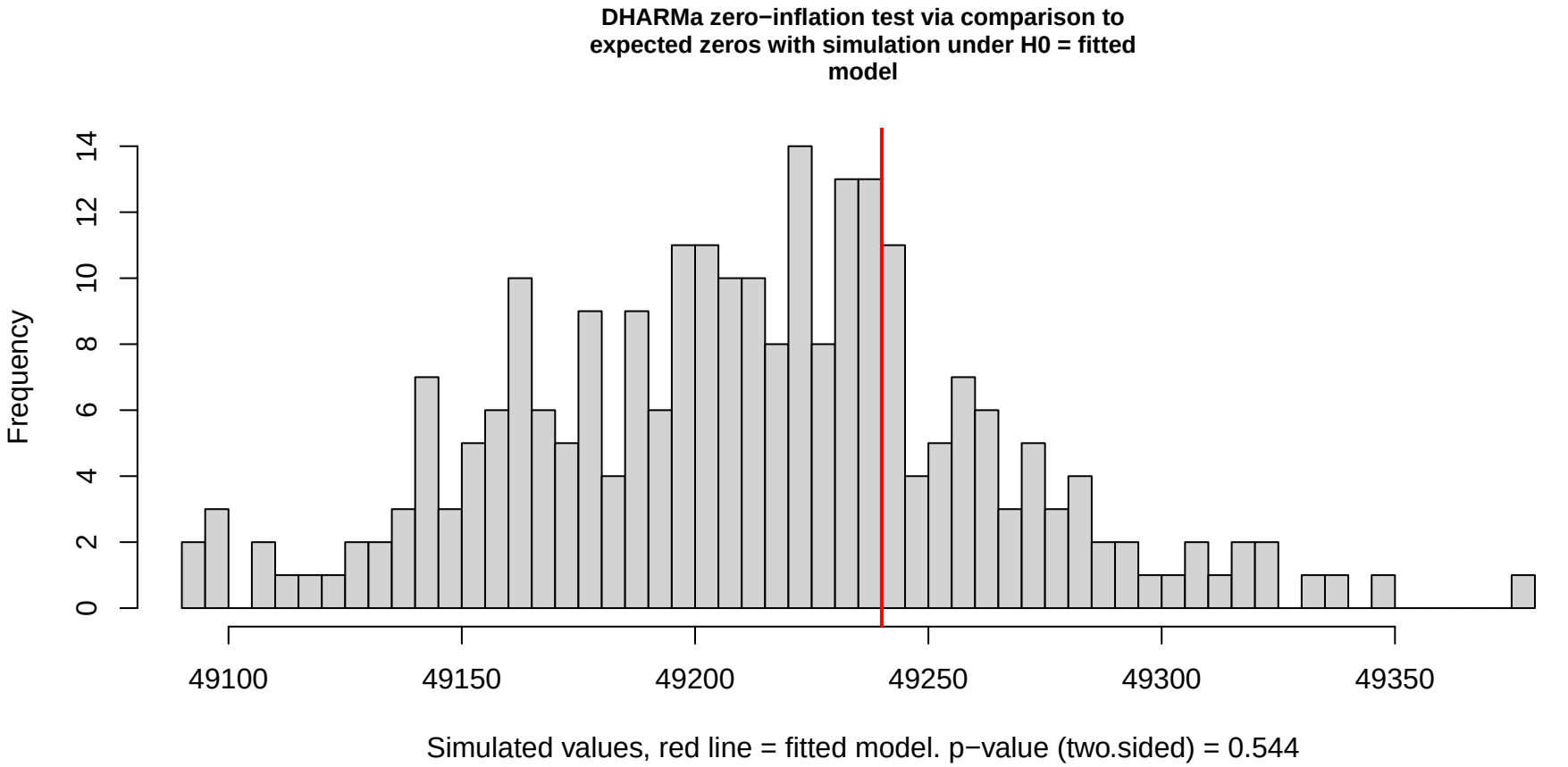

*Acer pseudoplatanus*

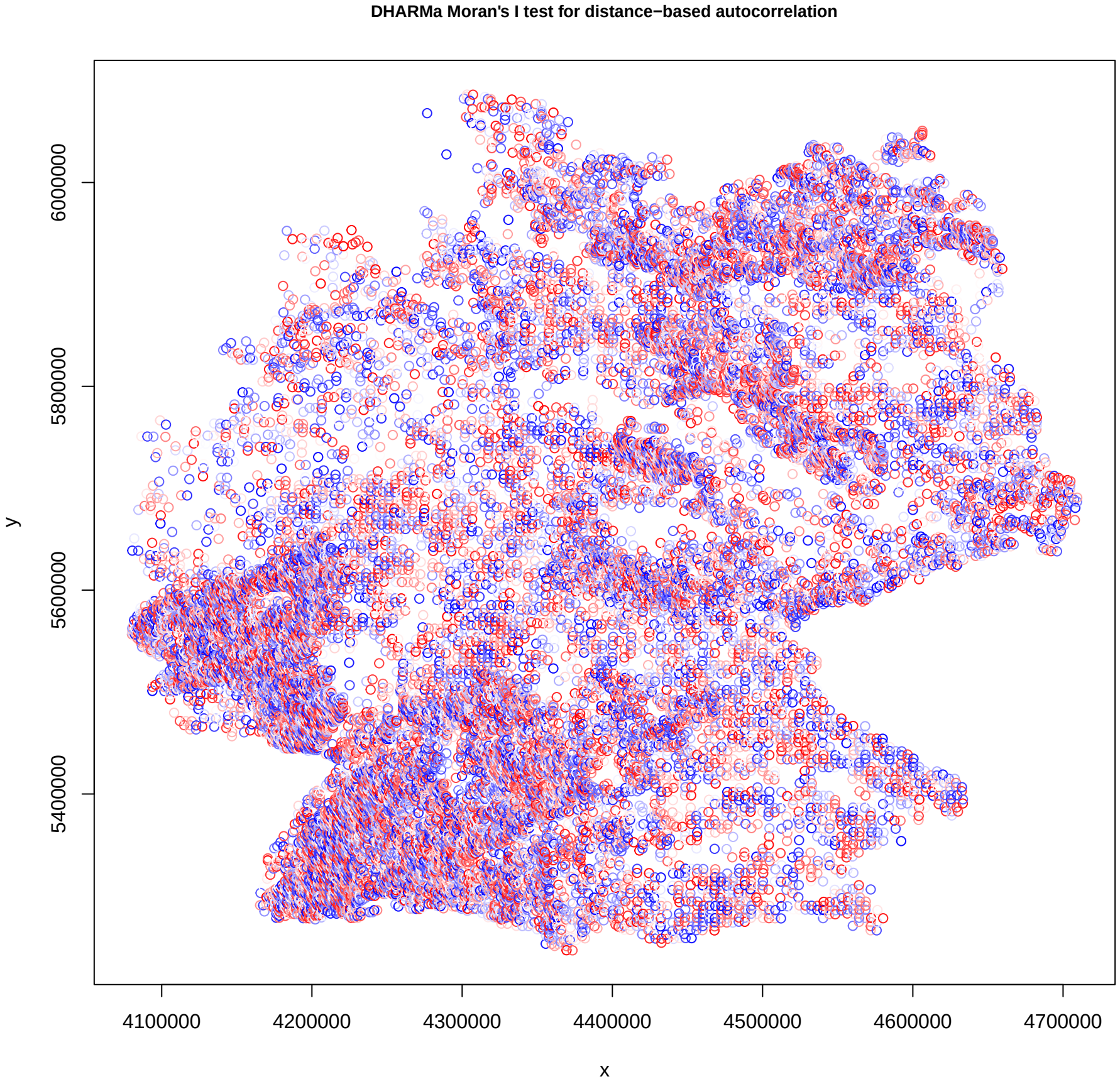

*Carpinus betulus*

DHARMa residual

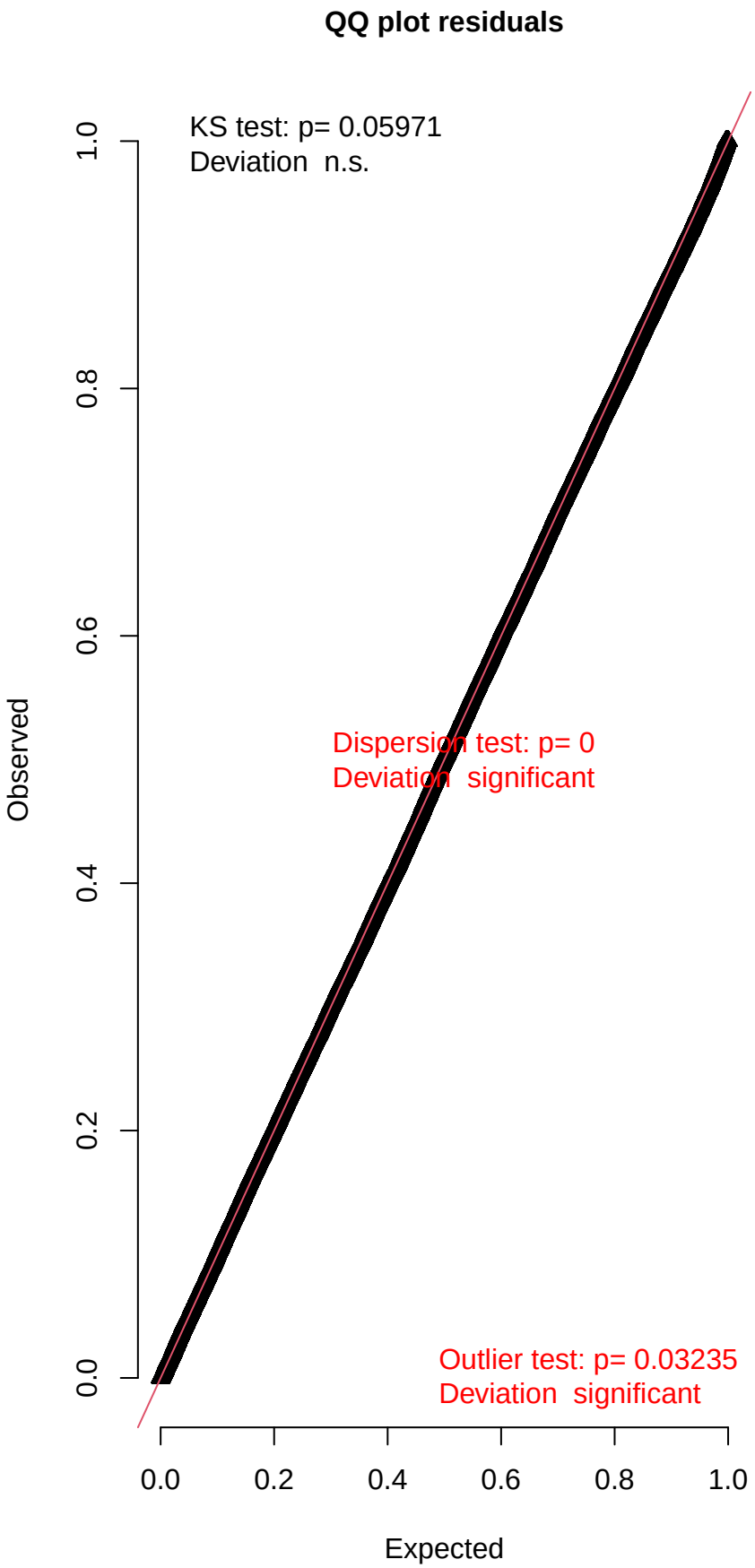


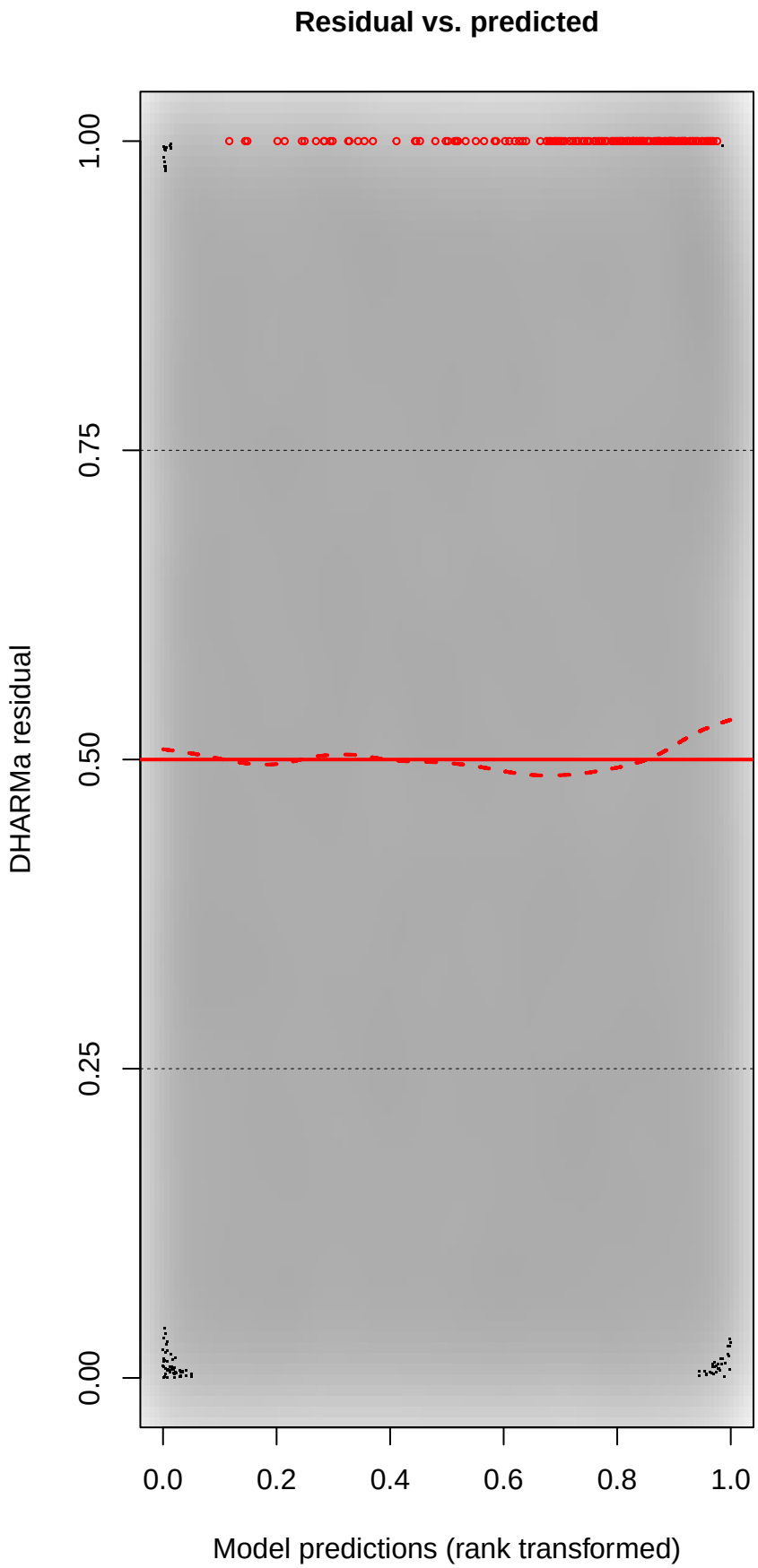

*Carpinus betulus*

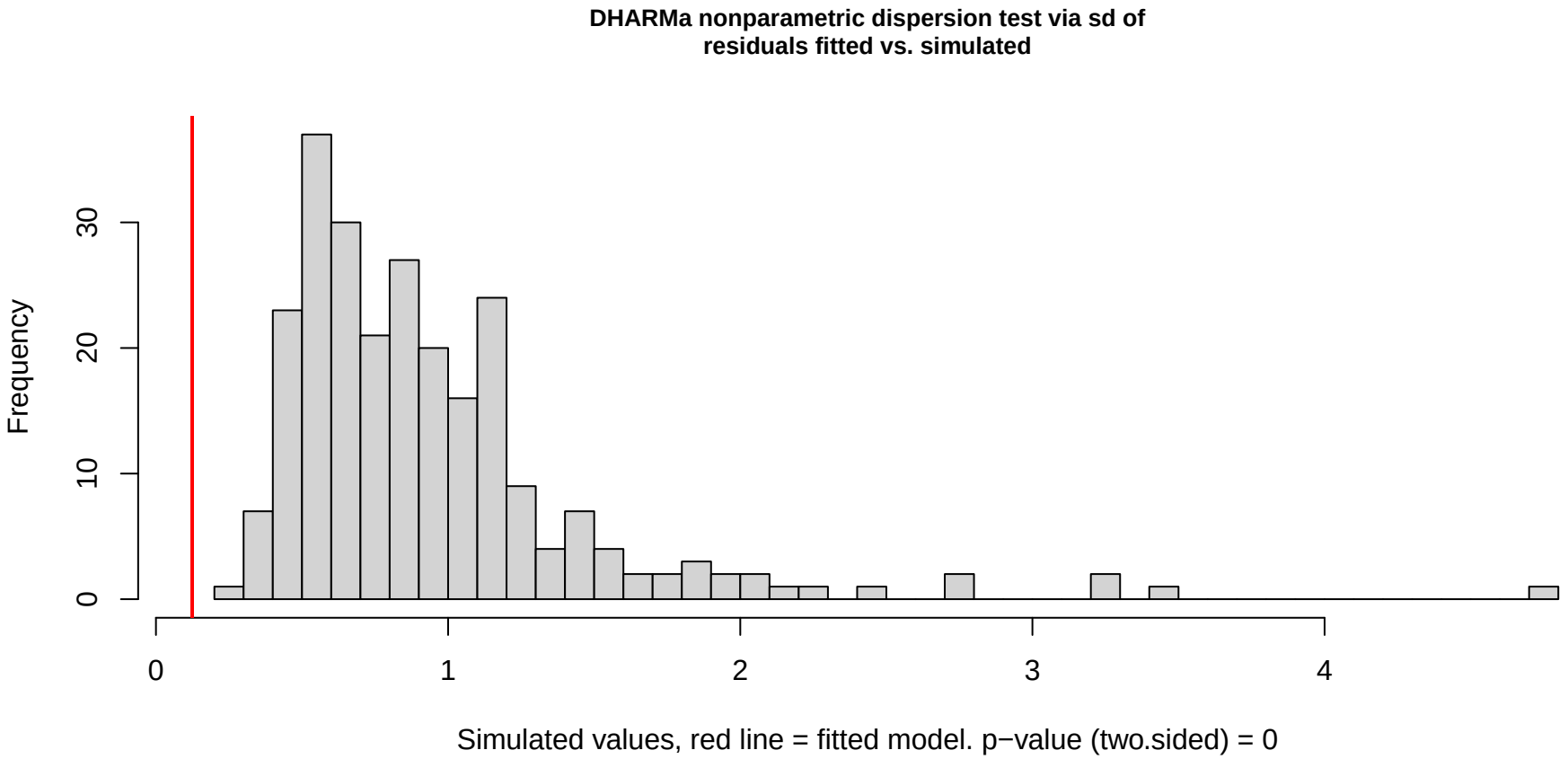


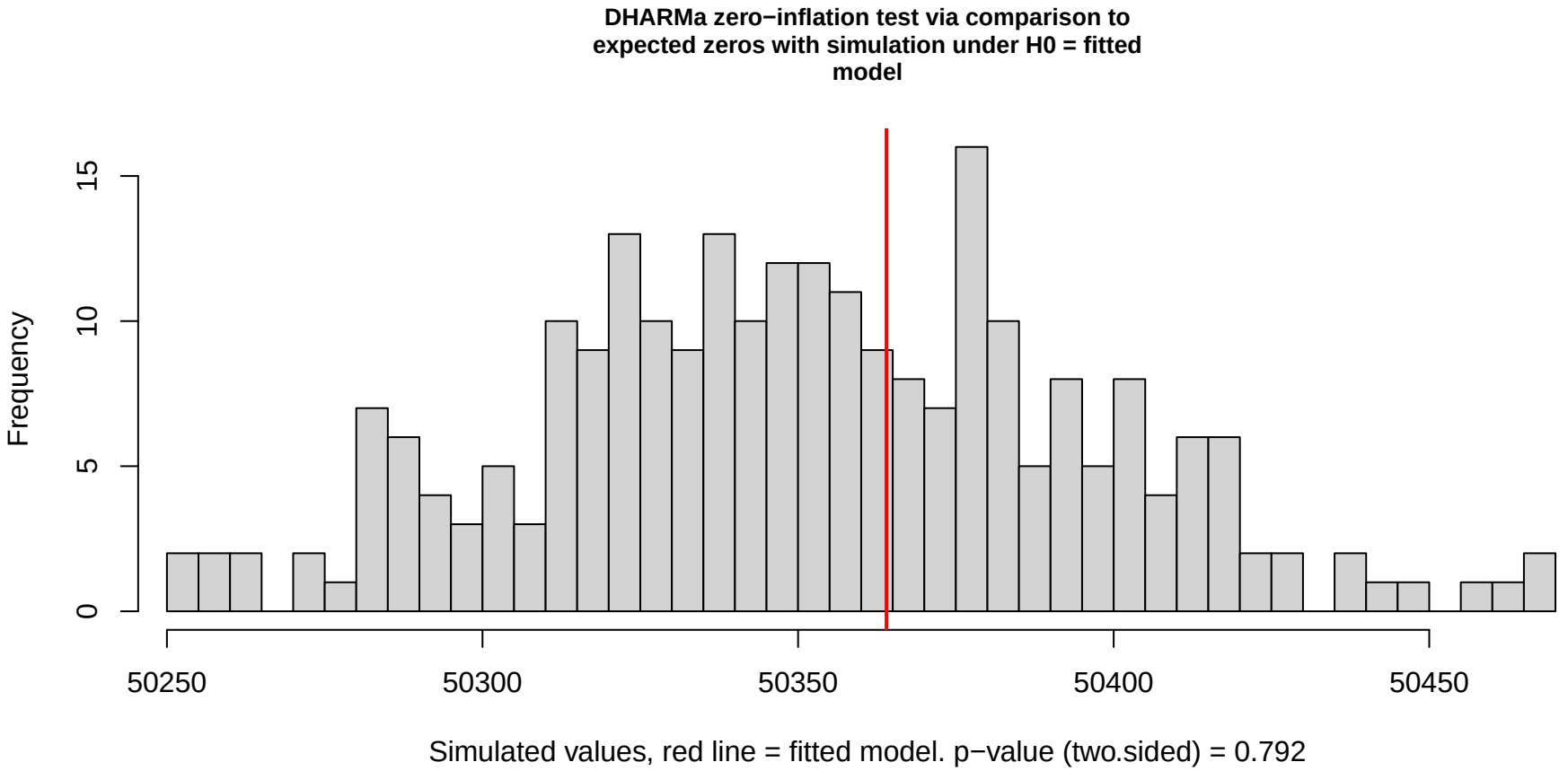

*Carpinus betulus*

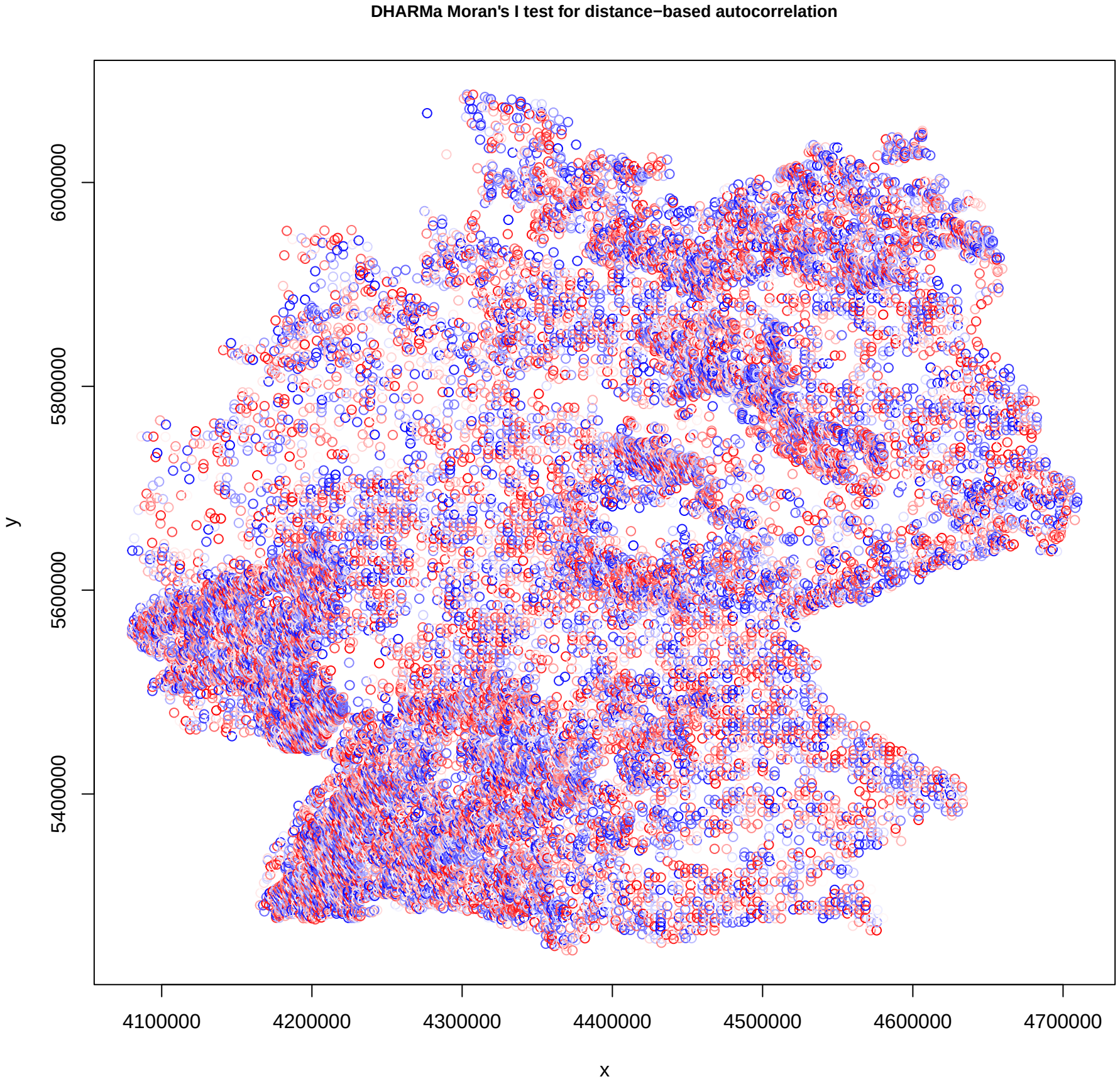

*Castanea sativa*

DHARMa residual

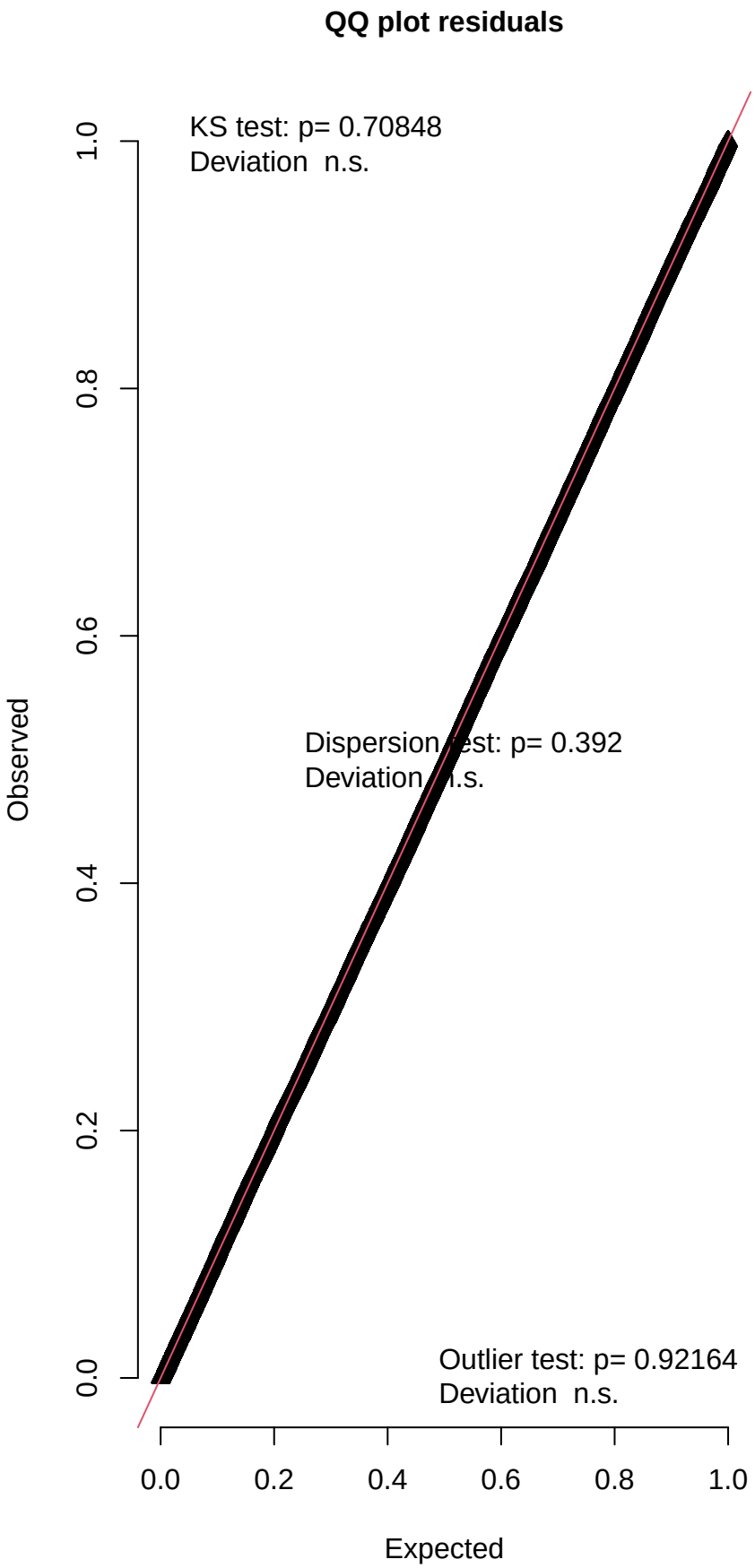


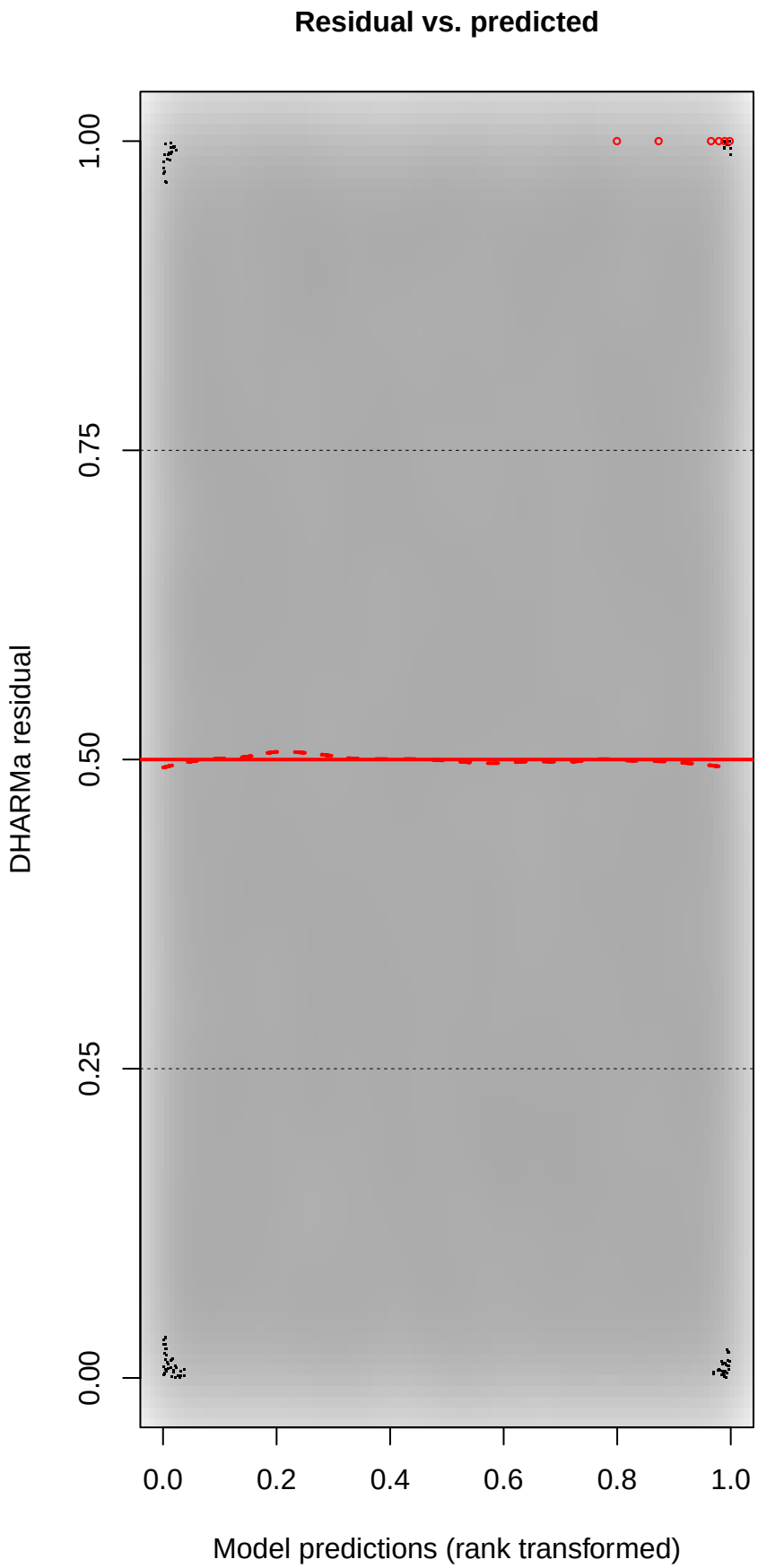

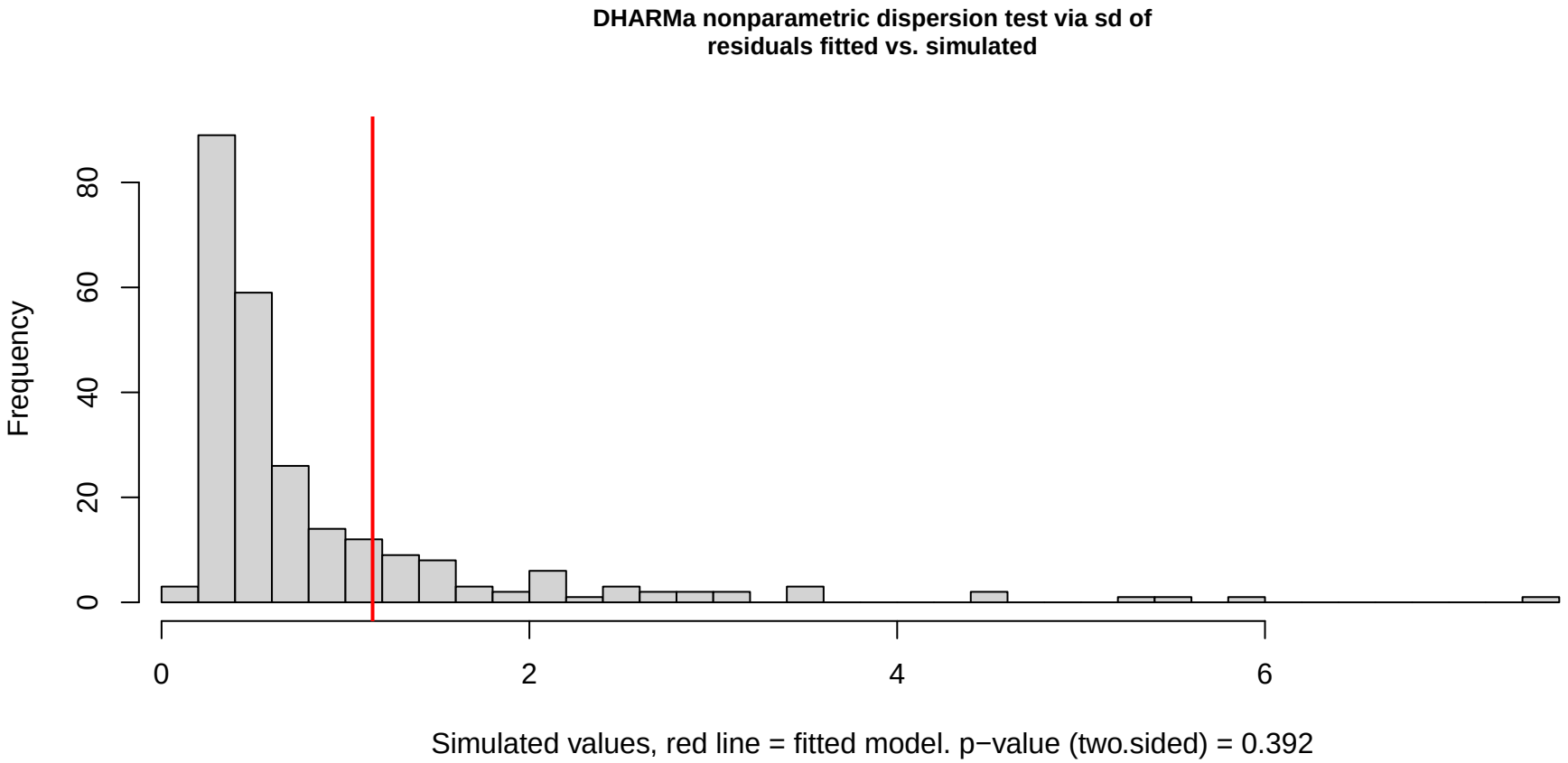
DHARMa nonparametric dispersion test via sd of residuals fitted vs. simulated
Frequency
0
20
40
60
80
0
2
4
6
Simulated values, red line = fitted model. p−value (two.sided) = 0.392

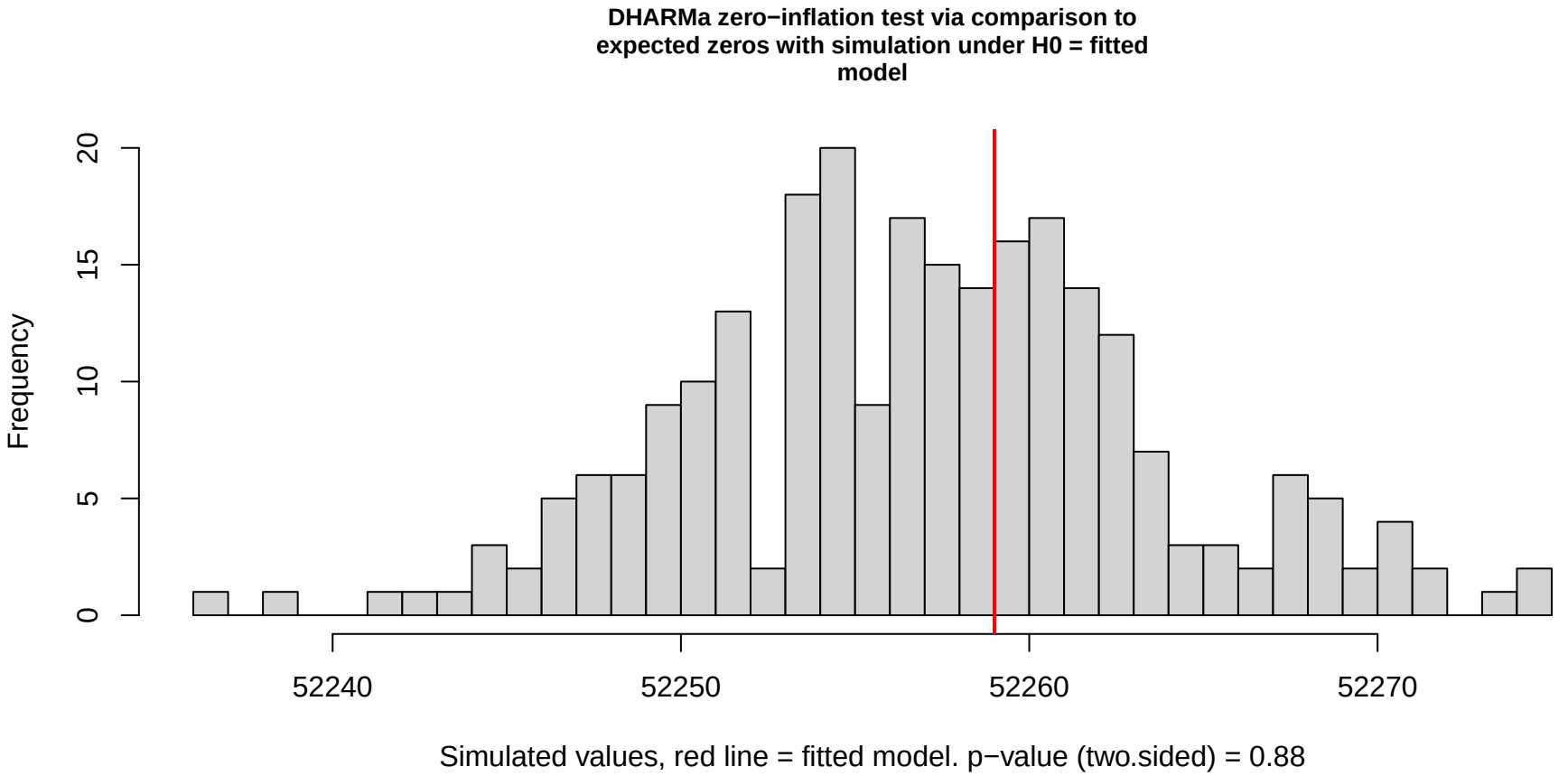
DHARMa zero−inflation test via comparison to expected zeros with simulation under H0 = fitted model
Frequency
0
5
10
15
20
52240
52250
52260
52270
Simulated values, red line = fitted model. p−value (two.sided) = 0.88

*Castanea sativa*

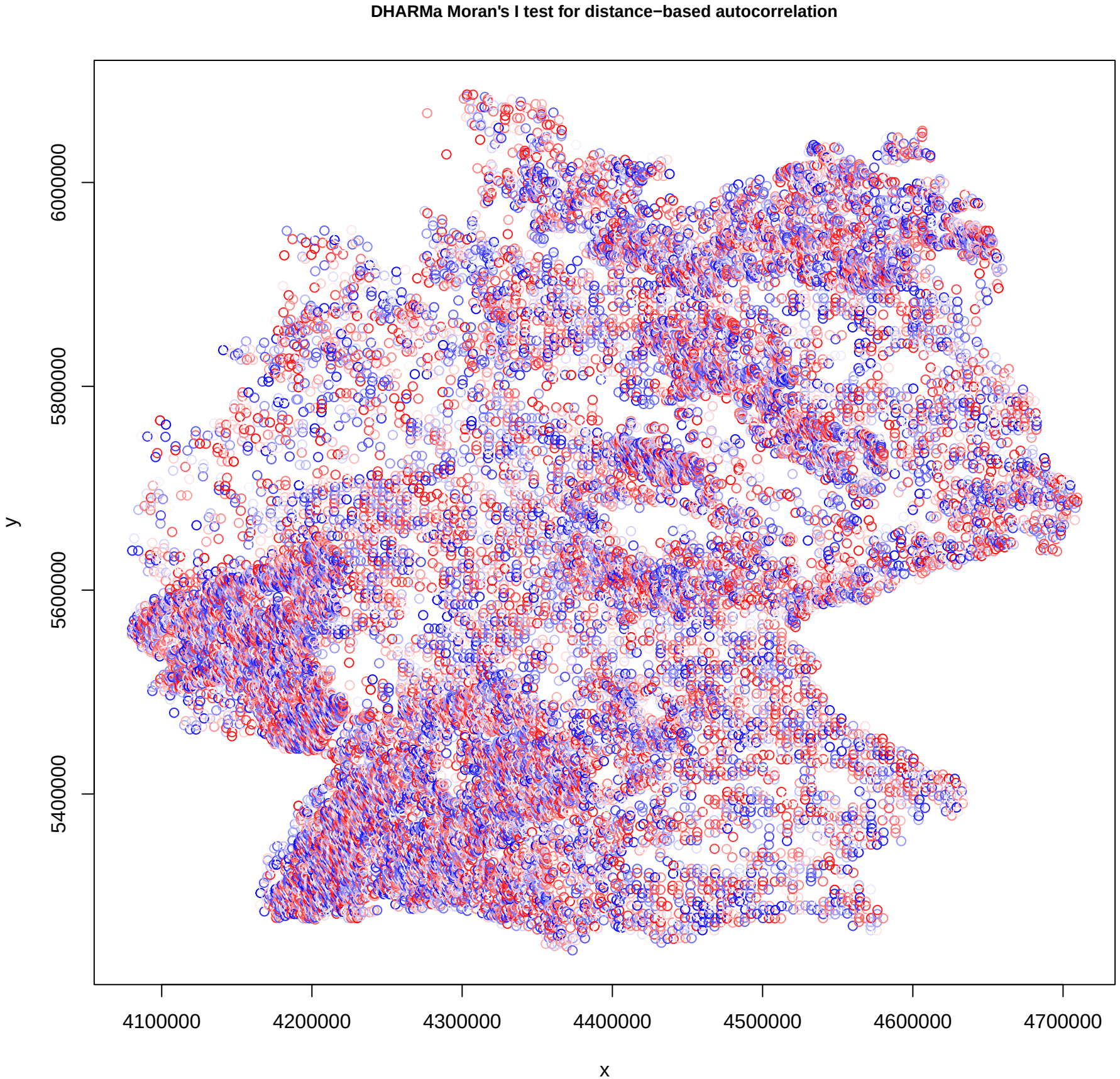

*Fraxinus excelsior*

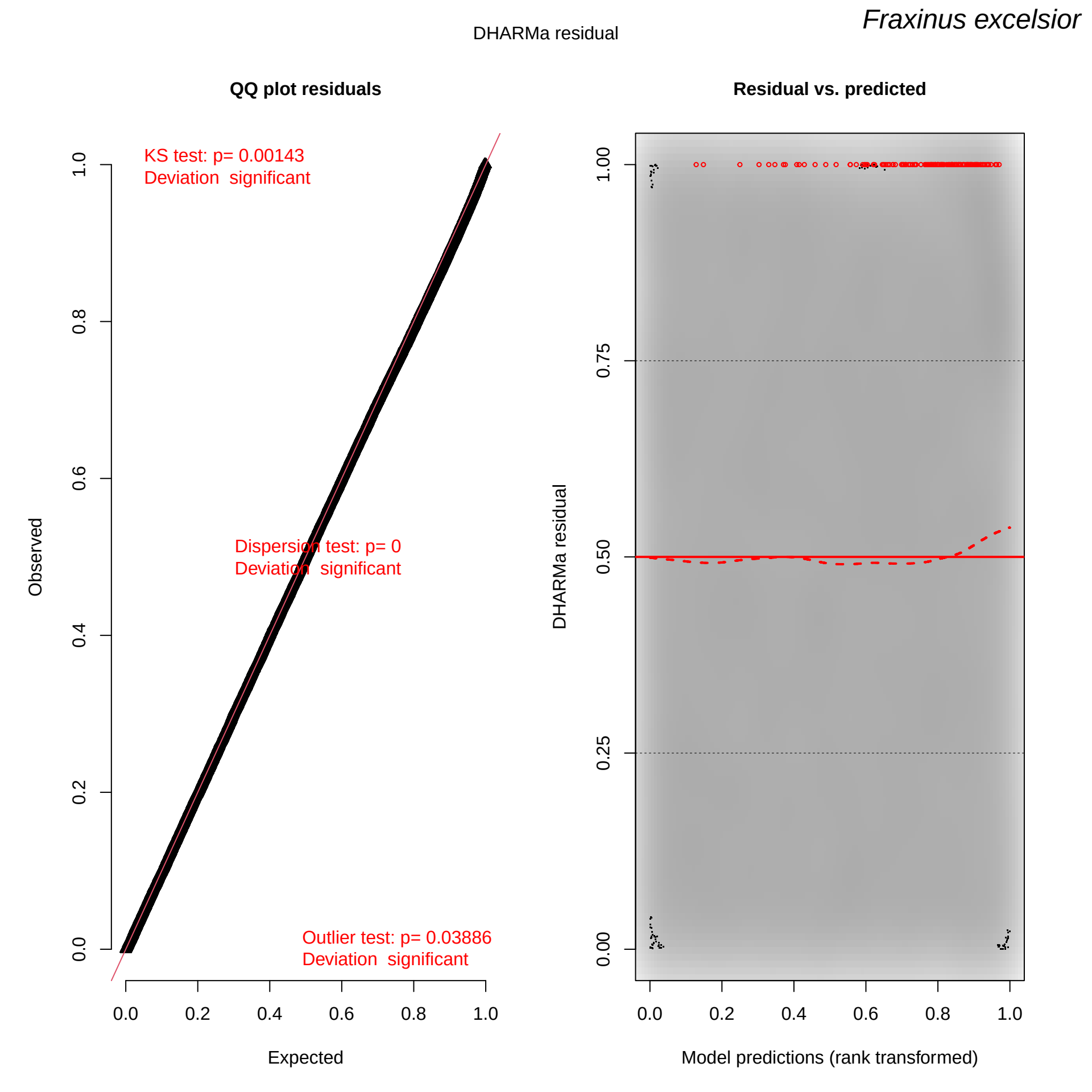

*Fraxinus excelsior*

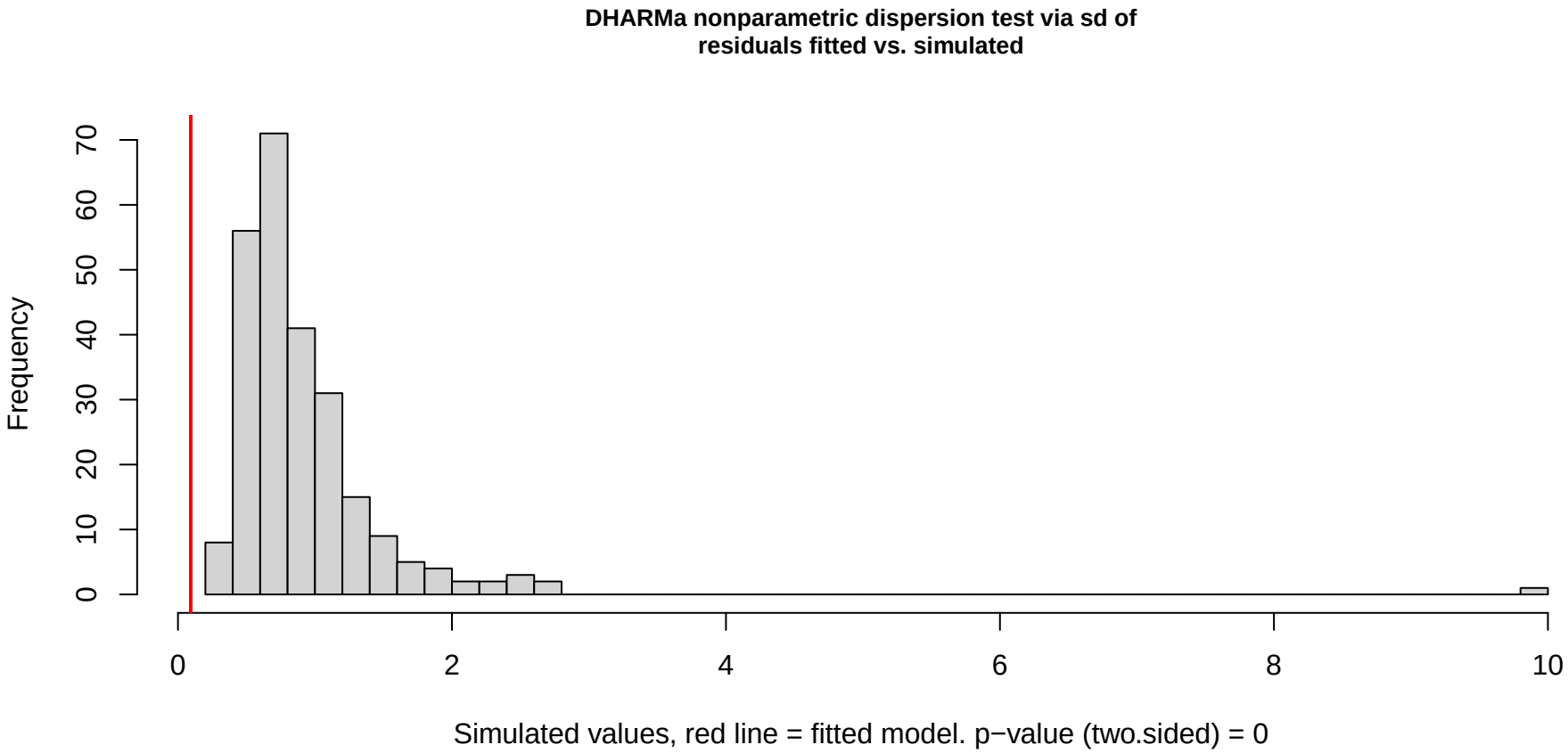


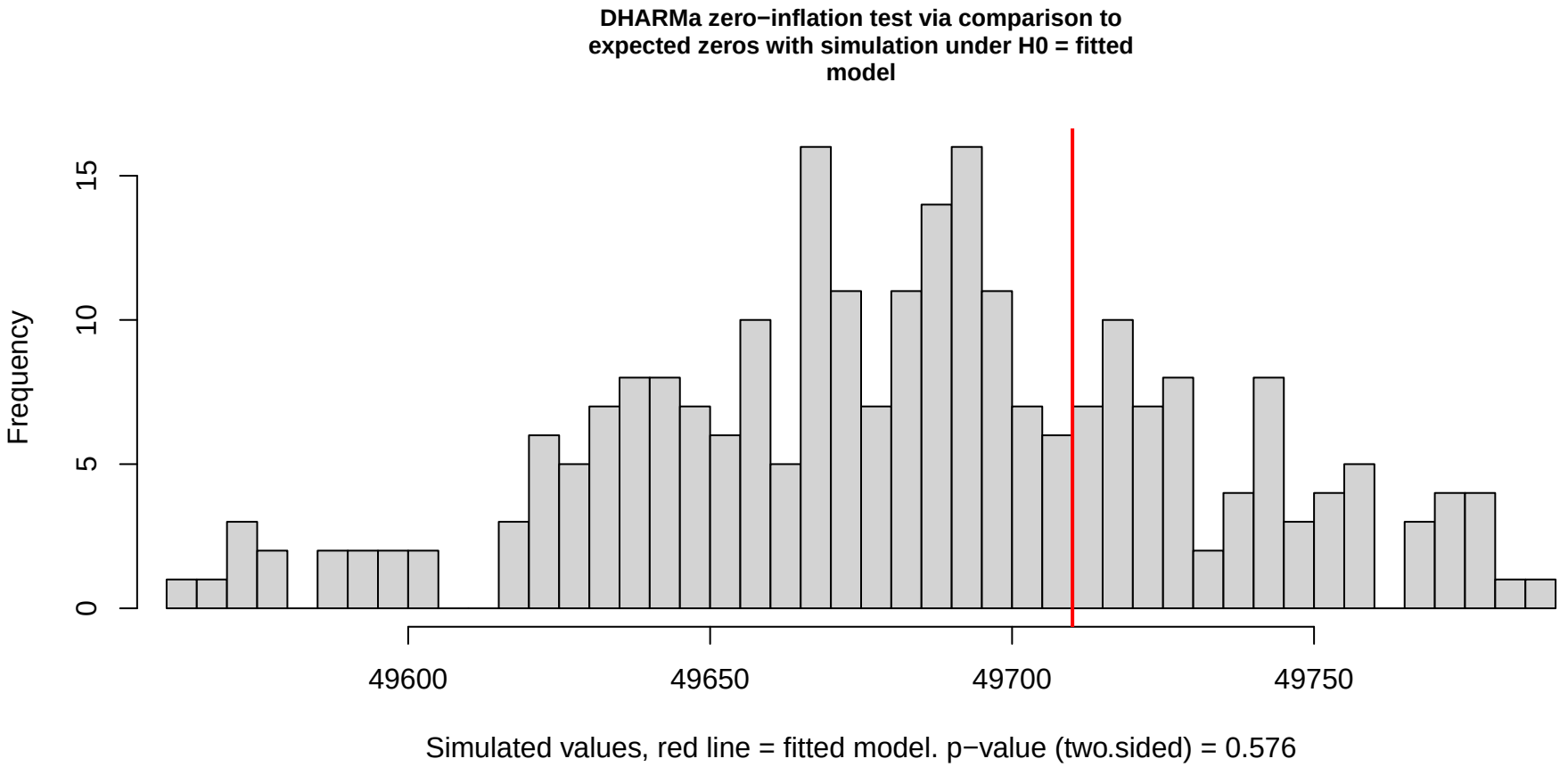

*Fraxinus excelsior*

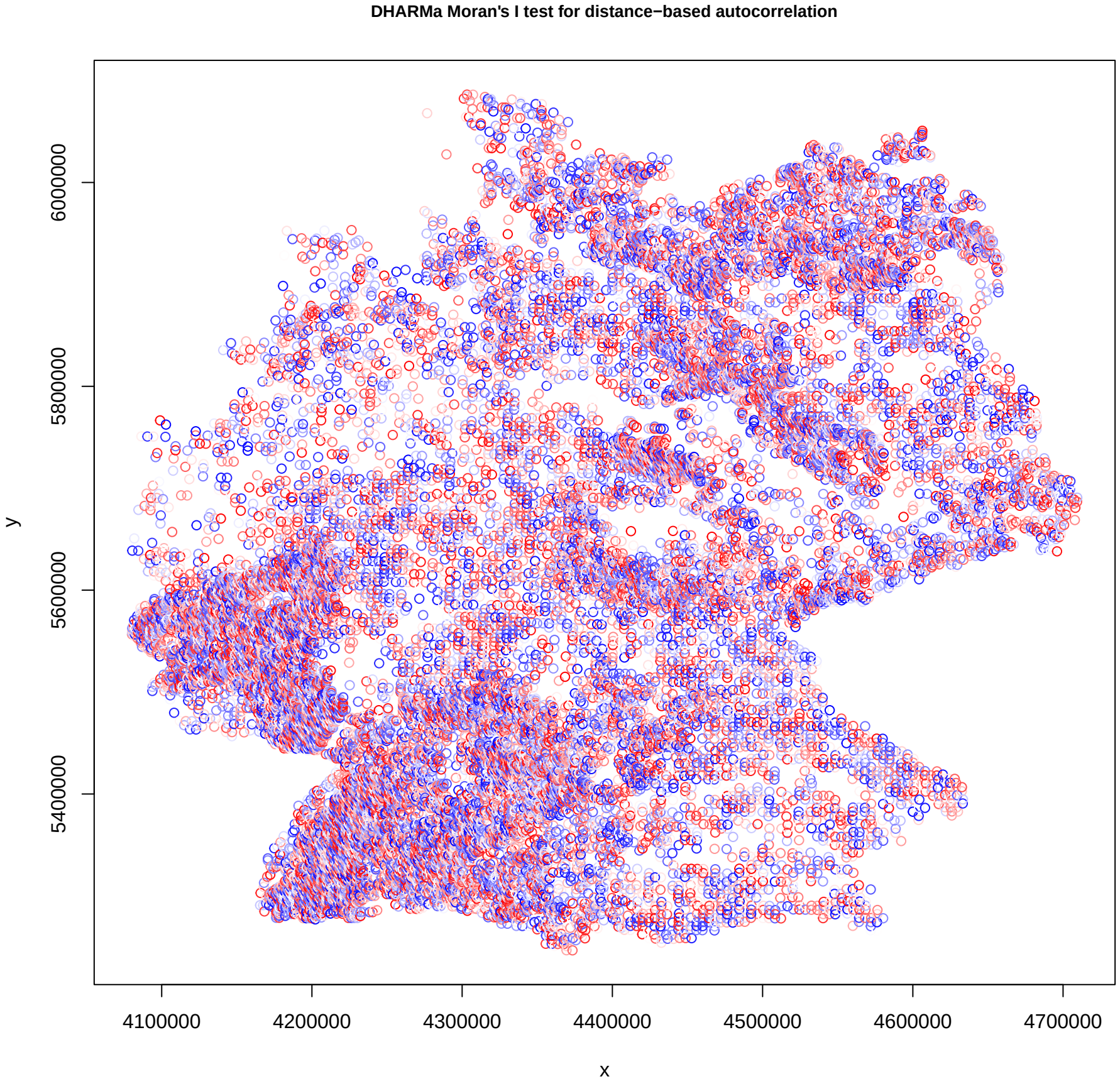

*Populus x.canescens*

DHARMa residual

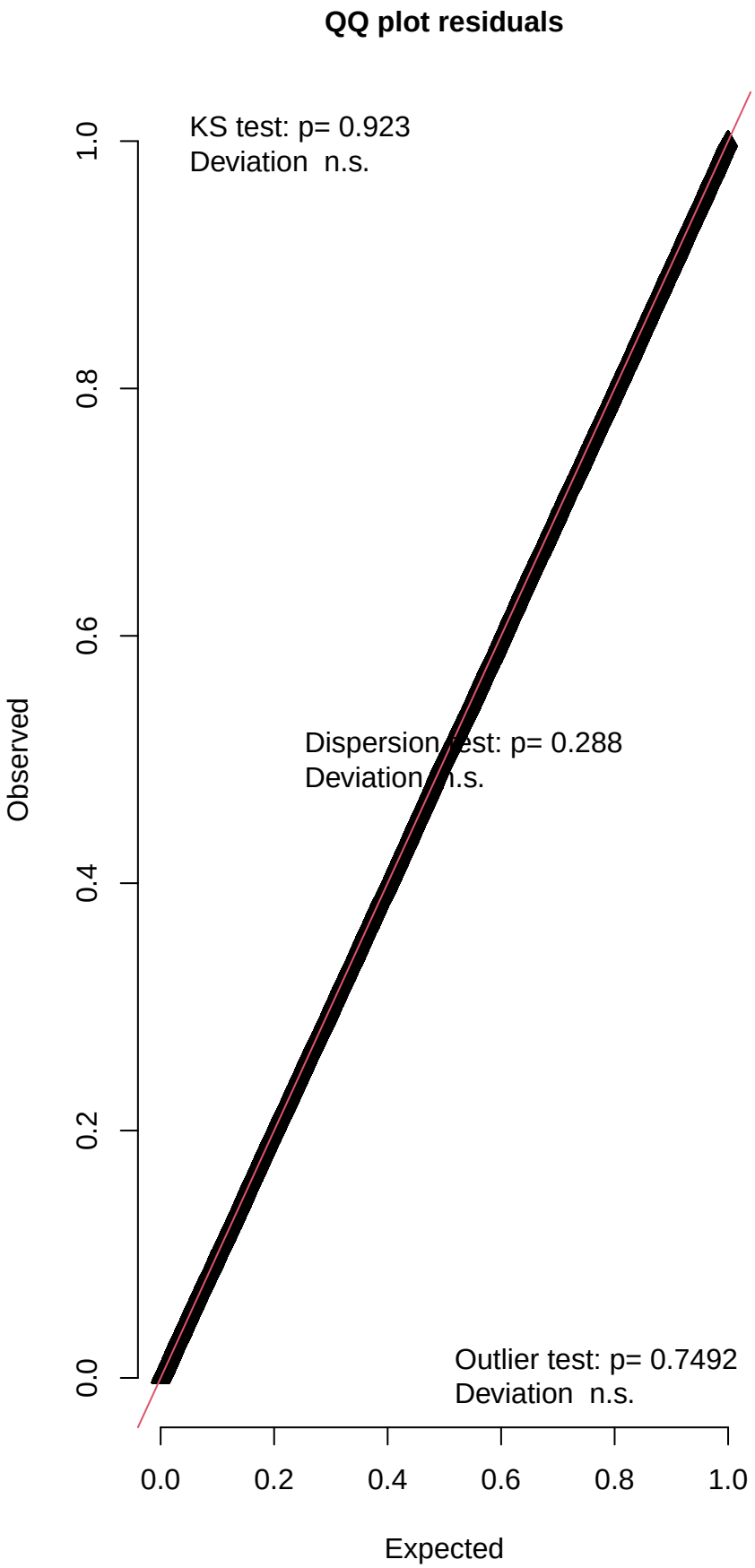


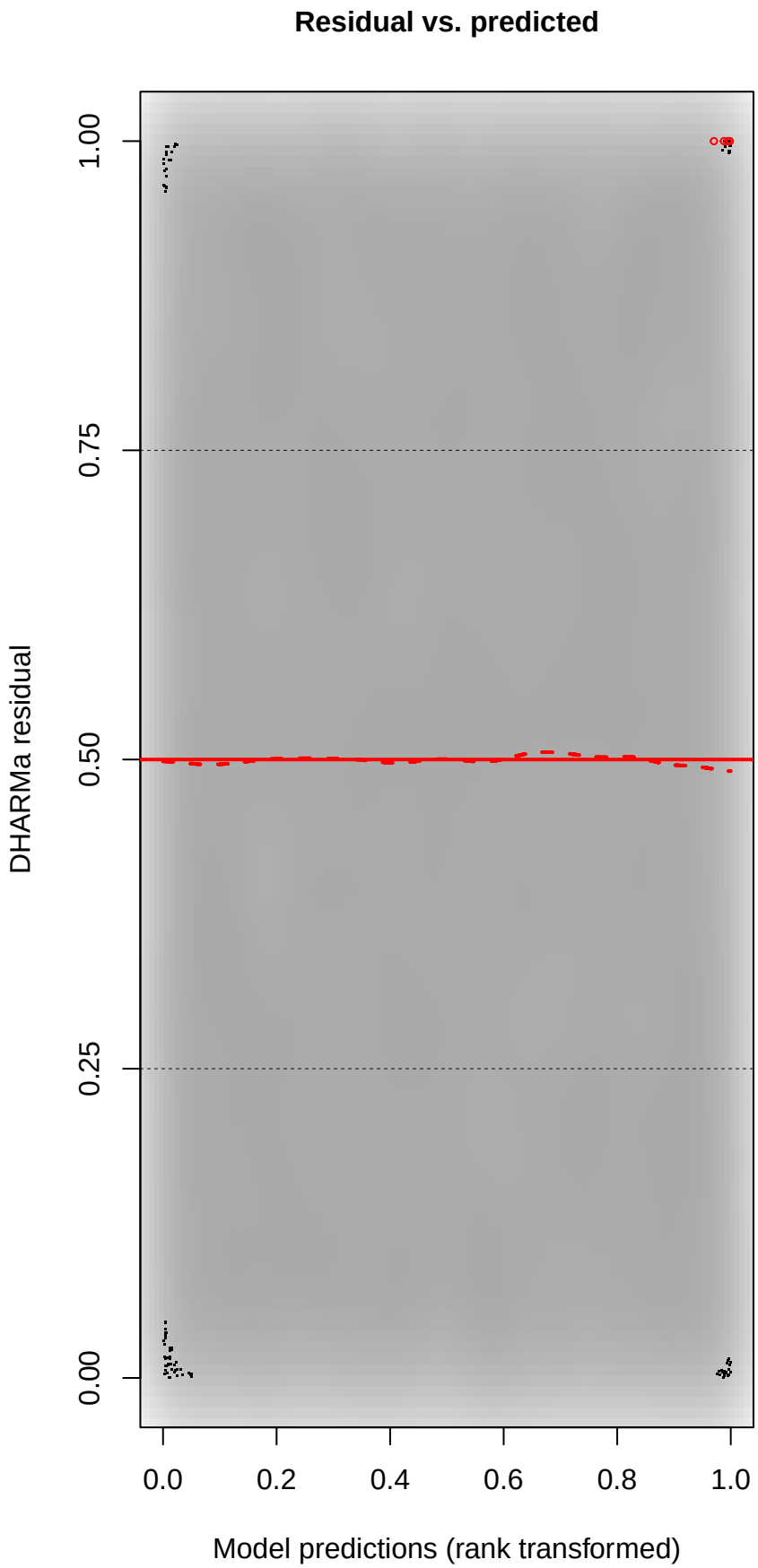

*Populus x.canescens*

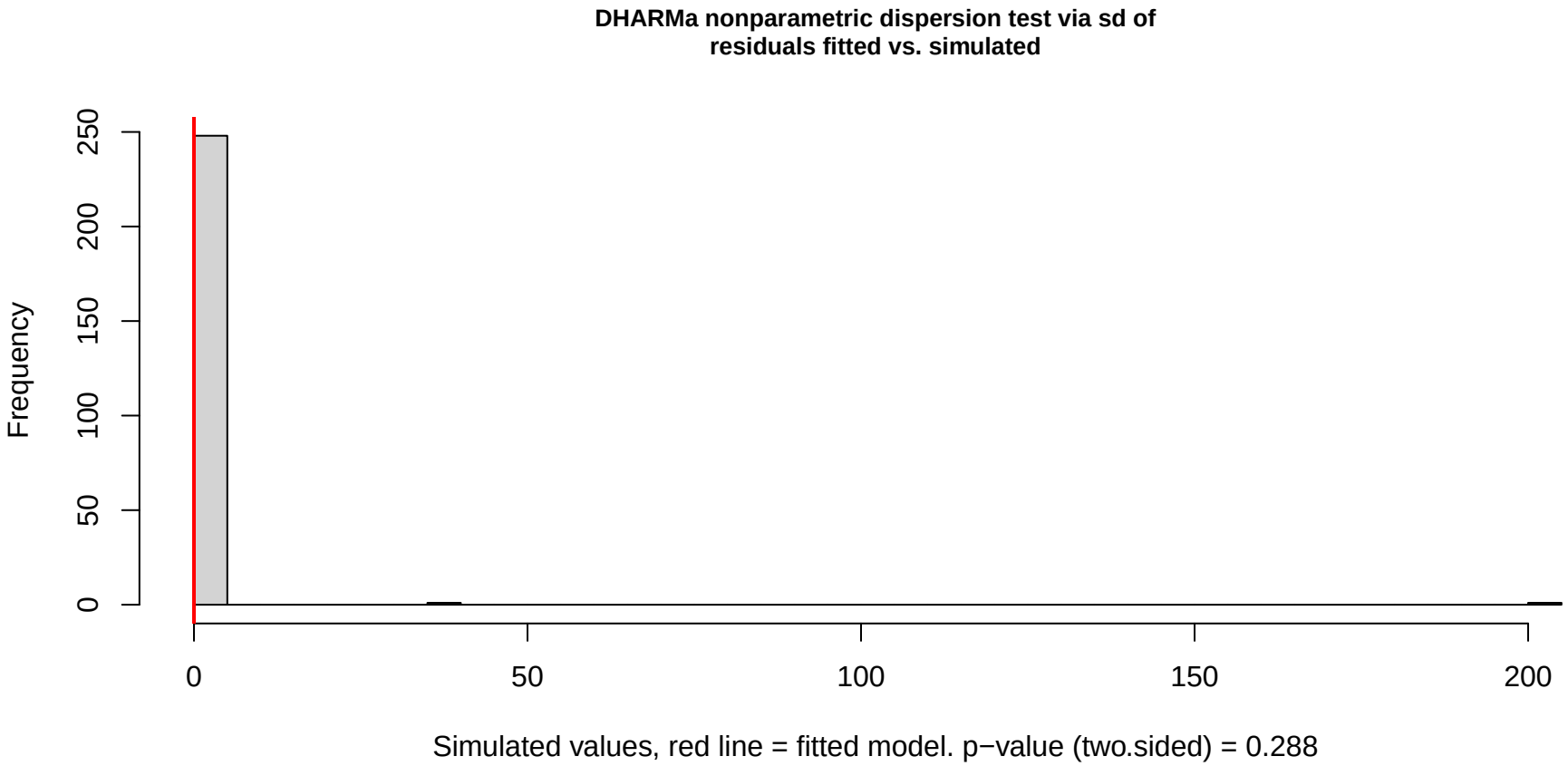


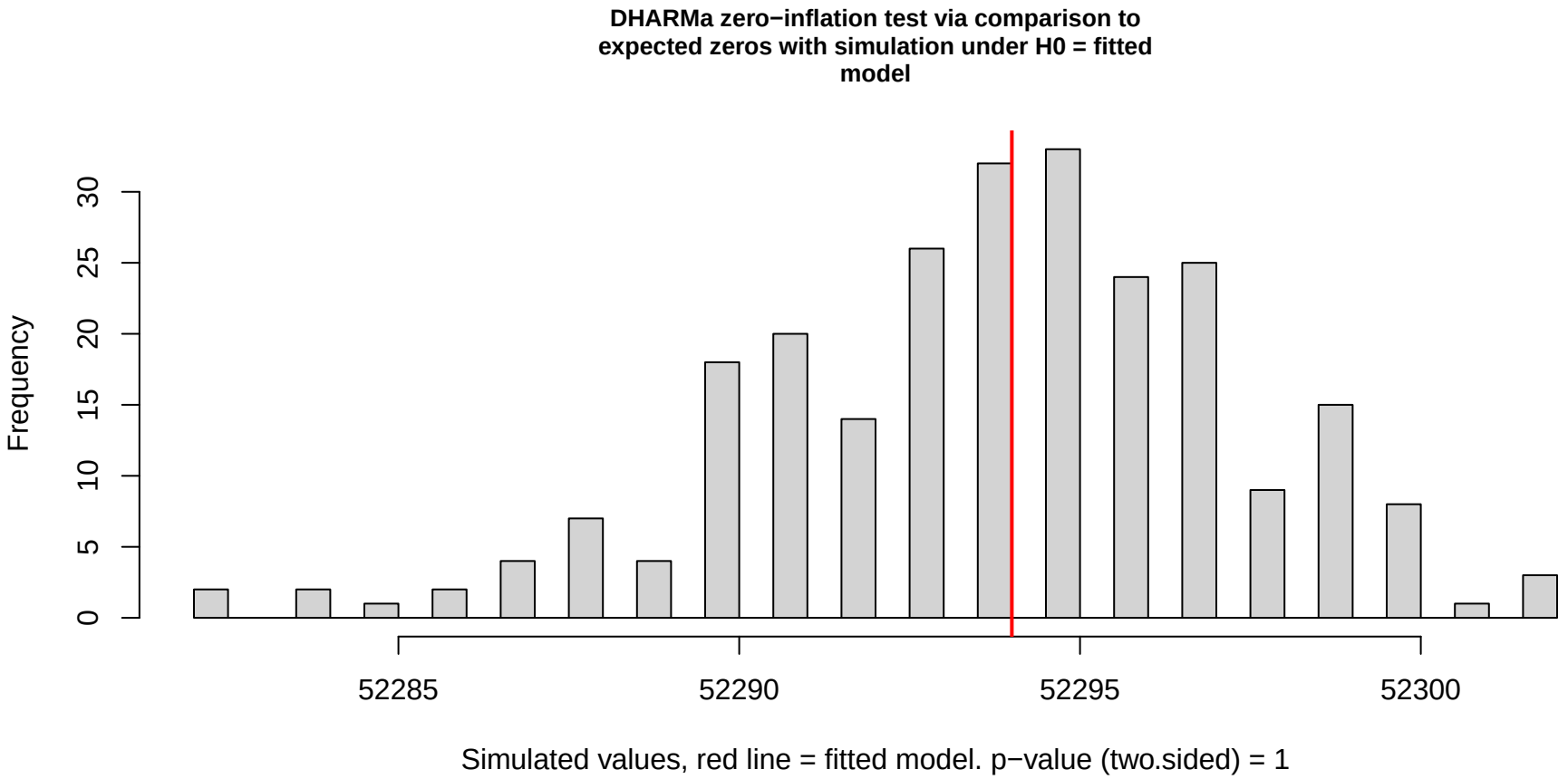

*Populus x.canescens*

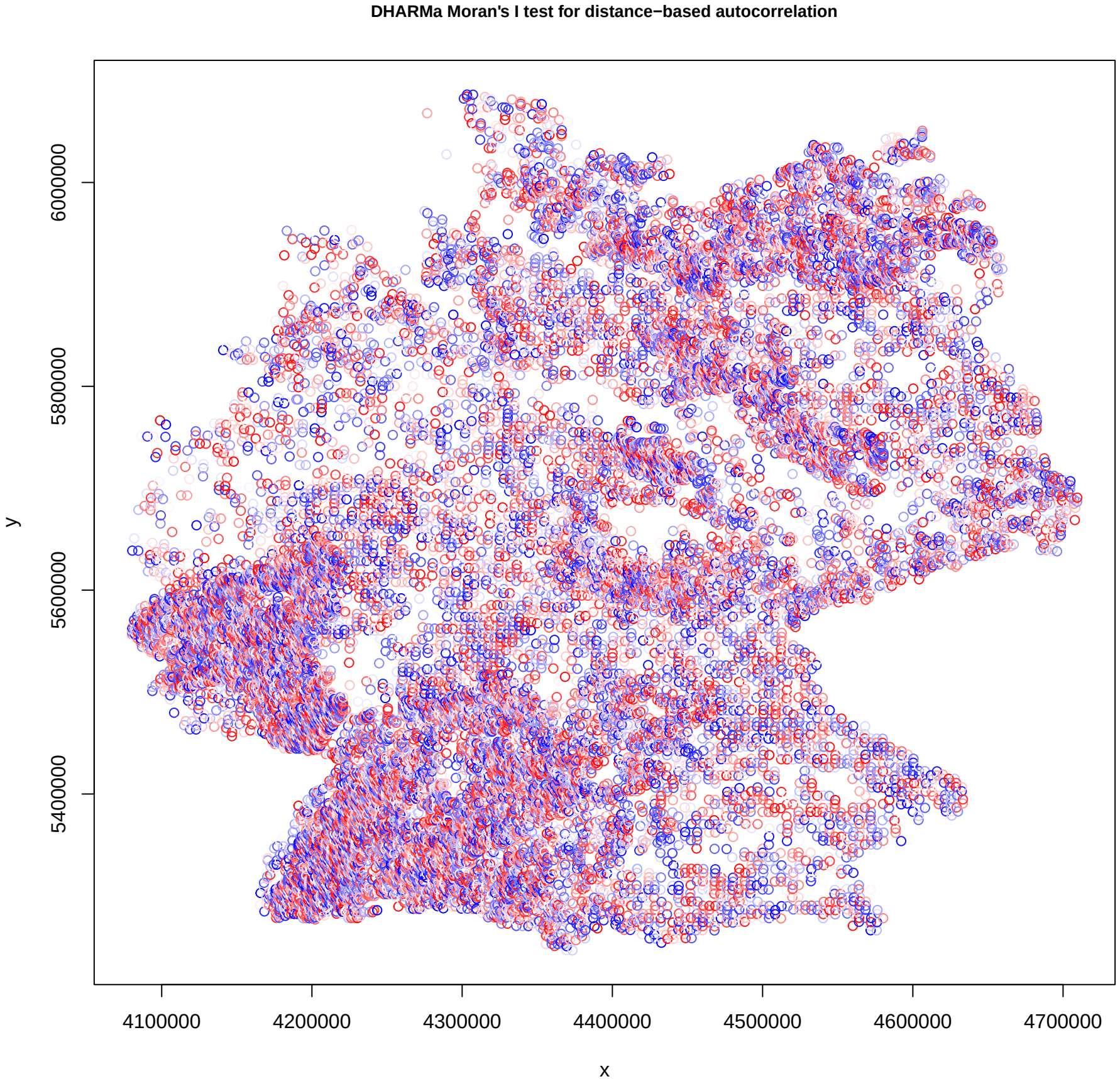

*Populus tremula*

DHARMa residual

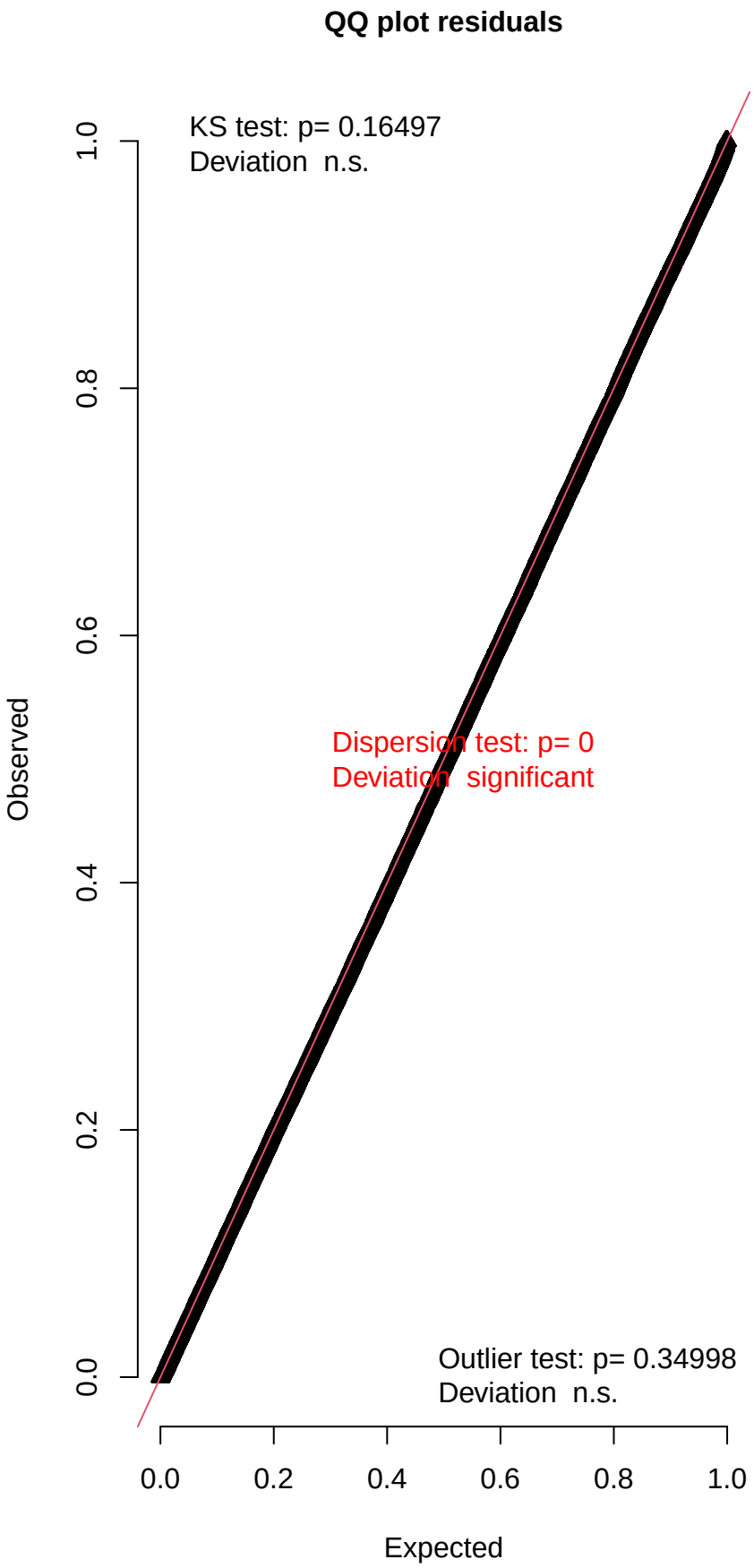


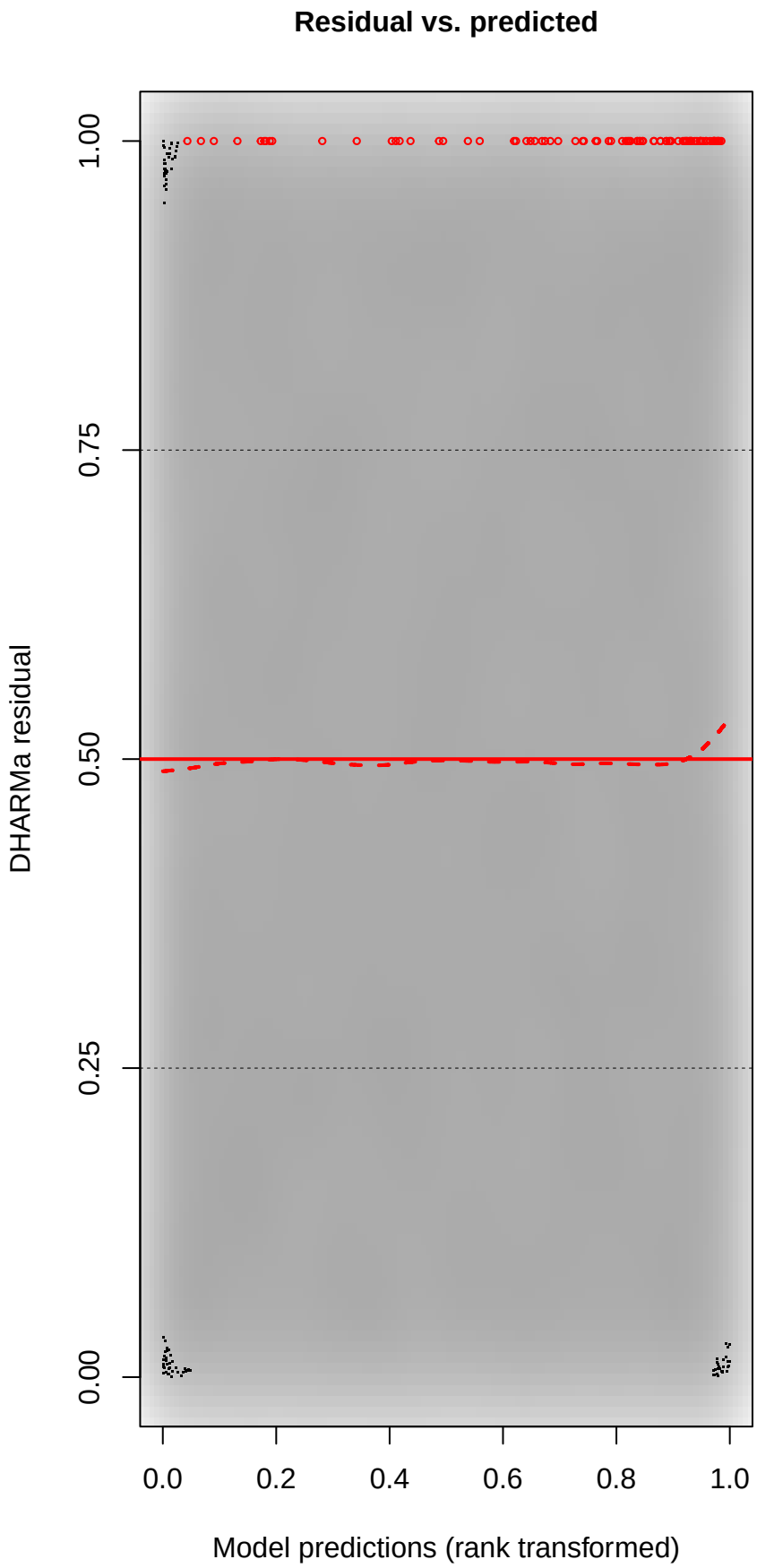

*Populus tremula*

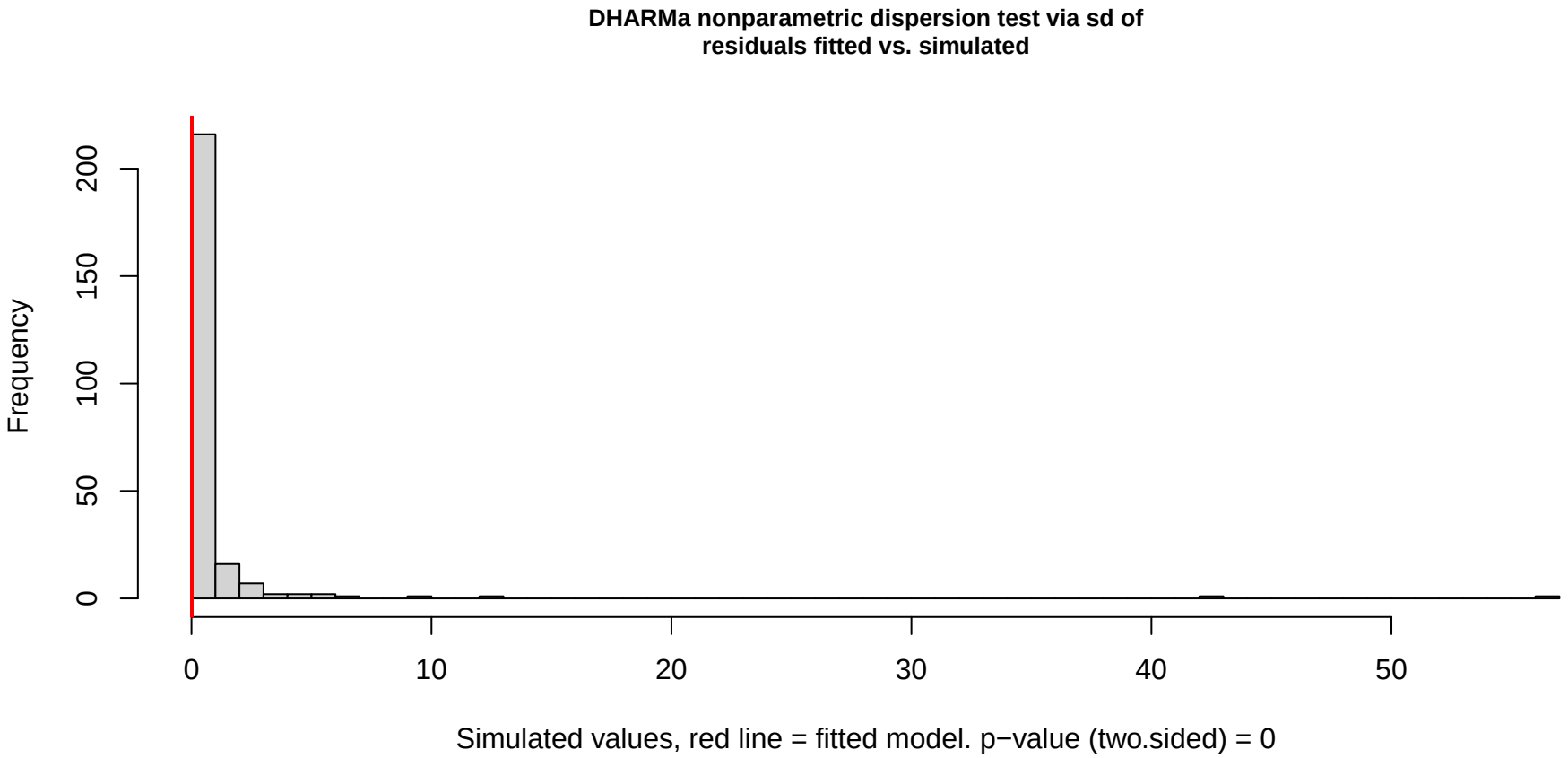


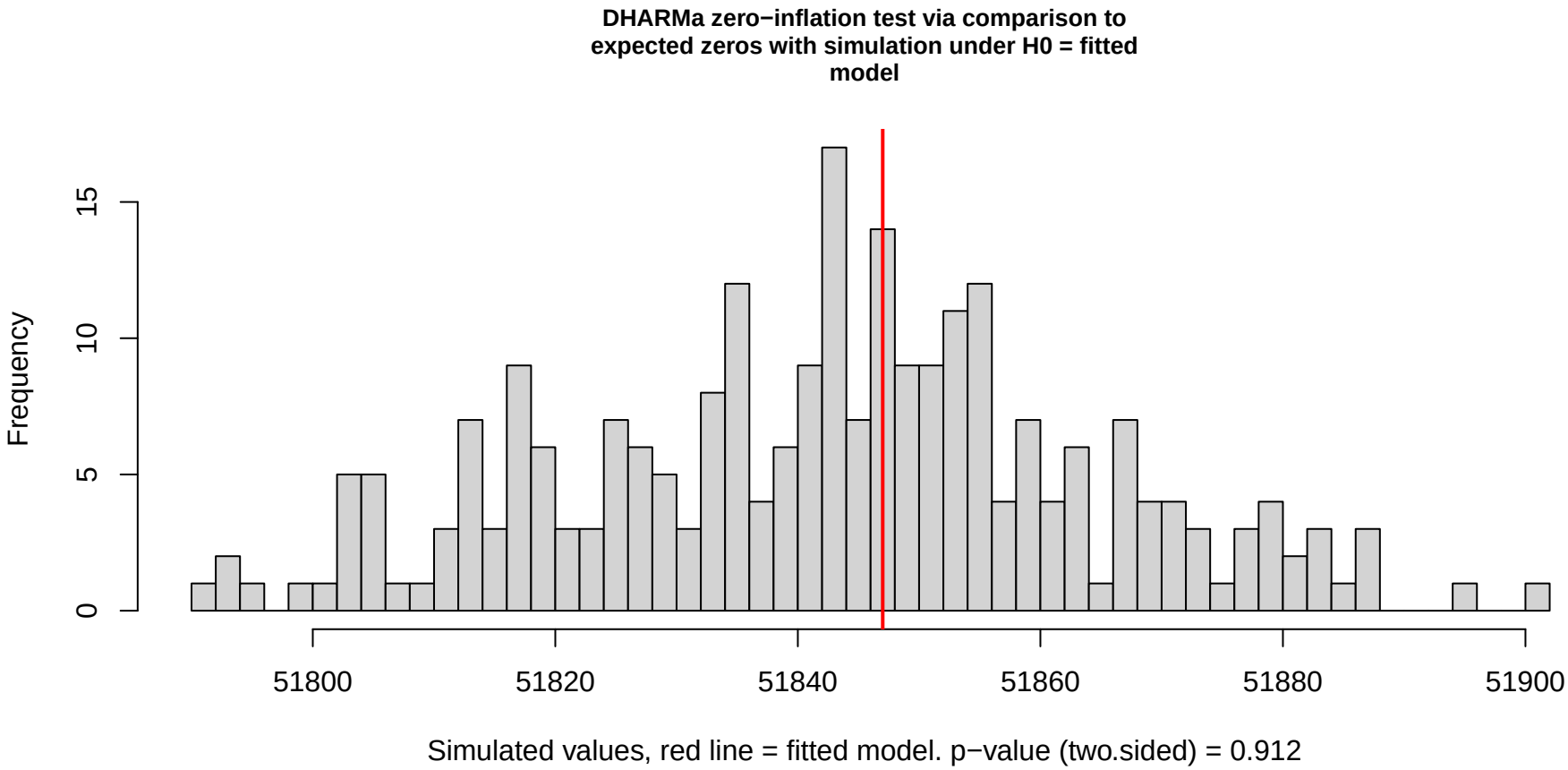

*Populus tremula*

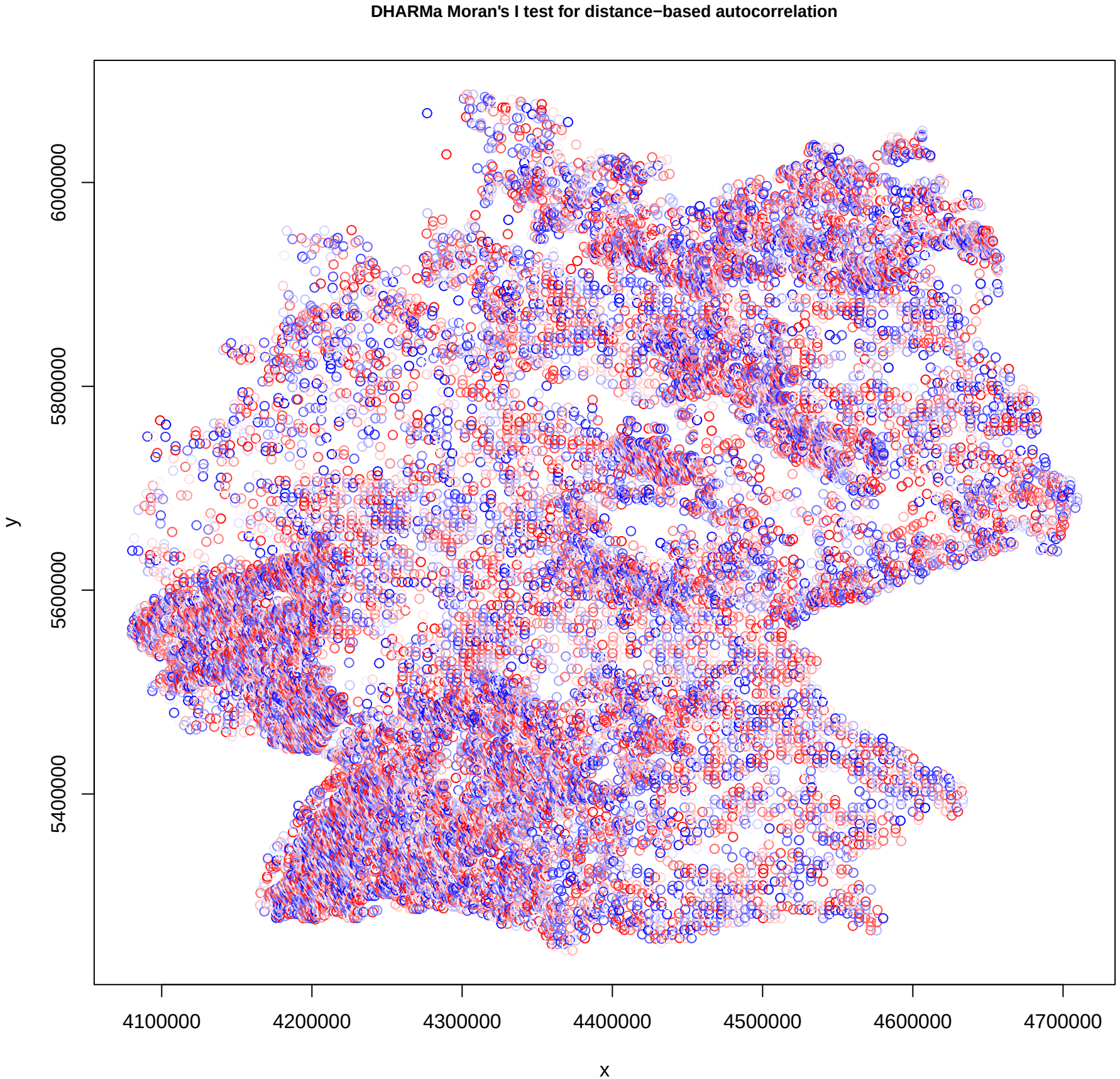

DHARMa residual

*Populus trichocarpa.x.maximoviczii*

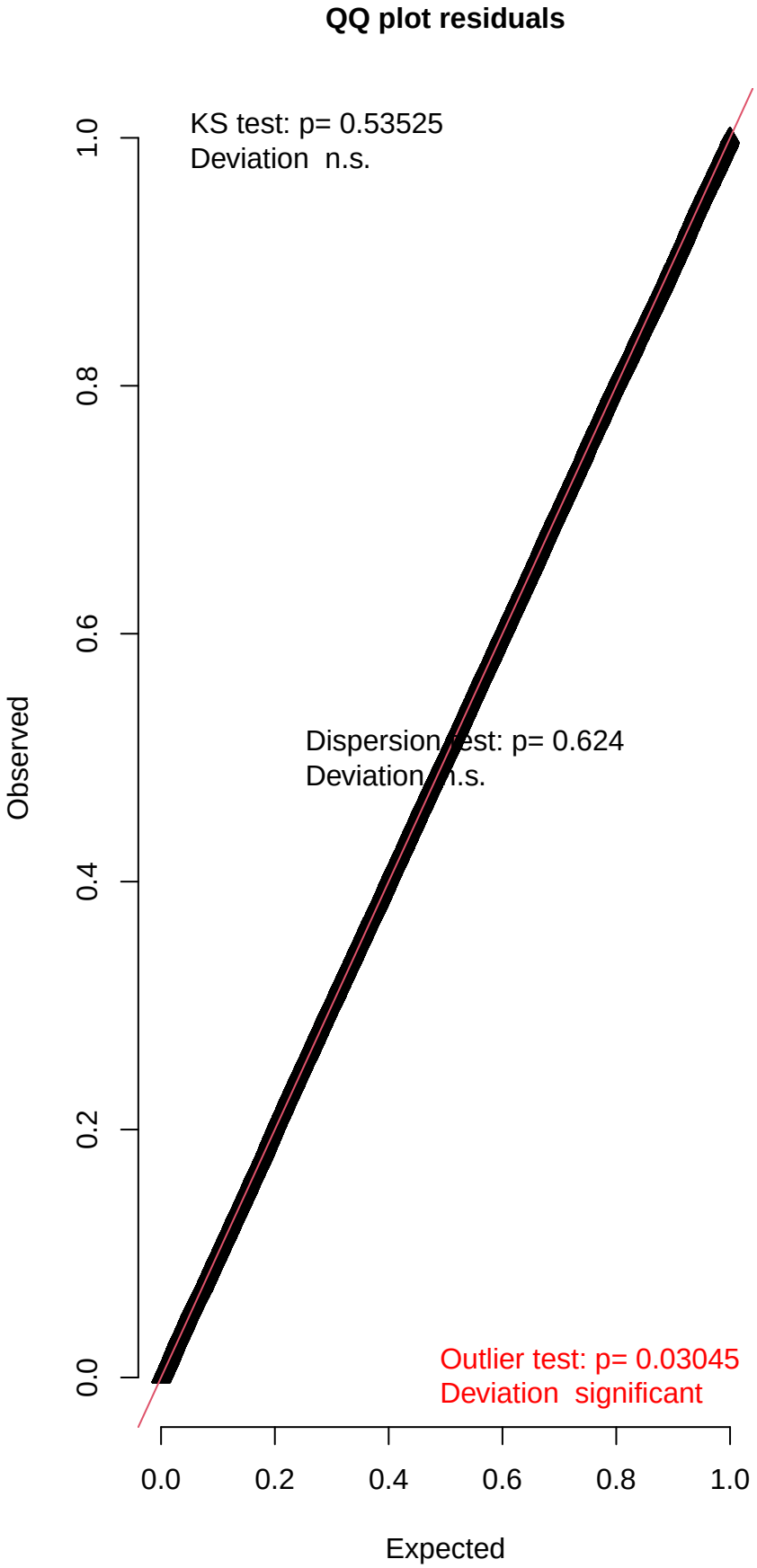


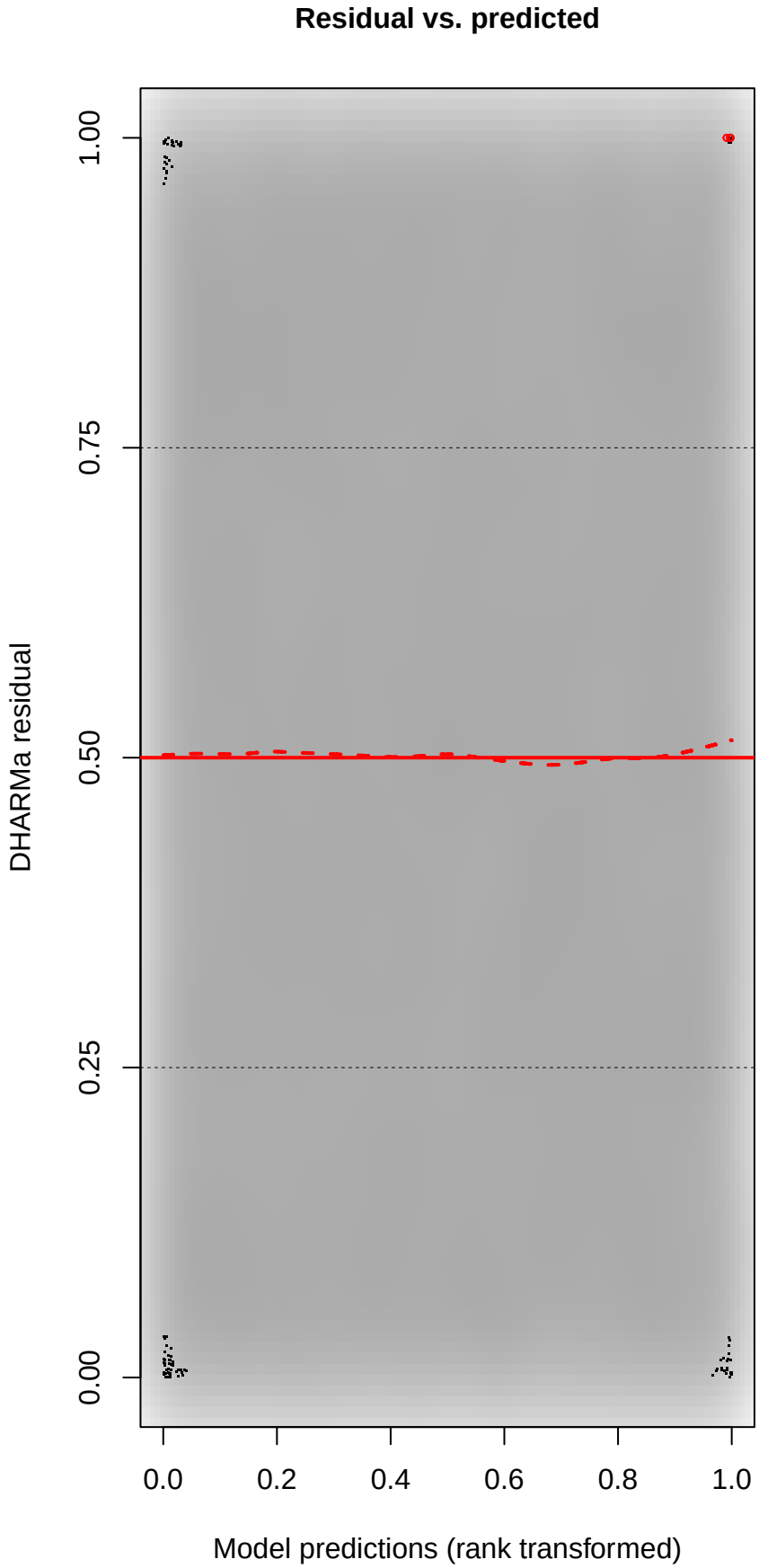

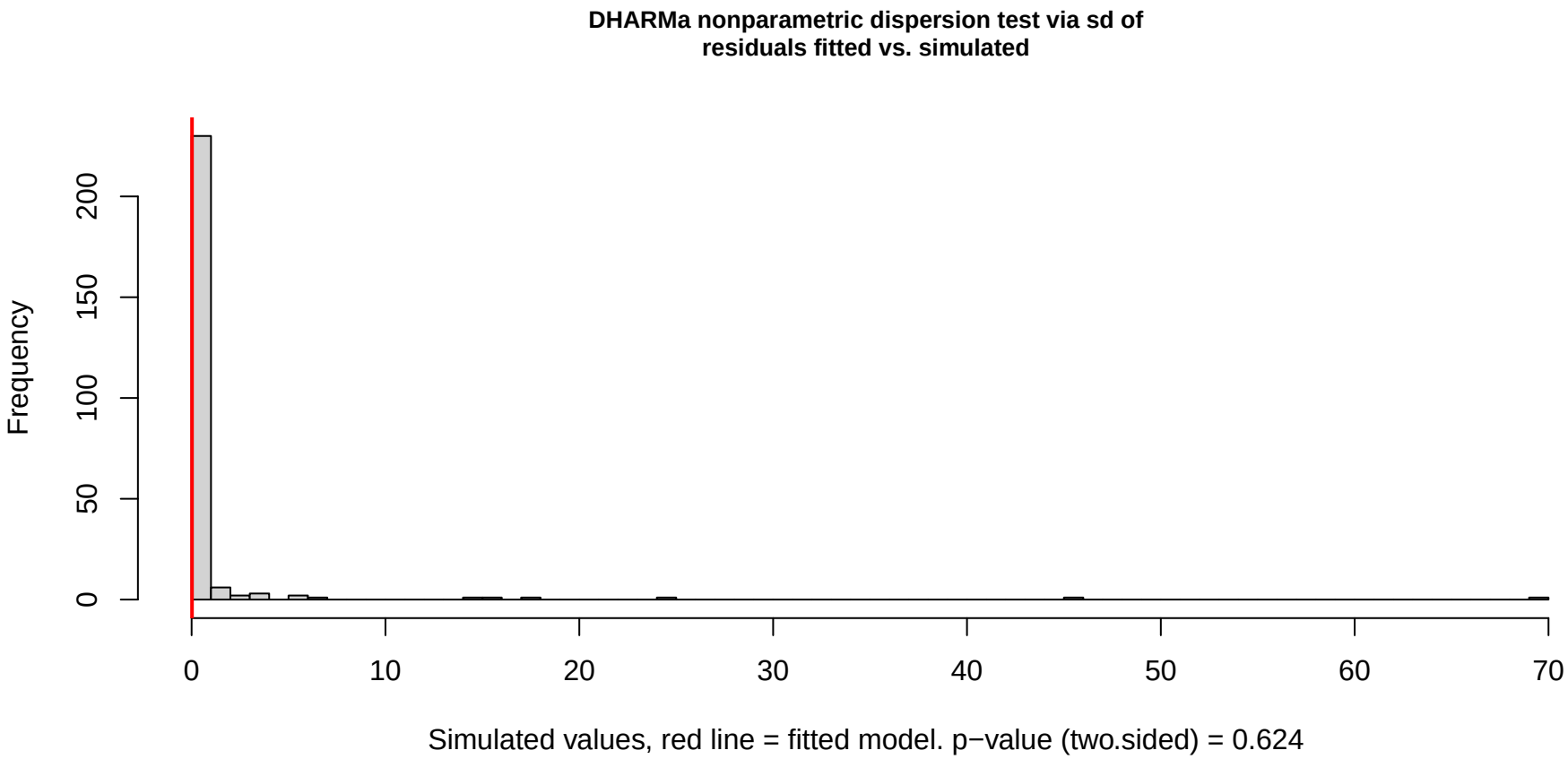
DHARMa nonparametric dispersion test via sd of residuals fitted vs. simulated
Frequency
0
50
100
150
200
0
10
20
30
40
50
60
70
Simulated values, red line = fitted model. p−value (two.sided) = 0.624

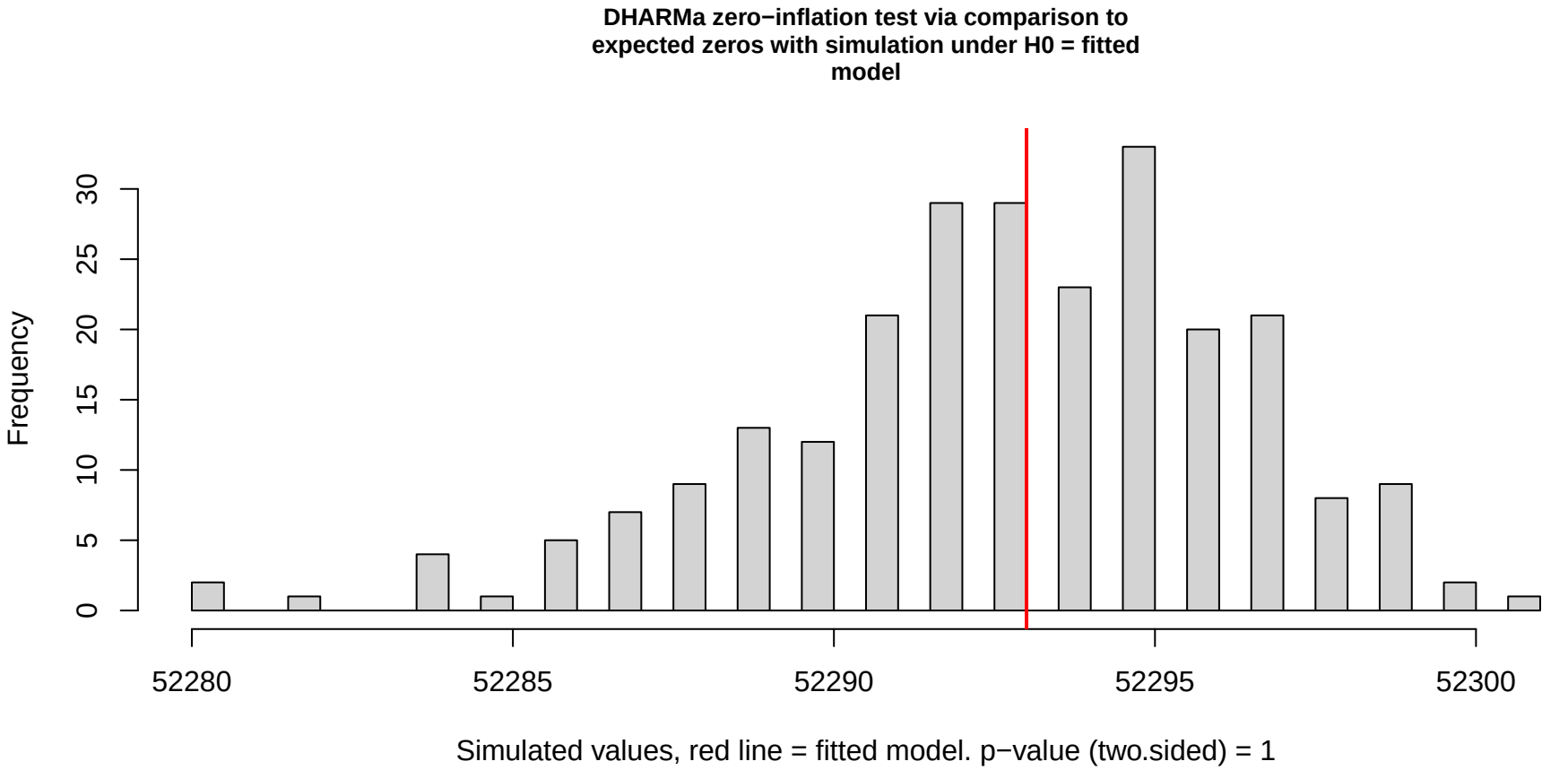
DHARMa zero−inflation test via comparison to expected zeros with simulation under H0 = fitted model
Frequency
0
5
10
15
20
25
30
52280
52285
52290
52295
52300
Simulated values, red line = fitted model. p−value (two.sided) = 1

*Populus trichocarpa.x.maximoviczii*

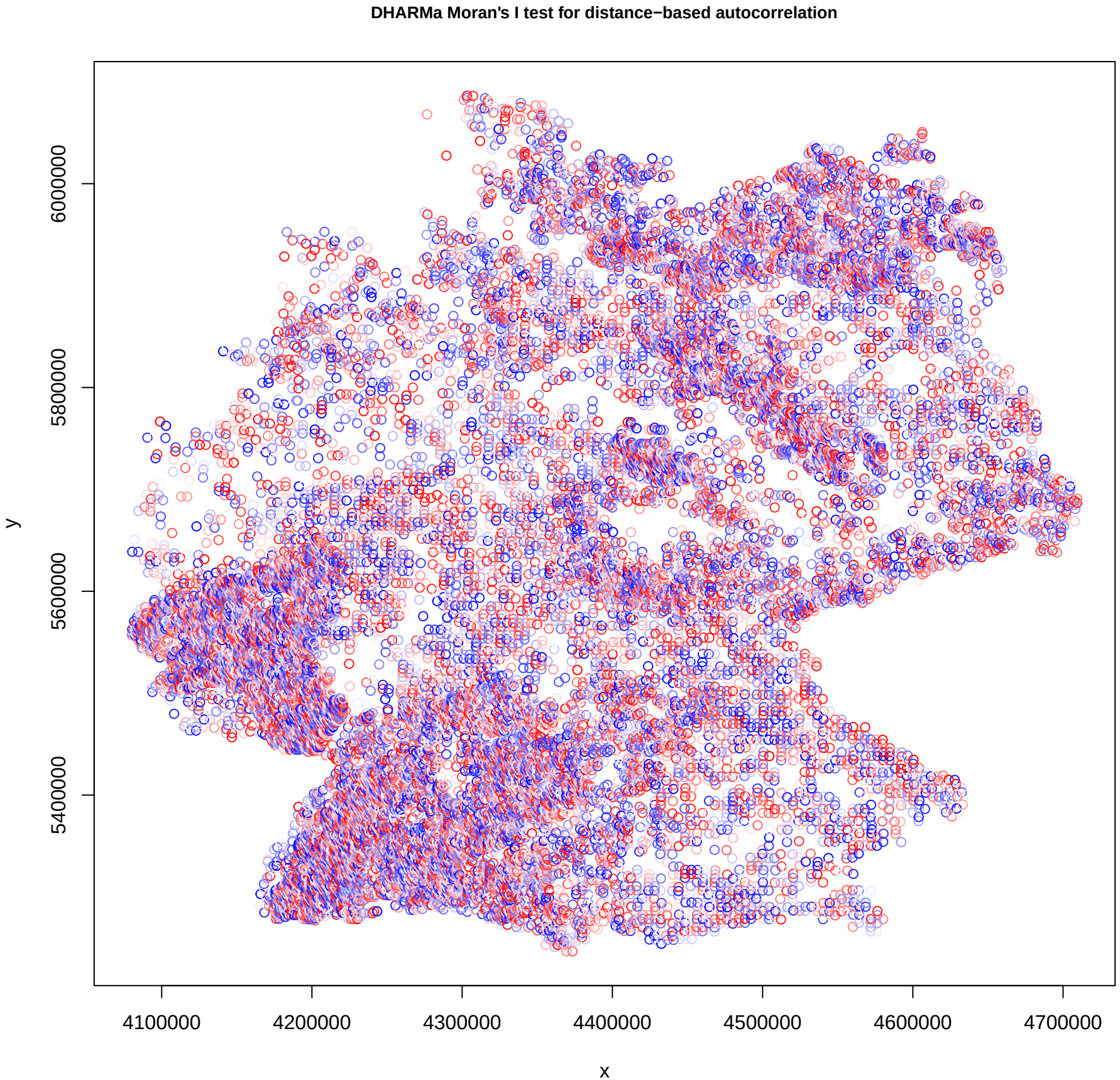

*Populus nigra*

DHARMa residual

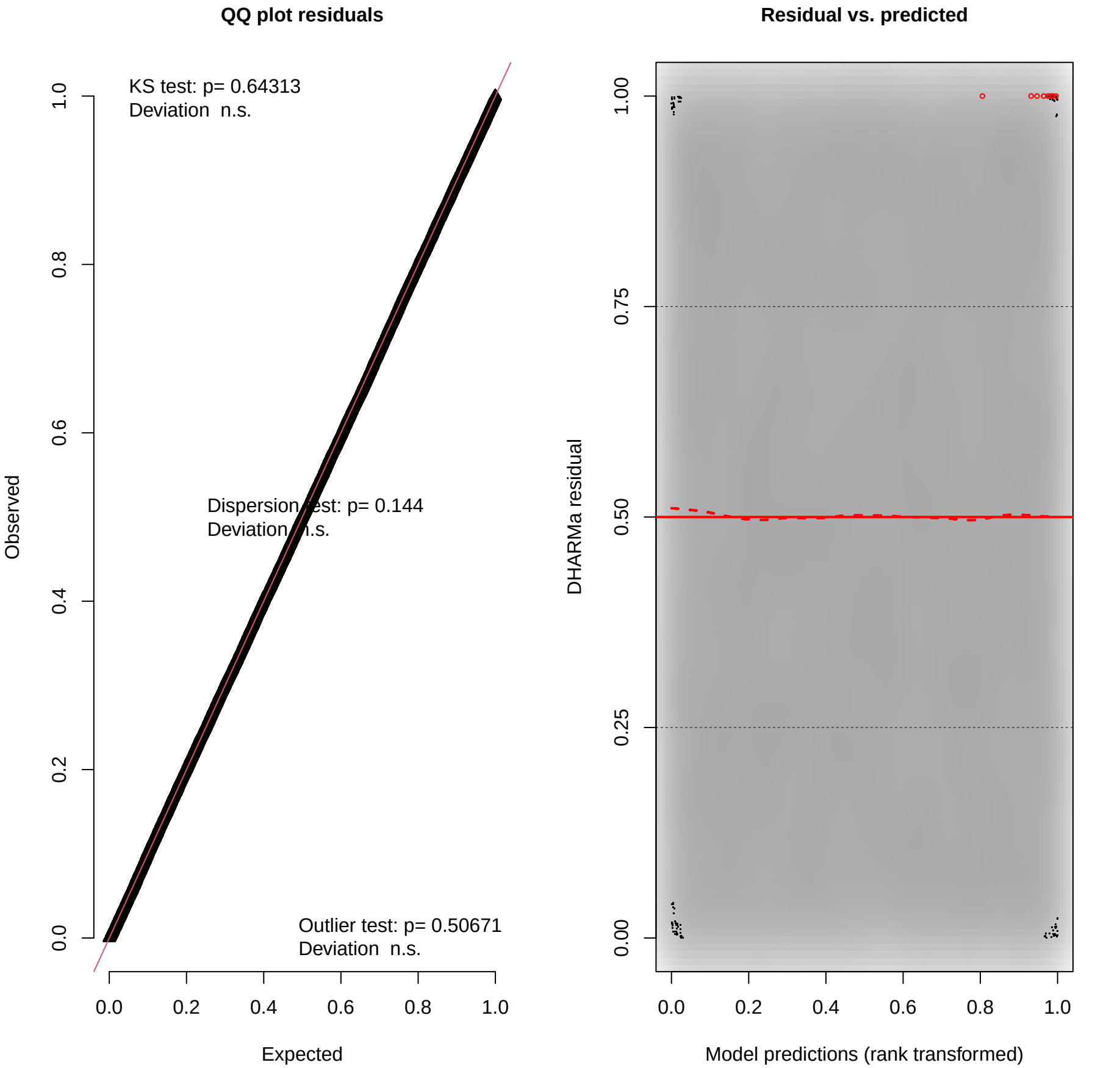

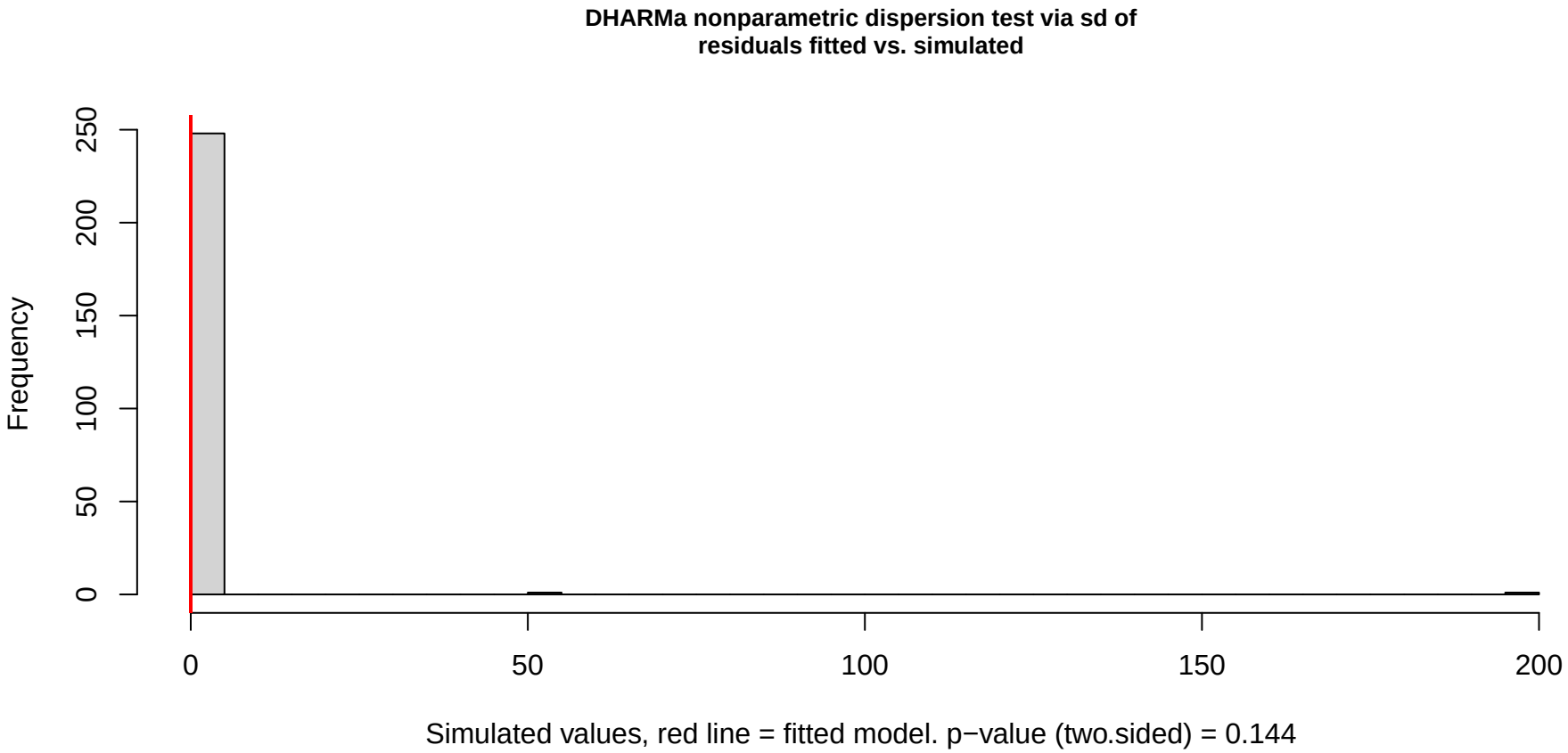
DHARMa nonparametric dispersion test via sd of residuals fitted vs. simulated
Frequency
0
50
100
150
200
250
0
50
100
150
200
Simulated values, red line = fitted model. p−value (two.sided) = 0.144

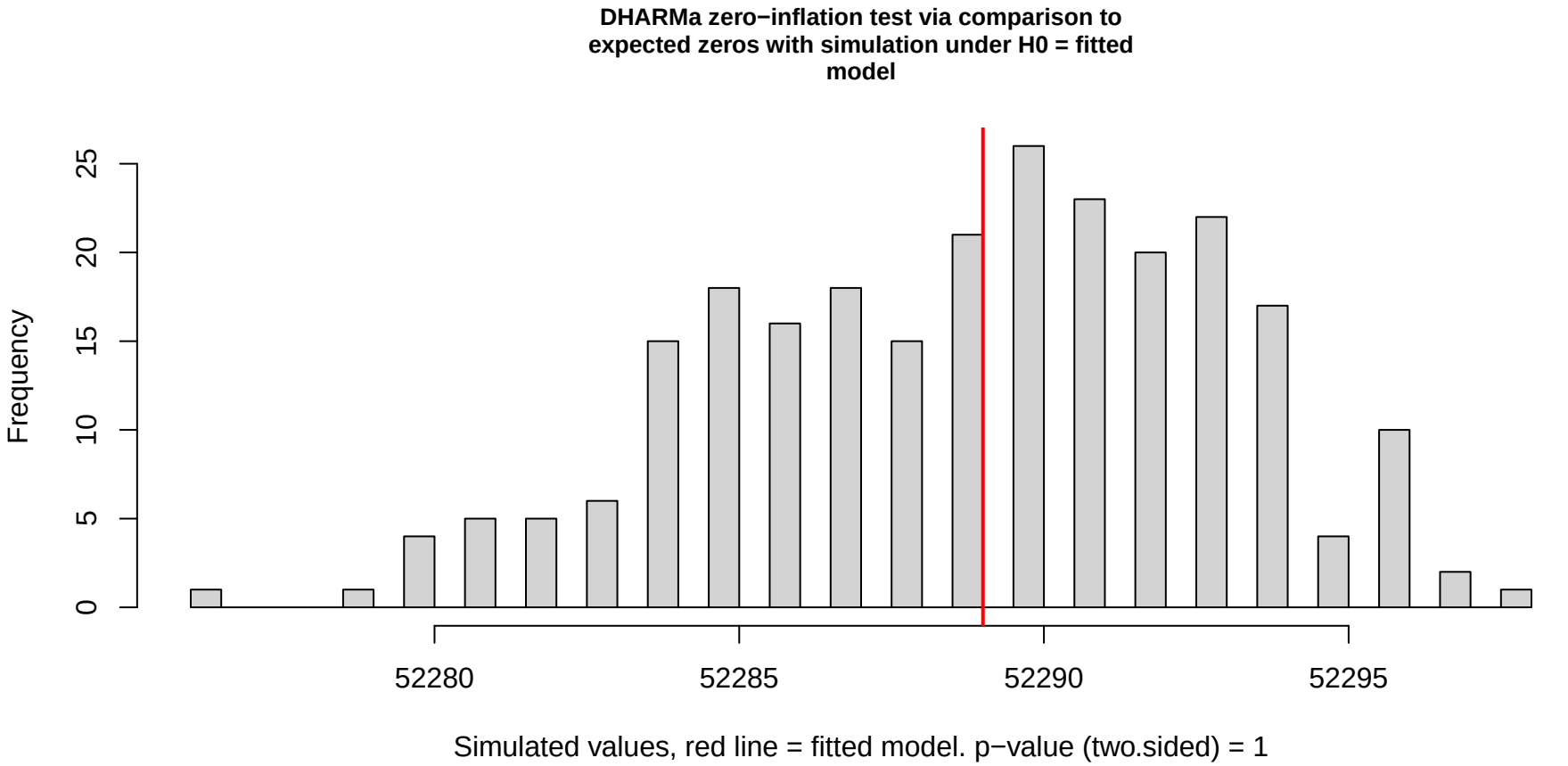
DHARMa zero−inflation test via comparison to expected zeros with simulation under H0 = fitted model
Frequency
0
5
10
15
20
25
52280
52285
52290
52295
Simulated values, red line = fitted model. p−value (two.sided) = 1

*Populus nigra*

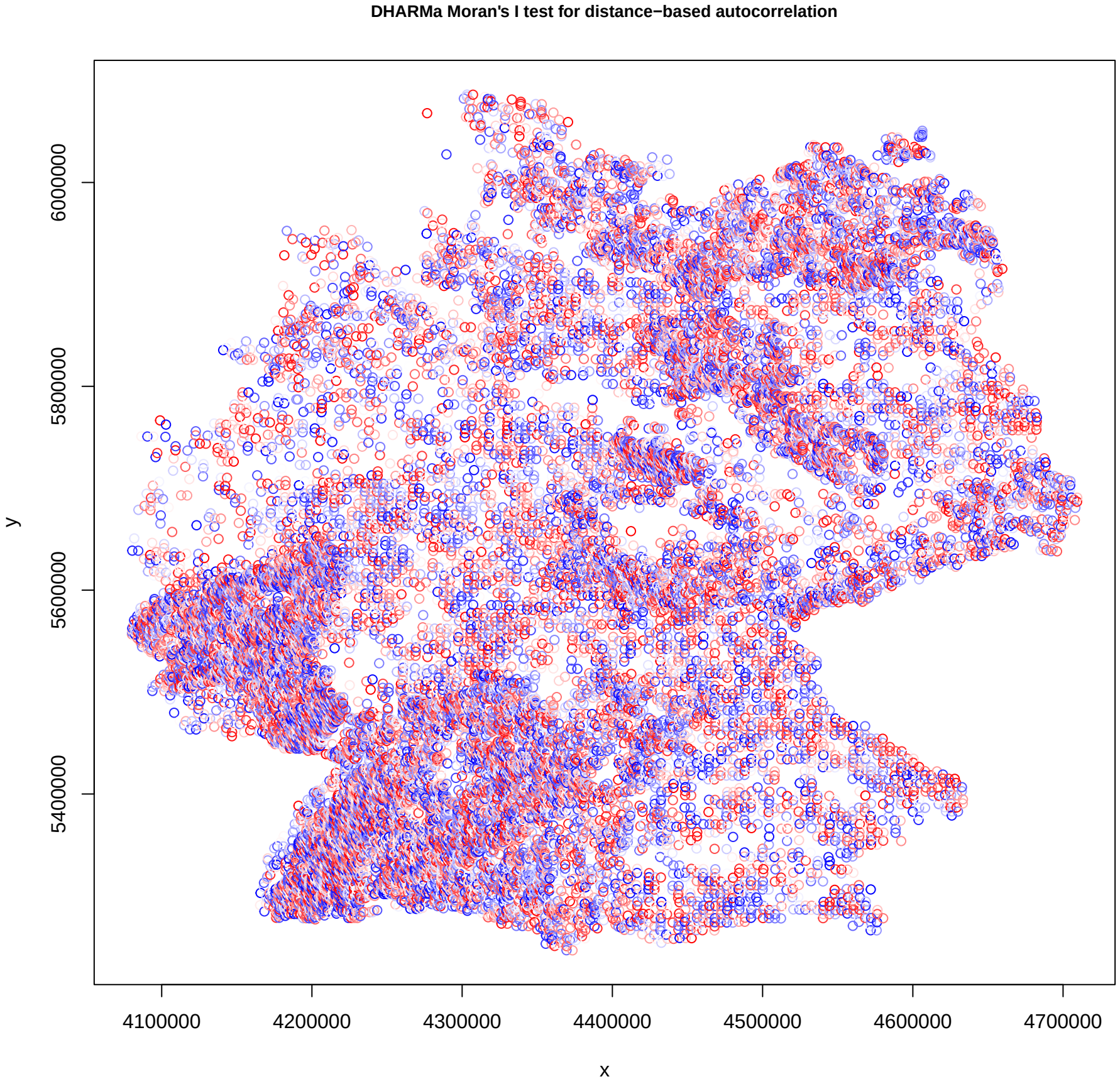

*Populus alba*

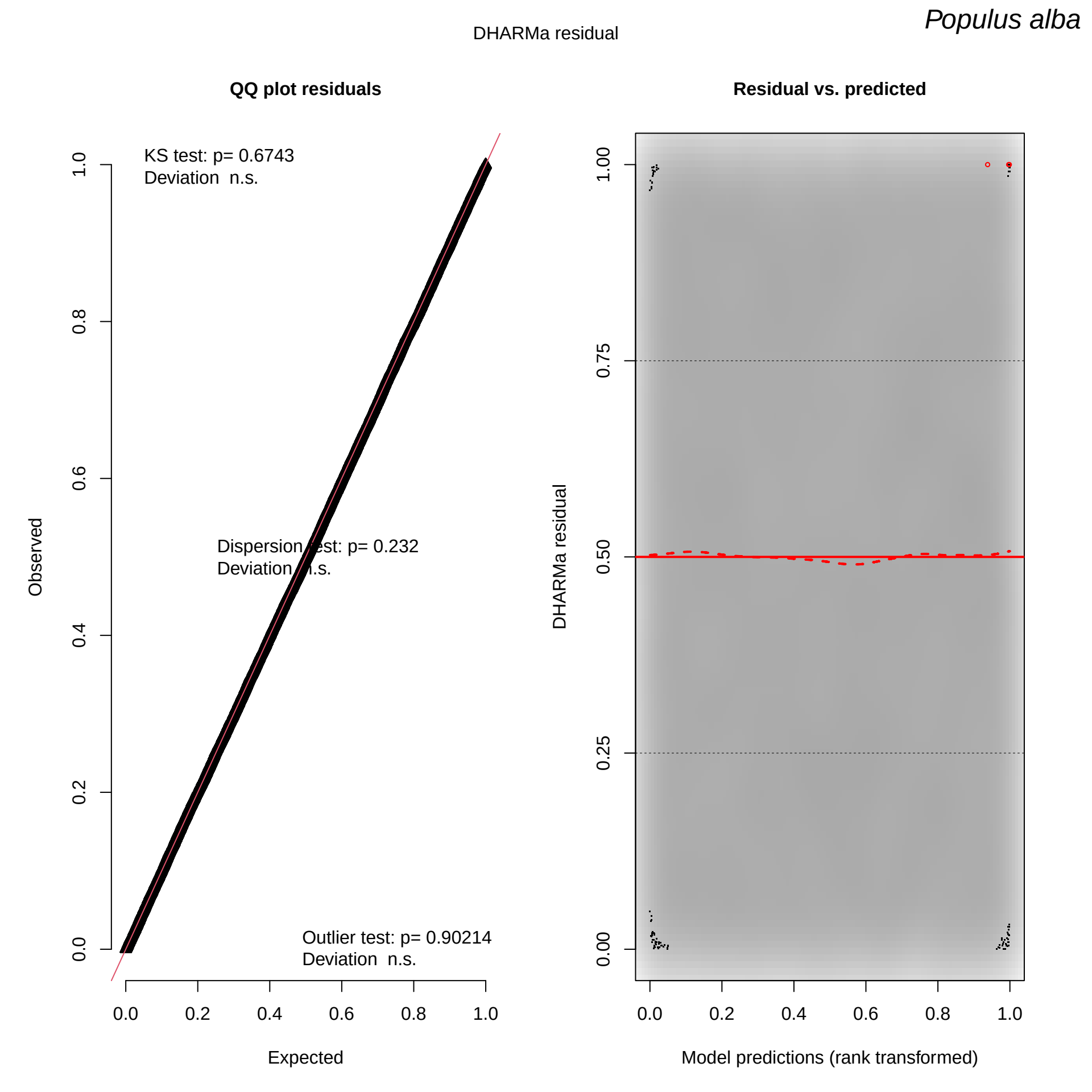

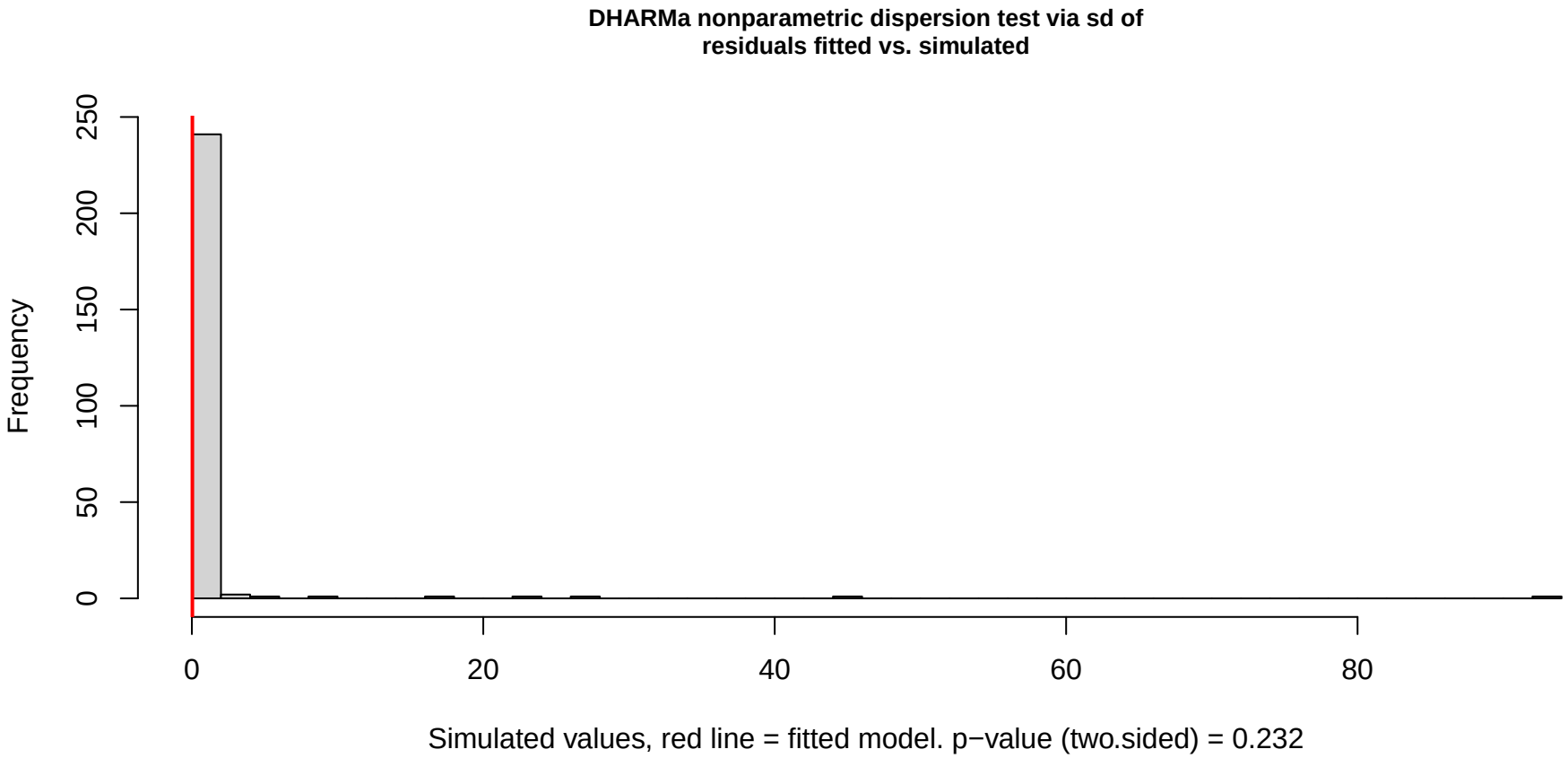
DHARMa nonparametric dispersion test via sd of residuals fitted vs. simulated
Frequency
0
50
100
150
200
250
0
20
40
60
80
Simulated values, red line = fitted model. p−value (two.sided) = 0.232

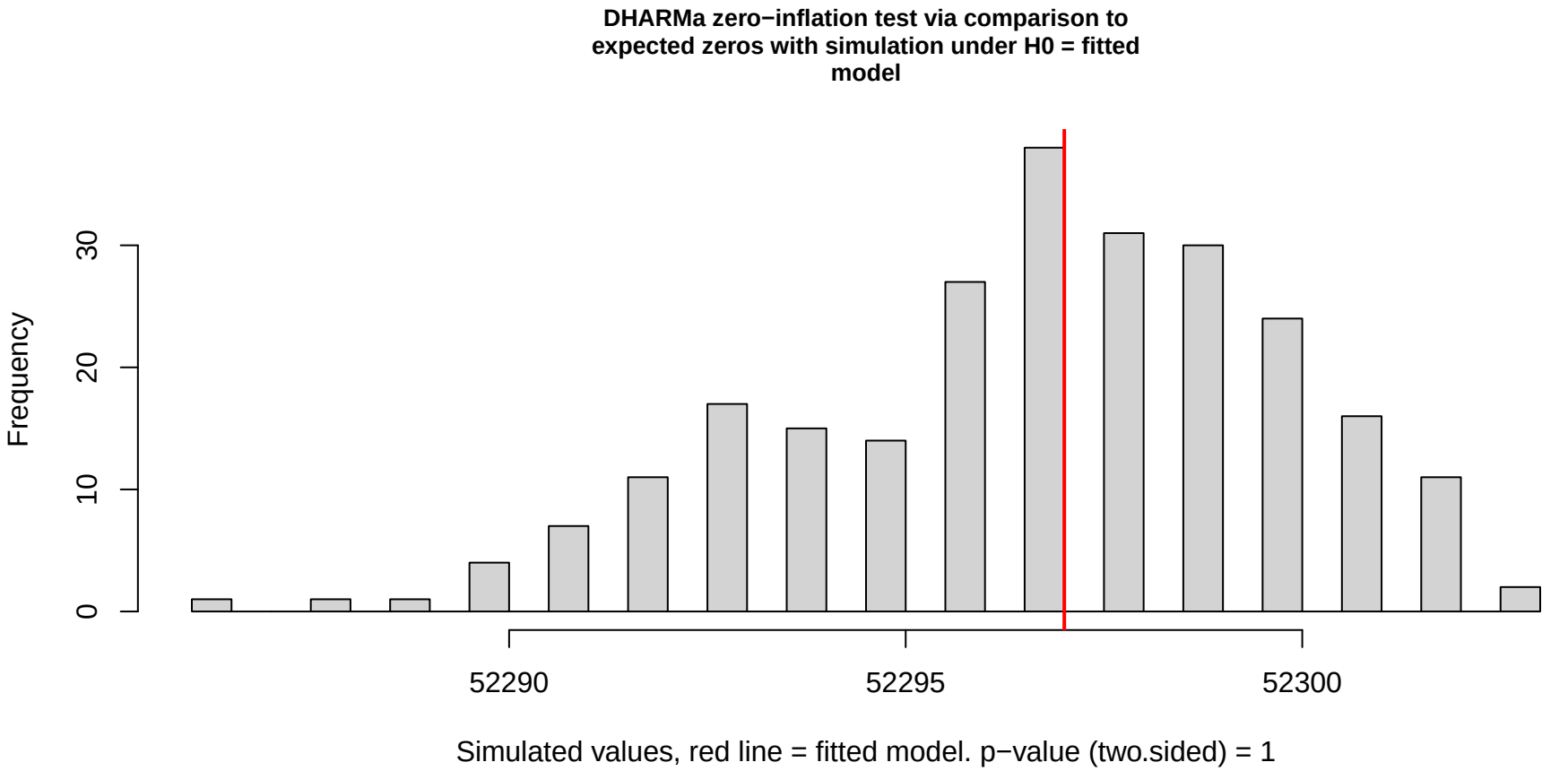
DHARMa zero−inflation test via comparison to expected zeros with simulation under H0 = fitted model
Frequency
0
10
20
30
52290
52295
52300
Simulated values, red line = fitted model. p−value (two.sided) = 1

*Populus alba*

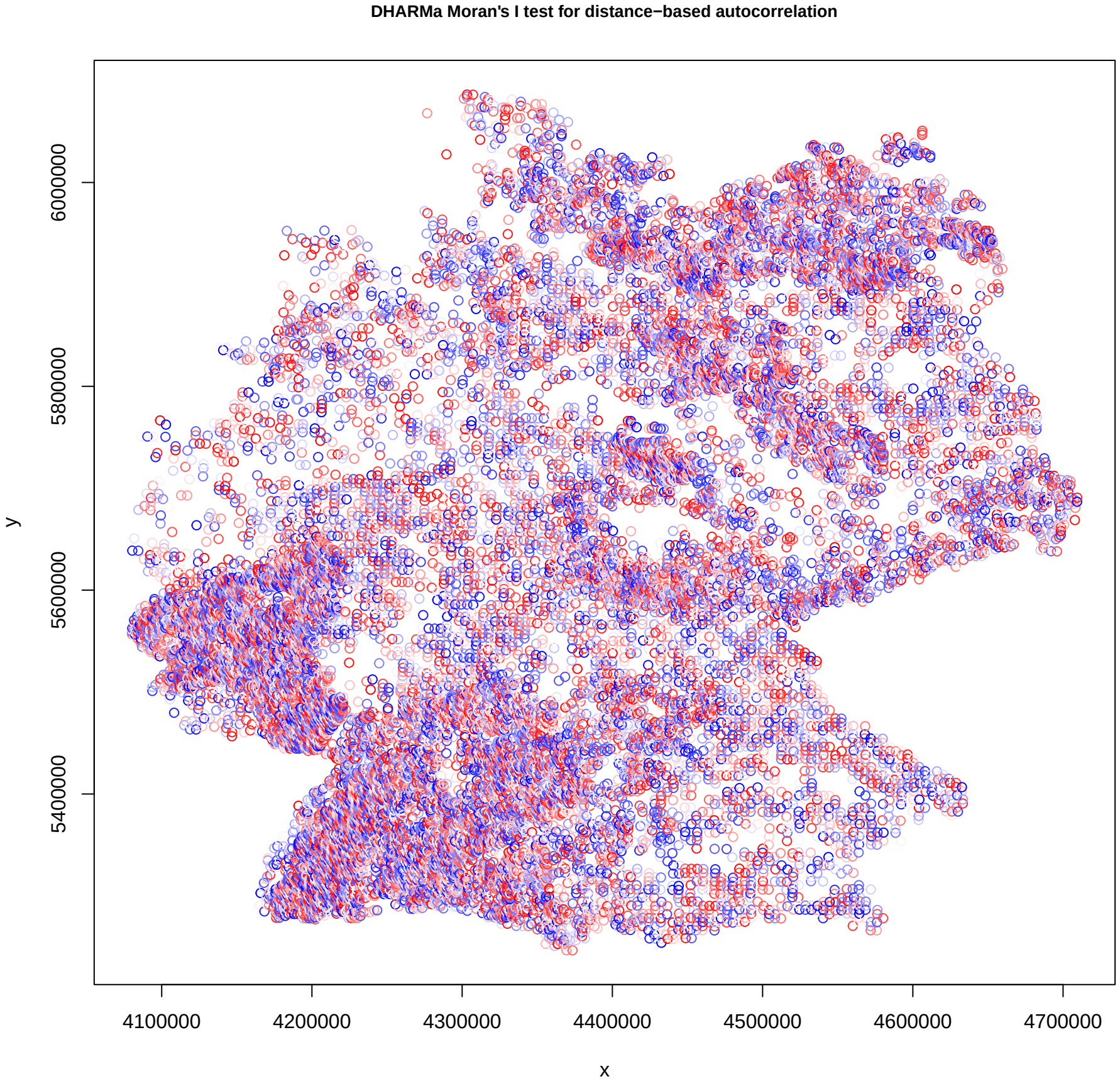

*Alnus glutinosa*

DHARMa residual

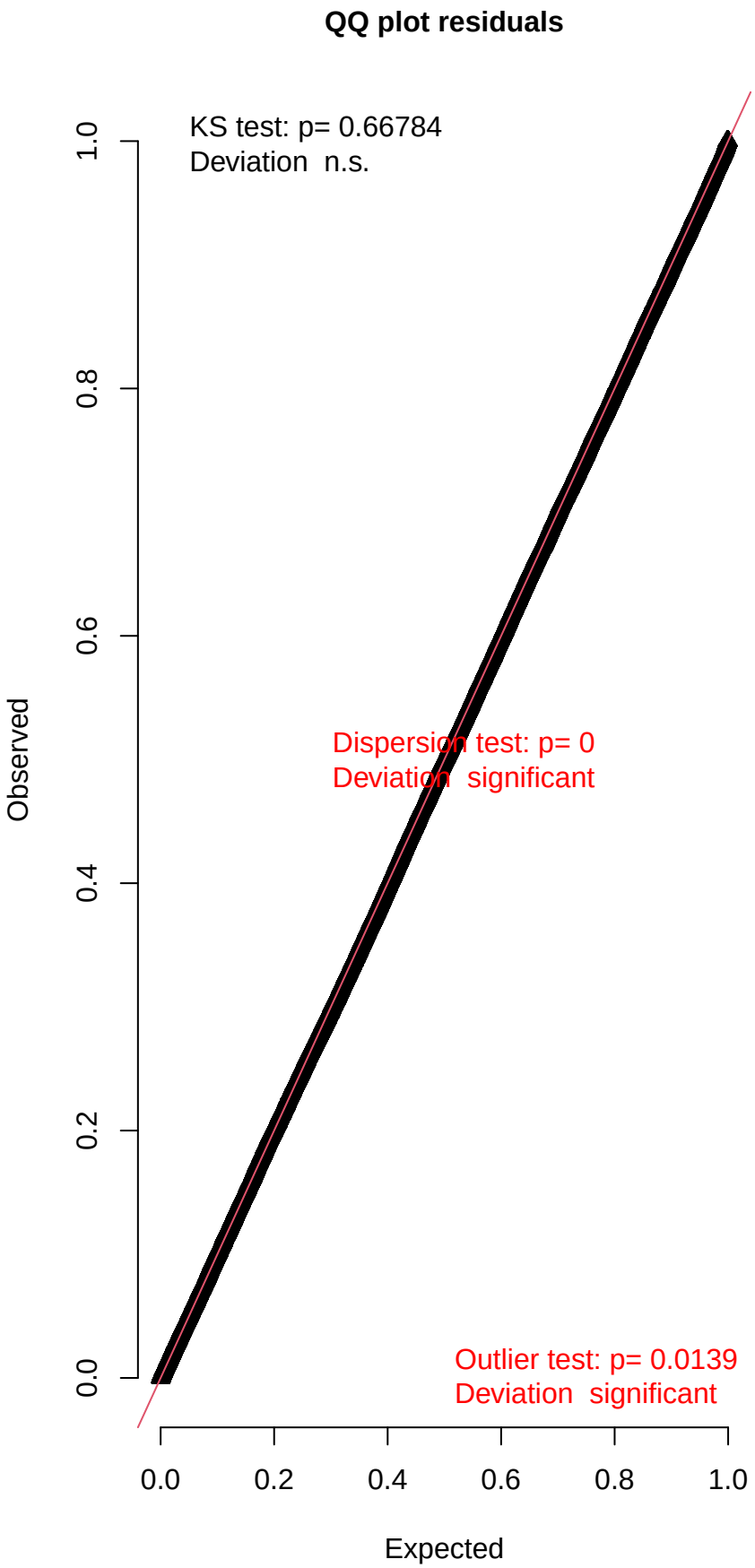


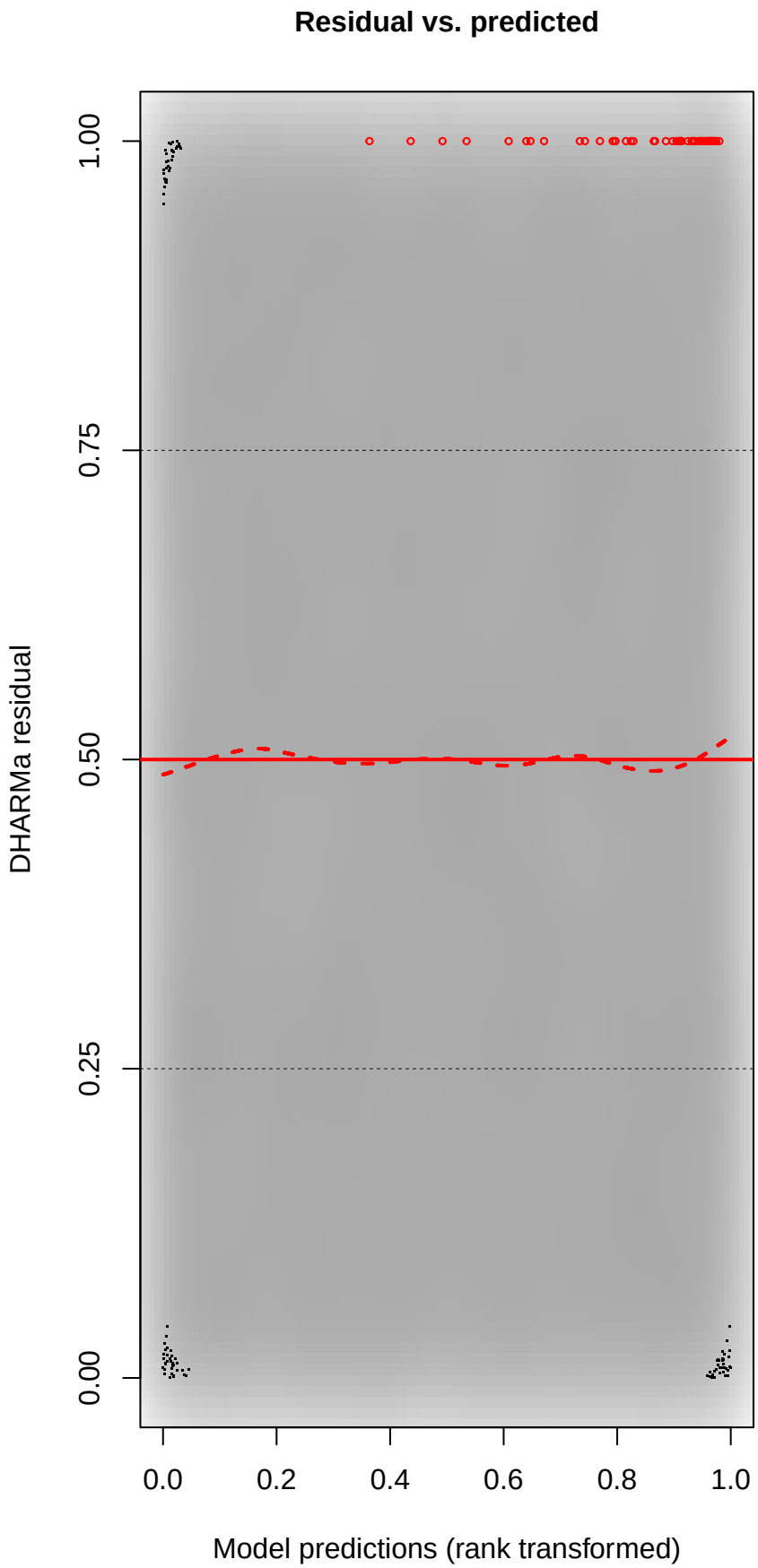

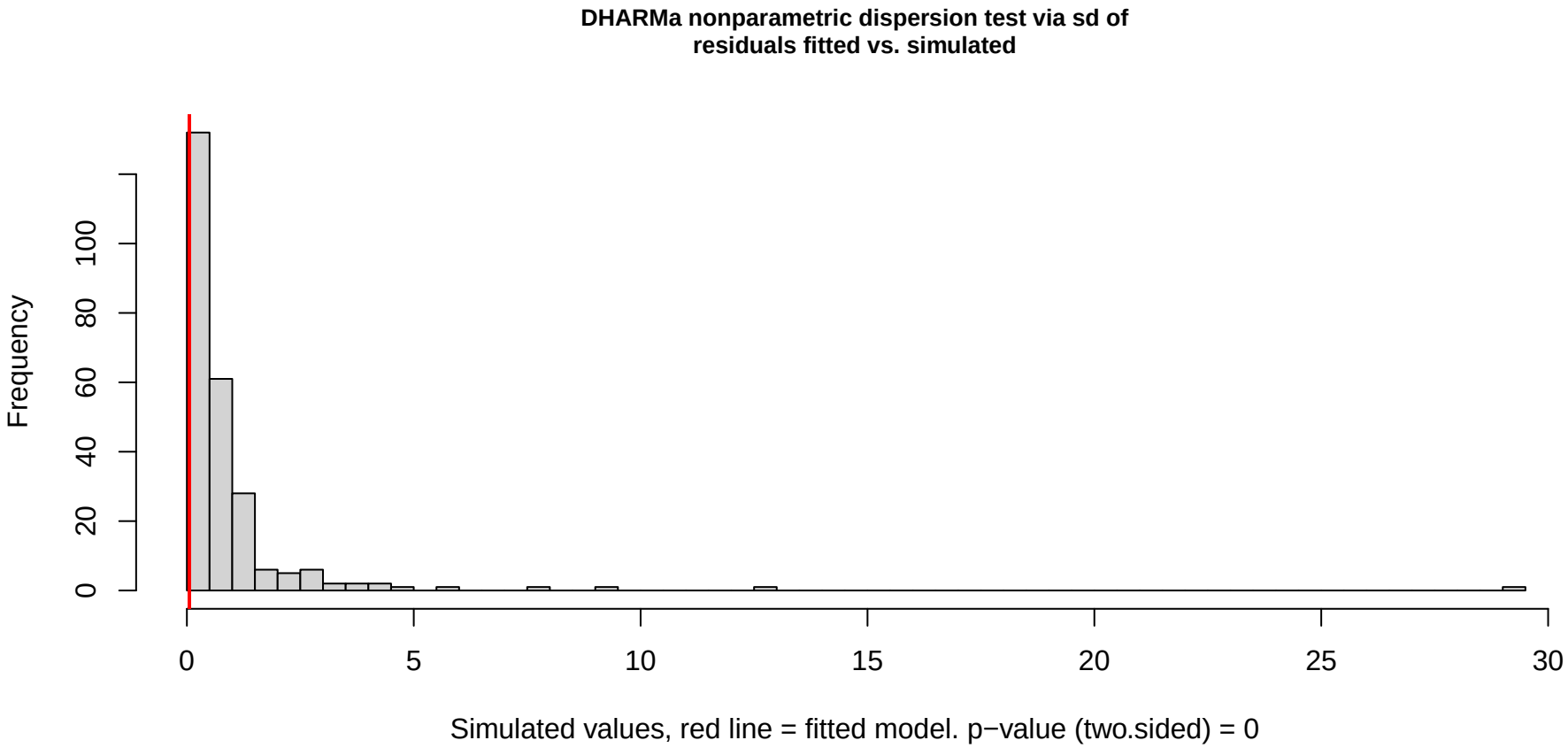
DHARMa nonparametric dispersion test via sd of residuals fitted vs. simulated
Frequency
0
20
40
60
80
100
0
5
10
15
20
25
30
Simulated values, red line = fitted model. p−value (two.sided) = 0

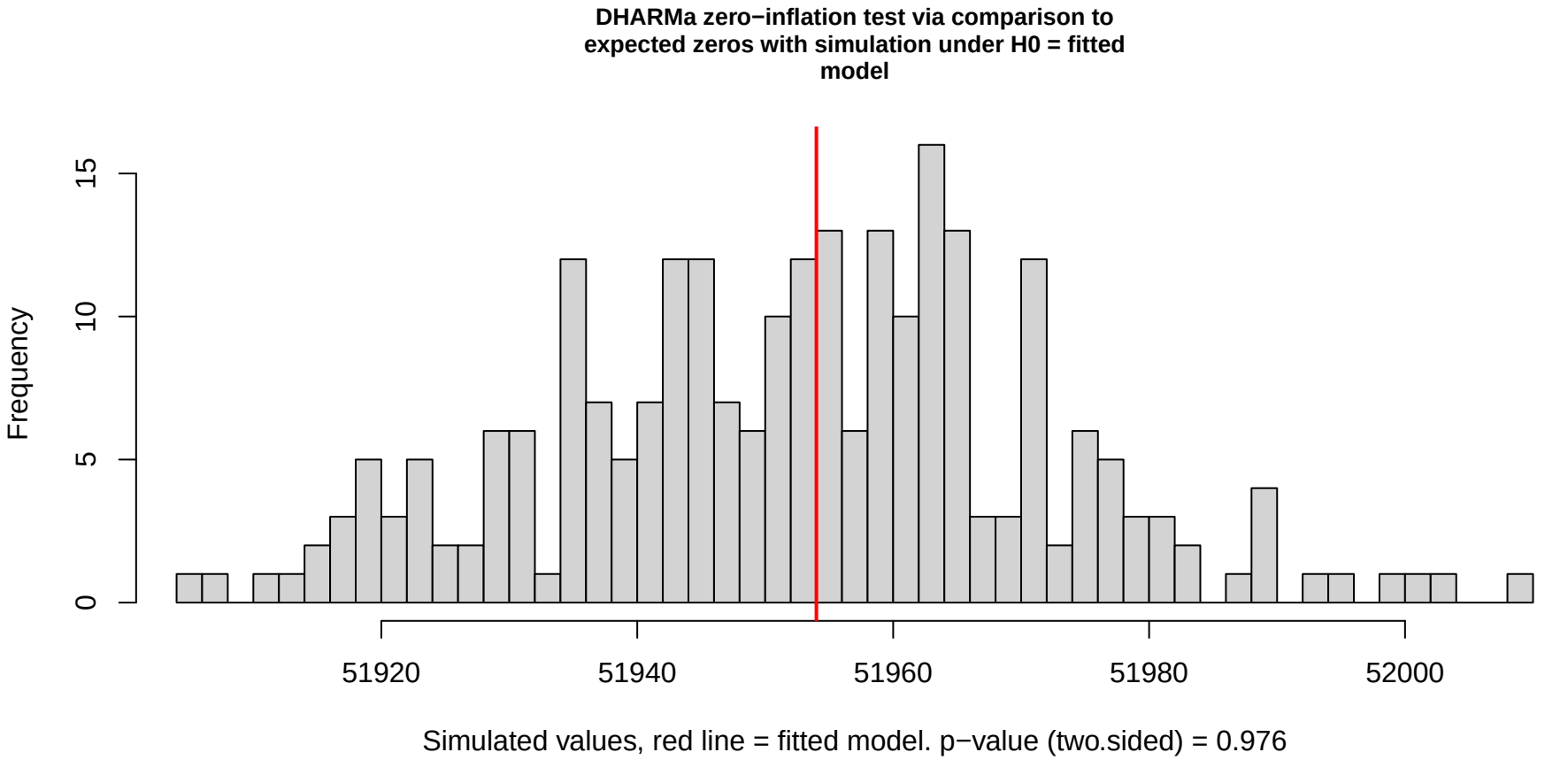
DHARMa zero−inflation test via comparison to expected zeros with simulation under H0 = fitted model
Frequency
0
5
10
15
51920
51940
51960
51980
52000
Simulated values, red line = fitted model. p−value (two.sided) = 0.976

*Alnus glutinosa*

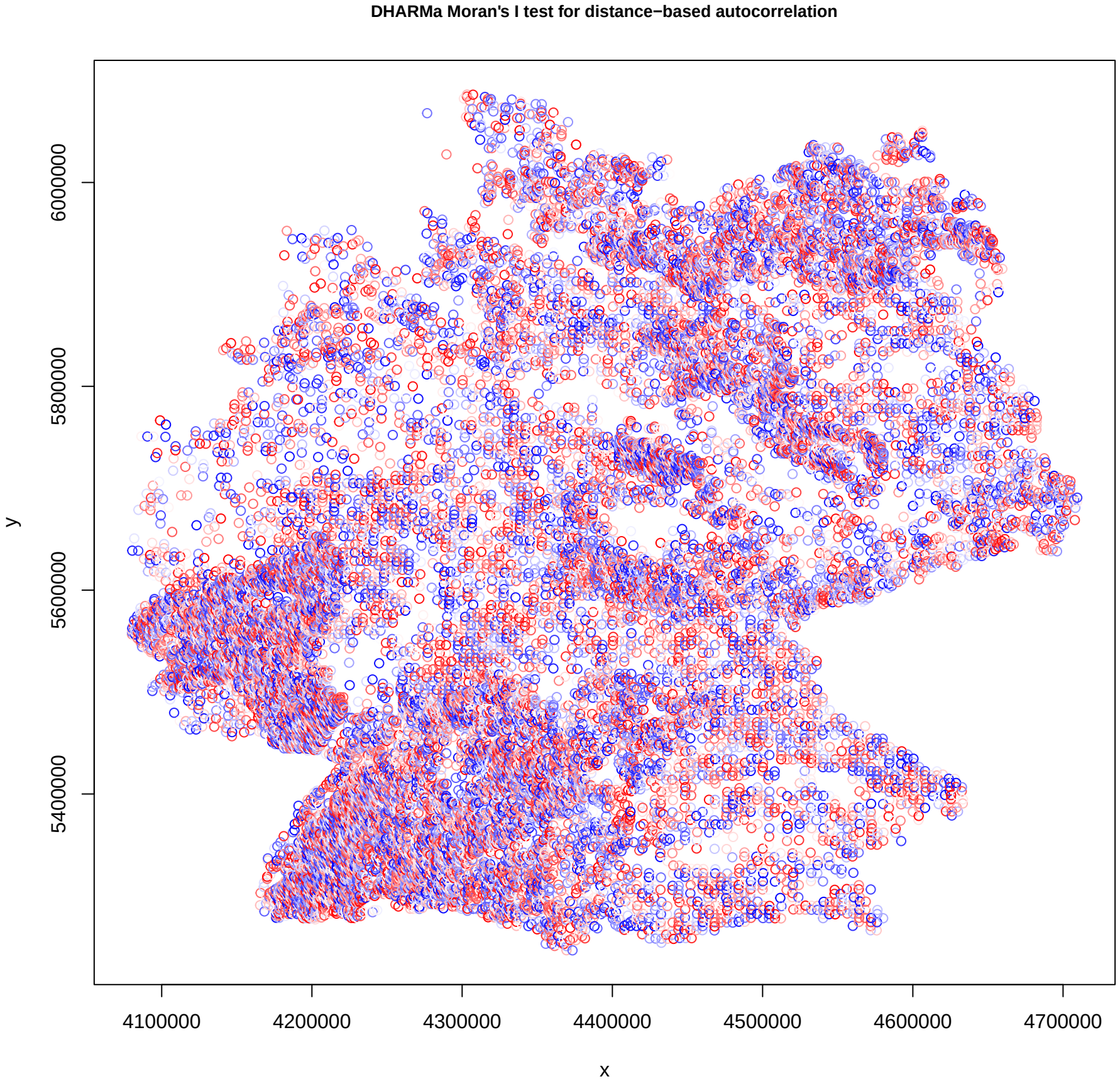

*Alnus incana*

DHARMa residual

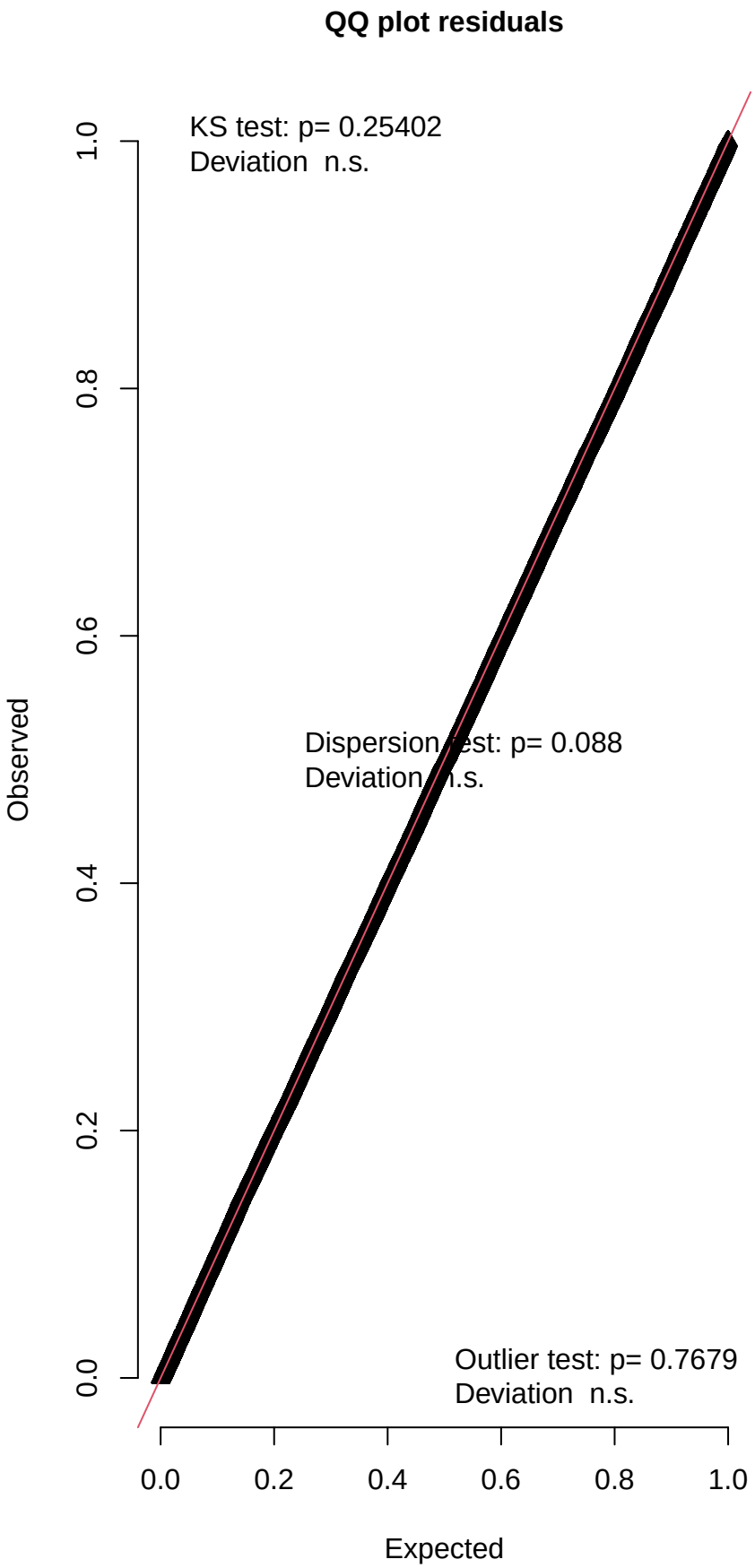


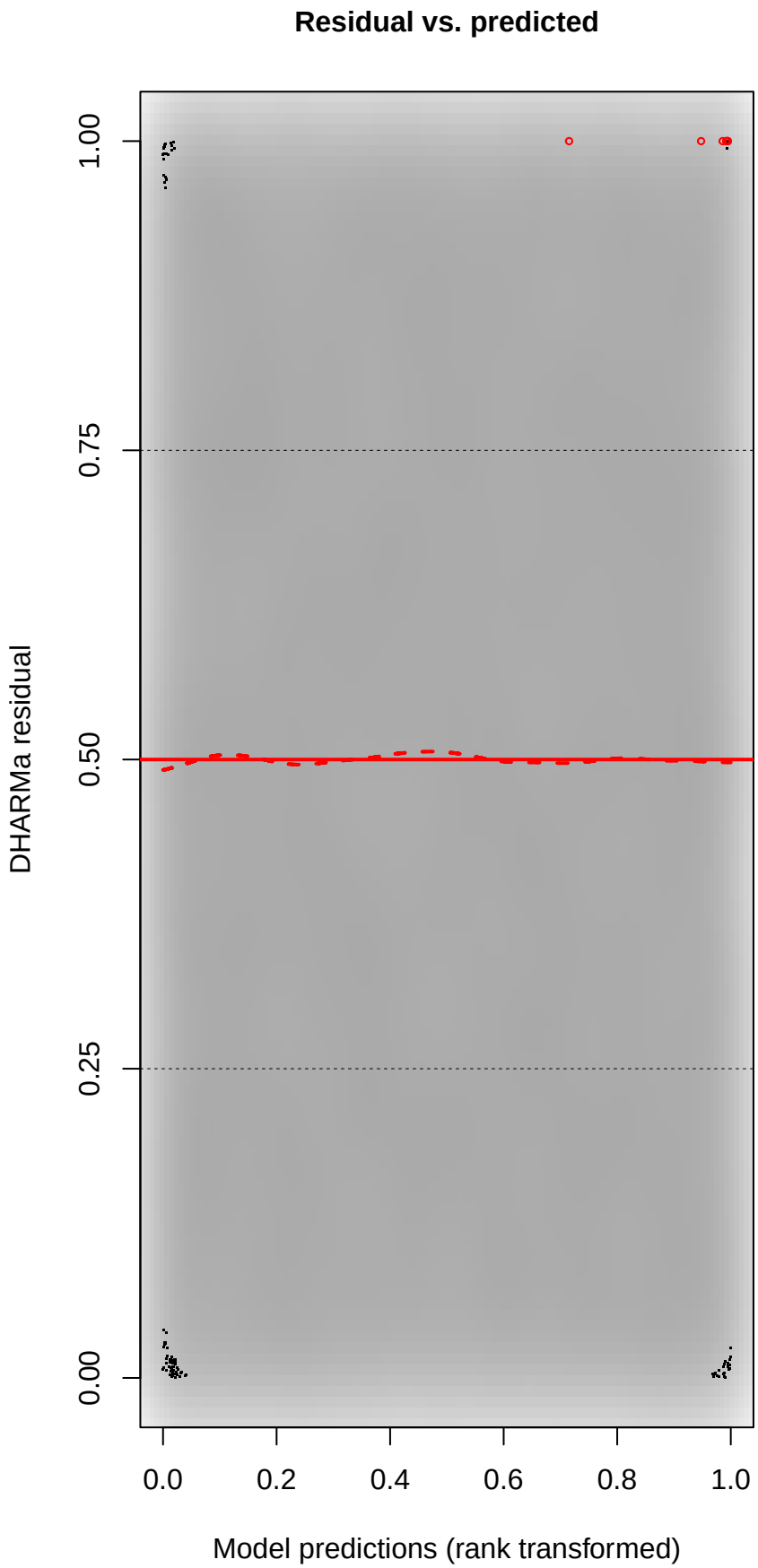

*Alnus incana*

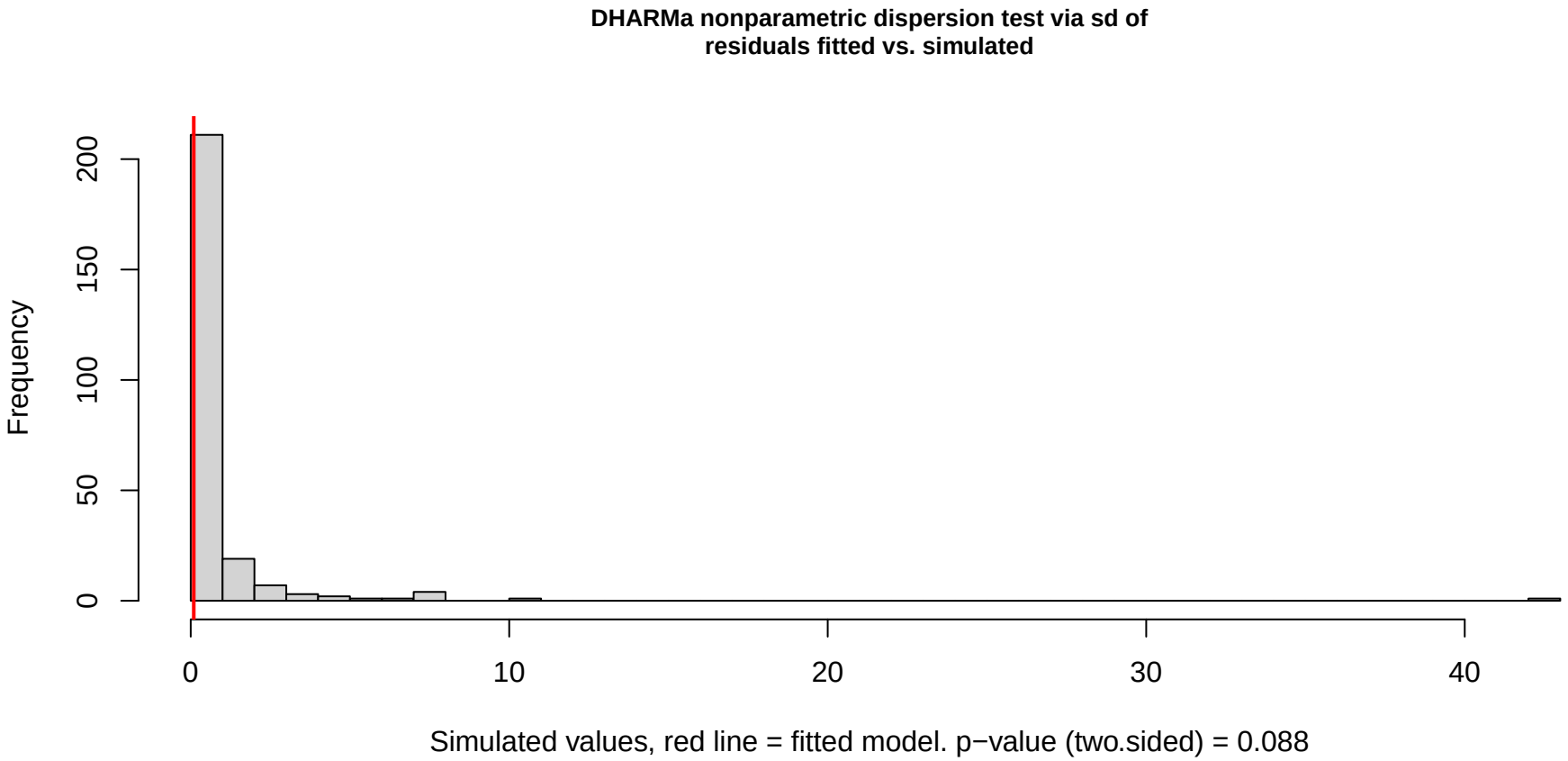


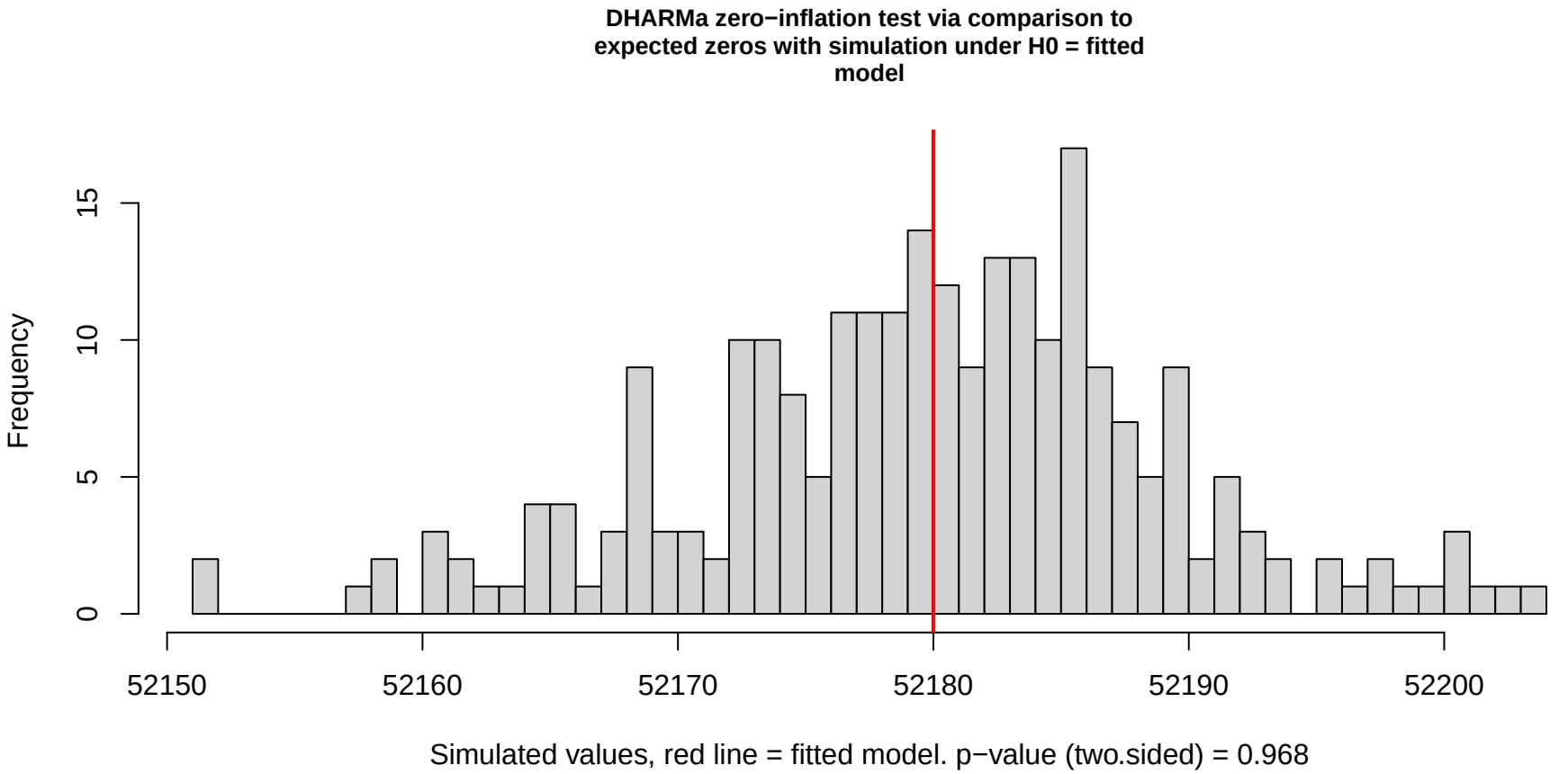

*Alnus incana*

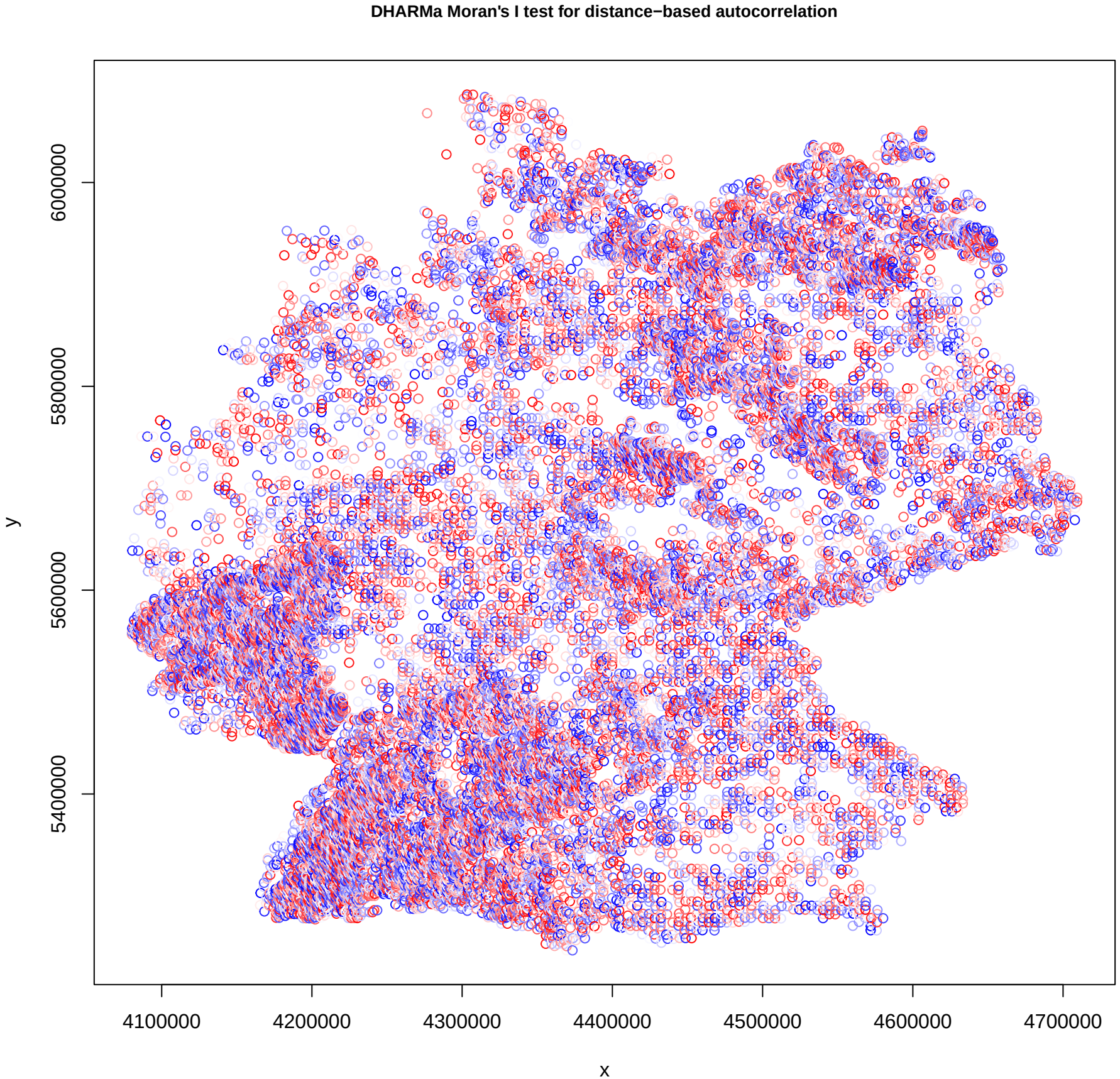

*Fagus sylvatica*

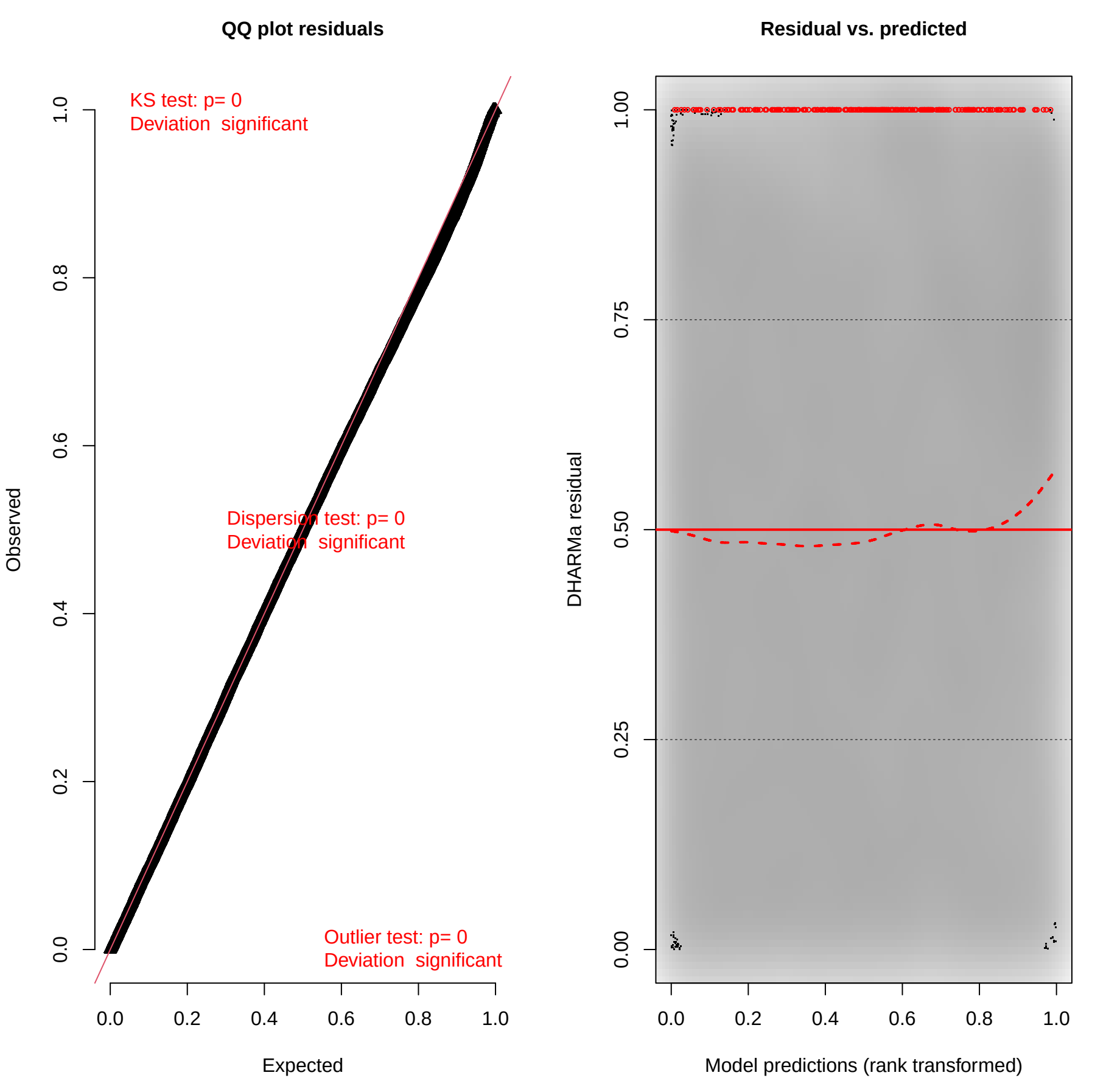

*Fagus sylvatica*

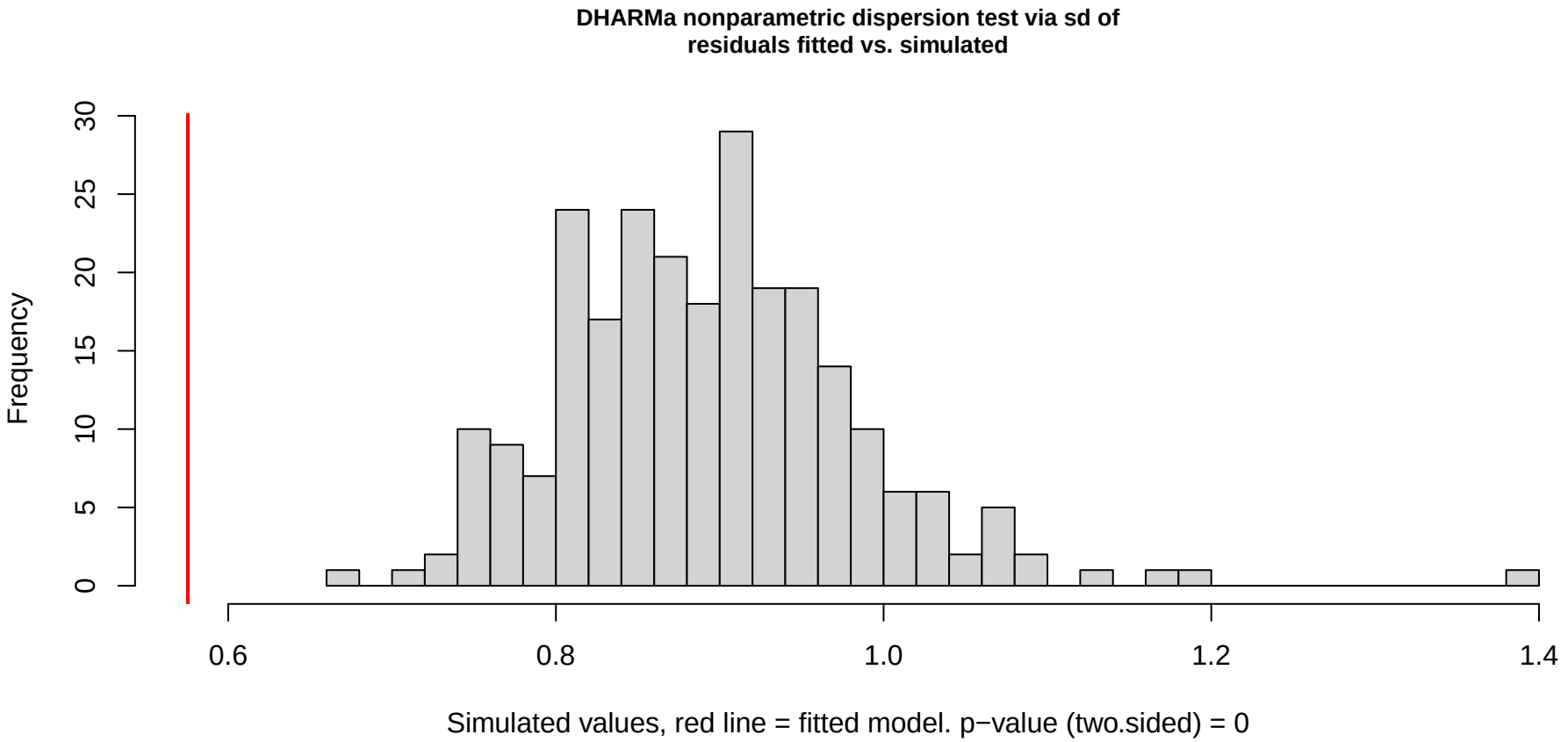


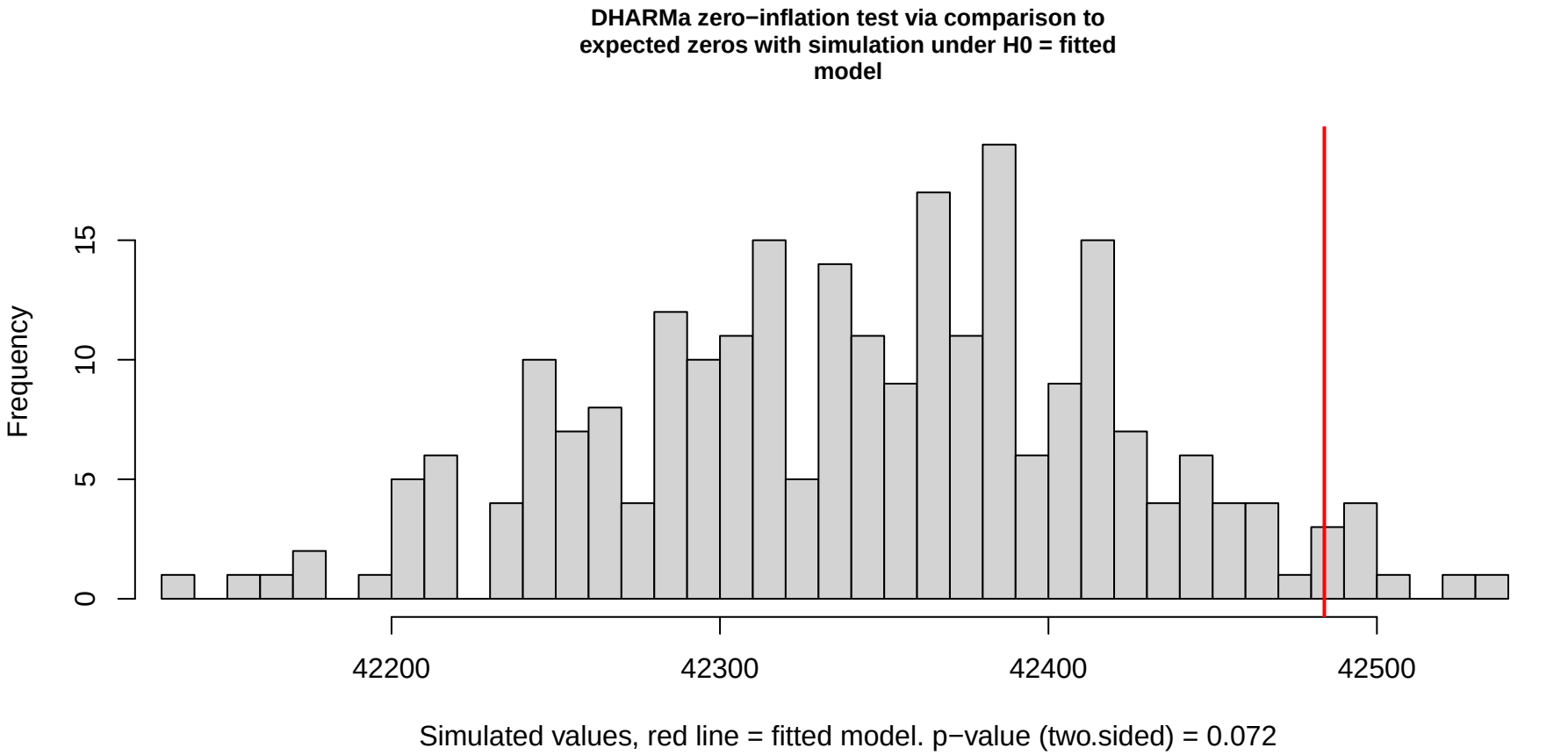

*Fagus sylvatica*

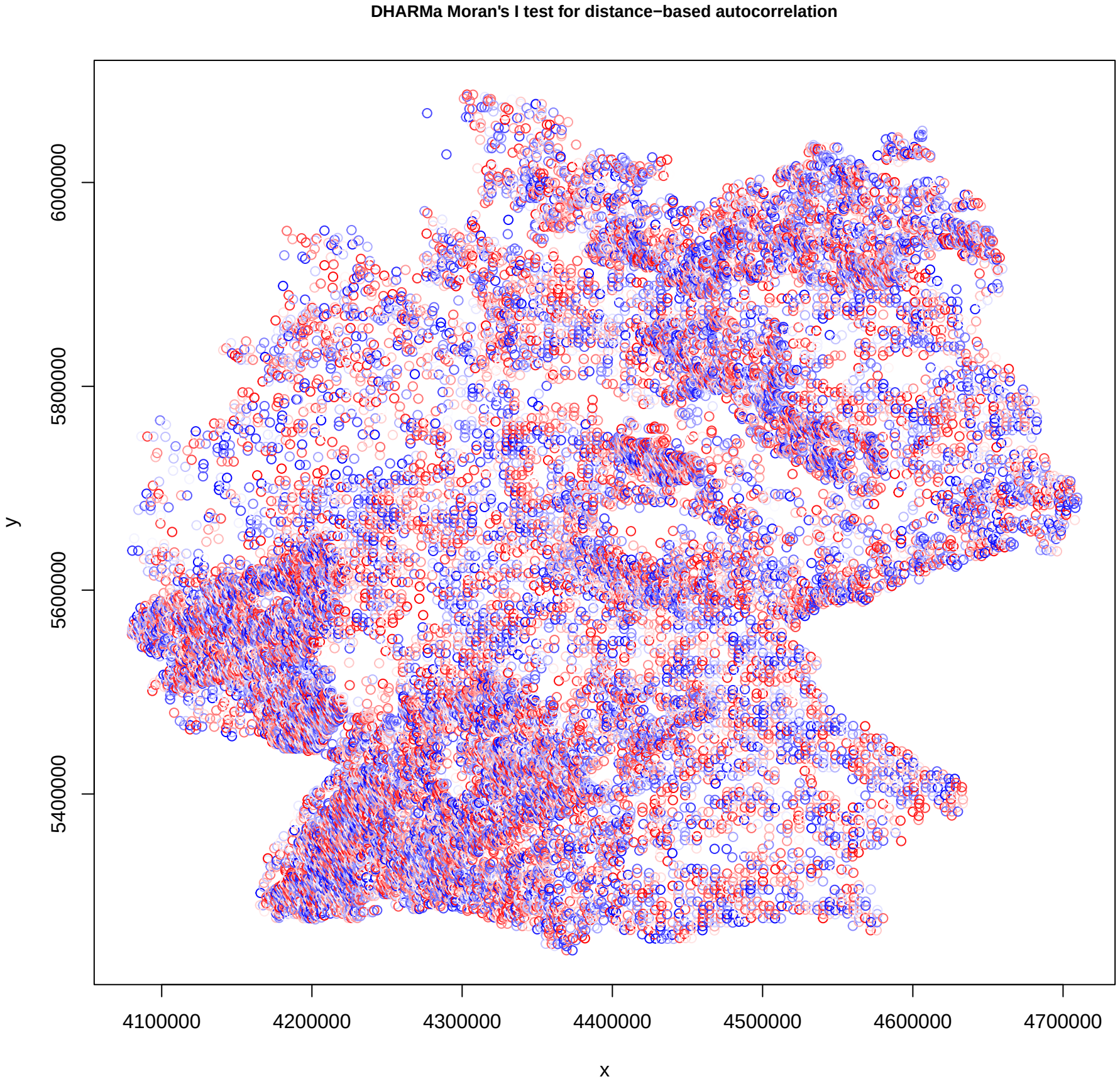

*Prunus serotina*

DHARMa residual

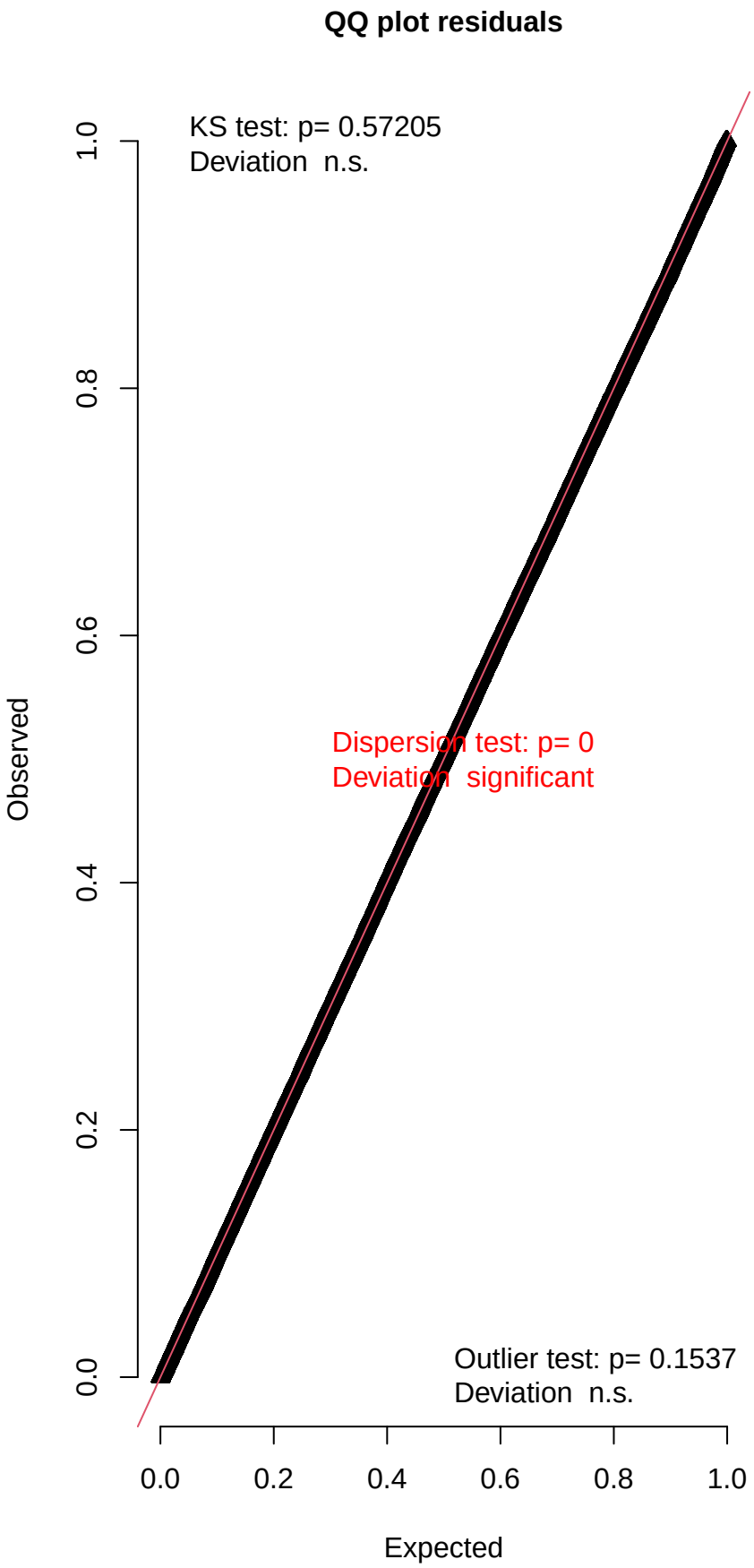


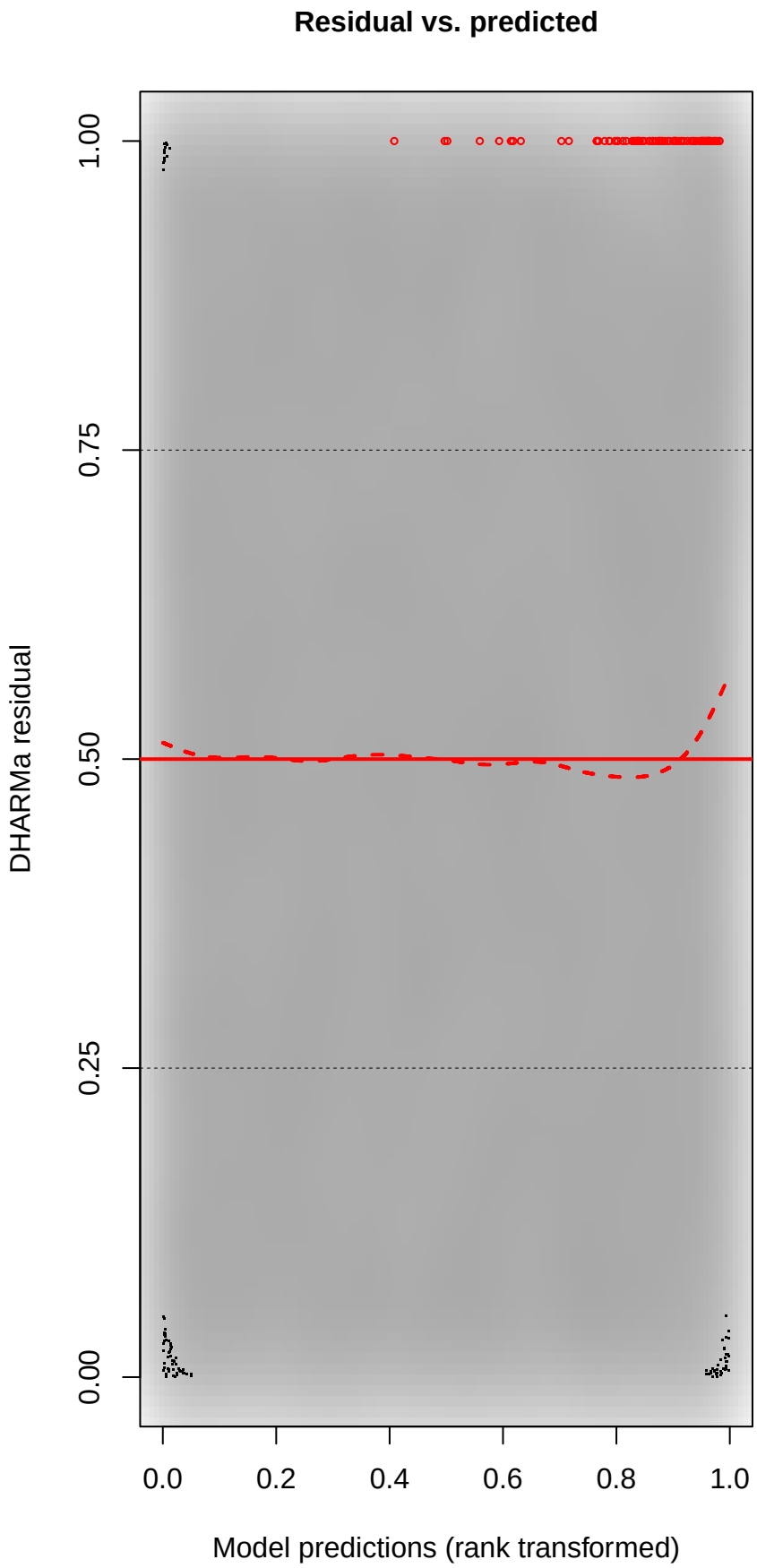

*Prunus serotina*

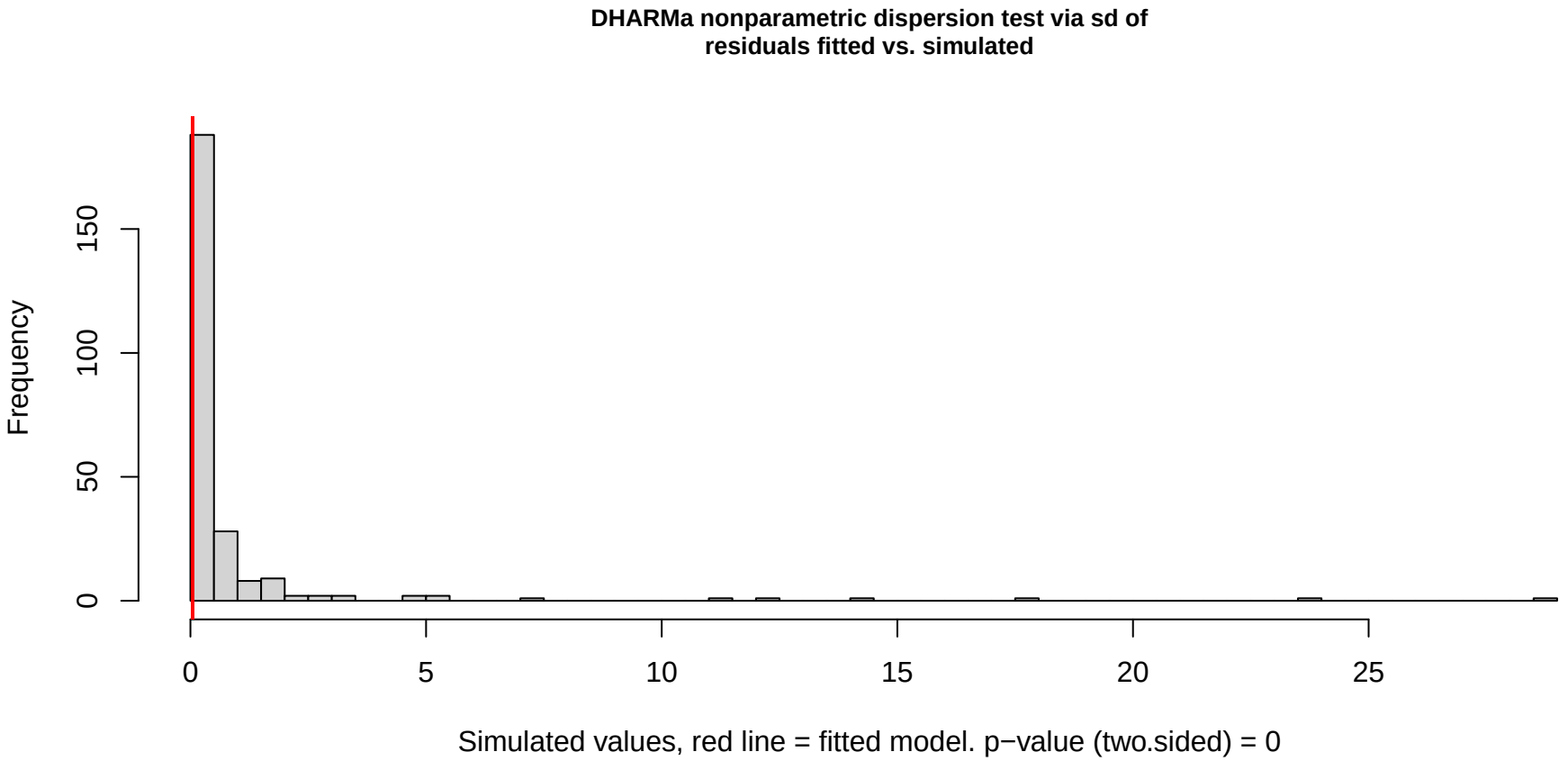


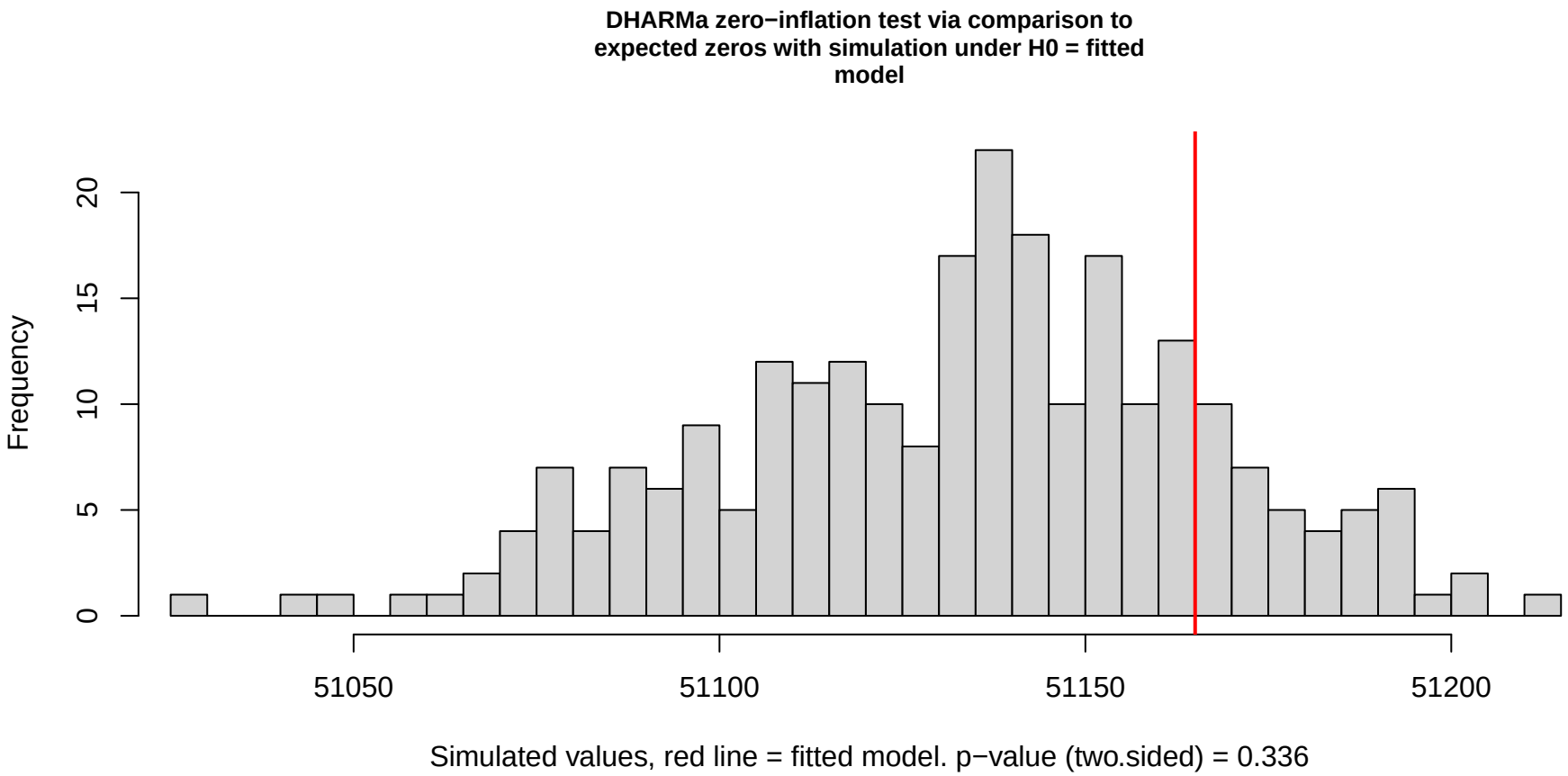

*Prunus serotina*

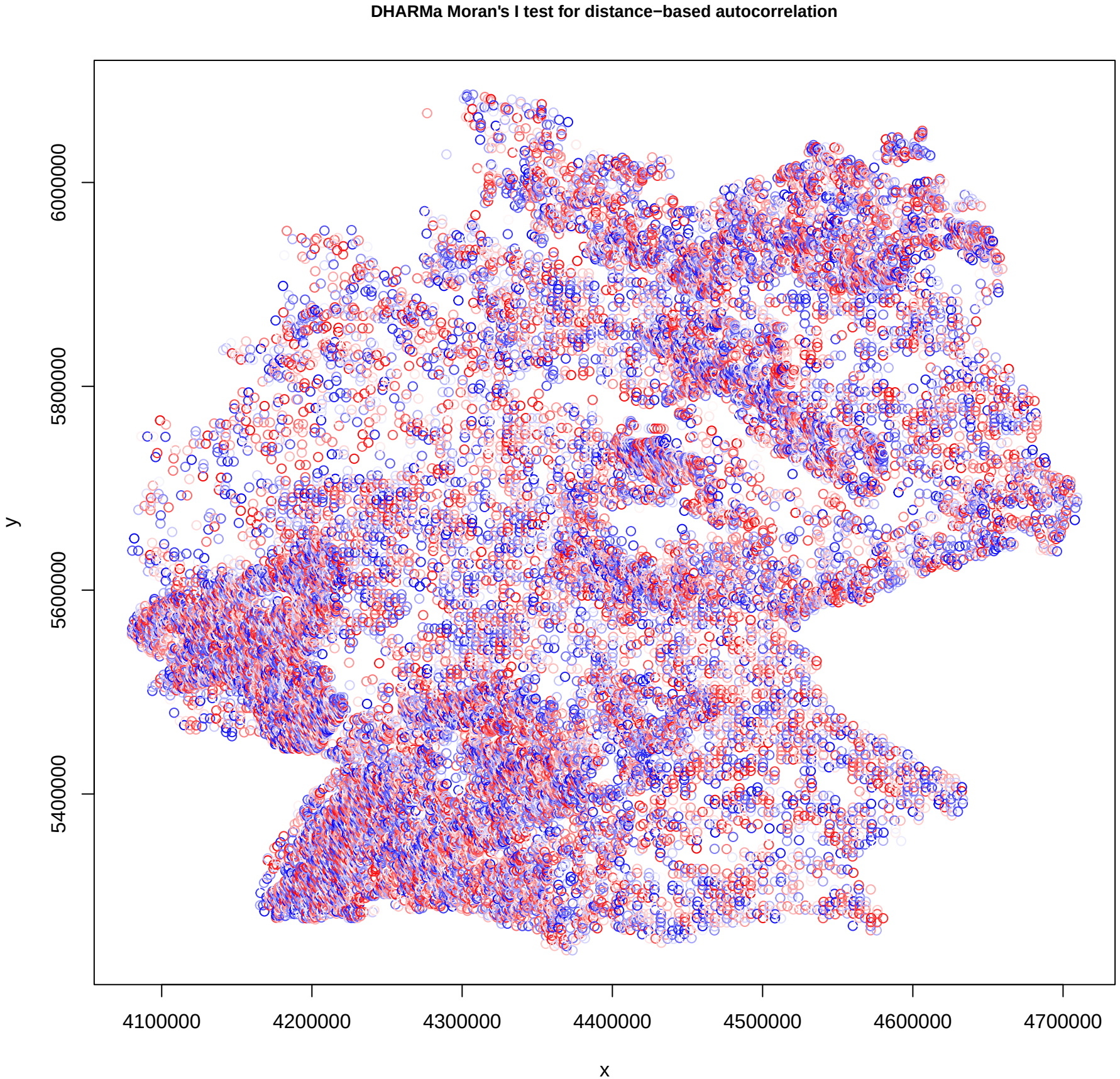

*Sorbus aria*

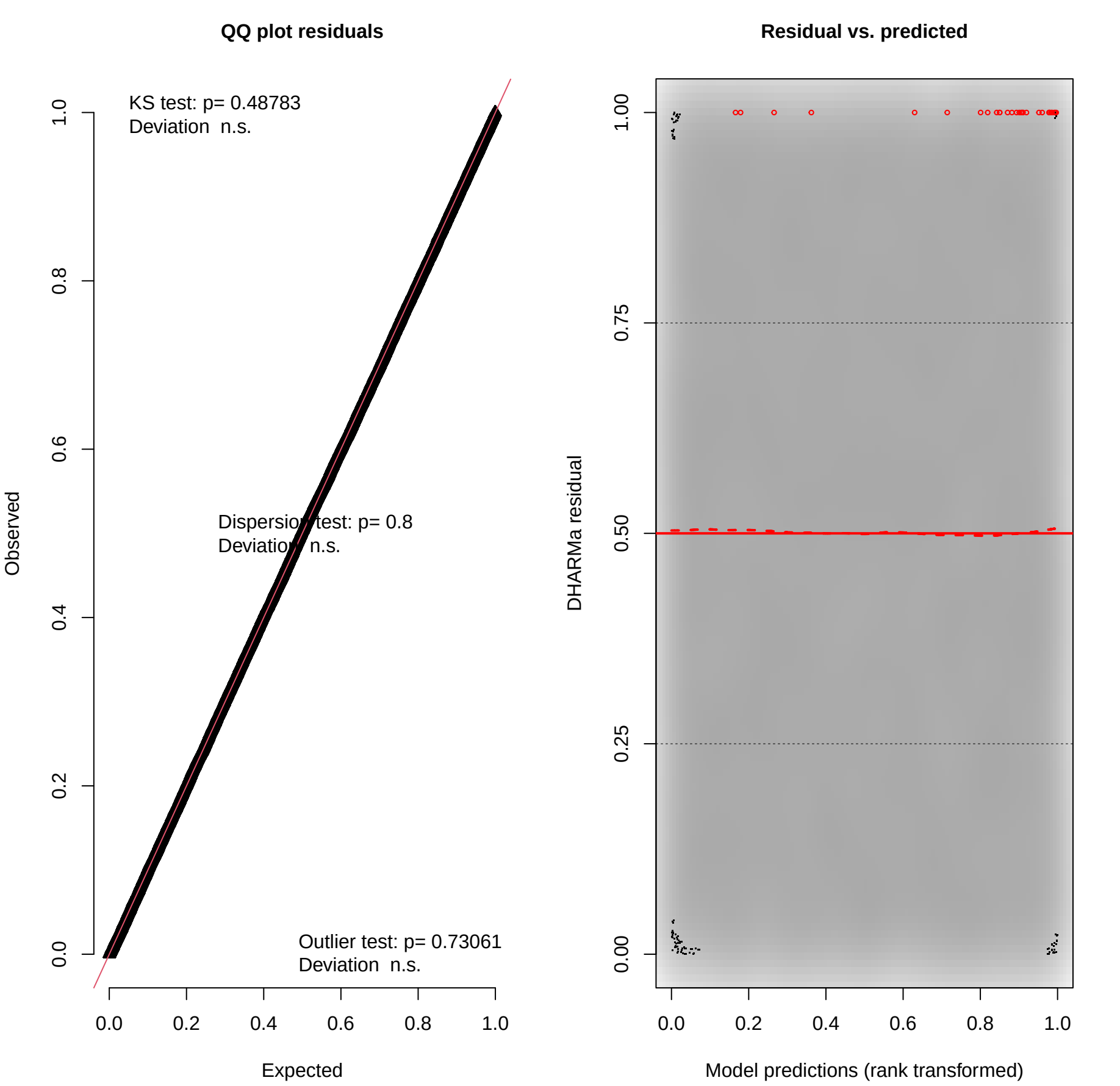
DHARMa residual
QQ plot residuals
KS test: p= 0.48783
Deviation n.s.
Dispersion test: p= 0.8
Deviation n.s.
Outlier test: p= 0.73061
Deviation n.s.
Observed
Expected
0.0
0.2
0.4
0.6
0.8
1.0
Residual vs. predicted
DHARMa residual
Model predictions (rank transformed)
0.00
0.25
0.50
0.75
1.00

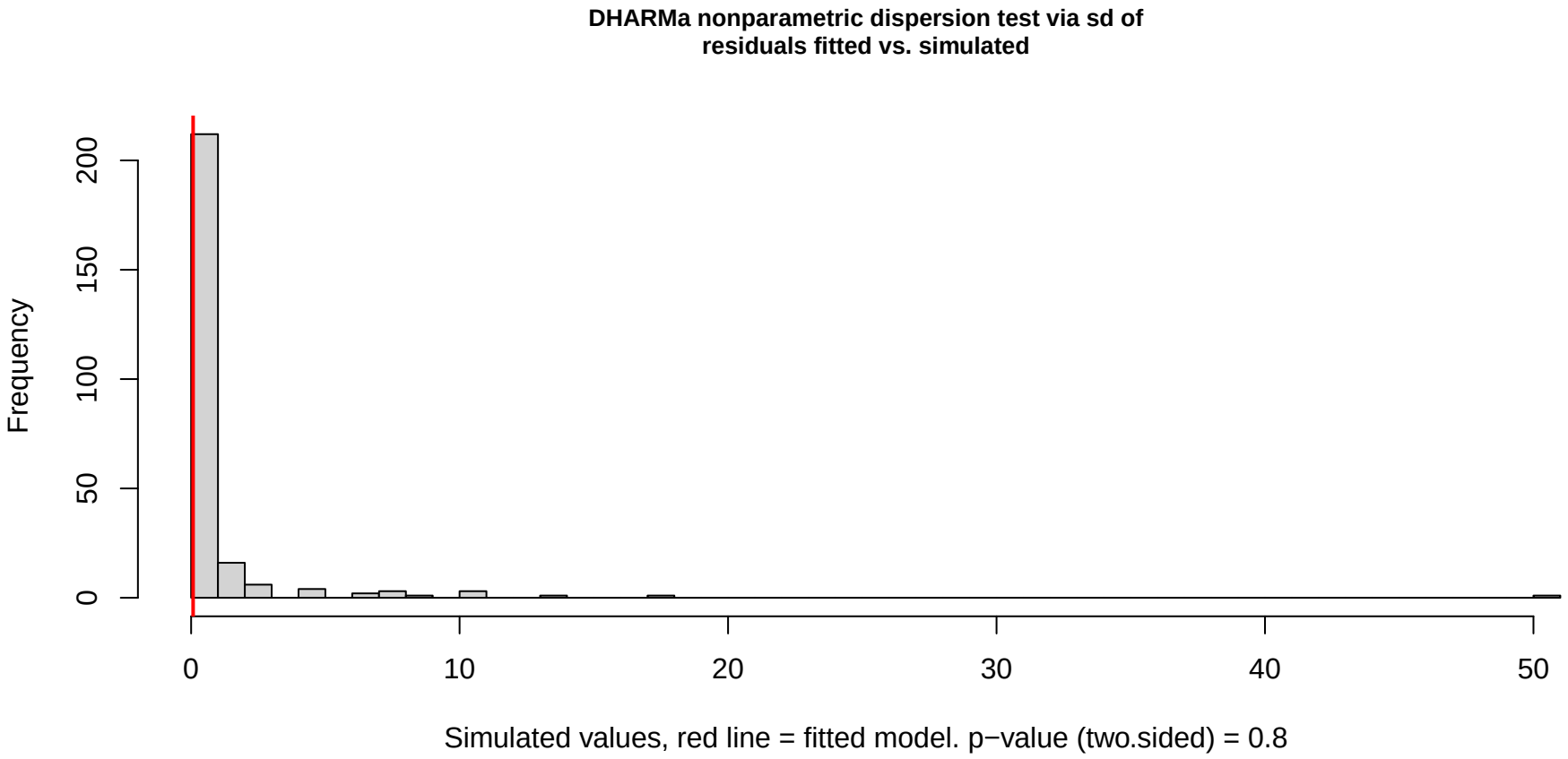
DHARMa nonparametric dispersion test via sd of residuals fitted vs. simulated
Frequency
0
50
100
150
200
0
10
20
30
40
50
Simulated values, red line = fitted model. p−value (two.sided) = 0.8

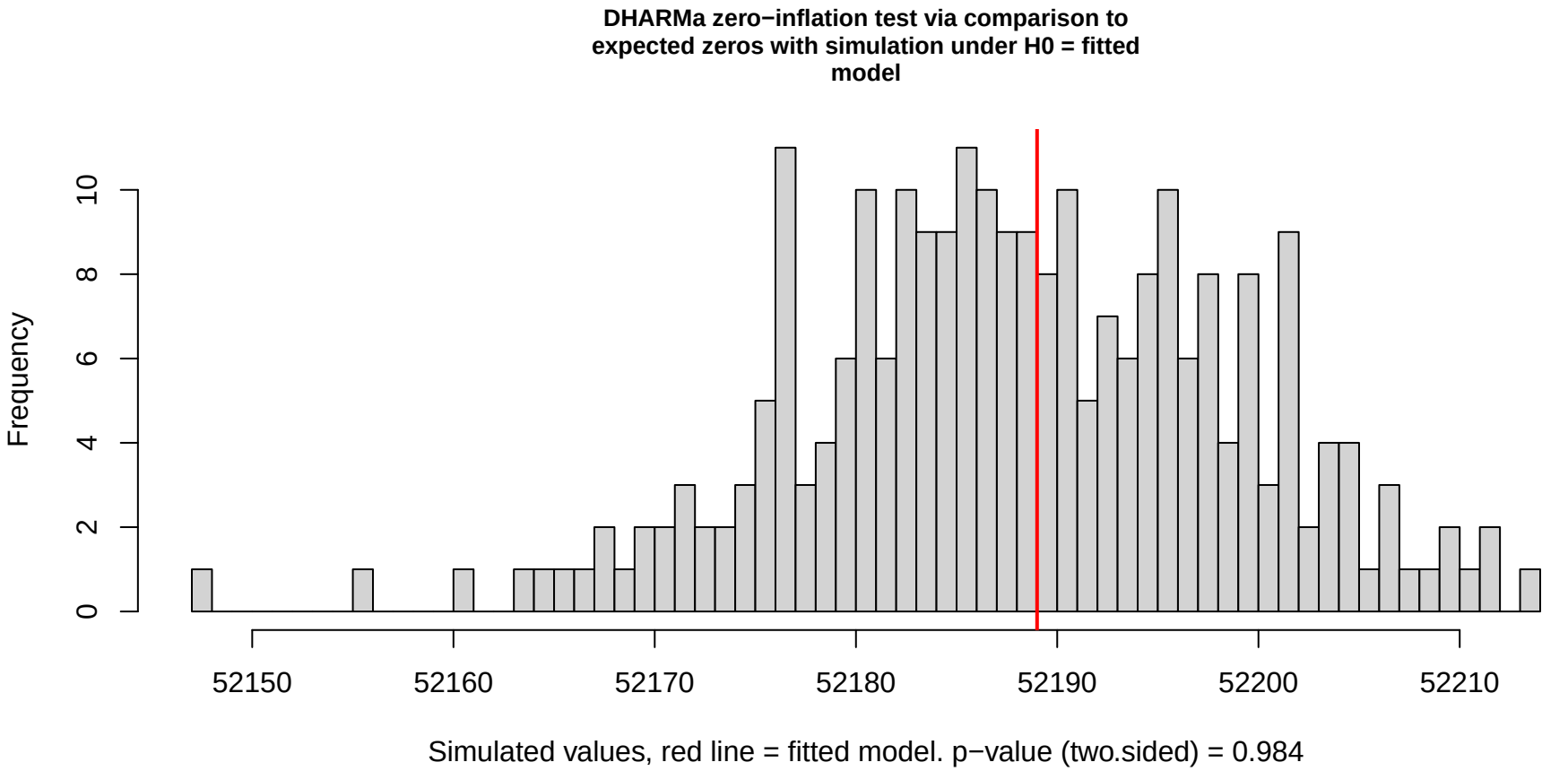
DHARMa zero−inflation test via comparison to expected zeros with simulation under H0 = fitted model
Frequency
0
2
4
6
8
10
52150
52160
52170
52180
52190
52200
52210
Simulated values, red line = fitted model. p−value (two.sided) = 0.984

*Sorbus aria*

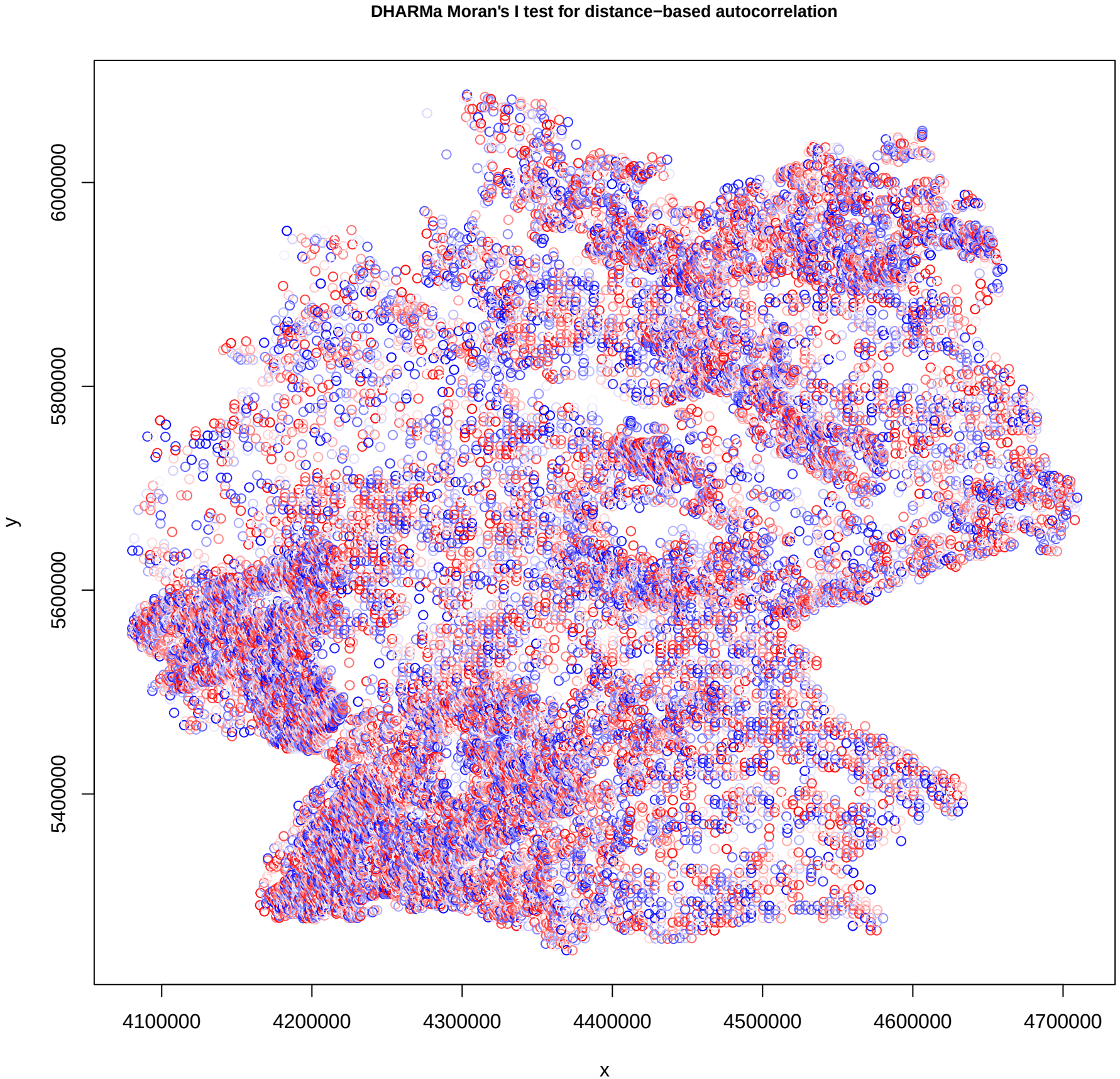
DHARMa Moran's I test for distance−based autocorrelation
y
6000000
5800000
5600000
5400000
4100000
4200000
4300000
4400000
4500000
4600000
4700000
x

*Prunus avium*

DHARMa residual

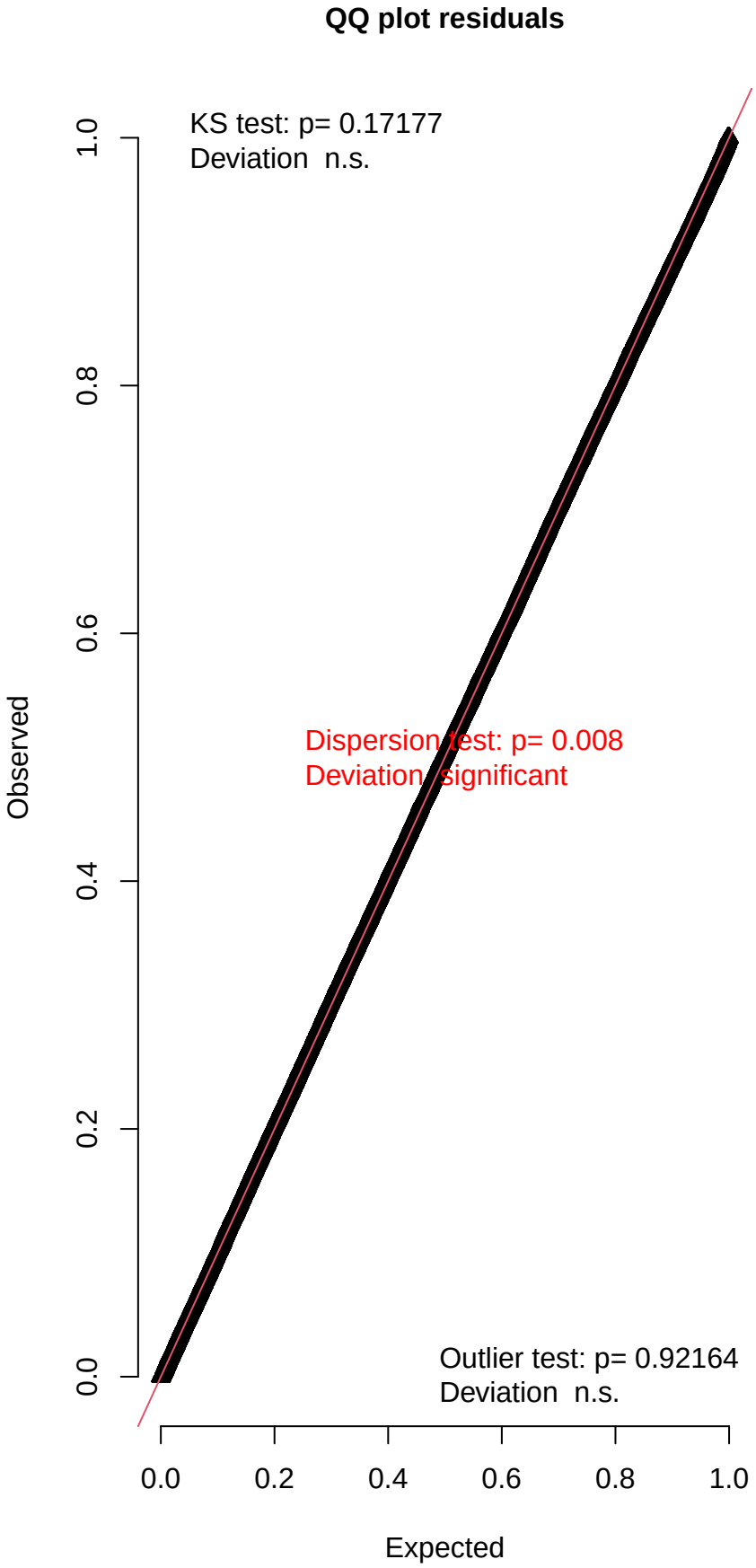


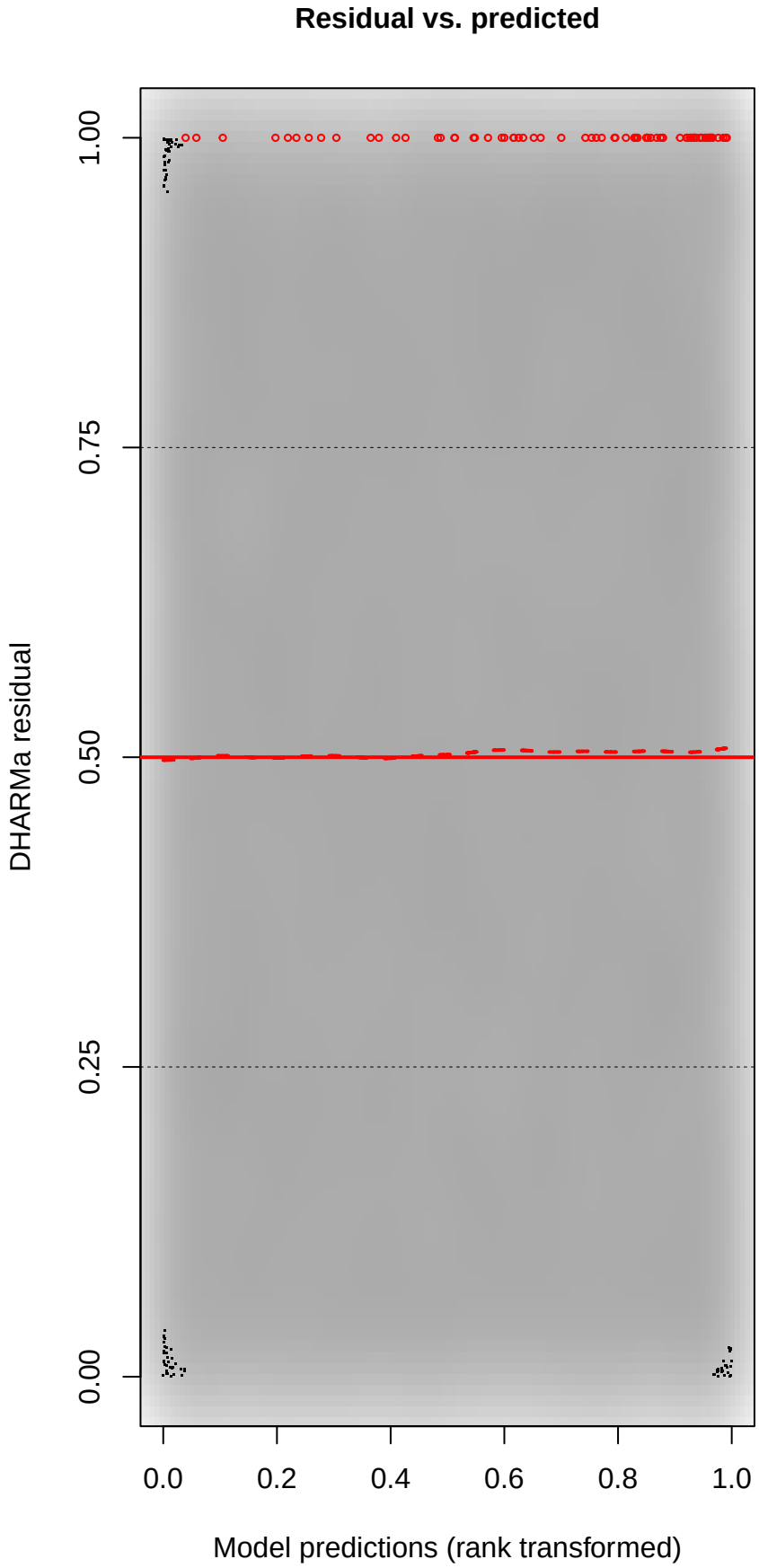

*Prunus avium*

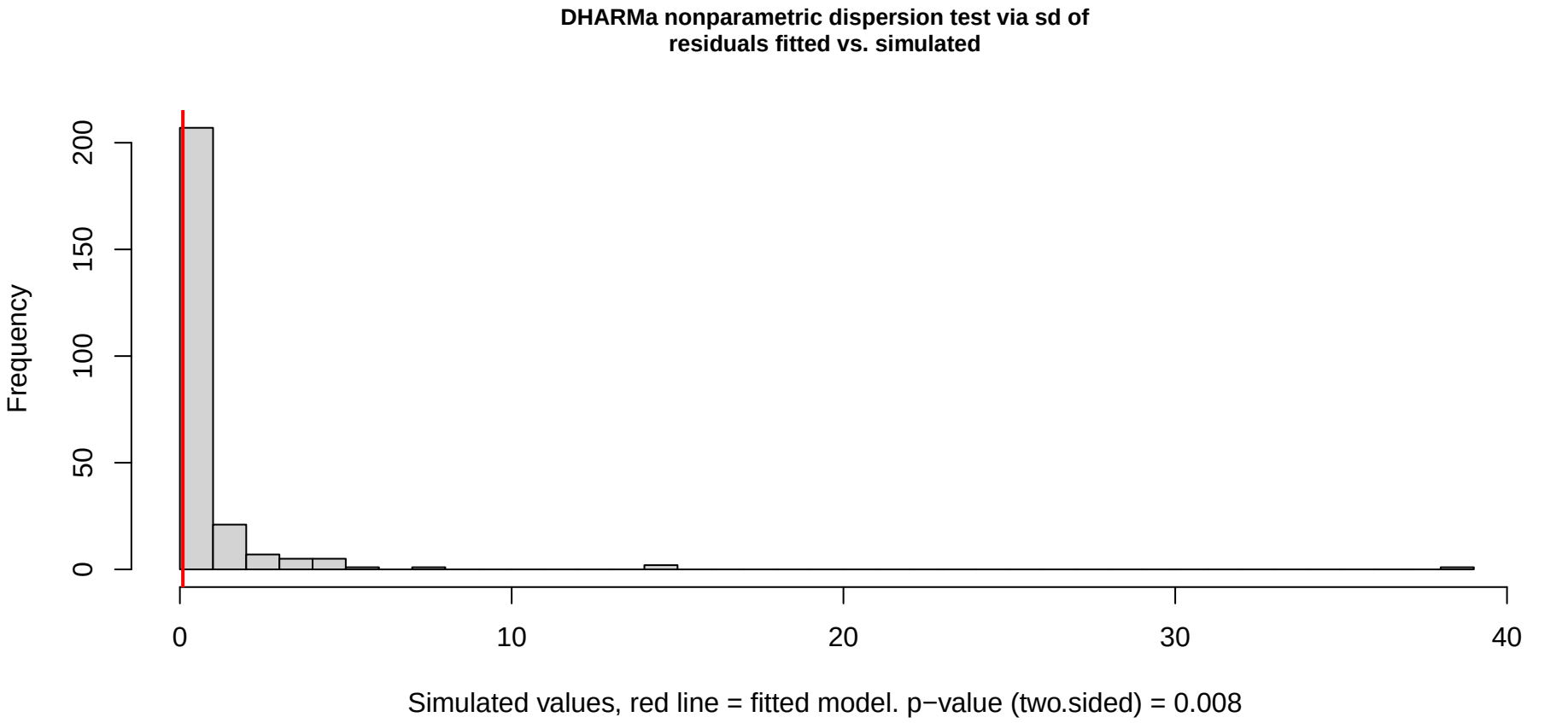


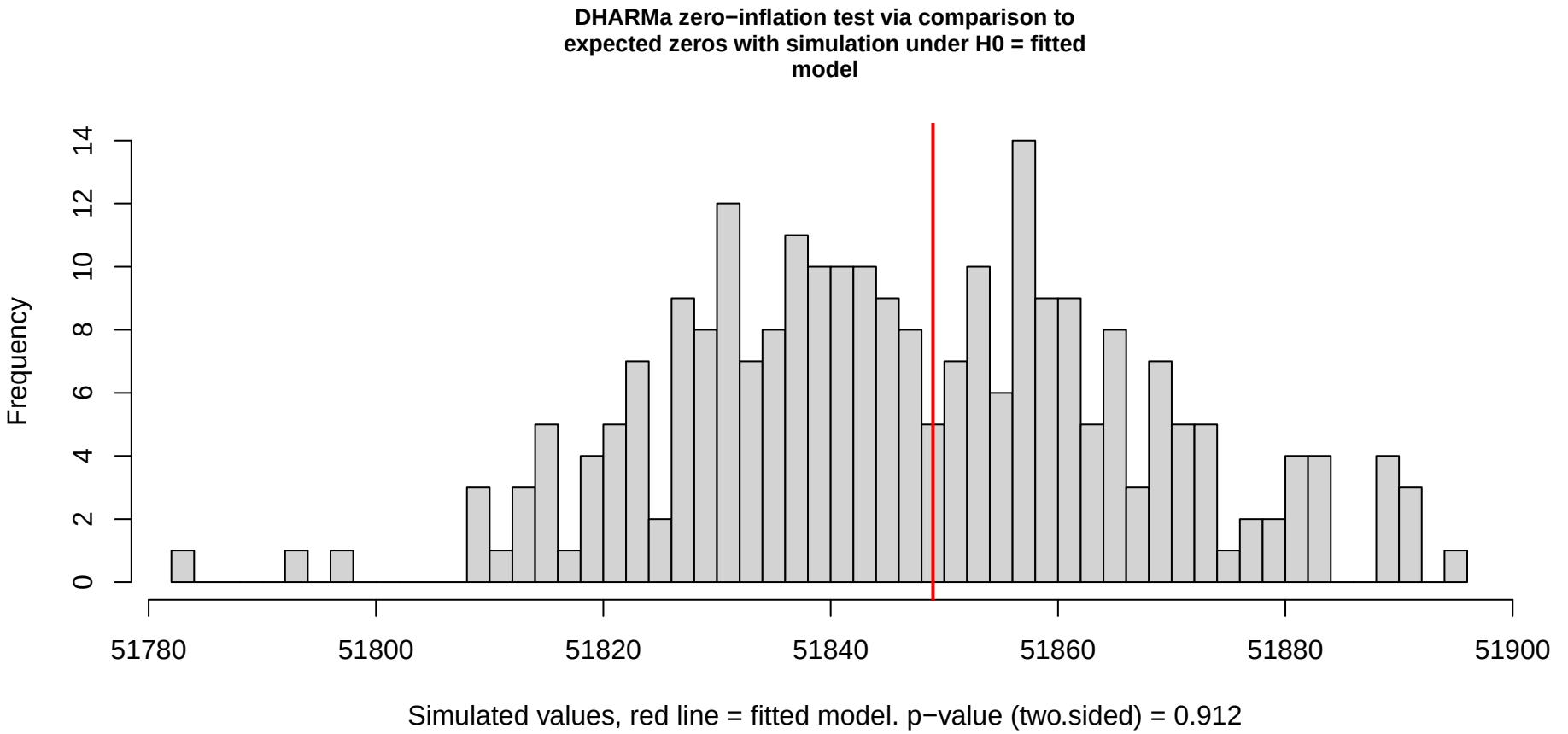

*Prunus avium*

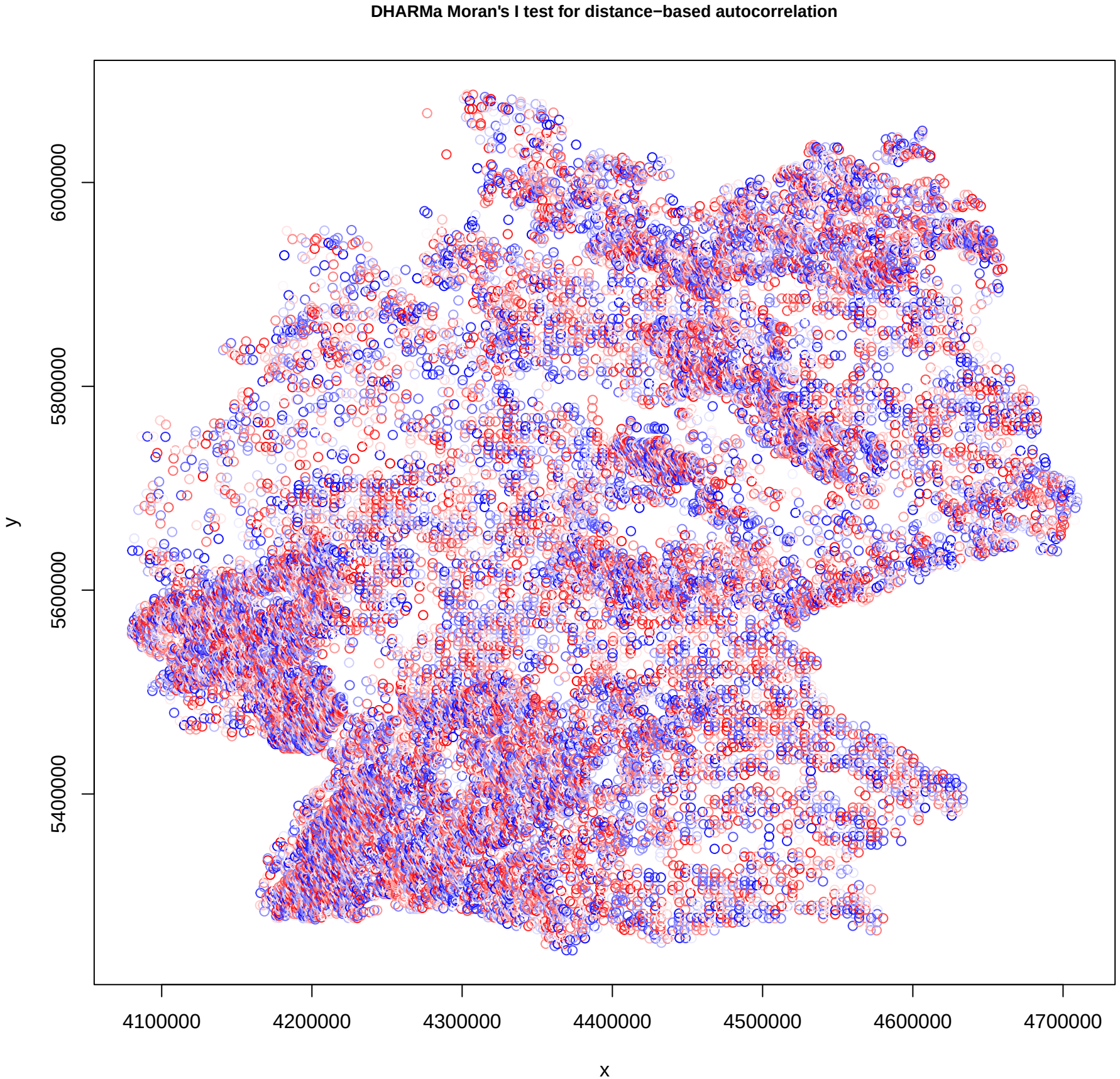

*Prunus padus*

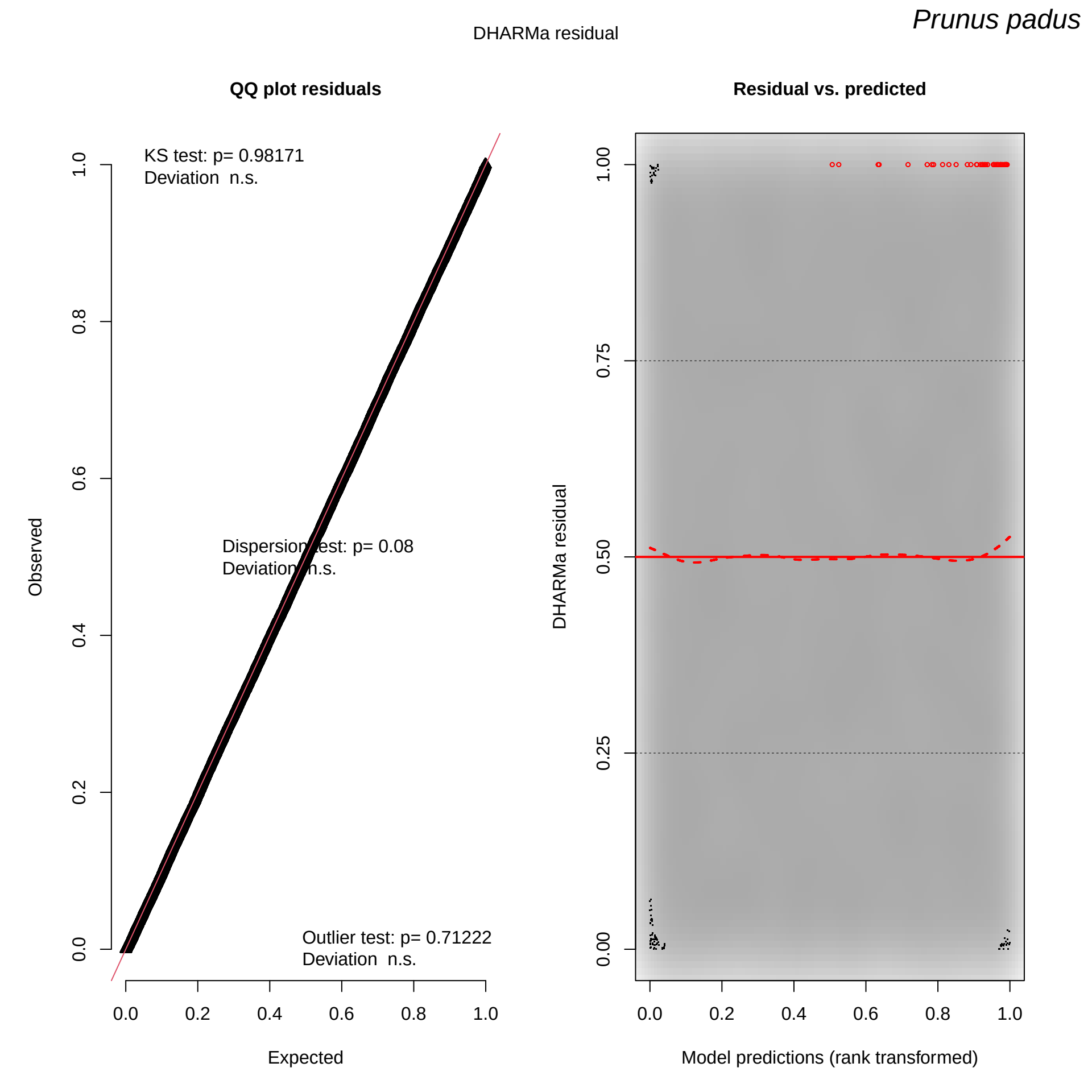

*Prunus padus*

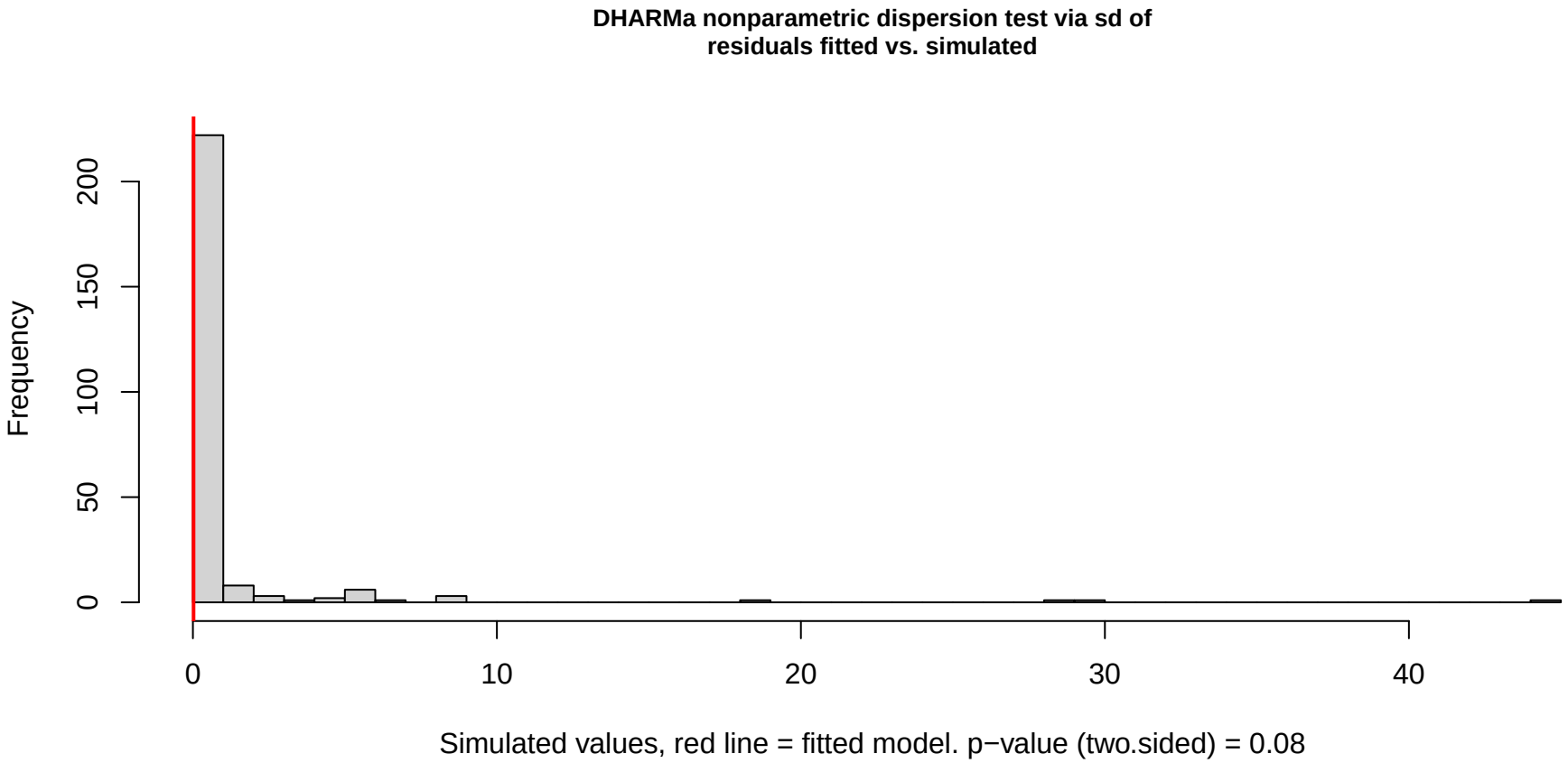


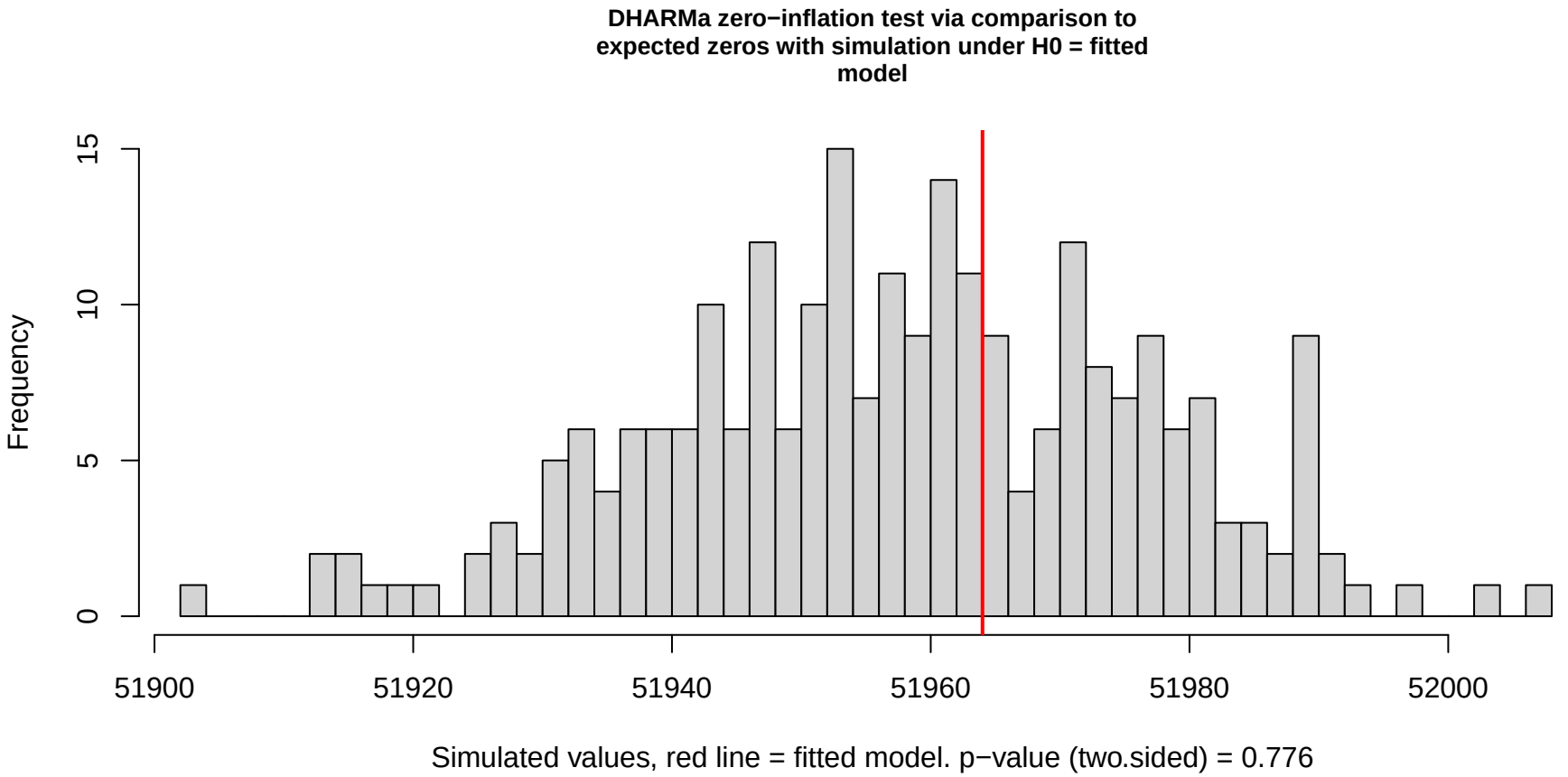

*Prunus padus*

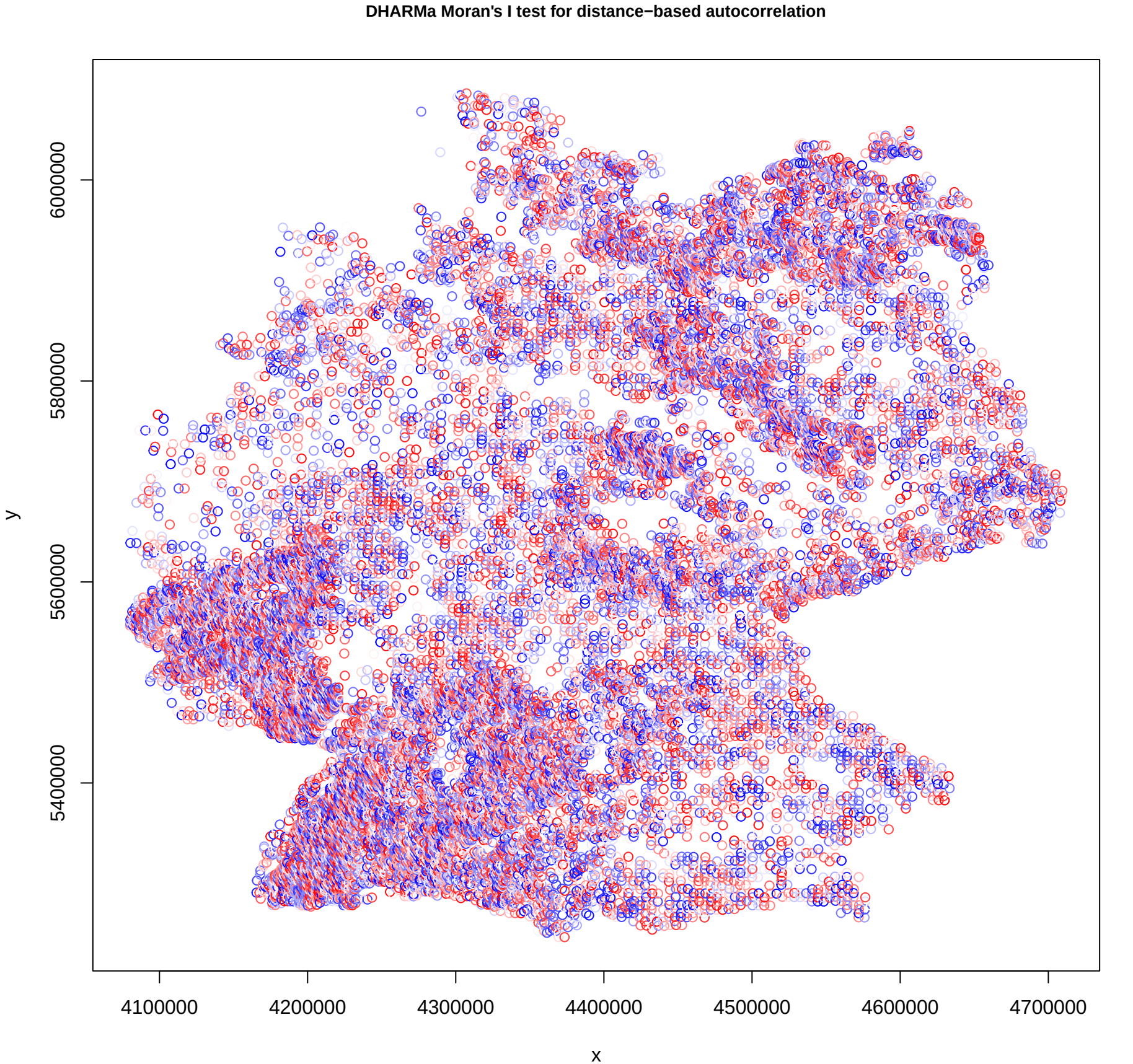

*Sorbus aucuparia*

DHARMa residual

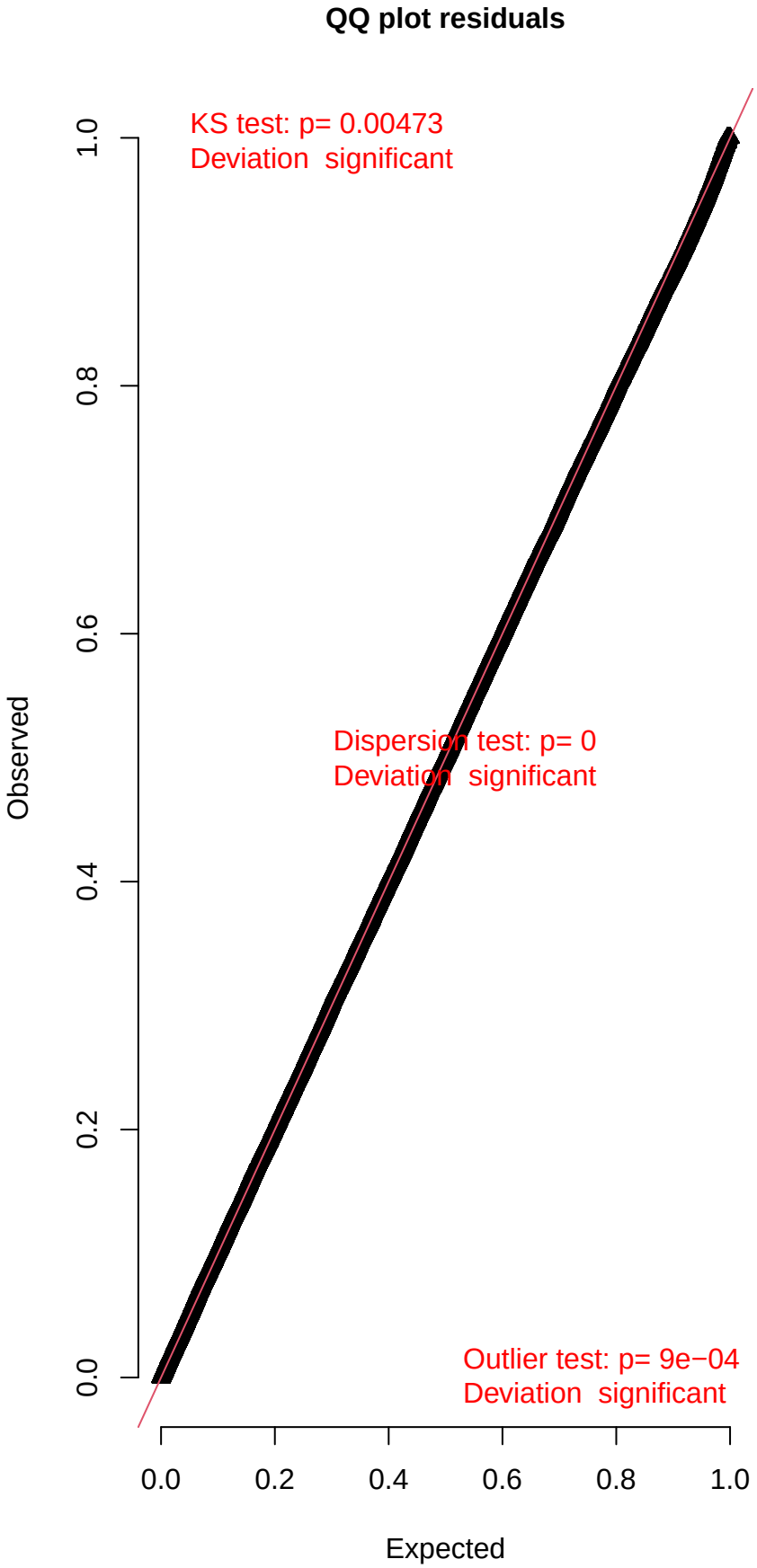


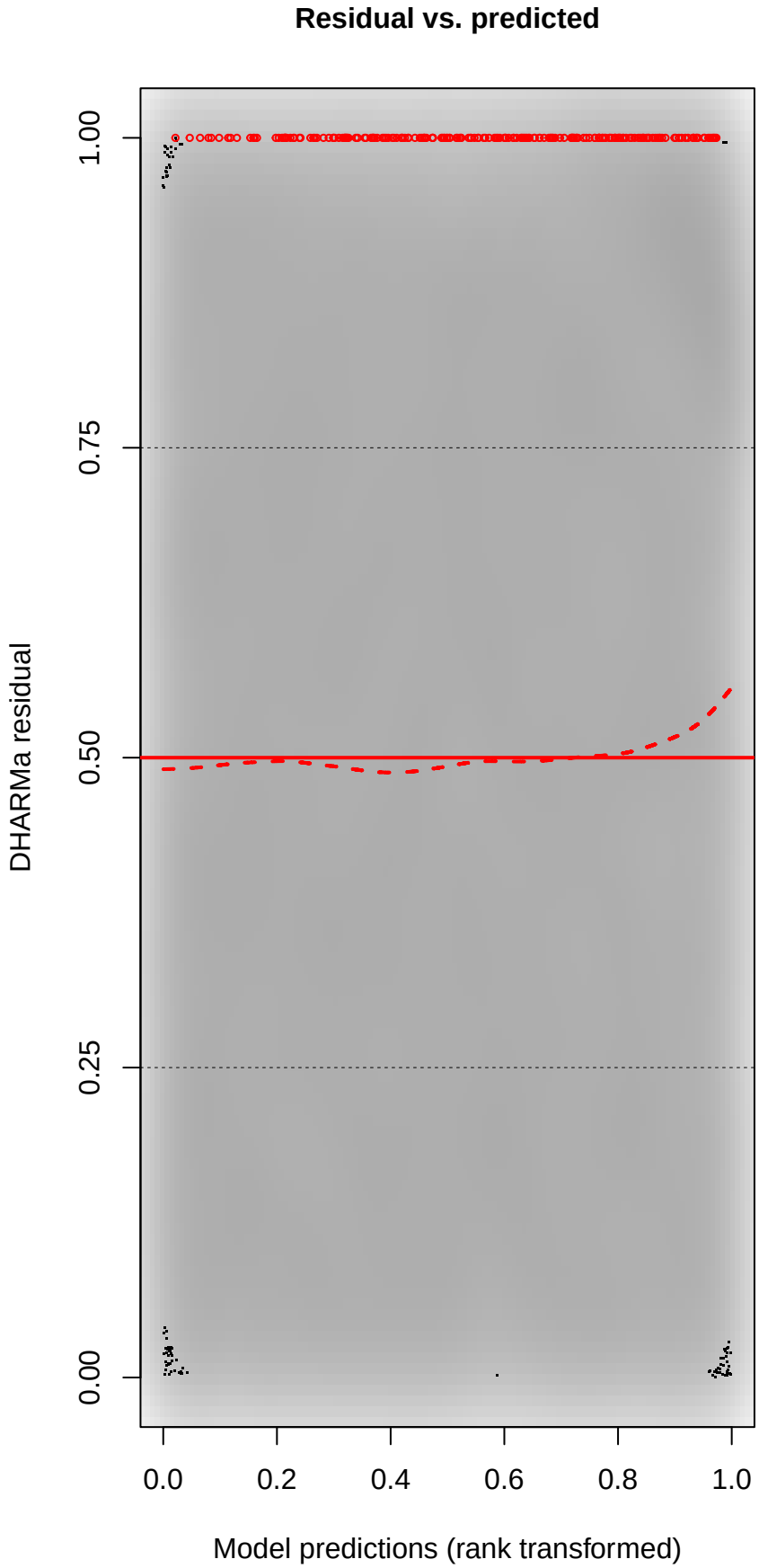

*Sorbus aucuparia*

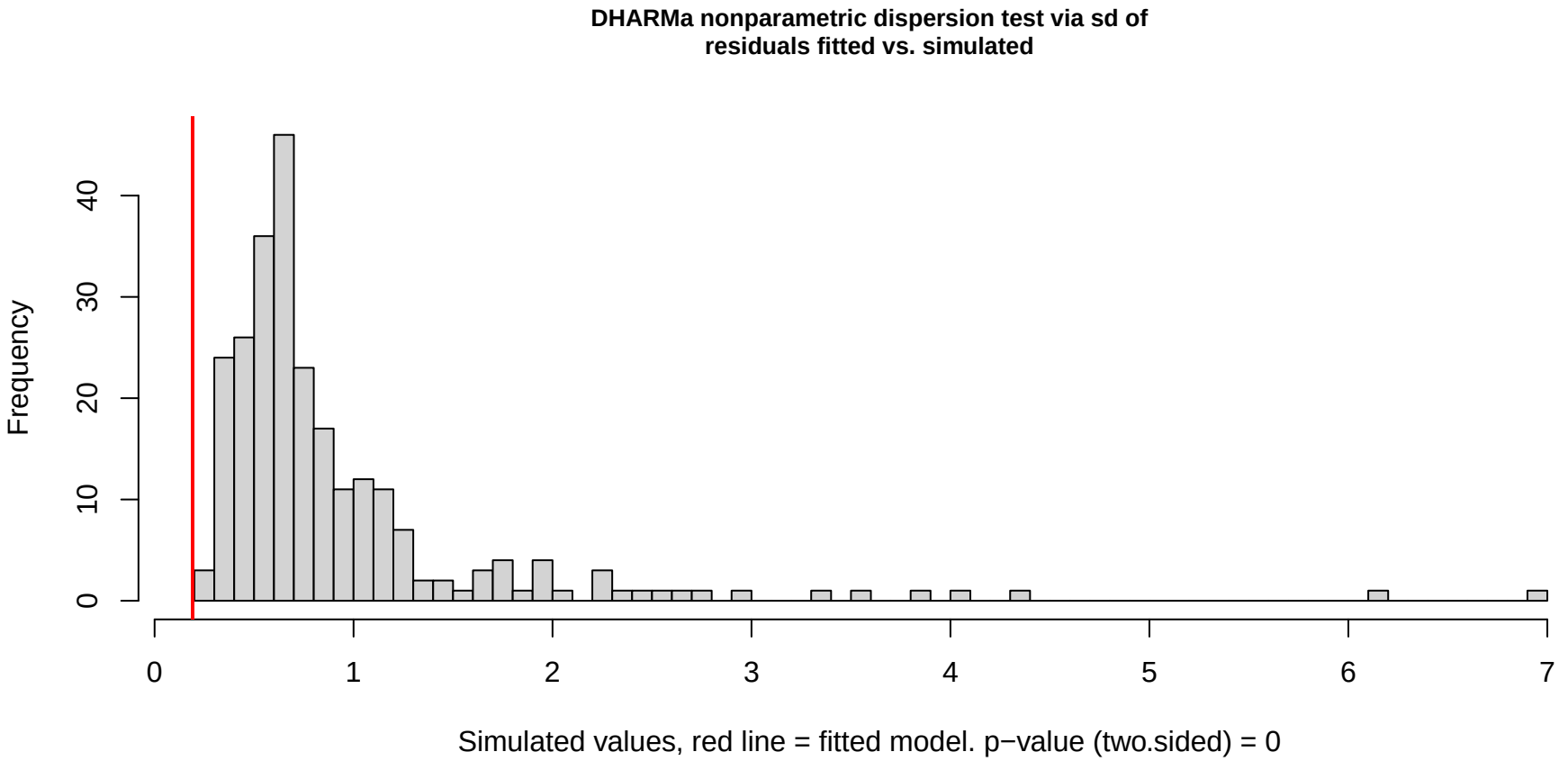


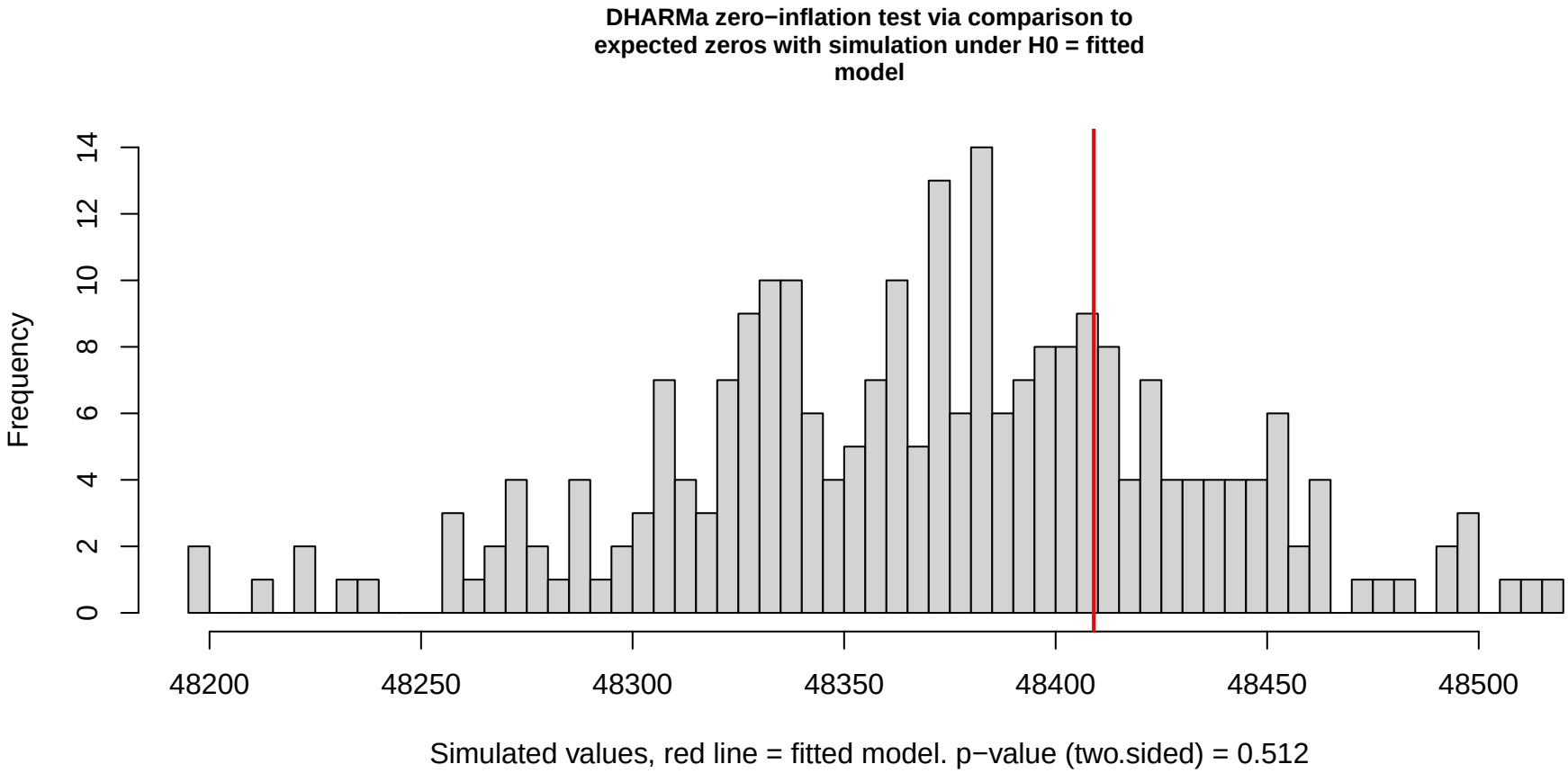

*Sorbus aucuparia*

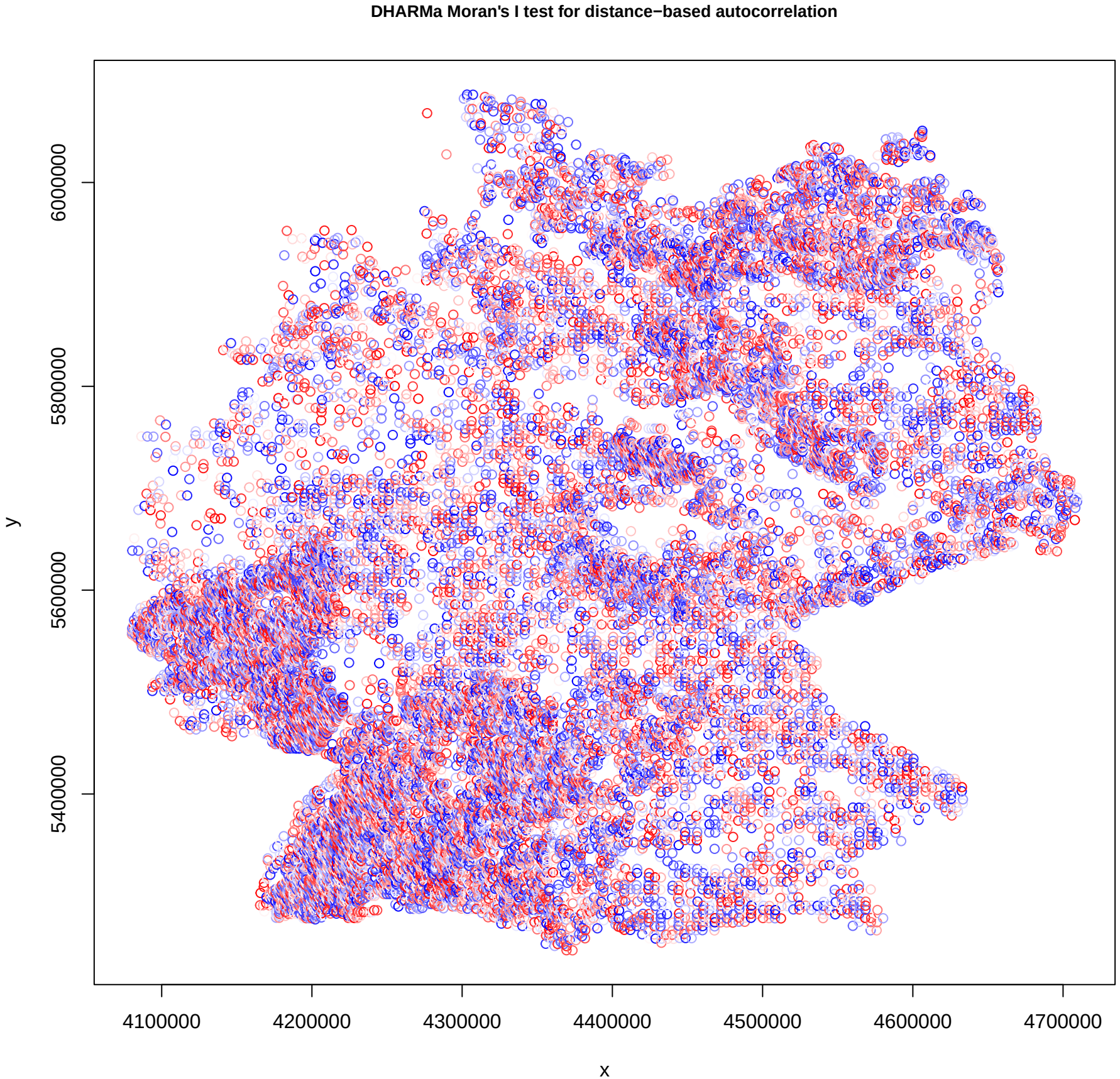

*Quercus petraea.robur*

DHARMa residual

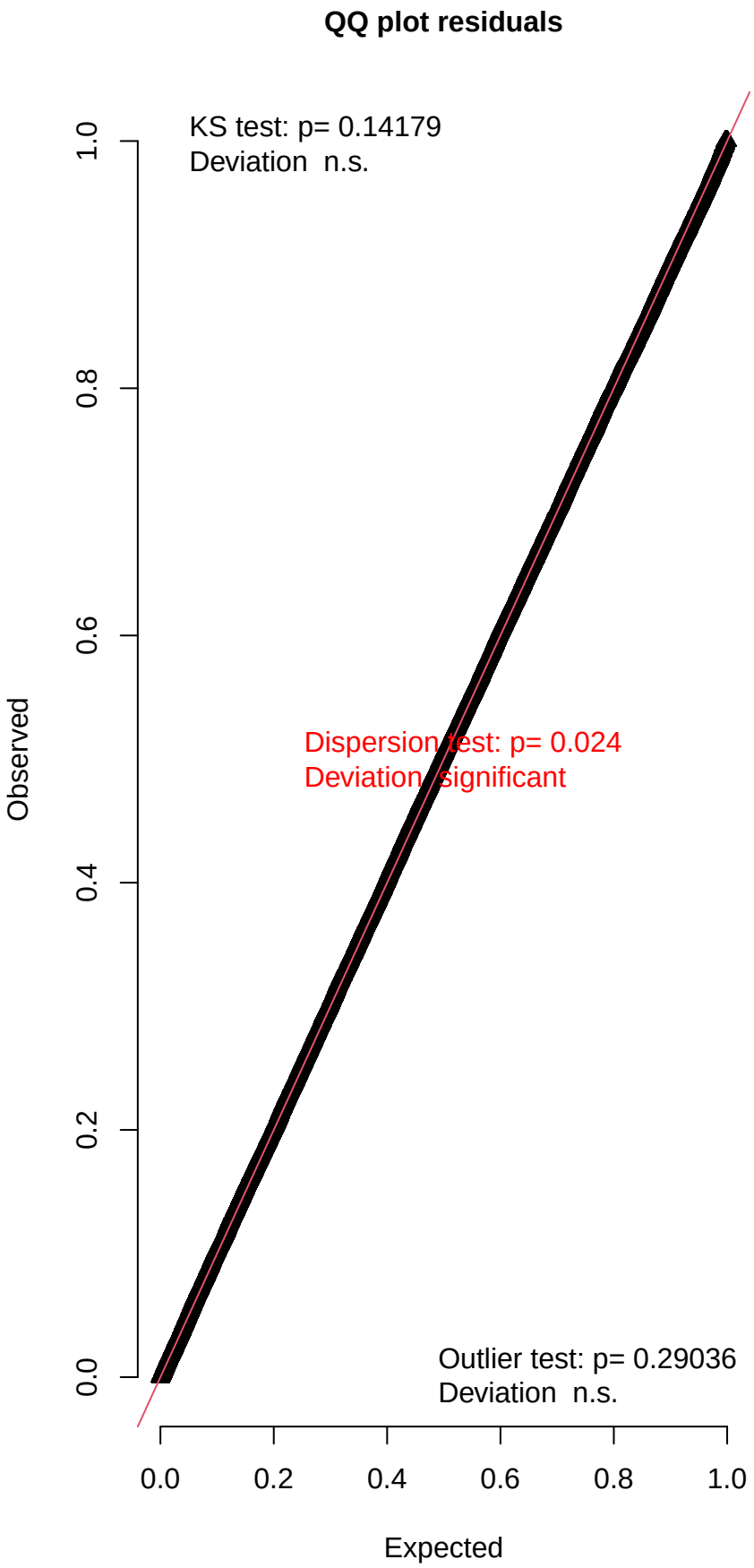


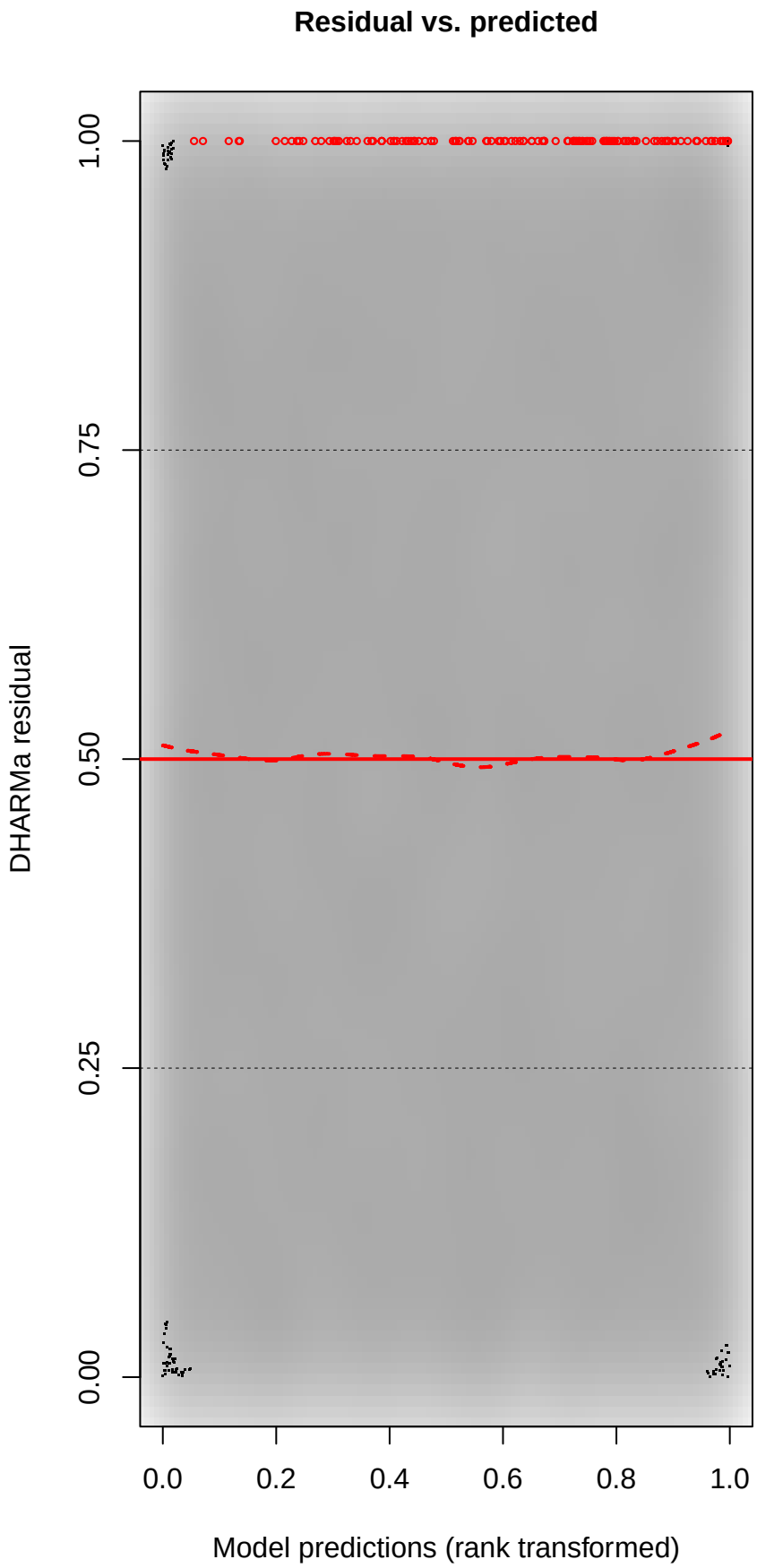

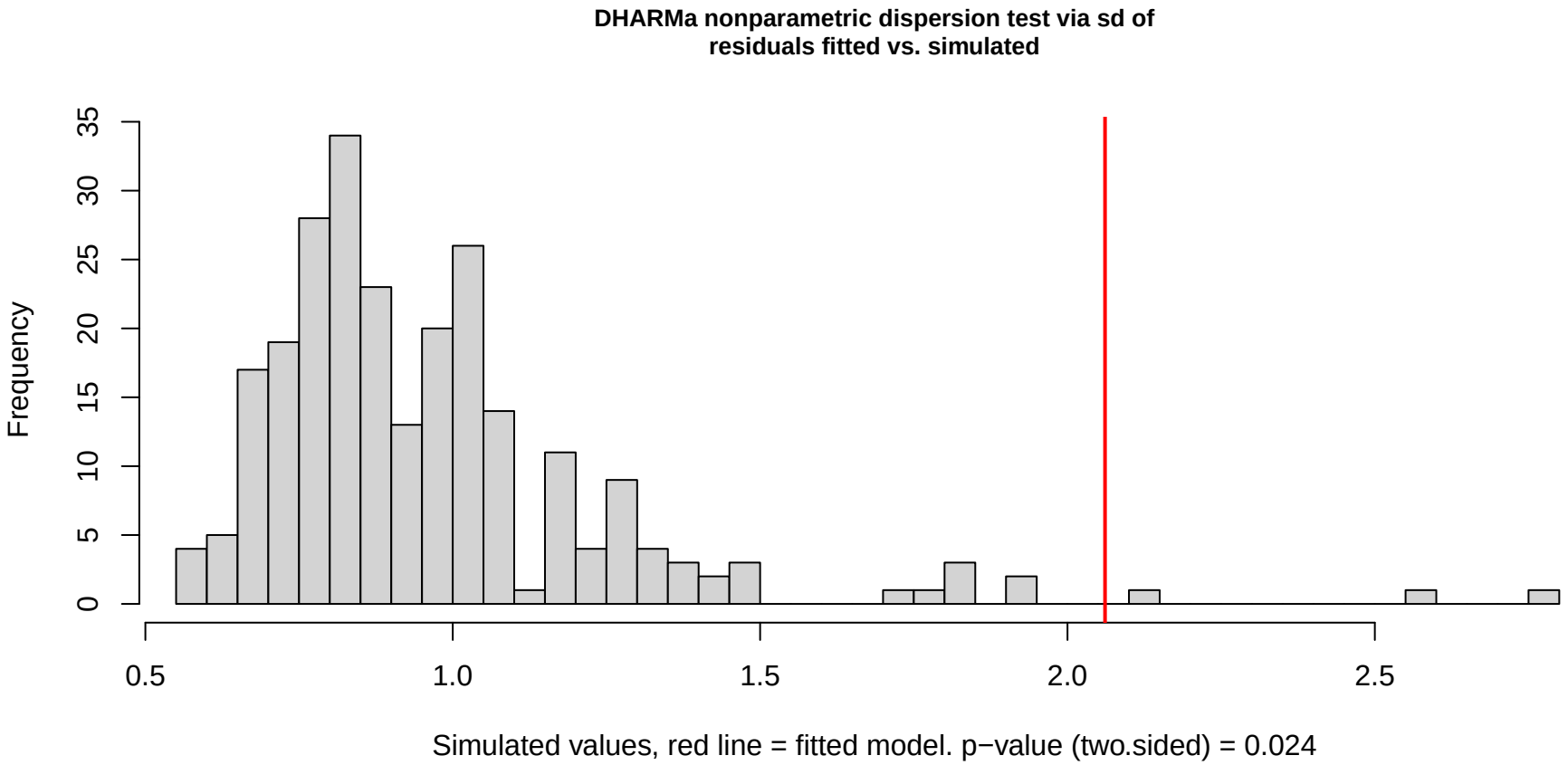
DHARMa nonparametric dispersion test via sd of residuals fitted vs. simulated
Frequency
0
5
10
15
20
25
30
35
0.5
1.0
1.5
2.0
2.5
Simulated values, red line = fitted model. p−value (two.sided) = 0.024

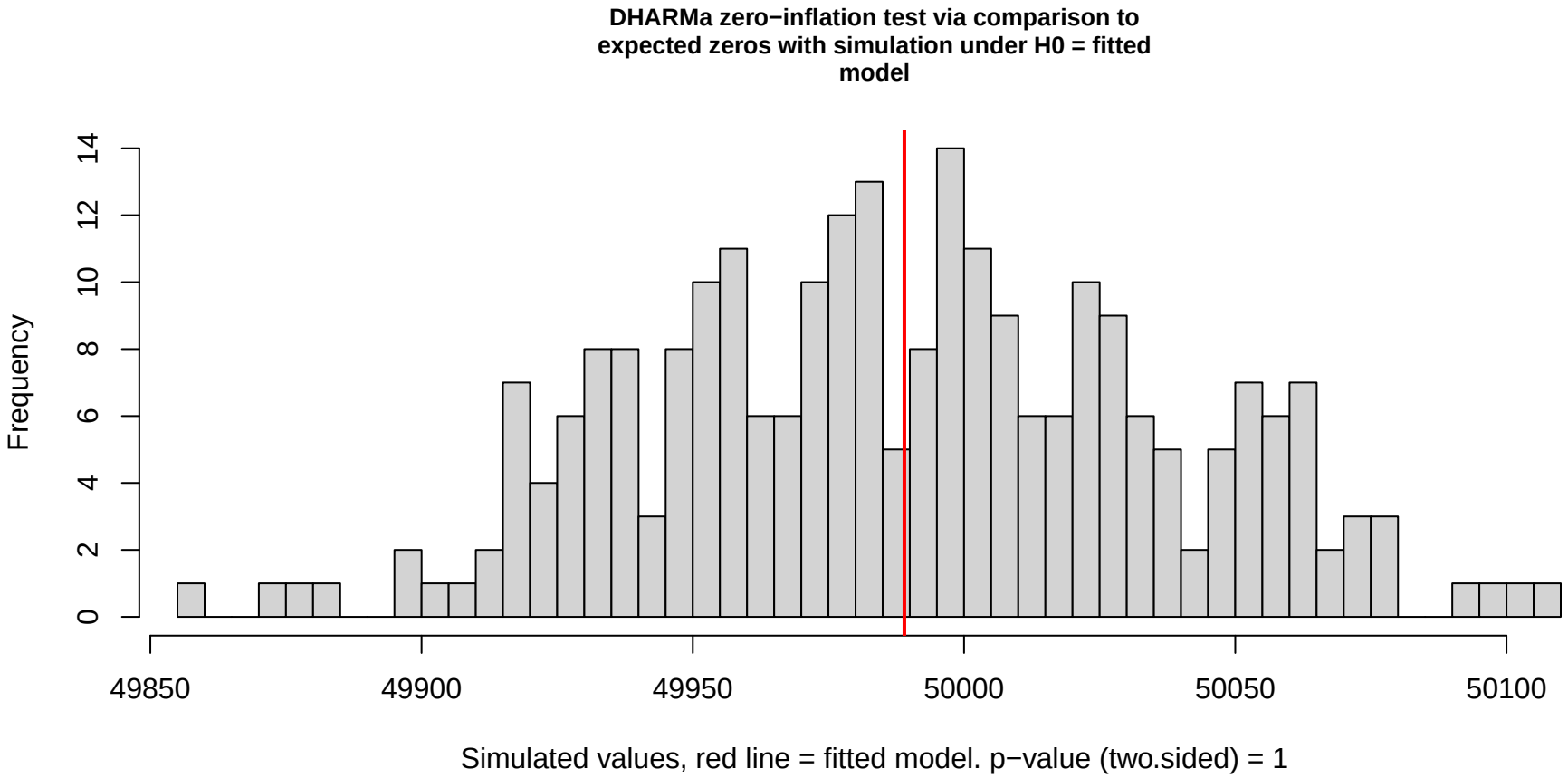
DHARMa zero−inflation test via comparison to expected zeros with simulation under H0 = fitted model
Frequency
0
2
4
6
8
10
12
14
49850
49900
49950
50000
50050
50100
Simulated values, red line = fitted model. p−value (two.sided) = 1

*Quercus petraea.robur*